THERMODYNAMIC AND ENVIRONMENTAL MODELLING OF THE AZURA EDO POWER PLANT IN EDO STATE, NIGERIA

BY

HENRY OKECHUKWU EGWARE
PG/ENG9900673
B.ENG, M.ENG (UNIBEN), MNIPES, MRAESON, COREN REGD

A THESIS WRITTEN IN THE DEPARTMENT OF MECHANICAL ENGINEERING AND SUBMITTED TO THE SCHOOL OF POST GRADUATE STUDIES. UNIVERSITY OF BENIN, BENIN CITY, NIGERIA, IN PARTIAL FULFILLMENT OF THE REQUIREMENTS FOR THE AWARD OF DOCTOR OF PHILOSOPHY(PhD) IN APPLIED ENERGY

SUPERVISOR: PROF. A.I OBANOR

CO SUPERVISORS: PROF. A.N. ANIEKWU AND

DR. O. I. OMOIFO

DEPARTMENT OF MECHANICAL ENGINEERING,
UNIVERSITY OF BENIN, BENIN CITY, EDO STATE, NIGERIA

AUGUST 2021

CERTIFICATION

This is to certify that the project titled "Thermodynamic and Environmental Modelling of the Azura Edo Power Plant in Edo State, Nigeria" was undertaken by Henry Okechukwu **EGWARE** with mat no. **PG/ENG9900673** of Mechanical Engineering Department, Faculty of Engineering, University of Benin, City,

Prof. A.I Obanor	Date
(Supervisor)	
Prof. A.N Aniekwu	Date
(Co -Supervisor)	
Dr. O.I. Omoifo	Date
(Co -Supervisor)	
Dr. S.A. Aliu	Date
(Ag. Head of Department)	

CERTIFICATION OF THE THESIS ON PLAGIARISM

We the undersigned attest and declare that the thesis of Henry Okechukwu **EGWARE** "Thermodynamic and Environmental Modelling of the Azura Edo Power Plant in Edo State, Nigeria" has successfully passed the anti-plagiarism test.

Prof. A.I Obanor	Date
(Supervisor)	
Prof. A.N Aniekwu	Date
(Co-Supervisor)	
Dr. O. I. Omoifo	Date
(Co-Supervisor)	
Dr. S.A. Aliu	Date
(Ag. Head of Department)	

DEDICATION

This study is dedicated to God Almighty for sparing my life and watering my education throughout the programme. Also, to my mother Mrs. Elizabeth Egware, my beloved wife Mrs. Josephine Ujiro Egware and dearly beloved children; Master Providence Oghenehalume Henry-Egware and Miss Passion Iluoghenedomero Henry-Egware, Miss Arerosuoghene Perpetual Henry-Egware and Master Prudence Ogheneyuome Henry-Egware for their patience and cooperation.

ACKNOWLEDGEMENT

I wish to express my sincere appreciation to my supervisor Prof. A. I Obanor for his support, guidance, and carefully reviewing this work and, providing me the opportunity to work under him in the department. Many thanks go to my co-supervisors Prof A.N. Aniekwu and Dr. O. I. Omoifo for their support and guidance during this research work.

My visit to Azura Edo Power Plant for data collection and other information about this research work was financed by Nigerian Bulk Electricity Trading PLC (NBET). Their financial support is highly appreciated and acknowledged. Many thanks to the Faculty of Engineering Research Group that conceived the idea of the collaboration that led to this research work.

I wish to acknowledge Associate Prof. Fei Duan and Dr. Baris Burak Kanbur of Nangang Technological University, Singapore for providing MATLAB code that assisted me in the area of environmental analysis. I am indeed grateful to STEAG Energy Services GmbH, Germany for the provision of Ebsilon Professional Software academic licence used in this study.

My thanks go to the owners and entire members of staff of Azura Edo Power Plant for their invaluable assistance when it mattered in this doctorial research work.

I will forever be indebted to the former Head of Department Dr. O. O. Ighodaro for his contribution to this study, also the present Head of Department Dr. S.A. Aliu and the entire staff of the Mechanical Engineering Department for their love and support throughout the programme.

My gratitude also goes to my family members, Mr. Duke Maro Egware, Miss Elizabeth Egware, Mrs. Victoria Idhigu, and late Barr. Vincent Idhigu. I would also like to acknowledge the immense support of my wife Mrs. Josephine Egware and our children Master Providence Oghenehalume Henry-Egware and Miss Passion Iluoghenedomero Henry-Egware, Miss Arerosuoghene Perpetual Henry-Egware, and Master Prudence Ogheneyuome Henry-Egware in the course of the study.

To my colleagues during this research work in the Department of Mechanical Engineering, it was a memorable experience working together.

Finally, l express my profound gratitude to Almighty God for divine assistance to achieve this goal.

ABSTRACT

In order to address the growing global energy demand and reduce the environmental impact from operating gas turbine power plants, the performance and how to improve existing gas turbine power plants need to be studied. In view of this, this research work aims at carrying out the thermodynamic and environmental analyses of Azura Edo Power Plant for design and off-design conditions.

Ebsilon Software is a commercially accepted energy and mass balance tool for power plant modelling. The performance of the Azura Edo Power Plant at design and off-design conditions were modelled using Ebsilon Software and the simulation exercise was validated. Energy, exergy and environmental analyses were conducted using operating data collected from the power plant to evaluate the thermal efficiencies, heat rate, energy losses and exergy destruction of each major component of the power plant and carbon dioxide emission rates with the aid of MATLAB software. The effects of ambient air temperature on the thermodynamic and environmental performances were carried out. Preliminary analyses of the effect of integrating an inlet air cooling system and heat recovery steam generator (HRSG) for future consideration were conducted.

The results obtained from model validation were -3.13% to 0.88% for design and -3.24% to 2.66% for off-deign conditions. This showed that the model data were found to be in good agreement with the International Standard Organization (ISO) and Azura Edo guaranteed data for both design and off-design conditions. Energy analysis results obtained showed that the average net thermal efficiency of the three units was found to be 29.79% at the ambient air temperature range from 21 to 35 ^{0}C, the compressor pressure ratio of 10.72 to 10.96 and net power output of 148.92 to 160. 70MW. Also, results obtained showed that there was a lower performance of the plant at high ambient air temperature and a lower compressor pressure ratio. The exergy analysis results indicate that the combustion chamber has the least exergy efficiency and highest exergy destruction efficiency compared to other components studied. Findings from the research revealed that the combustion chamber also has the largest improvement potential of 101.07 to 107.23MW among the components considered. The environmental analysis results obtained showed that the average emission of CO_2 for Azura Edo Power Plant was 707.741kgCO_2/MWh and 690,602,489.84kgCO_2/yr, which the latter is within the guaranteed values of 726,000,000 kgCO_2/yr. At high ambient air temperatures, low exergy and the second law of thermodynamic efficiencies, sustainability of fuel and high exergy destruction efficiency, depletion of fuel and CO_2 emission rates were observed. It was also observed from the preliminary analyses that the incorporation of air intake cooling system and HRSG caused 95.2341kgCO_2/MWh and 73,542.0651kgCO_2/yr; 181.52kgCO_2/MWh reduction in CO_2 emission respectively. The study established that the incorporation of an inlet air cooling system to maintain low compressor air inlet temperature, HRSG and steam turbine to utilize the high temperature of the flue gas to improve the plant performance was economically and environmentally feasible. Accordingly, the study has provided an understanding of suitable methods for efficient and waste minimization as ways of performance enhancement of Azura Edo Power Plant.

TABLE OF CONTENTS

LIST OF FIGURES

LIST OF TABLES

NOMENCLATURE

ABBREVIATION/SYMBOL

APH	Air Preheater
AR	Air Ratio
ASHRAE	American Society of Heating, Refrigeration and Air Conditioning Engineers
Aux	Auxiliaries
B	Width (m)
C	Compressor
CC	Combustion chamber
CCGT	Combined Cycle Gas Turbine
CCHP	Combined Cooling Heating and Power
CCS	Carbon Capture Sequestration
CHP	Combined heat and power
CIT	Compressor Inlet Temperature (^{0}C, K)
CO_2	Carbon dioxide
C_p	Specific heat capacity at constant pressure (kJ/kg K)
CSTIGT	Combined Steam Injection Gas Turbine
DBH	Diameter at Breast Height (m)
Dp	Depletion number
EIA	Environmental Impact Assessment
ER	Emission reduction
Ex	Exergy flow rate (MW)
FLT	First law of thermodynamics
FSPA	Fuel saving per annum

GE	General Electric
Gen	Generator unit
GHG	Greenhouse gas
GT	Gas turbine unit
HR	Heat rate (kJ/kWh)
HRSG	Heat recovery steam generator
I	Exergy loss (MW)
IBRD	International Bank for Reconstruction and Development
IEA	International Energy Agency
IFC	International Finance Corporation
IGV	Inlet Guide Vane
IPP	Independent Power Producer
IPPC	Intergovernmental Panel on Climate Change
ISO	International Standard Organization
KE	Kinetic Energy (kJ)
L	Length (m)
LCOE	Levelized Cost of Electricity
LF	Load factor (%)
LHV	Lower heating value (kJ/kg)
LNG	Liquefied Natural Gas
M	Molar mass (kg/kmol)
$\dot{m}$	Mass flow rate (kg/s)
MIGA	Multilateral Investment Guarantee Agency
MOPSO	Multi – Objective Particle Swarn Optimizer
MSCF	A Thousand Standard Cubic Feet

$\dot{n}$	Molar flow rate (kmol/s)
N	Number of moles
NBET	Nigerian Bulk Electricity Trading PLC
NIPP	National Integrated Power Plant
NOx	Nitrogen oxides
OMC	Operation and Maintenance Cost
OPT	Operation Time (s, h)
p	Pressure (bar)
P	Power (MW)
Q	Heat supply/removal rate (MW)
R	Universal gas constant (kJ/kgK)
r_p	Compressor Pressure ratio
s	Specific entropy (kJ/kgK)
$\dot{S}$	Entropy flow rate (MW/K)
SFC	Specific fuel consumption (kg/kWh)
SI	Sustainability Index
SLT	Second law of thermodynamics
SPPA	Siemens Power & Process Automation
SRK	Soave Redich Kweng
ST	Steam turbine
STIGT	Steam Injection Gas Turbine
T	Absolute temperature (^{0}C, K)
TC	Total cost
TCM	Test Centre Mongstad
TIT	Turbine Inlet Temperature (^{0}C, K)

$\dot{V}$	Volume flow rate (m^3/s)
v	Specific volume (m^3/kg)
W	Work done (MW)
W.R	Work ratio
WRPC	Warri Refining Petrochemical Company
X	Mole fraction

GREEK SYMBOLS

ξ	Carbon dioxide Emission Rate (kg/MWh)
ϕ	Relative Humidity
Δ_m	Change or difference in product of mass flow rate (kg/s)
η_c	Compressor isentropic efficiency
η_{cc}	Combustion efficiency
η_{gen}	Generator efficiency
η_{GT}	Gas Turbine Thermal Efficiency
η_{mech}	Mechanical efficiency
η_{net}	Net Thermal Efficiency
η_o	Overall Thermal Efficiency
η_{oav}	Average overall efficiency
η_{oc}	overall combined cycle efficiency
η_T	Turbine isentropic efficiency
η_{th}	Heat transfer efficiency
$\eta_{thermal}$	Thermal efficiency
η_{thgr}	Gross thermal efficiency

γ	Specific heat capacities ratio
E	Exergy efficiency
ε_d	Exergy destruction efficiency
λ	Fuel air ratio
P	Density (kg/m^3)
Ω	Moisture content

SUBSCRIPTS

a	Air
AC	Air compressor
Amb	Ambient
Aux	Auxiliaries
Av	Average
B	Width
CC	Combustion chamber
D	Destruction
da	Dry air
Elect	Electrical
f	Fuel
G	Exhaust gas
gen	Generator
GT	Gas turbine
I	In
Mech	Mechanical
O	Out

rd	Reduction
ref	reference/ambient
S	Steam
ST	Steam Turbine
T	Turbine
V	water vapour
W	Water
Xip	Exergy Improvement Potential

SUPERS CRIPTS

CHE	Chemical
M	Material
P	Mechanical
T	Thermal

CHAPTER ONE

INTRODUCTION

1.1 Background to The Study

The economic and technological developments of a country depend on available energy and power for all sectors of the economy. The direct increase in energy and power consumption is a result of the increase in urbanization, population, technological development and number of industries (Li and Lin, 2015; Shahbaz et al.,2015). In Nigeria, the electrical power supply is less than the demand for power (Olatomiwa et al., 2016). The poor power supply has hindered the economic and technological development strides in the country.

Due to the lack of adequate electrical power supply to her populace, the Federal Government of Nigeria (FGN) initiated the reform of the power sector in the past ten years that led to the privatization of the electrical power generation company (Gencos). When the Power Holding Company of Nigeria (PHCN) was being unbundled, the Nigeria government launched an ambitious capital investment program under the title of the National Integrated Power Plant (NIPP). The NIPP project consists of the gas-fired power plants and transmission lines, which was intended to add about 5000MW to the electrical generating capacity of Nigeria (NERC, 2020). The challenges of power generation in Nigeria after deregulation continued due to the difficulties in gas supply, evacuation of power generated, and payment guarantee.

The problems that arose from the implementation of the NIPP made the FGN also to state clearly that there were huge funds needed to be invested in the power sector and it cannot be done by the government alone. The Nigeria government made it clear that the private sector had to be involved to achieve the needed investment in the power sector. The issue led to establishing a credible regulatory and contractual frame work that would guarantee enough confidence for private

investors in the power sector. This made the FGN to come up with Independent Power Producer (IPP) policy. To achieve this, the Nigeria government requested for support from World Bank Group and other development financing institutions. In response to FGN request, Multilateral Investment Guarantee Agency (MIGA), International Bank for Reconstruction and Development (IBRD) and International Finance Council (IFC) worked together to form the Energy Business Plan (EBP) to manage the World Bank Group resources to support the reforms of Nigeria power sector. This was done to attract private investors in the Nigeria power sector, which will in turn provide additional generation capacity.

In order to enhance the growth of the power sector in the country, the Nigerian Electricity Regulatory Commission (NERC) gave licenses to 70 IPPs (Oladipo et al.,2018). Arising from this development, the following IPPs were built: Okpai Power Station with 480MW installed capacity, Afam IV Power Station with 642MW installed capacity, Ibom Power Station with 500MW installed capacity, AES Barge with installed capacity of 270MW, Omoku Power Station with 150MW installed capacity, Trans-Amadi Power Station with installed capacity of 136MW, Rivers IPP with 180MW installed capacity, Aba Power Station with installed capacity of 140MW and Azura Edo Power Plant with installed capacity of 459MW (Oladipo et al.,2018). Among the IPPs listed, apart from Okpai and Azura Edo others have challenges ranging from poor funding and technical problems (Oladipo et al.,2018).

As mentioned, the Azura Edo Power Plant was one of the IPPs which was funded under the EBP initiative. The project included the construction, operation, and maintenance of a 459MW gas – fired open cycle power plant near Benin City, Edo State Nigeria. The construction of 330kV transmission line connecting the power plant to the Benin Substation and an underground gas pipeline to connect the power plant to the Escravos Lagos Pipeline (ELP) was part of the contract.

The project was necessary to add power to the national grid (Siemens, 2018). The Azura Edo Power Plant was considered a priority project for the FGN, and it was the first green - field IPP post power sector reform that was built. Azura Edo Power Plant was the first IPP project almost fully financed by the private sector in Nigeria. The project company includes 97.5% shares from a consortium of private investors and 2.5% share from Edo State Government (WBG,2017). In this regard, it was regarded as a ground breaking project set to pave the way and set benchmarks for future private power sector - driven IPPs financed project in Nigeria.

It signals to private investors that despite challenges facing the country, bankable power projects can be successfully developed in Nigeria. The consortium led by Amaya Capital was supported by a syndicate of 15 international and local lenders including Siemens Financial Services. The plant is designed to run on natural gas. It is constructed under the turnkey Engineering, Procurement and Construction (EPC) contract by a consortium of Siemens (Mechanical and Electrical works) and Julius Berger Nigeria (civil works). The project will be developed in three phases, starting with this 459 MW open cycle gas turbine power plant. In the design, Siemens considered further extension and conversion to combined cycle over two phases, which will bring the total capacity of the plant up to 1,500 MW. This open cycle plant consisting of three SGT5-2000E gas turbines equipped with the SPPA-T3000 control system is designed and ready for combined cycle extension (Siemens, 2018)

The Azura Edo Power Plant signed an agreement with the FGN to buy over the facility in case of force majeure. The Power Purchase Agreement (PPA) was signed between Nigerian Bulk Electricity Trader (NBET) and Azura Edo Power Plant to guarantee that the power generated by the power plant will be bought by NBET. The agreement on the production of gas was signed

with Seplat Petroluem Development Company and that for the transportation of the gas was signed between Nigerian Gas Company (NGC) and Azura Edo Power Plant.

NBET, which guaranteed the buy over of the Azura Edo Power Plant in case of force majeure signed a contract with the Faculty of Engineering Work Group (FEWG) under the University of Benin Consultancy to monitor the construction and installation works. The contract was to ensure that the construction and installation works met the required specifications as well as building human capacity that will gain experience from the project. In view of this, NBET invited students to carry out research works to monitor the construction of the plant and its performance during and after installation. This is in line with what was suggested by Saravanamuttoo et al. (2009) and Simon et al. (2013) that the actual performance of gas turbine power plants should be monitored in their local sites where they are installed.

The project, whose development started in January 2016 was scheduled to be completed in December 2018. Be that as it may, with the completion of a massive portion of the project, the venture was finished 7 months ahead of time. It has additionally shown a good record of health and safety practices, having worked more than 4 million man-hours of work without a single lost-time due to injury as at the time the main unit was synchronized to the national electricity network (Siemens, 2018). The first turbine was synchronized to the country's electricity grid on 20th December 2017 and went through a battery of tests for more than five weeks. Tests on the next turbine were done towards the end of January 2018, with the tests on the third turbine happening towards the start of March 2018. The power station was commissioned at the end of April 2018 when the power station commenced its full commercial operation. The plant is operated and maintained by PIC Group Inc (a subsidiary of Marubeni) under a five-year operation and maintenance agreement. The SGT5 – 2000E gas turbine model installed in Azura Power Plant

has been designed to operate with good reliability, low NOx and CO_2 emissions, and ease of combined cycle integration.

The performances of all gas turbines are affected by local or ambient air conditions such as temperature, relative humidity, etc (ASHRAE, 2008). The rated capacities of all combustion turbines are based on the International Standard Organization (ISO) conditions of an ambient air temperature of 15 ^{0}C, relative humidity of 60% and ambient pressure of 1.01325 bar at sea level. Azura Edo Power Plant is located in an area having an average ambient air temperature of 26 ^{0}C, a relative humidity of 70%, and ambient pressure of 1.013bar. Ambient air temperature has a clear impact on the gas turbine power plant performance because the air mass is inversely proportional to its ambient air temperature and proportional to the power produced. So, it is important to study the effect of ambient air temperature on power output and other output parameters of gas turbine power plants as reported in Saravanamuttoo et al. (2009). The book also stressed that this is very important to the customer; at any specific condition, the performance of the power plant must be guaranteed readily by the manufacturer of the gas turbine. Simon et al. (2013) explained in their report that actual outcomes may differ depending on local site conditions. This makes it necessary to have design and guaranteed performance for gas turbine power plants when the site ambient air temperature differs from the ISO design ambient air temperature.

The Azura Edo Power Plant is fired by natural gas. Natural gas is classified as fossil fuel, which means it is finite and has emission problems such as Greenhouse gas (GHG), that causes global warming in the environment, climate change, and depletion of the ozone layer (Park et al., 2014). The effects of environmental impact, economic and limited reserves of natural gas and continuous increase in demand for electricity have led to research on efficient ways to manage the available fuel and its emission impact for power generation plants. The gas turbine cycle performance

improvement and reduction of its greenhouse gas emission had been of great concern to the industrial sector and researchers (Hoffmann et al., 2008; Ganjehkaviri et al.,2015; Howes et al., 2013).

Most of the existing thermal power plants still rely mainly on the utilization of fossil fuels, which emit greenhouse gas (GHG) (mainly CO_2) that cause environmental problems (Dell and Rand, 2004; Grant et al., 2016; Shahsavari and Akbari, 2018; Kırlı and Fahrioğlu, 2019). IEA (2016) reported that conventional hydrocarbon fuels had contributed approximately 67% of the total energy production in the world while 22% is contributed by renewable energy resources, which supports the claim by researchers mentioned earlier. To reduce the environmental impact from gas turbine power plants fired by natural gas, studies have shown that the incorporation of better technologies for performance enhancement and environmental sustainability should be considered.

Energy and mass conservation equations are used to determine the thermodynamic performance of each component and the total system for given input parameters (Kiameh, 2012). In designing and optimizing the performance of gas turbine power plants, the thermodynamic and environmental analyses are important evaluation methods utilized to maximize the usage of natural gas. The two essential thermodynamic methods in use are energy and exergy analyses. Energy analysis is the traditional way of evaluating the conversion /and or transfer of energy utilized during chemical or physical processing of materials in any system (Dincer and Rosen, 2007; Moran and Shapiro,2000). The use of the First and Second Laws of Thermodynamics to investigate the utilization of energy in thermal systems is referred to as exergy analysis (Dincer and Rosen, 2007).

Dincer and Rosen (2013) have provided reasons, such as the evaluation of losses during energy conversion process and efficient usage of gas turbine power for carrying out energy analysis. For types, locations, and causes of energy losses in the power plant, exergy analysis needs to be carried out (Oyedepo et al., 2015; Ibrahim et al., 2017). The evaluation of exergy will provide detailed information on how to reduce the wasted energy from the system and a more efficient way of managing the available resources for future purpose (Rocco et al.,2014). For gas turbine power plants performance evaluation, it is necessary to carry out both energy and exergy analyses because of their powerful and complementary nature as aforementioned. So, this explains the significance of carrying out both analyses. The environmental analysis is the study of the effect of emission of GHG in the utilization of fuel by thermal systems. Also, it is important to carry out the environmental analysis, in order to determine how much carbon dioxide is emitted to the atmosphere from the power plant.

Azura Edo Power Plant consists of 3 units of SGT5 – 2000E, GT11, GT12 and GT13 located in Ihobvor Community, Benin City, Edo State, Nigeria. For optimum performance of SGT5-2000E in this location, the thermodynamic and environmental analyses need to be undertaken in order to determine how the local weather affects its performance for design and off-design conditions. The actual performance will be compared with guaranteed values during the period of study.

1.2 Statement of the Problem

The increasing utilization of natural gas for generating power and the increase in energy supply costs have made researchers and manufacturers searching for systems with higher efficiency. The problem of shortage in power supply to end - users and the finite nature of natural gas resources have led to many power plant managers seeking to enhance the efficiency, specific fuel

consumption (SFC), heat rate (HR) of existing power plants and the performance of other thermal facilities. The efficiency and performance of power plants depend on some factors like operating conditions and component efficiencies. To improve the efficiencies and performance of existing energy facilities, it is essential to discover the components which have low performance and enhance their efficiency.

To achieve this, the thermodynamic analysis of the power plants should be carried out in order to identify the locations, types and causes of losses that occurred in them. Gas turbine power plants are environmentally sensitive, therefore there is a need to evaluate their performance to know how the ambient conditions affect them and suggest ways of improving them against negative environmental effects.

The gas turbine power plants also have negative impact on the environment as a result of emission from the combustion of fossil fuels that causes global warming and ozone layer depletion issues. The gas turbine power plants do release substances to the atmosphere, which contain carbon dioxide and other air pollutants. The research of systems to lower the emission of the GHG from power plant need to be studied. The main component of the exhaust gases that contributes to GHG is carbon dioxide as reported by Ong et al. (2011); Mukherjee et al. (2019). It has been reported in Anthony et al. (2015); Stechel and Miller (2013) that carbon dioxide emission from power plants into their surroundings is a universal alarm from previous theoretical models that provided information about its influence on climate change and global warming. The carbon dioxide buildup in the atmosphere is about 1 tera ton (Mikkelsen et al., 2015); IEA (2015) and Robert (2020) model proposed that to maintain 2 ^{0}C temperature increase by 2050, the levels of carbon dioxide in the atmosphere annually should not be greater than 15 gigatons. Environmental and economic performances of the power plant are crucial matters in designing and optimizing the performance

of power plant production systems (Babaelahi et al., 2019). Thus, it is essential to estimate the carbon dioxide emission of power plants that use fossil fuels to ascertain its emission level. To effectively monitor the performance of Azura Edo Power Plant, these aforementioned problems should be addressed.

1.3 Aim and Objectives

1.3.1 Aim

The aim of this study is to undertake the thermodynamic and environmental modelling of the Azura Edo Power Plant in order to evaluate its thermal performance and determine some environmental parameters.

1.3.2 Objectives

To achieve the aim of the research, the objectives are to:

i. develop models to evaluate the performance of Azura Edo Power Plant at design and off-design conditions and validate them with design and actual operating data.

ii. determine the Azura Edo Power Plant performance and energy losses using the First Law of Thermodynamics.

iii. evaluate and identify the Azura Edo Power Plant exergy consumption and destruction sources for its various components.

iv. identify which of the components are more significant for performance exergy improvement potential, determine the sustainability index (SI) and depletion of fuel for Azura Edo Power Plant.

v. quantify the carbon dioxide (CO_2) emissions rates from Azura Edo Power Plant.

vi. develop models that will be useful for future phases integration and performance monitoring.

1.4 Relevance of The Study

Research work is very relevant to the development and sustenance of our energy infrastructure which are important for our industrialization. Thermodynamic and environmental analyses are beneficial because they provide a comprehensive rundown of the losses, in terms of waste energy emission and irreversibility, for the overall plant and its individual components. These analyses are very important because they are useful, suitable, and straightforward methods for evaluating and enhancing the performance of power generation stations. The study will provide how Azura Edo Power Plant is performing at design and off–design conditions. It will also provide models that will be helpful for the Azura Edo Power Plant future phases integration.

1.5 The Scope and Limitation of The Study

The scope of this study is limited to thermodynamic and environmental modelling of the Azura Edo Power Plant. It involves evaluation of the energy and exergy performance of the major components of this plant such as compressors, combustors and turbines with a view to identifying the ones that require improvements for optimum performances of the plant. The actual performance data of the plant will be deployed for these purposes.

CHAPTER TWO

LITERATURE REVIEW

2.1 Basic Gas Turbine Cycle

The majority of the power plants in the country are gas turbine power plants because of its low cost, short installation period and abundant availability of natural gas. The gas turbine power plants can operate as a simple open cycle system, a combined cycle system, or combined heat and power system in the power plant generation setup (Kaviri et al.,2013; Vélez et al.,2012). The shaft or propulsion power and heat applications of gas turbines in an area of industrial, automotive, commercial, and other applications had become reliable and popular. (Ahmadi et al., 2016; Tlili, 2015; Tlili and Musmar, 2013; Colonna et al., 2015). The Nigerian government has encouraged the establishment of independent power plants (IPPs) to complement her effort in making more power available to her citizens. To that effect, Azura Edo Power Plant which is an IPP project in Benin City with SGT5 – 2000E open cycle gas turbine power of 459 MW capacity was initiated.

The performances of all gas turbines are affected by local or ambient air conditions such as temperature, relative humidity, etc (ASHRAE, 2008). The rated capacities of all combustion turbines are based on the International Standard Organization (ISO) conditions of an ambient air temperature of 15 ^{0}C, relative humidity 60% and ambient pressure 101.325 kPa at sea level. The majority of gas turbine power plants in Nigeria are located in areas where they rarely operate at ISO conditions, thereby, affecting their optimum performance. Azura Edo Power Plant is located in an area of an average ambient air temperature of 26 ^{0}C, a relative humidity of 70%, and ambient pressure of 1.013bar. Ambient air temperature has a clear impact on the gas turbine power plant because the air mass is inversely proportional to its ambient air temperature and directly

proportional to its power produced. So, it is important to study the effect of ambient air temperature on power output and other output parameters of gas turbine power plants as reported in Saravanamuttoo et al. (2009). The report also stressed that this is very important to the customer; at any specific condition, the performance of the power plant must be guaranteed readily by the manufacturer of the gas turbine. This makes it necessary to have design and guarantee performance for gas turbine power plants when the site ambient air temperature differs from the design ambient air temperature.

Most existing thermal power plants still rely mainly on the utilization of fossil fuels, which emit greenhouse gas (GHG) (mainly CO_2) that cause environmental problems (Dell and Rand, 2004). IEA (2016) reported that conventional hydrocarbon fuels had contributed approximately 67% of the total energy production in the world while 22% is contributed by renewable energy resources. This supports the claim of Dell and Rand (2004). To reduce the environmental impact from gas turbine power plants fired by natural gas, studies have shown that the incorporation of better technologies for performance enhancement and environmental sustainability should be considered.

Gas turbine power plants in Nigeria use natural gas as a source of fuel to fire them. Natural gas is classified as fossil fuel, which means it is finite and has emission problems such as Greenhouse gas (GHG), that causes global warming in the environment, climate change, and depletion of the ozone layer (Park et al., 2014). The effects of environmental impact, economic and limited reserves of natural gas and continuous increase in demand for electricity have led to research on efficient ways to manage the available fuel and its emission impact for power generation plants. The gas turbine cycle performance improvement and reduction of its greenhouse gas emission had been of great concern for the industrial sector and researchers (Hoffmann et al., 2008; Ganjehkaviri et al.,2015; Howes et al., 2013).

Results from various research works have shown that the thermodynamic and environmental analyses of gas turbine power plants vary from location to location for the same/different power plant models, because operating ambient conditions are not the same. The thermodynamic and environmental performance evaluation of the Azura Edo Power plant has not been previously carried out. Thus, it is necessary to carry out this study.

All gas turbines operate on the thermodynamic cycle known as the Brayton cycle (Saravanamuttoo et al.,2009). The sectional view of the gas turbine-set is illustrated in Figure 2.1. Figure 2.2 shows a typical schematic diagram of an open cycle simple gas turbine plant, while Figure 2.3 shows a T-s diagram of an open cycle gas turbine. Simple gas turbine major components are compressors, combustors, turbines, and generators. It operates continuously by taking in the fresh air at state 1 into the compressor. The air is then compressed to high pressure in the compressor and discharged into the combustors at state 2. Here the compressed air is mixed with fuel and burnt continuously after ignition to liberate its energy at constant pressure. At state 3, the combustion products with high pressure and temperature flow into the turbine, the burnt gas thermal power is converted to mechanical shaft power in the turbine, which in turn drives the generator shaft. The mechanical shaft power is converted to electrical power by the generator. At state 4, the flue gases are discharged into the atmosphere at constant pressure after expansion through the turbine to low temperature and pressure.

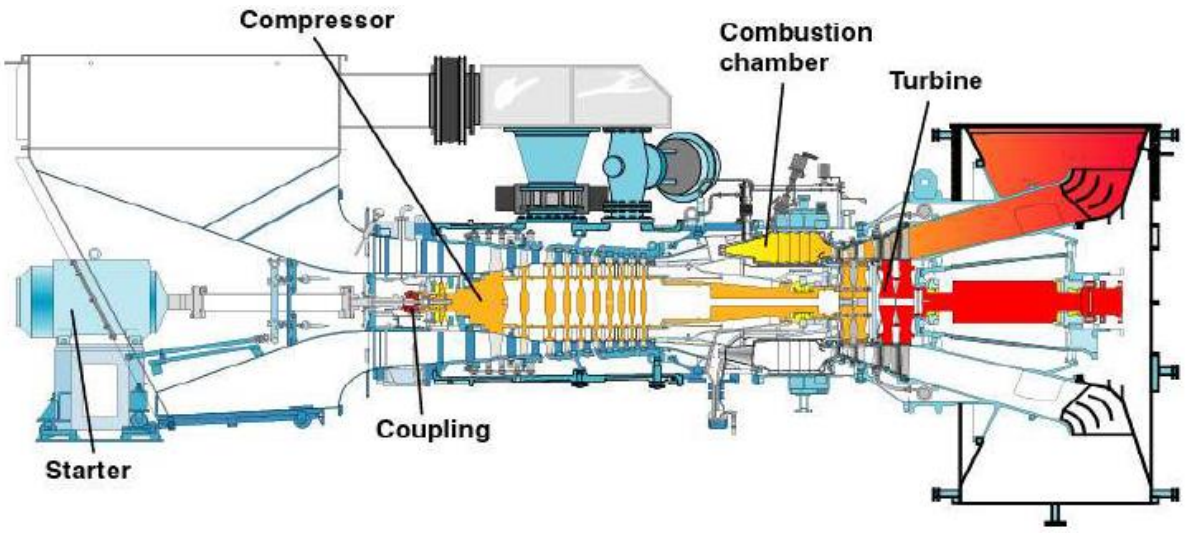

Figure 2.1: Overview of a Gas Turbine - Set (Nordstrom 2005)

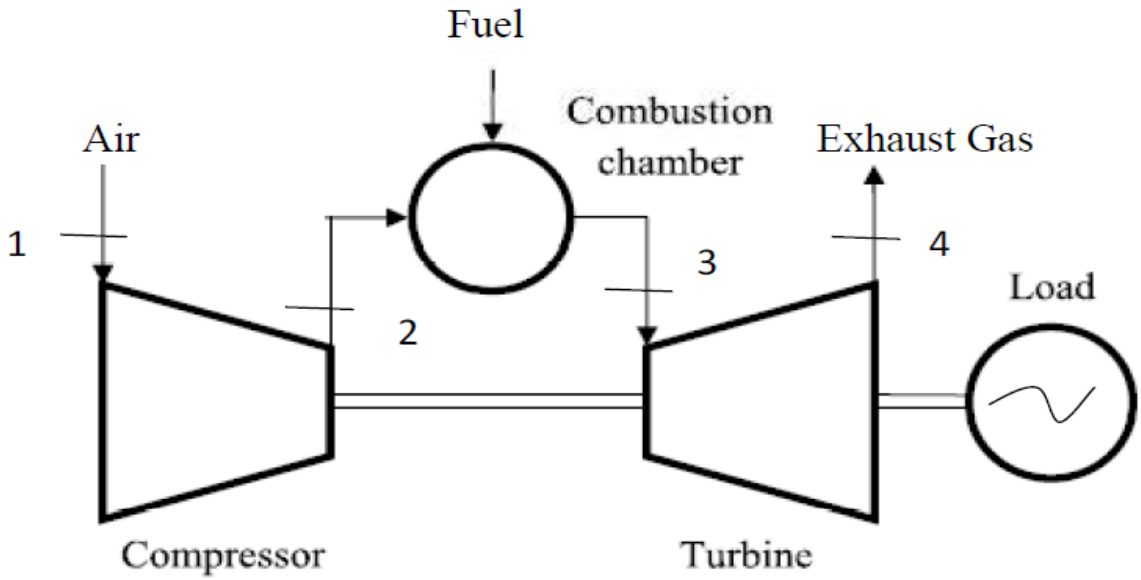

Figure 2.2: A Typical Gas Turbine Plant Schematic Diagram.

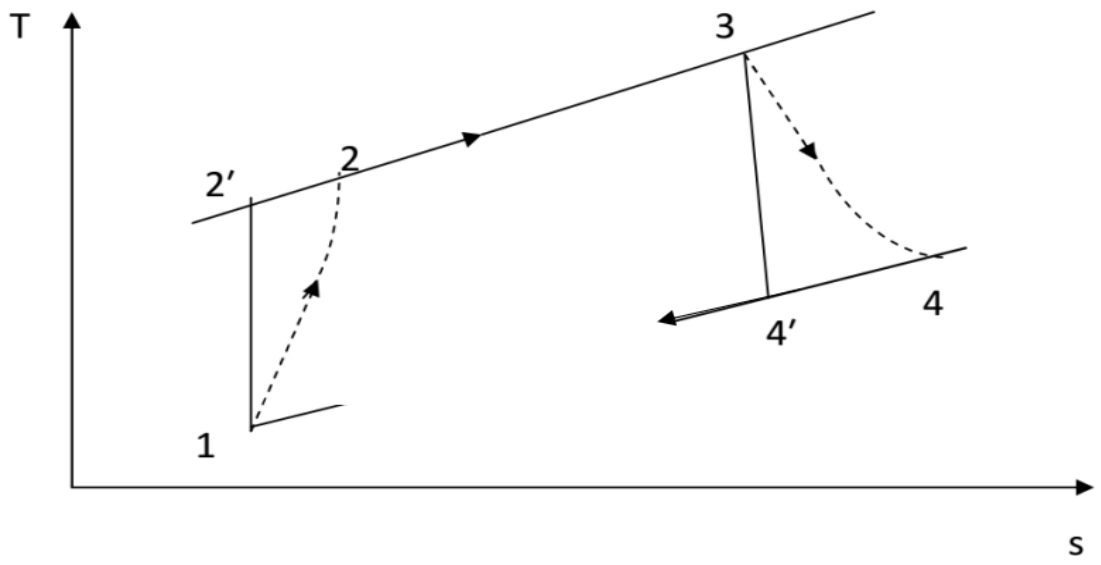

Figure 2.3: Temperature (T) – Specific Entropy (s) Diagram of an Open Cycle Gas Turbine

2.2 Gas Turbine Main Components

The description of the main components of a gas turbine is as follows:

2.2.1 Compressor

The compressor of a large power gas turbine is an axial flow type that compresses a bulky volume of air efficiently. It usually contains many individual stages in a series of operations. The number of stages depends on the design and unit capability.

Each stage of the compressor is made up of rotating and fixed rows of blades called rotors and stators respectively. In the compressor, the intake air velocity is increased by the rotor and the air kinetic energy (KE) is converted to pressure increase by the stators. In the inlet of the compressor, there are Inlet Guide Vanes (IGV) consisting of stationary blade sets that direct the intake air smoothly into the first set rotor of the compressor. In some types of gas turbine plants, variable IGVs are used to control the volume of air that enters into the compressor (Saravanamuttoo et al 2009).

At the compressor discharge, there is a cone-shaped diffuser that consists of stationary blades to obtain maximum pressure increase before the air flows into the combustion system.

Air is extracted from the compressor which can also be utilized as a means of sealing and cooling air for bearings, wheels, turbine nozzles, and other hot gas path parts that need cooling.

2.2.2 Combustion System

In the combustion chamber, many liners allow the injection of fuel into it to combust the air from the compressor. The turbine section is connected by these liners by transition pieces. The atomization of the fuel for proper combusting is done by injecting the fuel into the liners by corresponding fuel nozzles. The electric spark plug in the combustion system is used to ignite the fuel initially. As soon as it starts burning, self – sustained and continuous burning will take place as long as air and fuel are supplied to the combustion chamber.

2.2.3 Turbine Section

The turbine section contains many stages (depending on design specification), each stage is made up of a set of a fixed row of blades and a rotating row of blades known as nozzle and rotor respectively. The nozzle is attached to the turbine case while the rotor is attached to the turbine shaft. The nozzle increases the velocity of high energy gases and pushes it in the direction of the rotor. The rotor blades help to convert the kinetic energy from the high-velocity gas to the rotating motion of the turbine. The turbine is driven by the available energy from the combustor and it can be altered by changing the amount of fuel that flow into the combustor.

2.3 Performance Enhancements on A Gas Turbine Power Plant

Usually, some factors which affect the performance of the gas turbine power plant are not controllable. The power plant configuration (like a simple or combined cycle) and the planned

site location are some of these factors. To improve the performance of simple open cycle gas turbine power plants, some performance enhancement techniques need to be considered.

To address growing universal energy demand and reduce the environmental impact from gas turbine power plants, improvement in energy generation and conversion processes had to be developed. The use of systems that will decrease the generation costs of products and reduce the emission of gases causing climate change have to be employed (Isam et al., 2018; Ghaem Sigarchian et al. 2018). Many researchers have analyzed various combinations of regenerative and other gas turbines cycles (Khan et al., 2017; Xue et al., 2007; Khan and Tlili, 2018; Shengya et al., 2017) that can improve the simple gas turbine performance. Studies to enhance the performance in the Azura Edo Power Plant have not been previously carried out. So, it will be necessary to consider it in this study.

2.3.1 Inlet Air Cooling

The ambient temperature effect curve shown in Figure 2.4, indicates that turbine output and heat rates are enhanced through the lowering of compressor inlet temperature. The integration of chillers or evaporative coolers in the compressor air intake arrangement can be utilized to decrease the compressor inlet temperature.

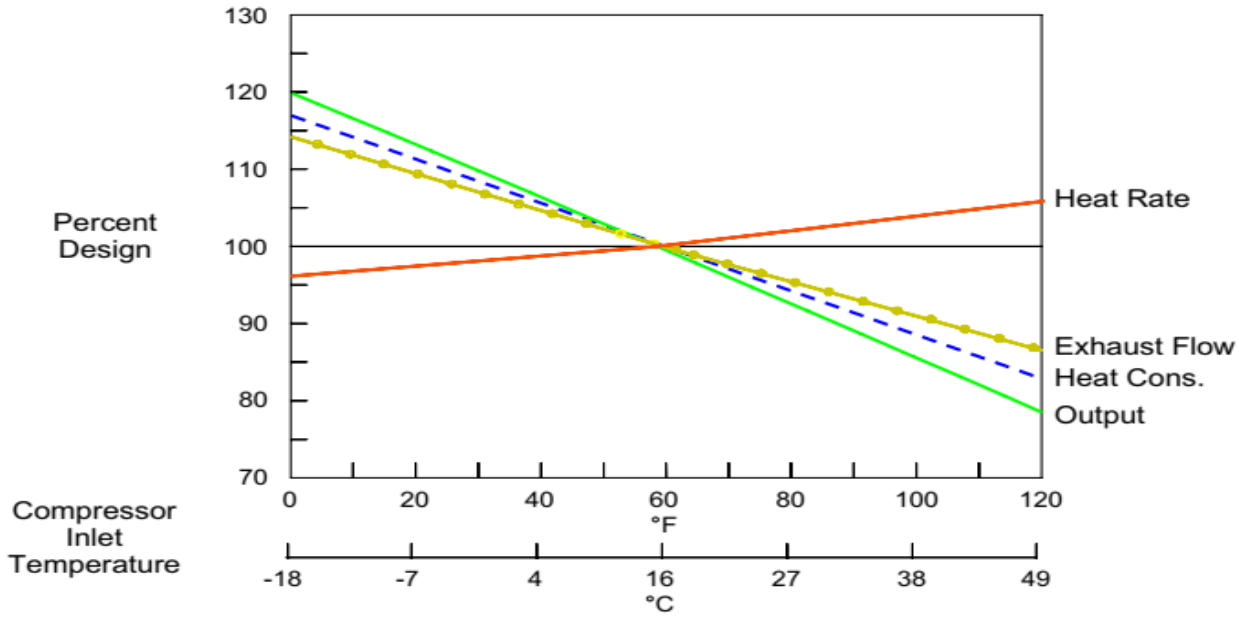

Figure 2.4: Effect of Ambient Temperature on Gas Turbine Power Plant (Brooks 2000)

The evaporative cooling system is a direct technique that cools the compressor inlet air by mixing the air with spray atomized water (Wang et al., 2009). This cooling system has been widely studied and applied successfully in gas turbine power plants operating in hot and dry regions (Ameri et al 2004; 2007; Alhazmy et al 2006). The evaporative cooling system is simple, cheap, and helps to reduce the content of NOx emitted from gas turbine power plants. The effectiveness of 85% to 90% of coolers has shown economic benefit when applied in gas turbine power plants (Brooks 2000; Hosseini et al., 2007; Baakeem et al., 2018).

Caution is needed in applying these systems of cooling to avoid lowering performance and exacerbating fouling of compressor caused by carryover or condensation of water. The carryover moisture will be reduced by coalescing pads or moisture separators immediately after the evaporative cooler.

The gas turbine differs from other prime movers in being particularly sensitive to ambient air temperature. The power output for a given turbine inlet temperature increases markedly at low air

temperatures, the efficiency also improves but less markedly; this is mainly because the compressor, at a given speed, aspirates a mass of air roughly proportional to the density (Wood 1981; Zeitoun, 2021).

Mahto and Pal (2013) reported that for the summer period, there is a rise in demand for power. On the other hand, Meher-Homji and Mee (1999) stated that the net power output drops by 0.91% for every 1 ^{0}C rise in ambient air temperature from their study. Yang et al. (2009) concluded in their works that employing the inlet air cooling system in gas /steam combined cycle produced higher efficiency at ambient air temperature ranging from 15 – 20 ^{0}C. The study of integrating inlet cooling can be considered since the Azura Edo Power Plant operates mostly between 22 – 35 ^{0}C which is higher than the ambient air temperature considered by Yang et al. (2013).

Ehyaei et al (2012) evaluated the effect of integration of absorption cooler in a simple open gas turbine power plant in two Iranian cities. The application of the absorption chiller air intake cooling technique revealed that the net power output improved by 10.3% and 11.5% for Bushehr and Tabas cities respectively and is economically viable. Furthermore, the paper indicated that there was 29.4 and 22.9% improvement in second law efficiency and 2.9 and 5.04% reduction in electricity generation cost for Bushehr and Tabas respectively. The effects of integrating a fogging inlet cooling system for a combined cycle power plant on its performance were studied by Ehyaei et al. (2015). The increase in the average power output, first and second laws efficiencies were determined to be 17.25, 3.6, and 3.5% respectively for incorporating an air intake cooling system as reported in their paper.

Yazdi et al. (2015) undertook the study of integrating air intake cooling with a heat pump to the gas turbine power plant using a novel system configuration for the temperate climate of Tehran

and hot arid region of Yazd. The impact of incorporating the inlet cooling technique on the power plant performance showed that there was an increase in average power output by 10% and 11.5% for Tehran and Yazd respectively; this led to a 10% and 11% reduction in power production cost for Tehran and Yazd respectively. The paper also reported that the incorporation of the inlet cooling technique resulted in a 35% and 10% reduction in the rate of pollutants emitted in Tehran and Yazd respectively. The paper concluded that the payback periods achieved by the inlet air cooling system for Tehran and Yazd are 2.5 years and 2 years respectively. The aforementioned studies in this section have shown the benefits of incorporating inlet air cooling systems. This has not been studied previously for the Azura Edo Power Plant. So, the effect of integrating inlet air cooling system will be considered for this study.

2.3.2 Steam and Water Injection for Power Augmentation

The injection of water or steam into the combustor head end has helped to increase the mass flow rate, which leads to increasing the power output and reduction in NOx emitted. Normally, the NOx requirement for operating cost minimization and impact on inspection determine the amount of water needed to be injected into the combustor.

For the past three decades, General Electric (GE) gas turbines had made available the option of augmenting power by injecting steam into the combustor (Brooks 2000). The steam can be either injected into the combustor or the compressor discharge casing of the gas turbine for power augmentation.

As shown in Figure 2.5, the heat rate and output are equally affected by steam injection. GE does make room for up to 5% of the compressor airflow for steam injection to the combustor when designing their gas turbines (Brooks 2000).

Ziółkowskia et al. (2019) carried out the study of retrofitting combined heat and power (CHP) plant by applying the method of steam injection gas turbine and combined steam injection gas turbine. The results achieved in Steam injection gas turbine (STIGT) and Combined steam injection gas turbine (CSTIGT) show that the electric power output increased by 1.33 MWe and 2.68 MWe and reduced the heating power by 52.90 MWth and 31.75MWth respectively. The study also revealed that exergy losses occur in the combustor with a value of 61.30 MW. Finally, the work mentioned the reduction of temperature in the combustion chamber kept the NOx emission at 8b/MWh limit for both models. The study demonstrated the importance of steam injection in enhancing power plant performance.

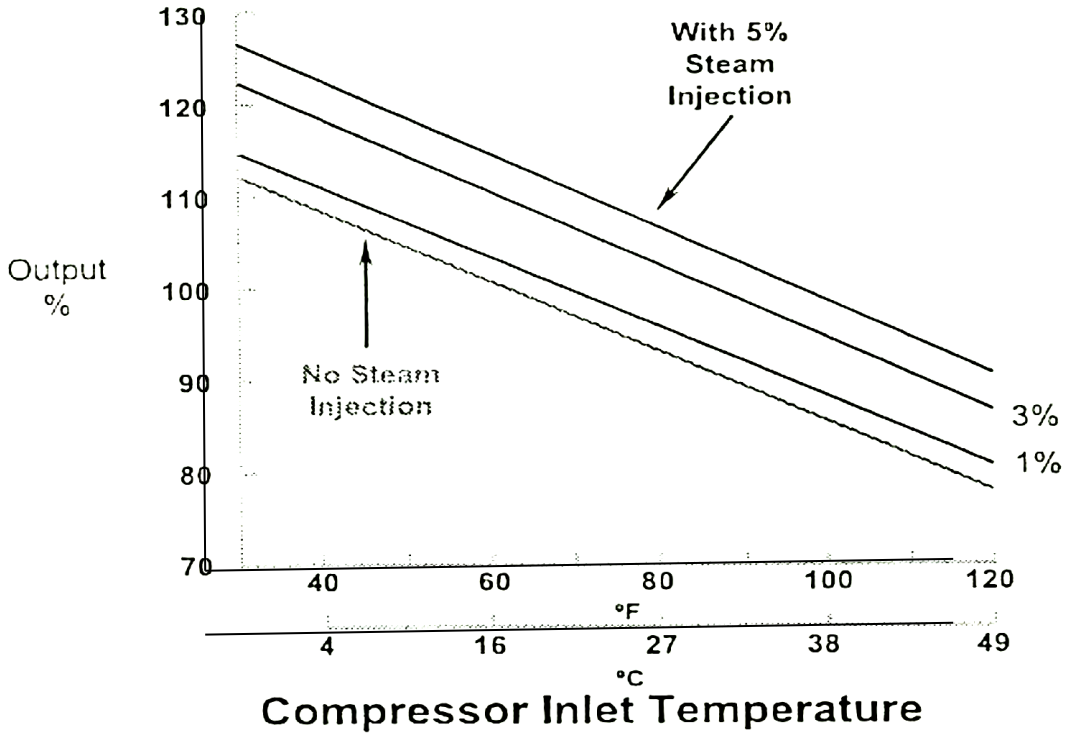

Figure 2.5: Effect of Steam Injection on Output and Heat Rate

2.3.3 Combined Cycle Arrangement

The installation of Heat Recovery Steam Generator (HRSG) and steam cycle components to form a combined cycle power plant does not need much modification to the existing gas turbines. Minimum plant downtime and loss in production capability will be experienced during the steam cycle integration process because of no interference with the existing gas turbine cycle. These reasons have made the installation of the bottom cycle to form a combined cycle arrangement attractive (Boyce, 2012; Saghafifar and Gadalla, 2016; Zohuri and McDaniel, 2017).

The gas turbine exhaust, normally at a temperature of 500 – 600 ^{0}C, is utilized to generate steam in the HRSG (Allen and Kovacik, 1984; Jaszczur et al.,2020). This steam is then used in the steam turbine to drive a generator. Normally, there is unburnt oxygen in the gas turbine flue gases, which can be utilized for supplementary firing in the boiler to increase steam generation when the gas turbine exhaust temperature is relatively low (Pilavachi, 2000; Diesel and Gas Turbine Worldwide 2004). The exhaust from the HRSG may be used in a process such as paper drying, brewing, heating of the building, sterilizing, or for preheating combustion air for the furnace at a carbon producing facility, this process is known as combined heat and power (CHP) or cogeneration.

Although the characteristic compactness of the gas turbine is sacrificed in binary cycle plants, the efficiency is much higher than is obtainable with the simple cycle that such turbines are now widely used for large – scale electricity generating station (Saravanamuttoo et al 2009, Ighodaro and Aburime 2011). The incorporation of the steam cycle in a simple gas turbine power plant to form a combined cycle power plant is an economically viable and attractive investment (Farrell, 1988; Wicks, 1988; Gadalla and Saghafifar, 2017; Saghafifar and Poullikkas, 2017). An example of a combined cycle schematic diagram is presented in Figure 2.6.

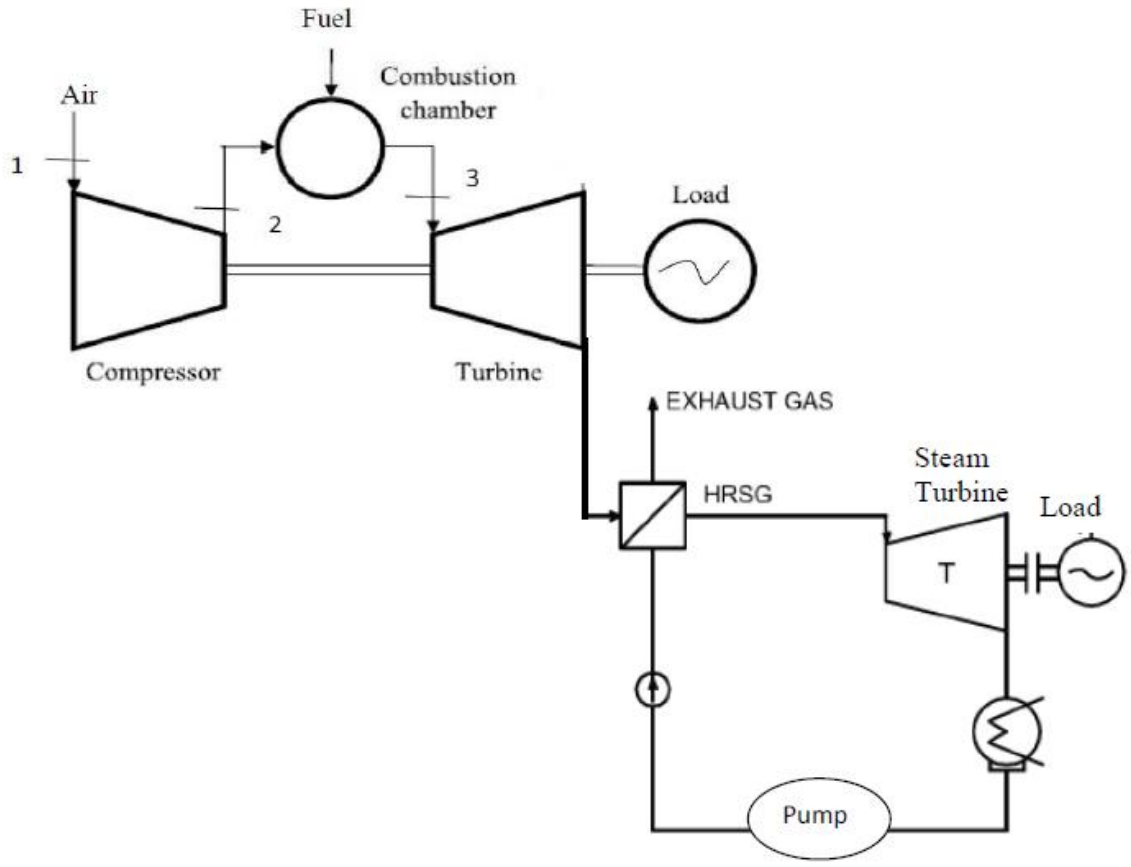

Figure 2.6: A Combined Cycle Power Plant Schematic Diagram

The optimal operation of CHP units has been widely studied and modeled in the thermodynamic field. The proposed thermodynamic model characterizes all the devices in the CHP units in detail to simulate and monitor their operating conditions, and obtains wide applications in the optimal operation research of an individual CHP plant as in (Jarre et al., 2016; Nazar et al., 2016. Liszka and Ziebik, 2009; Kotowicz and Bartela, 2011; Kaviri et al., 2012; Chen, 2017). Based on a detailed thermodynamic model, the operation of CHP units considering the energy performance and pollutant emissions is analyzed in Jarre et al. (2016), and the optimal operating conditions are studied in Nazar et al. (2016) and Liszka and Ziebik (2009), with the effect of key parameters on the operating cost and efficiency investigated in Nazar et al. (2016). Kotowicz and Bartela (2011)

illustrate the optimal features design of CHP units and present a sensitivity analysis, and Kaviri et al. (2012) discussed the multi-objective optimal operation of a CHP plant. A comprehensive introduction to the thermodynamic model of CHP units and the optimal operation is given in Chen (2017). Duran et al. (2013) proposed a method for developing the design of an HRSG, which has three sections (economizer, evaporator and one super heater) by obtaining a small heat transfer area and low-pressure losses.

Pooneh (2012) carried out performance prediction and integration of a gas turbine with heat recovery steam generator (HRSG). The study considered the single, dual and triple pressure HRSG to extract maximum heat energy from flue gas to steam for the combined cycle. The finding from the work revealed that dual pressure HRSG was selected based on higher combined cycle efficiency. Valdes et al. (2003) presented a generic algorithm optimization method of a single and triple pressure HRSG. Attala et al. (2001) described a definition of production cost objective function for combined cycles as well.

Aminov et al. (2016) analyzed the fossil fuel savings and CO_2 and NOx emission reduction of a conventional power plant using a Combined Cycle Gas Turbine (CCGT) technology. The modified plant consists of a 300MW gas turbine (GT), HRSG and a 160MW existing steam turbine (ST). The outcomes from the analysis revealed that the efficiency of the conventional cycle of 34.5% was increased to 58.28% in the modified plant as well as an annual reduction of 1760.18t NOx/annum and 981 ktCO_2/annum.

Mohammadi et al. (2018) carried out thermo – economic analysis of a modified gas turbine power plant with an air bottoming combined cycle. The study considered eight various hybrid systems integration for recovering heat from a gas turbine with air bottoming cycle to generate power as

well as for heating and cooling purposes. The results achieved from the study showed that the utilization of waste heat using their proposed model was cost-effective and proposed it for integration for residential and industrial systems applications.

Colmenar-Santosa et al. (2018) carried out a study on technological improvement in energy efficiency and sustainability in an existing Combined Cycle Gas Turbine (CCGT) power plant. The study employed computer simulation to calculate efficiency and emission using data from the existing CCGT power plant. The work also looked at triple – pressure steam reheated combined cycle (CCC3PR) with 400MW of net power by integrating a regenerator and 50MW renewable solar energy sources. Results obtained from the study showed 2.25% to 3.29% increase was achieved from integrating the regenerator and solar hybridization model. In addition, a 6.25% to 9.45% reduction in gas consumption, which led to a reduction in emission by 26,167 t/year was also obtained. The study concluded that an increase in performance, efficiency, and reduction in emission by integrating a regenerator with solar hybridization showed that the incorporated model was successful and interesting.

Janusz Kotowicz and Brzeczek (2018) carried out "a comprehensive thermodynamic analysis of various gas turbines improvements in a modern combined cycle". The paper analyzed the sequential combustion, closed steam cooling, closed air cooling, open-air cooling integrated with the combined cycle. The integrated model improved the net electrical efficiency to 0.63 and 0.65 as reported in their work.

Chen et al. (2020) proposed a novel CHP model employing the heat exchange process in HRSG and the economic analysis showed that it is an attractive investment.

From the combined cycles research works considered using HRSG, they have shown that the combined cycle efficiency is higher than the simple gas turbine efficiency. The integration of HRSGs were economically and environmentally viable. Various researchers that studied the various levels of HRSG pressure considered one factor such as efficiency in selecting their best choice. This study intends to use more than one criterion such as efficiency, payback period and reduction in CO_2 emission in selecting the best HRSG option.

2.3.4 Turbine Inlet Temperature (TIT)

Within the limits prescribed by the metallurgical conditions of turbine blades, a rise in the turbine inlet temperature considerably affects the life and performance of the turbine units with regards to its power output and consequent thermal efficiency, its exergetic efficiency, and the exergy destruction. The life span of the turbine blades is greatly dependent on the TIT. Ebadi and Gorgi-Bandpy (2005) studied the effects of increased turbine inlet temperatures on the exergetic efficiency and exergy destruction of gas turbine plants. While the increase in exergetic efficiency was not very significant for a 120% increase in TIT, the exergy destruction was noticed to decrease by about 23% with the same increase in TIT. El Hadik (1990) also stated that the TIT value depends on the ratio of fuel to air and material specification used. Mishra et al. (2020) also studied the variation of blade cooling mass fraction with TIT and mentioned that the TIT is constrained by the materials used for making the blade. Soltani et al. (2013) concluded in their paper that the increase in TIT led to increases in energy and exergy efficiencies increase, and the reduction in flow rate of air.

Having highlighted above the advantages and effects of TIT, the monitoring and regulation of TIT become indispensable. Effective monitoring and regulation of TIT will protect the life of the units

since it will ensure that the blade's metallurgical limits are not exceeded and enhance both the gas turbine unit's thermal and exergetic efficiencies while reducing the amount of exergy destroyed.

Previous research works had shown that increasing TIT will improve gas turbine power plant performance. This improvement is limited by the metallurgical property of the blade material which cannot be changed after installation. It may not be encouraged for installed power plants because of this challenge. Thus, it was not considered for this study.

2.4 Energy Analysis

The traditional way of evaluating energy utilization in an operation concerning chemical and physical processing of materials and conversion and/or transfer of energy is referred to as energy analysis. It typically involves the application of the First Law of Thermodynamics (FLT) in evaluating energy balances and efficiencies. Energy conversion and losses from inefficiencies can be determined by employing energy balance, and also used for waste reduction through the heat recovery process.

Presently, energy analysis of power and heat cycles is the frequent method used in assessing thermal systems such as electrical efficiency and fuel utilization. The energy analysis has been developed to as well - established thermal evaluation tool since the last century (Coplan, 2005; Cengel and Boles; 2010). Energy analysis has also been utilized in analyzing microturbine performance (Gimelli and Sannino, 2018).

Energy analysis is established on the principle of continuity equations and together with the FLT for each component and the total plant; it has become a powerful analytical method. (Jassim et al.,2009; Abam and Moses,2011; Angelis-Dimakis et al., 2011). The main goal of energy analysis

is to determine the losses involved in energy conversion and optimizing the thermal efficiency of a system.

The power output, efficiency, work ratio, specific consumption (SFC), and heat rate (HR) are used to qualify the performance of gas turbine power plants. These parameters are determined by utilizing the energy analysis method. Many parameters influence the performance of power plants fired by natural gas such as compressor inlet temperature, compressor pressure ratio, turbine inlet temperature (TIT), etc. (Mahmood and Mahdi, 2009; Rahman et al., 2010). De Sa and Al Zubaidy (2011) studied the effects of ambient pressure, ambient temperature along with flue gas temperature on the performance of a gas turbine power plant. The outcomes obtained from the work revealed that as the ambient air temperature increases, there was a noticeable drop in power output. The paper further states that when the air intake temperature was increased from ISO condition of 15 ^{0}C to 30 ^{0}C, a 10% reduction in net power output was observed (Boonmasa et al., 2006). This analysis has shown that study of ambient air temperature changes with gas turbine power plant performance can be undertaken in locations where the temperature changes from 22 to 35 ^{0}C all over the year like Azura Edo Power Plant Location.

In the application of the energy analysis method to determine the performance of various gas turbine power plants. Pattanayak, (2015); Ibrahim et al., (2017); Rahman et al. (2011); Kurt et al. (2009); Memon et al. (2013); Polyzakis et al (2008); Sahu et al. (2017) have studied the performance of various open simple gas turbine cycle using energy analysis method. Bolatturk et al. (2007); Ahmadi et al. (2011); Barzegar Avval et al. (2011) have used the analysis to evaluate the outcome of the gas turbine with regenerative cycles. The performance of gas turbine cycles with intercooling and reheating configuration has also been studied using the energy balance method by Kayadelen and Ust (2017). The energy analysis was applied in carrying out

performance evaluation of cogeneration and CHP plants by Karaali and Ztrk (2015) and Ahmadi and Dincer (2010) respectively. This method of analysis has been used to evaluate performance improvement of efficiency in a gas turbine with integration such as solid oxide fuel cells (Haseli et al.,2008); multigeneration systems (Ahmadi et al., 2013; Arsalis and Alexandrou, 2014; Mousafarash), hybrid solar gas turbine plants (Olivenza-Len, 2015). Energy analysis has been applied by (Blumberg et al. 2017; Chmielniak et al., 2016; Ersayin and Ozgener, 2015; Gogoi, 2014; Kalina, 2017; Kaviri et al., 2012; Rovira,2005) to carry out performance evaluation in combined cycle power plants. Many research works have been done using energy analysis to assess the performance of gas turbines cycles and with various modifications, but these few are mentioned to ascertain its wide application in energy systems.

The power output, efficiency, and other output parameters for the gas turbine module can be calculated using data from its operating conditions (Horlock, 2003). Nevertheless, in gas turbine power plants, input parameters such as compressor inlet temperature, ambient pressure and relative humidity do not provide optimal performance in some situations. In order to obtain optimal performance of the gas turbine power plant, these input parameters can be controlled. To manage the operating conditions of a system, a parametric study on the effect of input operating conditions on the system is needed (Rahman et al., 2011; Ibrahim, and Mohammed, 2015; Balli, 2017).

The rise in natural gas utilization for generating power and an increase in energy supply costs have made researchers and manufacturers looking for systems with higher efficiency. This situation has resulted to carrying out some studies like the effect of ambient air temperature on the rate of irreversibility and the overall efficiency of the thermal power plant in Turkey by using energy analysis (Kopac and Hilalci,2007; Ehyaei and Mozafari, 2010).

Lebele-Alawa and Jo – Appah (2015) carried out a "thermodynamic performance analysis of a gas turbine in an equatorial rain forest of Southern Nigeria". The data used were collected from the plant's Mark IV speedtronics system and logbook. In their analysis, thermodynamic relations and equations were used to evaluate the gas turbine performance such as net power output, thermal efficiency, specific fuel consumption, heat rate, and compressor work by varying the operating parameters such as ambient air temperature, exit temperature of the compressor, TIT, flue gas temperature and fuel mass flow rate. The outcomes got revealed that the net power output and thermal efficiency decreased by 1.37% and 1.49% respectively; and the compressor work, SFC and HR increased by 0.3%, 2.17% and 2.16% respectively as the ambient air temperature was increased by 1^0C. They concluded in their work that the enormous power drop observed was as a result of the impact of site ambient data rather than design parameters.

Ibrahim et al. (2017) undertook the energy analysis of a gas turbine power plant to evaluate its thermal performance. The findings from the work revealed that the compressor inlet temperature affected the power plant adversely. The paper suggested that the compressor inlet air temperature should be lowered, the combustion chamber should be modified to have a better air-fuel ratio and the gas turbine capacity should be increased to allow high inlet temperature in order to enhance the power plant efficiency.

Ankit et al. (2017) undertook the thermodynamic analysis of an open cycle gas turbine power plant. The impact of functional parameters such as relative humidity, ambient temperature, the pressure ratio of the compressor, isentropic efficiencies of compressor and turbine and TIT on power output, thermal efficiency and heat rate of the gas turbine power plant were considered. The outcomes achieved from the study showed that the pressure ratio of the compressor, ambient temperature, air to fuel ratio, the compressor, and turbine isentropic efficiencies have a strong

effect on the power plant thermal efficiencies. Furthermore, a rise in ambient air temperature and air-fuel ratio led to a reduction in power output and thermal efficiency and an increase in heat rate and SFC of the power plant.

Carneiro and Gomes (2019) evaluated the performance of hybrid waste – to - energy power plants in Bilbao using energy, exergy, environmental and economic analyses. The result of their case study, namely plant power output, thermal efficiency, ecological efficiency, thermal waste input and levelized cost of electricity (LCOE) generation were 107MWe, 36%, 89%,155MWt, and US$ 64 – 89 per MWh respectively. The results obtained showed that the investment in this technology was very attractive. The findings from the study also showed that hybrid waste – to – energy power plants have good potential in the energy conversion system.

The study of evaluating recuperative Brayton cycle with various models such as reheating hybrid and intercooling stages with solar power using pressurized air receiver from the solar tower was undertaken by Mohammadi et al. (2019) using energy analysis. Results obtained in their work revealed that the integration of four reheating and intercooling stages had the highest efficiency among other models and the least LCOE of $80/MWh. The work also revealed the aforementioned model increased the Brayton cycle thermal efficiency from 32% to 53.6%.

Khan and Tlili (2019) used a new method for improving gas turbine performance. Energy analysis was employed as thermodynamic tools for the proposed model, which included a combined cycle, regenerative gas turbine cycle, and was compared with the simple gas turbine cycle. The outcomes of the study revealed that both thermal efficiency and net power output were increased using the same amount of fuel rate compared to the simple gas turbine cycle.

Delgado-Torres (2018) studied the effect of an ideal gas model with temperature-independent heat capacities on thermodynamic and performance analysis of open-cycle gas turbines. The paper stated that the use of perfect gas assumption in open cycle gas turbine energy analysis may result in increasing the uncertainty in the outcome parameters. The research also reported that the increase (amplification) of uncertainty observed relies on the technique utilized to evaluate the heat capacities and which affected the performance of output parameters variously. It was also reported in the paper that for compressor pressure ratios between 5:1 and 40:1 and the turbine inlet temperature between 1200K and 1800K, the maximum relative errors occurring in the net specific work output were 4.4% and -19.2% respectively depending on the specific heat capacity at constant pressure values used for fixed compressor inlet air temperature. For the SFC, the maximum relative errors obtained are -19.51% and 3.95% respectively.

Bontempo and Manna (2019) studied advanced gas turbines optimization aimed at improving network done and thermal efficiency by integrating an intercooler, reheat, and intercooler and reheat cycles using energy analysis. These cycles were compared with the simple gas turbine cycle. The results obtained showed that an overall pressure ratio was established when the network done and thermal efficiency was maximized for the three-model cycles. The maximized value of network done and thermal efficiency when increasing the overall pressure ratio for simple, intercooled, reheat, and intercooled and reheat obtained were 8.550 and 18.26; 14.95 and 25.039; 20.846 and 39.984; and 73.109 and 73.109 respectively. The work also reported that the various model cycle maximized network done was doubled and thermal efficiency improved by 24.966% compared to the simple cycle.

Simon et al. (2013) explained in their report that actual outcomes may differ depending on local site conditions. These analyses are important for electrical power generating utility managers for

making effort to manage and enhance performance like efficiency, specific fuel consumption (SFC), and heat rate (HR) of their facilities. So, the energy analysis will be studied to determine the performance of Azura Edo Power Plant which has not been previously undertaken under the period of this study.

2.5 Exergy Analysis

The limitation of the FLT is overcome by using the exergy analysis method because its idea is founded on both the FLT and the Second Law of Thermodynamics (SLT). The type, location, and cause of energy degradation in a process are indicated by exergy analysis and can thereby, lead to enhancing the operation and technique. Exergy can also quantify thermal energy in a waste stream. The major objective of this method is to ascertain significant exergy efficiencies and the cause of exergy loss and its magnitudes. The use of FLT and SLT to appraise the performance of energy utilization in the thermal system is referred to as exergy analysis. Dincer and Rosen (2007); Cengel and Boles (2010) defined the exergy of a system as "the maximum shaft work that can be obtained by the composite of a system and at a reference environment". Normally, the specific environment is categorized by mentioning its pressure, temperature and chemical composition, which can be in equilibrium, infinite and enclosing other systems. So, exergy is a property of both the reference environment and a system, but not just a thermodynamic property. The characteristics of exergy and the importance of exergy analysis in gas turbine power plants are reported in Dincer and Rosen (2007).

The exergy analysis helps the designer to focus on the maximum practical technical efficiency at the least sensible expense under the predominant specialized, monetary, and legitimate conditions

and representing moral, biological, and extraordinary results and targets. Some alternative process configurations are then proposed (Noh and Hang, 2019).

The increase in the use of exergy analysis and acknowledging its usefulness in designing and optimizing power plant performance have been noted in many research works (Edgerton, 1992; Moran and Sciubba, 1994; Dincer, and Rosen, 2013).

The connection between exergy and financial aspects, especially the compromises that ordinarily happen among efficiency and expenses, has been a significant worry for quite a long time and keeps on being so. Economic techniques dependent on exergy, otherwise called thermoeconomics or exergoeconomics, have advanced and are applied in evaluating power plant performance (Dincer and Rosen, 2003). Likewise, the natural effects and non-sustainability of energy use have happened to huge concerns as of late, and exergy techniques have been utilized as progress endeavors to (i) decrease emission from the environment and extending the lives of assets through improving efficiencies and (ii) evaluate the possible effects of gasses emitted (Connelly and Koshland, 1997; Dincer and Rosen, 1999). Thermoenvironomics or exergoenvironomics consolidates exergy and environmental investigations to decide thermodynamic efficiency and development of ecological effects on power plant parts. The investigation uncovers the relationship between thermodynamic analysis and environmental effects among power plant parts (Buchgeister, 2010).

Ofodu and Abam (2002) utilized the idea of exergy in evaluating the performance of Afam IV Thermal Power Plant (TPP). The Grassman and Sankey diagrams were used to represent the analysis, that provide exergy and energy amounts at specific states in the power plant. The outcomes indicated that the turbine and the exhaust diffuser experienced the highest loss of exergy,

the followed by the combustor. The paper concluded that the losses were a result of unburnt gas, high temperatures and mechanical losses experienced in different components of the power plant.

Fagbenle et al. (2007) undertook the study of a "53 MW_{th} (net) biogas fired integrated gasification steam injected turbine (BIG/STIG)" power plant with 41.5% and 45.0% thermal efficiency for power and cogeneration respectively using the First and Second Laws of Thermodynamic analysis. The analysis indicated that the highest irreversibility, which is about 79% of the overall plant exergy loss occurred in the combustion chamber. Techniques to decrease the huge exergy loss experienced were suggested. The suggestions made were spraying of water in the combustor and preheating of the reactants before entering the combustor, and the utilization of exergy left in the stacks from HRSG.

Rajkumar and Ashok (2009) undertook the identification of losses in a 55 MW Thermal Power Plant (TPP) at an output of 40MW and 55 MW respectively using energy and exergy analyses. The exergy destruction that occurred in the boiler was above 57.822%. The paper stated that the overall plant efficiency based on first and second laws ranged from 24.208% to 25.015% and 19.938% to 22.208% respectively. Additionally, the study presumed that exergy evaluation is a genuine standard for estimating any thermal systems performance.

Balkrishna (2009) analyzed the energy and exergy performance of a blast furnace gas-fired steam power plant. The outcomes obtained from the energy analysis revealed that the highest energy loss occurred in the condenser with 64% and trailed by the boiler with 19%. The boiler has the highest exergy destruction efficiency of 75%, followed by the steam turbine with 11%, and the least occurred in the condenser with 8%. It was reasoned in the paper that the majority of the power

plant exergy destruction occurred in the boiler and it was as a result of high irreversibility that took place in the boiler during the combustion process.

Aljundi (2009) carried out the performance evaluation of the Al-Hussein power plant in Jordan using energy and exergy balance methods. The use of component-wise modelling was applied in assessing the complete energy degradation and loss of exergy for the power plant performance. The outcome of the analysis indicated that highest degradation of energy took place in the condenser (134MW), whereas the least took place in the boiler (13MW). The highest exergy destruction was discovered in the boiler (77%), next was the boiler (13%), and the least was the condenser (9%). Thus, the boiler has the highest source of irreversibilities in the power plant, which was due to the combustion process that occurred in it. The work suggested that the boiler exergy destruction can be lowered by preheating the air before combustion and decreasing the ratio of air to fuel.

Ganapathy et al. (2009) carried out an exergy study on an existing 50 MWe unit of steam power plant fired by lignite, to evaluate the power plant energy and exergy efficiencies. The outcomes indicated that the highest energy loss of 39% took place in the condenser, while the highest exergy loss of 42.73% took place in the combustion chamber.

Abam and Moses (2011) undertook the exergy analysis performance of a 33 MW gas turbine power plant with the aid of computer simulation. The outcome from the study indicated that the highest and the lowest quantity of exergy destruction took place in the combustor and the gas turbine respectively.

The exergy study of a 240 MW_{el} TPP to be fired by ten various types of Turkish lignite was carried out by Ehsana and Yilmazoglub (2011). The mass and energy conservation principles with exergy

destruction of an open steady-state system were used to evaluate the exergy destruction of each part. The study indicated that the net energy efficiency and exergy efficiency obtained for the power plant were 37.16% and 34.84% respectively. Also, the evaluation of the power plant performance showed that the 299.10MW was obtained as the largest exergy destruction found in the boiler, which accounts for 83.29% of the whole plant exergy destruction.

Ighodaro and Aburime (2011) undertook an exergy evaluation of Delta IV Power Station, Ughelli in Nigeria. The analysis utilized the First and Second Laws of Thermodynamics. In each of the components, the mass and energy conservation principles were applied. The highest exergy efficiency of 95.4% was obtained in the turbine and 45.7% for the overall plant. The largest exergy destruction efficiency of 56% occurred in the combustor and 58.5% occurred in the whole plant.

Exergy analysis of a steam cycle with twofold reheat and turbine extraction was done by Rashidi et al. (2014). Three high-pressure and three low-pressure heaters with deaerator were used in this analysis. The outcome of the investigation indicated that the largest exergy losses took place in the boiler and the least occurred in the turbine. The outcomes likewise revealed that as the pressure of the condenser rises, the overall thermal and second law efficiencies reduce for fixed boiler exit temperature. Besides, for increased boiler temperature the overall thermal and second law efficiencies tend to increase at any given pressure. In the appraisal of existing thermal power plants, component exergy destruction obtained is an indication of the thermodynamic inefficiency in the component, which give a chance on how to lower the cost of investment, and the effect of the environment related with each component and the total system. Hence, the paper concluded that it is worth considering the appraisal of environmental effects and economics of the existing thermal power plant from an exergy analysis perspective.

Seyyedi et al. (2011) evaluated the "exergy analysis of GT cycles with air preheat". In this analysis, the impact of air preheater (APH) on exergy and economic enhancements in the thermodynamic cycles was researched. The outcome from the paper indicated that the presence of APH improved the cycle exergy efficiency and environmental effects cost stream rate, though it lowered the overall cost stream rate.

Kumari (2015) compared the impact of different cycle operating parameters on the thermodynamic performance of a simple gas turbine and gas turbine integrated with intercooled cycles. The work stated that the exergy efficiency of the simple gas turbine cycle is less than the intercooled gas turbine cycle. Also, the paper mentioned that the simple gas turbine cycle has higher total plant exergy destruction than the intercooled gas turbine cycle. The assessment from the research showed that intercooled gas turbine cycle performed better than the basic gas turbine cycle.

Awaludin et al. (2016) carried out an exergy study of the gas turbine power plant of 20MW in Pekanbaru – Indonesia using data from the power plant logbooks. The FLT and SLT, along with the conservations of mass and energy principles were applied to each component. From the results obtained the largest exergy destruction occurred in the combustor up to 71.03% or 21.98MW, while, the lowest exergy destruction took place in the compressor at 12.33% or 3.15MW. Furthermore, the gas turbine power plant efficiency was 33.77% using the First Law of Thermodynamics and was 32.25% using the Second Law of Thermodynamics. They compared the results of their work with other research works and reported that generally, their results agreed with those of other authors. They concluded that irreversibility occurred because there is a huge temperature difference between the combustion chamber and the working fluid.

Otunuya and Emeka (2017) used Non – Dimensional Sorting Genetic Algorithm (NSGA) to carry out energy and exergy analyses of a 100MW Delta IV Ughelli Gas Turbine Power Plant Unit. Operating variables such as compressor isentropic efficiency, compressor pressure ratio, TIT, isentropic efficiency of turbine, air and fuel mass flow rates were varied and while ambient pressure and temperature were held constant at 1.013bar and 303K respectively. The results obtained from the study showed that thermal efficiency increases as compressor pressure ratio increases and reduction in exergy destruction were observed as compressor isentropic efficiency increases. The work also reported that increased compressor isentropic efficiency and turbine inlet temperature played very important roles in exergy destruction reduction in the combustor and fuel consumption reduction. In addition, the work stated that the decrease in mass flow rates of air and fuel also influenced the reduction of total plant exergy destruction.

Kumar et al. (2017) did a comprehensive review of energy, exergy, exergoeconomic and economic (4E) study of thermal power plants. The work concluded that for the steam cycle, the condenser possesses the highest energy loss, followed by the boiler. The largest exergy destruction took place in the boiler. The boiler and steam turbine have the highest exergy cost compared to the other components. The paper concluded that from exergy analysis studies, the combustion chamber was the major source of exergy destruction and the highest ineffective component in GT and combined cycle power plants.

Almansoori and Dadachi (2018) simulated the performance of the Natural Gas Combined Cycle (NGCC) Power Plant generating 620MW of electrical power using the ASPEN HYSYS V9.0 commercial software and the Soave – Redich – Kweng (SRK) equation of state. The authors applied exergy–based analysis to determine the exergy efficiency and environmental impacts under normal situations. The results obtained showed that the major source of exergy destruction

was from combustor with 75.65%. Conversely, the lowest exergy destruction efficiency of 5.63% and the highest exergy efficiency of 94.37% took place in the HRSG. Also, the exergy efficiency of the total plant is 53.28%. The comparative difference of exergy-related environmental effect was used as a performance indicator for each of the power plant components and environmental effect for generating electrical power also to assess the complete power plant. The outcomes of the research indicated that the combustion chamber and the HRSG have the largest and lowest environmental impacts of 52.19% and 5.96% respectively. The environmental effect in terms of kWh of electricity generated was 34.26 mPts/kWh based on exergy destruction and 34.42 mPts/kWh based on exergy loss and destruction.

Ahmadi et al. (2018) undertook a comprehensive review of the thermodynamic and economic study of thermal power plant performances. Findings from the review showed that in GT and combined cycle power plants fired by natural gas, the major location of exergy destruction is the combustion chamber. The study suggested that performance can be enhanced in various ways and the degree of saving can be increased by operating the power plant with increasing efficiency. This demand can be achieved through the rigorous efforts of the research community in this dominion. It also stated that operating conditions and each component efficiency are factors which affect the performance of modified power plants. In an attempt to improve power plant efficiency, it is essential to discover the components with the least performance and enhance their efficiency.

Kanbur et al. (2017) studied the thermodynamic evaluation of a combined cycle for a small-scale LNG cold utilization. Ambient air temperature varying from 288.15K to 313.15K and the compressor pressure ratio varying from 3 to 4 was used for conducting the parametric studies. The study used thermodynamic analysis to evaluate the rate of power generated and thermal efficiency. The work also compared the performance between the conventional micro-cogeneration and

combined system using the exergy cost analysis. In the study, the rates of power generated, energy and exergy efficiencies increased by 7.8%, 1% and 2.4% respectively at the micro gas turbine real pressure ratio. It was also reported that at pressure ratios of 3, 3.64, or 4, the reductions in emissions of 3.9%, 7.8%, or 8% were observed respectively. It was deduced that at lower pressure ratios, the unit cost estimated for the components of the system showed that the highest unit fuel was obtained in the combined model. Furthermore, the simple system is approximately 25% less than the combined system in terms of levelized product cost at the real pressure ratio.

Shamoushaki and Ehyaei (2018) undertook the exergy, exergoeconomic, and exergoenvironmental analysis of a gas turbine cycle and its improvement by Multi-Objective Particle Swarm Optimizer (MOPSO) calculation. Complete cost rate, exergy efficiency of the cycle, and CO_2 discharge rate were used as objective functions. The plan factors considered were the pressure ratio of the compressor, combustor inlet temperature, turbine inlet temperature, while compressor and gas turbine isentropic efficiencies were considered as design parameters. The impacts of turbine inlet temperature and compressor pressure ratio on thermal efficiency and carbon dioxide discharge were examined. The outcomes from the investigation revealed that as the compressor pressure ratio and turbine inlet temperature increased, the exergy efficiency of the cycle increased. Also, the amount of carbon dioxide emitted was found to decrease as the exergy efficiency of the cycle increases.

Başoğul (2019) used exergy analysis to evaluate the actual operating conditions performance of a geothermal power plant. The outcomes from the study revealed that the equipment exergy destruction contributed to 98% of the geothermal power plant's total environmental impacts. The work then proposed that to mitigate this shortcoming, instead of disposal, operation and maintenance, and construction system changes; enhancement of equipment exergy efficiency

should be considered. Better condenser and pump performance were also proposed to improve the exergy efficiency and environmental impact of the power station.

Nascimento Silva et al. (2019) studied the exergy and CO_2 emission of an advanced gas turbine power plant on an offshore petroleum production platform. The study compared the effect of oxyfuel gas and an amines-based post-combustion carbon capture systems integration to an existing gas turbine cycle in terms of reducing atmospheric CO_2 and increasing exergy efficiency. The outcomes achieved from the work revealed that the oxyfuel gas turbine power plant has a cycle efficiency of 27.01% and a lower specific CO_2 emission of 0.015kgCO_2/toil; the amines-based cogeneration has a cycle efficiency of 54.34% of the advanced configuration.

Wang et al. (2019) undertook the energy, exergy, environmental and exergoeconomic study of a solar-based combined cooling, heating and power (CCHP) gas turbine system. In the cooling load operation, energy and exergy efficiencies results obtained were 83.6% and 24.9% respectively, while for the heating load operation the energy and exergy efficiencies obtained were 66.0% and 25.7% respectively. The work mentioned that the off-design study illustrated that using energy and exergy efficiencies analysis only was not enough to show the input of solar hybridization in the system. Therefore, applying exergoeconomic analysis, considering energy level, the market pricing technique for electrical power exergy costs unit, using hot water for heating operation (or chilled water for cooling operation) and domestic hot water are 2.1, 7.8, and 8.3 times more than the cost of using natural gas fired plant respectively.

The power plant performance can be enhanced by reducing its irreversibility, to achieve this, it is very important to obtain its optimal operating parameters (Ighodaro and Aburime, 2011; Neserian et al., 2016; Khosravi et al., 2014; Otunuya and Emeka, 2017). This makes exergy analysis a

reliable tool in evaluating gas turbine power plant performance. Thus, in order to know the location of these irreversibilities in Azura Edo Power Plant, its exergy analysis, exergy improvement potential, sustainability index and depletion number of the fuel will be examined in this work. No previous study of these parameters for Azura Edo Power Plant was found in the literature so far.

2.6 Environmental Analysis

From a wider impact and policy perspective, GHG emissions are the most significant environmental issue for industries while recognizing that other environmental impacts are potentially significant, especially at the local level. Relevant studies have shown that natural gas combustion mainly emits carbon dioxide, nitrous oxide, and sometimes methane when unburnt. The utilization of fossil fuel for power generation has been indicated to be the main source of carbon dioxide emission, though natural gas combustion has emitted less carbon dioxide than coal (Raghuvanshi et al., 2006; Allam et al., 2013; Mousavi et al., 2017). Memon et al. (2014) stated that this is the reason researchers are interested in exploring various environmental impact mitigation strategies while considering the use of fossil fuel for power generation.

Environmental issues are such a danger that individuals everywhere in the world ought to have a concern. While innovation keeps on at a fast pace, nature has been debased earnestly in past decades. Environmental researchers have categorized carbon dioxide (CO_2) as the most notable anthropogenic ozone-harming substance (Smith et al., 2003; Stangeland, 2007; Dey and Dhal, 2019). It has been rising by 39% (280 ppm to 380 ppm) since the start of the Industrial Revolution (Wright and Boorse, 2011). There is a chance of CO_2 influencing human wellbeing if air with CO_2 of 426 ppm or more is breathed in for quite a while; the body might be quickly affected from 600ppm and above (Robertson, 2006). Carbon dioxide concentration in metropolitan regions is

probably going to be more than 426 ppm as a result of expected increase in population and human exercises; CO_2 causing activities must be reduced in order to avoid the increase of CO_2 concentration in the atmosphere (Mc Pherson, 1998).

Gas turbine power plants generate exhaust heat apart from electricity production. The flue gas emitted to the power plant surroundings contains carbon dioxide and other gases which pollute the air and contribute to GHG. An average carbon dioxide emission intensity or rate for simple open gas turbine has been determined in EIA (1999) as 557gCO_2/kWh. Robert et al. (2020) also mentioned in their paper that the carbon dioxide emission rate varies from 274 to 720gCO2 per kWh, depending on technology and region. For gas turbine power plants fired by natural gas, the amount of carbon dioxide intensity emitted by using the heat and power method is 404 g/kWh (Ong et al, 2011; Schivley et al., 2018; Rahman et al., 2017). Allam et al. (2013); Carapellucci et al. (2016) stated that the majority of the contribution to GHG emission from gas turbine power plants is carbon dioxide. In order to reduce the rate of CO_2 released into the atmosphere from power plants, Owusu and Asumadu-Sarkodie (2016) suggested that the percentage of fossil fuels should be replaced with renewable fuels. Research work on carbon dioxide emission from fuel consumption in Iran was carried out by Lotfalipour et al. (2010); the results reveal that carbon dioxide emission will increase by 2.1 times by 2025.

Saravanamutto et al. (2009) stated in their book that a large amount of excess air is needed in gas turbine combustible engines which lead to considerable amount of oxygen in the exhaust gases. The work, also explained that the exhaust gases of any gas turbine consists mainly of CO_2, H_2O, O_2, and N_2, and the combustion products can be expressed as either gravimetric (by mass) or molar (by volume) composition. With this explanation, CO_2 is the main gas that is harmful to the environment. It is a greenhouse gas that contributes to global warming. So, this makes it necessary

to carry out the study of its emission and also suggest ways to reduce its effects on the immediate gas turbine power plant environment.

The discharge of CO_2 from fossil fuel-fired power plants as reported by Steen (2000) relies upon

i. the measure of electric power produced by petroleum products
ii. the fuel – blend utilized through its carbon content, and
iii. the thermal efficiency of the non-renewable energy source burning plants

Studies have shown that the damaging effects caused by greenhouse gas emissions on the climate were obtained from anthropic activities (Figueroa et al., 2008; IPCC, 2014). The aforementioned fact has spurred government, private companies, and research bodies to look at energy techniques that will help lower the effect of natural gas and oil sectors' environmental impact on the overall budget of carbon dioxide emission (IEA, 2015). The reliance on fossil fuel for power generation will continue because of its extensive infrastructure for fuel production and distribution, and the level of ongoing usage of renewable energy resources.

Carbon dioxide has been said to be the most important greenhouse gas (Brink, 2003). The proceeded utilization of petroleum derivatives to meet most of the world's energy requests is compromised by expanding the centralization of CO_2 in the environment and worry over an Earth-wide temperature boost (Yu et al., 2003; Demirbas et al., 2004). The burning of petroleum derivatives is responsible for 73% of the CO_2 emitted into the atmosphere (Wildenborg and Lokhorst, 2005).

The keen attention to the dangerous global warming problem has expanded enthusiasm for the improvement to lessen GHG emitted into the atmosphere (Lombardi, 2003). The idea that carbon

dioxide is the main GHG gas from the gas turbine power plant is clear from previous research works. This provided initiative to investigate its emission and how to reduce it. In the effort to lower the emission of carbon dioxide into the atmosphere from power plants, as mentioned in (Mach and Mastrandrea,2014; IPCC,2015); recent techniques have focused on the following:

(i) to decrease energy utilization

(ii) to raise the efficiency of energy conservation or usage

(iii) change to fuel with lesser carbon content

(iv) to capture and store CO_2, and

(v) to enhance natural sinks for CO_2.

Lowering fossil fuel utilization for power generation would noticeably decrease the amount of CO_2 emitted, along with lowering the level of pollution gases (Demirbas, 2006). The quest for non – fossil fuels usage will help to lower CO_2 emission; this is gaining attention to resolve the issue concerning global warming as a result of growth in fossil fuel dependence (De Olivera et al.,2005). To decrease the net contribution of GHGs such as CO_2 to the air, natural carbon sequestration has to be studied to ascertain if it can be used as a potential alternative to other forms of carbon capture.

In reality, a well-expanded energy matrix design will help to minimize the problem of carbon dioxide emission (Boait et al., 2015; Zhang et al., 2014). IEA (2017) reported that carbon capture and storage (CCS) techniques have been used to reduce carbon dioxide emission, and this will account for under 10% of the reduction of CO_2 emission by 2040. This makes it necessary to look at other techniques for CO_2 emission reduction to complement the CCS technology. Various CCS techniques have been reported and well explained in Leung et al. (2014); Carranza-Sánchez and Oliveira (2015).

The study on CO_2 emission by Manceralla and Chicco (2009); Nazari et al. (2010); Hendriks et al. (2009) using CO_2 emission factor stated that the emission of CO_2 is on the increase.

Thermoenvironmental and economic investigation of simple and regenerative gas turbine (GT) cycles with regression modelling and optimization were carried out by Memon et al. (2013). Complete modeling and optimization of a simple and regenerative gas turbine were investigated in this study. The outcome of the investigation indicated that when the compressor inlet temperature was reduced and the r_p and TIT were increased, the power output and thermal efficiency increase, while the emission of CO_2 to the atmosphere was reduced. Moreover, the optimization of five objective functions was done to maximize net power output, energy and exergy efficiencies, and minimize emissions of CO_2 and the costs of the cycle. The optimization result obtained shows a compromise between thermoenvironmental benefits and extra expenses. The examination presumed that, from the thermoenvironmental perspective, TIT ought to be chosen as high as could be expected under the circumstances, notwithstanding, this prompts an expansion in the capital expense and levelized cost of electrical power.

Memon et al. (2014) investigated the impacts of significant working parameters on the overall cycle performance and CO_2 emission of the gas turbine cycle model. The paper likewise looks at the impacts of these parameters (compressor inlet temperature, compressor ratio and turbine inlet temperature) on the plant performance. In addition, they developed “multiple polynomial regression models to correlate the response variables and predictor variables”, and operating parameters were optimized. Their results showed that the investigated operating parameters have an important effect on the performance of the cycle and emission of CO_2. The lowest exergy efficiency and largest exergy destruction were obtained in the combustor from the results of their work. They also reported that the regression models developed are good in estimating the response

variables. The optimal values of CIT, TIT, and r_p obtained were 288K, 1600K, and 23.2 respectively for maximum performance.

Oyedepo et al. (2015) studied the CO_2 emission of 11 selected GT power plants using the combustion equation. The study analyzed the variation of CO_2 emission with TIT and exergy efficiency. Findings from the work showed that an increase in the exergetic efficiency of the GT plants resulted in a reduction in CO_2 emission.

Kanbur et al. (2017) also used the combustion equation method to analyze the CO_2 emission of a combined cycle for a small-scale LNG Cold plant. The findings from the environmental analysis revealed that the combined cycle system had a lower CO_2 emission rate than the single system because it produced a higher power rate while both systems emitted the same amount of CO_2 to the atmosphere.

Babaelahi et al. (2019) assessed the environmental and economic viewpoints, and streamlining of another two-venture solar-powered gas turbine cycle by applying a new multi-step Emergo-Exergo-Economic and Emergo-Exergo-Environmental methodologies. The outcomes from the analysis showed that the exergetic, money-related and environmental performance of the cycle can be upgraded genuinely by changing the choice factors.

Karapekmez and Dincer (2020) analyzed the environmental impacts and efficiency of the solar-assisted combined cycle with various fuels. The results obtained revealed that sawdust and wet wood have the least environmental impacts with 11.37kg/s and 11.78kg/s of CO_2 emission respectively, which can be the rewarding alternative to natural gas.

Robert et al. (2020) stated in their research work that to maintain global warming at a temperature below 2 ^{0}C, an ambitious way of mitigating climate change problems from power facilities needs to be studied by continuous monitoring of carbon dioxide from the facilities. Though Azura Edo is a new power plant, with these suggestions, it is necessary to monitor its CO_2 emission by estimating the amount of CO_2 emitted periodically. This study has not been undertaken previously. Also, the SGT5 – 2000E gas turbine model has a good record regarding low NOx and CO emissions. A major constituent of the exhaust gas from the Azura Edo Power Plant is CO_2. Thus, this work intends to evaluate the quantity of CO_2 emitted from the power plant.

2.7 Modelling and Simulation of Power Plant

Numerical modelling and simulations help to determine the efficiency and correctness od a design before the construction of the actual system. The gas turbine power plant to be investigated requires a detailed mathematical model in order to accurately assess the performances of power plants in ambient temperature variation and part load function A good number of modelling tools have been utilized for power plant simulations and analysis. From various programming software accessible, for example, APROS, Aspen, Autodynamics, HYSYS, gProms, SIMODIS, PowerSim, MMS, and ProTRAX; the EBSILON Professional package was chosen. This product package considers far-reaching power plant process cycle usage for steady-state and semi-dynamic simulations and plant parameters advancement measures. Albeit, physical equations depicting all the components of the EBSILON Professional programming condition are valid for steady-state estimation and the dynamic impacts by carrying out the arrangement of reenactments on a little timescale. It is acknowledged by having a blend of “time Series” and “ebsScript” included at the programming level to make and simulate such semi-dynamic systems

EBSILON Professional 14 and ASPEN Software are both good simulating programming software with sequential modular. The features of EBSILON Professional 14 are medium library, fast convergence speed, high accuracy and medium in learning cost, while ASPEN features are large library, medium convergence speed, very high accuracy and very high learning cost. EBSILON Professional 14 are specifically developed for power plant application, while ASPEN software focus on process, oil refining and chemical industries applications. Based on their different applications mentioned, and this study involves thermodynamic and environmental modelling of a gas turbine power plant, EBSILON Professional is preferable for this study.

2.8 Model and Simulation with Ebsilon Professional

EBSILON Professional is one of the most utilized energy and mass balance computation programming tool in the European Countries that speak the German language. It shows high convergence stability, high computational speed, and is adjusted to Microsoft environments. EBSILON has all the features needed for the investigation of gas turbine power plant, which is applicable for this study.

OEM-GTLib, created by STEAG – Energy Service GmbH in cooperation with VTU Energy GmbH, contains countless gas turbine models. These are changed under genuine performance conduct and depend on legitimate producer information. Accordingly, one can choose the ideal gas turbine for one's capacity plant to study. The library contains models of gas turbines from Alstom, Siemens, Rolls Royce, General Electric, Solar Turbines, Centrax, and Hitachi.

Ebsilon software has been used for various research works in power plant analysis by Miguez Da Rocha (2010) on the study of retrofitted solar-powered Combined Cycle Power Plant; Jaszczur and Dudek (2019) in the thermodynamics investigation of a gas turbine combined cycle

incorporation with a high-temperature nuclear system; Garcia Sanchez – Cervera (2010); Wojcik and Wang (2018) in steam power plant optimization of energy for an effective process of a post-combustion of CO_2 capture plant; and Wallentinen (2016) in the analysis of a concentrated solar power gas turbine with thermal storage. Zyrkowski and Zymelka (2019) analyzed the behaviour of 2 225MW coal units by utilizing Ebsilon Professional Software. The model results were validated using test results from the power plant. Matjanov (2020) also used the software in modelling and analysis of the Tashkent CHP enhanced with an air inlet cooling system. Design data were used to validate their models in their various researches. There are many studies carried out using Ebsilon software, but these few are mentioned to ascertain that Ebsilon software has been previously used for research work. It has been employed as an accurate tool, precise and powerful tool to support the design, modification, retrofitting of power plants and further development of power plant (Wallentinsen, 2016; Olausson, 2017; Gacitua et al.,2018).

2.9 Modeling and Simulation of Gas Turbine Utilizing MATLAB 2017

MATLAB 2017 is a software that has a mathematical computation environment with a multi-paradigm. MathWorks developed the programming language for MATLAB 2017, which is exclusive to them (MATLAB, 2017). It is applied in manipulating the matrix, algorithms implementation, data and functions plotting, user interface creation, and interfacing with programming languages such as JAVA, PYTHON, FORTRAN, C++ and C. Though, this software was mainly designed for numerical computation and alternative toolbox for MuPAD symbolic engine utilization, it also has the abilities for symbolic computation. MATLAB 2017 possesses an extra package known as Simulink; which comprises graphical multi-domain simulation and model-based for dynamic and embedded systems.

Dispatching of virtual, inheritance, classes, packages, pass-by-reference, and pass-by-value semantics is object-oriented programming supported by MATLAB 2017. Nonetheless, languages used for conventions of calling and syntax in MATLAB 2017 are significantly not the same as other languages. MATLAB 2017 has two classes namely reference classes and value class. A reference class handles super classes while a value class handles non-super classes.

Oyedepo et al. (2015) successfully used MATLAB software to carry out the thermodynamic and environmental analysis of eleven selected gas turbine power plants in Nigeria. In the work, actual operating parameters were used to validate the outcomes of the study by applying error analysis. Kanbur et ai. (2017) also utilized MATLAB successfully to provide the numerical solution in the thermodynamic and environmental analyses of a combined cycle for a small - scale LNG cold utilization. Ankit et al. (2017) developed MATLAB code from the mathematical formulation that was utilized in carrying out the gas turbine power plant performance.

Colera et al. (2019) carried out a numerical scheme for the steady-state thermodynamic analysis of gas turbine engines. A simulator was formulated that can be applied in MATLAB by the authors using mathematical techniques such as sparse solver and quasi-Netwon methods. The study reported that good results were obtained when the formulated simulator was applied to predict the performance of a real gas turbine power plant. Chen et al. (2020) used MATLAB to carry out economic dispatch analysis of combined heat power plant.

The research works reviewed showed that MATLAB is a good software for mathematical calculation and plotting of graphs. This study intends to deploy it for the thermodynamic and environmental analyses computation because of its “hand off “calculation ability.

2.10 Summary of Previous works Reviewed

After an extensive literature review of energy, exergy, and environmental analyses of gas turbine power plants, the following are the highlights of pertinent findings:

(i) Energy and exergy analyses are reliable methods that can be used in the design, optimization, performance appraisal of gas turbine power plants, showed that their performances are affected by ambient temperature, pressure ratio and turbine inlet temperature.

(ii) Exergy analysis is used to determine the exergy destruction in various components in gas turbine power plants; the combustion chamber has been identified as the major source of exergy destruction in the plant.

(iii) The results from the review also identified that extensive research should focus on the combustion and ambient temperature variation on the various appraisal methods.

(iv) The review also indicated that CO_2 is a major pollutant constituent of the exhaust gases to the environment. The emission of CO_2 from gas turbine power plants should be examined because of its effect on global warming.

(v) The review also showed that thermodynamic and environmental analyses of gas turbine power plants vary from location to location for the same/different gas power plant models because the various results obtained were not the same.

2.11 Research Gap

Based on the findings from the literature review, the following research gap were identified.

(i) The thermodynamic and environmental performance evaluation of the Azura Edo Power Plant has not been previously carried out.

(ii) The preliminary study to enhance the performance of the Azura Edo Power Plant by modified cycle such as combined cycle has not been previously undertaken.

(iii) The effect of incorporating inlet cooling system study has not been studied previously for Azura Edo Powe Plant.

(iv) The study of how the variation of ambient air temperature affect the performance of Azura Edo Power Plant which is located in a region where the annual temperature changes from 22 ^{0}C to 35 ^{0}C has not been found in the in literature so far.

(v) Studies have shown that thermal efficiency, specific fuel consumption and heat rate are important indices for electrical power generating utility managers for assessing their facilities and these performances evaluation have not been carried out previously for Azura Edo Power Plant.

(vi) In order to know the location of irreversibility in Azura Edo Power Plant its exergy analysis, exergy improvement potential, sustainability index, and depletion number of the fuel are intended to be examined in this work. No previous study of these parameters for Azura Edo Power Plant was found the literature so far.

Thus, the study is set out to determine how the local weather affects the performance of the aforementioned plant for design and off-design conditions, integration of inlet air cooling and combined models, which differs from similar past studies.

CHAPTER THREE

METHODOLOGY

3.1 General Overview of Azura Edo Power Plant

The Azura Edo Independent Power Plant is located in Ihovbor Community, Benin City Edo State in the south-south geo-political zone of Nigeria. The power plant has an installed generating capacity of 459 MW (3 X 153MW). The power plant is fired by natural gas, which is delivered through Nigeria Gas Company (NGC) pipeline networks, allied with Seplat Nigeria Limited. It consists of 3 units of SGT5 – 2000E; namely GT11, GT12 and GT13. The power plant is situated on latitude 6^{0} 24' 45.49 N and longitude 5^{0} 40' 45. 38 E, northeastern outskirts of Benin City, Edo State, the southern part of Nigeria. The power plant location was chosen because the site is close to the Benin Transmission Substation for easy evacuation of power generated, the Escarvos Lagos Pipeline for easy natural gas supply to the power plant, has good road access, is in a relatively peaceful area and within Edo state, as per Azura Power's partnership with the Edo State Government.

The mechanical and electrical works on site were done by Siemens, a German company; while the civil work was carried out by Julius Berger Nigeria Limited. There is an agreement between the Azura Edo Power Plant and Nigerian Bulk Electricity Trading PLC (NBET) for the purchase of generated power. Also, Azura Edo Power Plant has another agreement with Seplat on the gas supply to fire the power plant. The project, whose development started in January 2016 was foreseen to be completed in December 2018. Be that as it may, with the completion of a massive portion of the project, the venture was finished 7 months ahead of time. It has additionally become a leading figure for good health and safety practices, having worked more than 4 million man-hours of work without a solitary lost-time in injury as at the time the main unit was synchronized

to the national electricity network. The first turbine was synchronized to the country's electricity grid on the 20th of December 2017 and went through a battery of tests for more than five weeks. Tests on the next turbine were done toward the end of January 2018, while the tests on the third turbine started in early March 2018. The power station was commissioned at the end of April 2018 and when the power station commenced its full commercial operation. The plant is operated and maintained by PIC Group Inc (a subsidiary of Marubeni) under a five-year operation and maintenance agreement. A typical sample of the SGT5 – 2000 E is shown in Figure 3.1 and the pictorial views are presented in Appendix IV.

The SGT5-2000E model features a single – shaft, single casing design, and two laterally flanged, large volume, a silo-type combustion chamber, a 16 multi-stage compressor, and a four-stage turbine. There is an air-cooled generator attached to the cold (compressor) end. The SGT5-2000E had been previously installed in Nigeria. There are 3 Nos of SGT5 – 2000E gas turbine each was installed in the Geregu I (414MW) and Geregu II (434MW) Power Plants; Two gas turbines of the same model are installed in the power block Afam V (276MW).

SGT5 – 2000E is a unique gas turbine model because the generator is coupled to the shaft at the compressor side. This configuration allows easy modification for the combined Cycle model unlike other models which have their generator coupled on the turbine side. It consists of two silo combustors for efficient burning of fuel and compressed air mixture to minimize NOx and CO emission. The model also has a robust ability to operate at high levels of reliability and even provision of burning liquid and gaseous fuel.

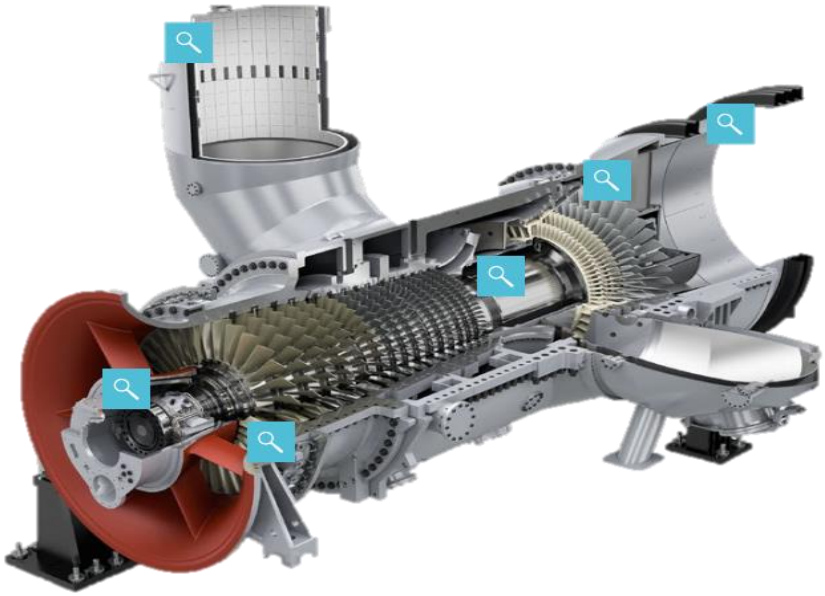

Figure 3.1: A Typical Sample of the SGT5 – 2000 E

3.2 Thermodynamic Operational Principle of Azura Edo Power Plant

The Azura Edo Power Plant operates on the Brayton cycle. The schematic and temperature–specific entropy (T – s) diagrams of Azura Edo Power Plant are illustrated in Figures 3.2 and 3.3 respectively.

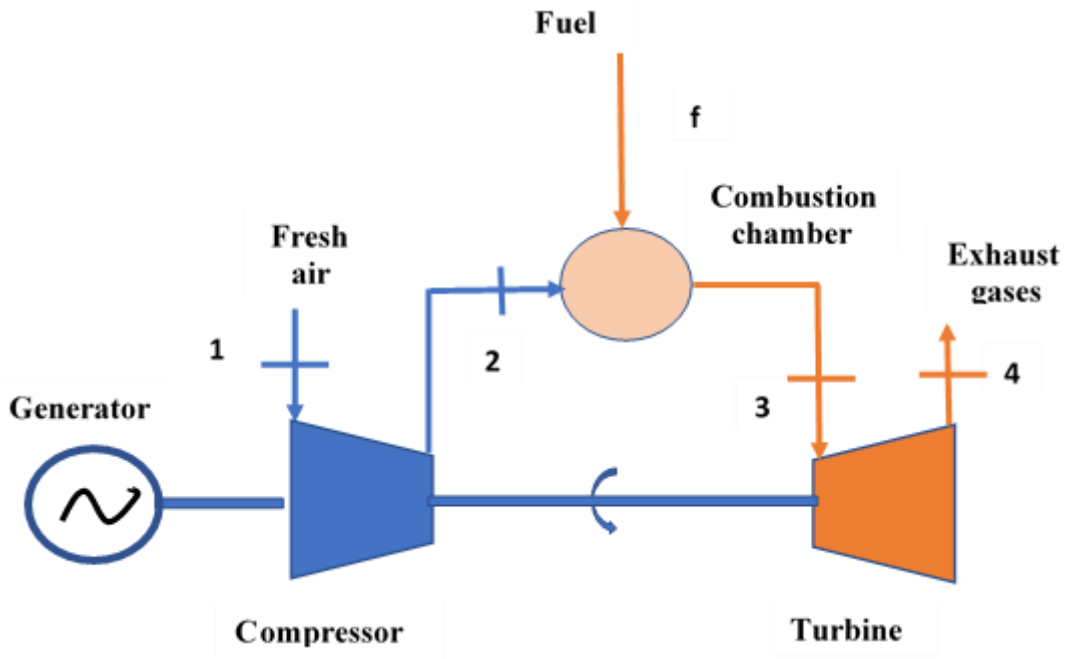

Figure 3.2: A Typical Schematic Diagram of Azura Edo Power Plant

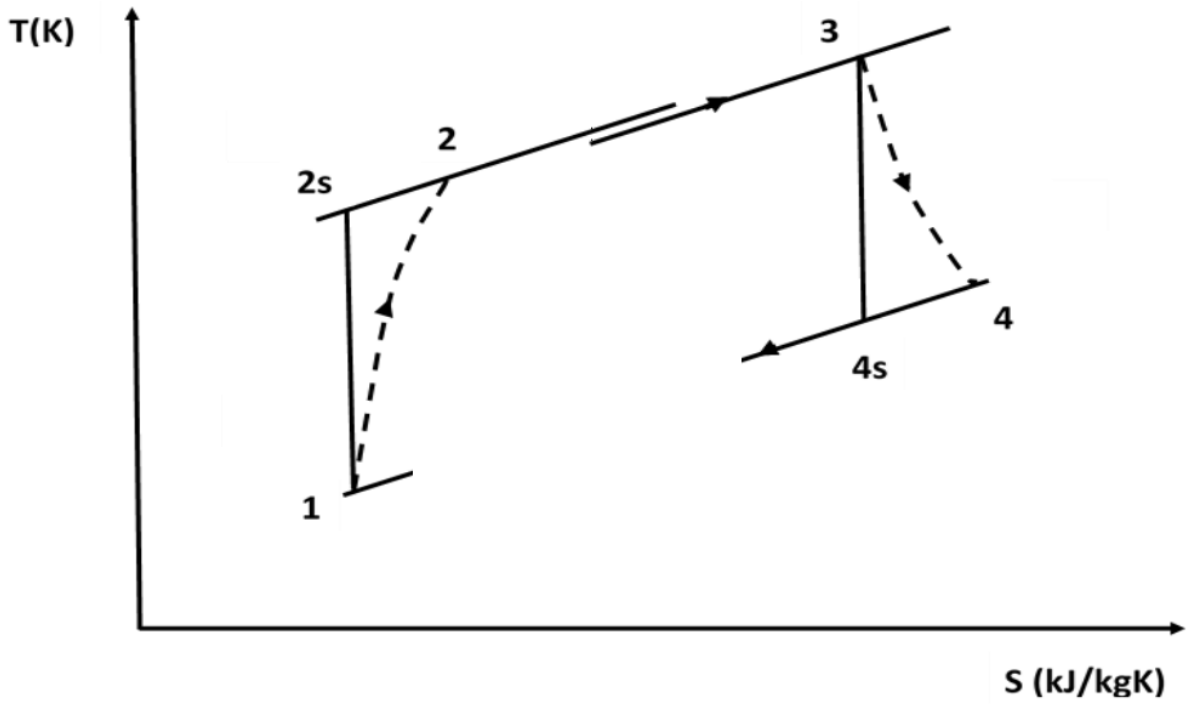

Figure 3.3: A Typical T- s Diagram of Azura Edo Power Plant Cycle

For the initial starting of the power plant, the air compressor (axial flow type) is initially driven by an electric motor until 60% of the turbine shaft speed is achieved. The maximum net thermal

efficiency of the Azura Edo Power plant operating on the open simple cycle will always be less than 40% because 60% of the turbine shaft power is used to drive the air compressor.

At the point when the turbine starting structure is activated, the air intake plenum takes fresh air from the surroundings air, filters it at state 1 and compresses in the 16-stage air compressor. At the 11^{th} stage, the air extraction valve is opened and the variable IGVs are closed during start-up for pulsation protection. The extraction bleeding valve closes automatically at 95% speed of the turbine shaft, which allows the compressed air to enter into the silo combustor annular space at state 2 and then enters liners of the combustor. For appropriate combustion, the compressed air flows into the burning zone through the metering hole in each of the combustor liners.

Fuel is supplied to the liners equally, each stopping at a fuel nozzle. The fuel is introduced into the burning chamber by the nozzles at a steady rate depending on the load and speed required by the gas turbine. The fuel blends in with the compressed air and the mixture is exploded utilizing either of the spark plugs. At the moment when the fuel blend is lighted in one burning chamber; fire is spread through cross-interfacing fire cylinders to all other ignition chambers. At the point when the turbine rotor approximates the working rate, the pressure of the combustion causes the spark plugs to withdraw subsequently eliminating their electrode from the hot zone. It is planned for appropriate dilution and cooling in the combustion chamber.

At state 3, the hot gas flows into a 4-stage turbine after expanding into different progress pieces joined to the aft end of the chamber liners from the combustor. In every turbine nozzle, the hot gas kinetic energy is raised as the drop in pressure occurred in after each row of rotating blades. Part of the burnt gas kinetic energy is transferred into useful work on the rotor of the turbine.

The flue gases, after flowing through the third stage of blades, are coordinated into the fumes hood and diffuser, which contains a progression of rotating vanes to divert the gases from axial flow to radial flow directions with the least fumes hood losses. At state 4 the gases flow into the fumes plenum and are released with the air through the fumes stack.

The turbine uses part of the power generated to drive the air compressor as earlier mentioned and the rest is obtainable for valuable work at the gas turbine output flange, which is coupled to a 3000-rpm generator at the compressor side. The generator will convert the mechanical power to electrical power, which is supplied to the national grid.

3.3 Azura Edo Power Plant Main Components

The relevant data on the three SGT5 – 2000E turbine units are presented in Sections 3.3 – 3.4. The information in this section is obtained from Siemens (2011) and Azura Edo (2017).

3.3.1 General Design Data Operating at Full Load.

Gas turbine model series - SGT5 – 2000E

where S – Siemens, GT – Gas Turbine, 5 – 50 Hz, 2000 – Rating class identifier, E – Efficiency class identifier

Gas turbine application – generator drive

Cycle – simple

Shaft rotation – counterclockwise

Shaft speed - 3000 rpm

Control – SSPA –T3000

3.3.2 Gas Turbine Ratings

Load output – 153 MW

Inlet temperature – 26 ^{0}C

Inlet pressure – 1.013 bar

Exhaust temperature – 541 ^{0}C

3.3.3 Compressor Section

Number of stages – 16

Compressor type – Axial flow, heavy-duty

Casing split – Horizontal flange

Inlet guide vanes – variable

Relative Humidity – 70%

3.3.4 Turbine Section

Number of stages – 4

Casing split – Horizontal

Nozzles (4 stages) – fixed area

3.3.5 Combustion Section

Silo Combustion type

Two large combustors with an annular arrangement

3.3.6 Generator Section

Generators – 3 Nos of SGEN – 100A

Type – Air-cooled

Rated output – 153 MW

Rated speed – 3000 rpm

Rated voltage – 15kV

Frequency – 50 Hz

Power factor – 0.8 lagging

3.4 Design Specification Data

The design data are manufacturer specifications and ratings of all the units. The data for LHV, pressures, pressure ratio, temperatures, volume flow rate, density and isentropic efficiencies were obtained from Siemens (2011) and Azura Edo (2017). The data for specific heat capacities at constant pressure and gas constant of various fluids were obtained from previous works like Ighodaro (2006), initially used for preliminary computation and were found suitable for this study.

Type of fuel – Natural gas

Lower Heating Value (LHV) – 45011 kJ/kg

Air inlet temperature, $T_1 = 26\ ^0C$

Atmospheric pressure, $p_1 = 1.013$ bar

Compressor pressure ratio, $p_2/p_1 = 12{:}1$

Generator output power, $P_{electrical} = 153$ MW

Specific heat capacity of oil, $c_{poil} = 2.001$ kJ/kgK

Specific heat capacity of water, $c_{pw} = 4.182$ kJ/kgK

Specific heat capacity of air $c_{pa} = 1.005$ kJ/kgK

Specific heat capacity of fuel at constant pressure, $c_{pf} = 1.54$ kJ/kgK

Specific heat capacity of exhaust gas, $c_{pg} = 1.148$ kJ/kgK

Gas constant for air $R_a = 0.287$ kJ/kgK

Gas constant for fuel $R_f = 0.451$ kJ/kgK

Gas constant for exhaust gas $R_g = 0.29$ kJ/kgK

Lube oil flow rate $V_{oil} = 80 m^3/h$

Density of lube oil , $\rho_{oil} = 900 kg/m^3$

Cooling water volume flow rate, $V_w = 150\ m^3/h$

Density of cooling water, $\rho_w = 1000\ kg/m^3$

Isentropic efficiency of compressor, $\eta_c = 85\%$

Isentropic efficiency of turbine, $\eta_T = 90\%$

The Edo Azura Power plant guarantee performance data which were obtained from Edo Azura EIA (2013) and Edo Azura (2017) are as follows:

i. plant net electrical power output – 459000 kW (153000 kW per unit)
ii. plant net heat rate – 10528 kJ/kWh
iii. emission of CO_2 – 2,178,000 tonnes/year.

3.5 Software for Modelling and Analysis

In this study, the modelling was done using Ebsilon Professional and the MATLAB software was utilized for the operating data analysis. The description of the Ebsilon and MATLAB softwares, and how they solve the problem when utilized are presented in this section.

3.5.1 Model and Simulation with Ebsilon Professional

EBSILON Professional is one of the tmost utilized energy and mass balance computational programming in the European Countries that speak the German language. It shows high convergence stability, high computation speed, and is adjusted to Microsoft environments. EBSILON has all the highlights needed for this investigation and is the ideal apparatus for this study. This part quickly sums up the principal highlights of this product.

(i) Basic Characteristics

EBSILON is the contraction for "**E**nergy **B**alance and **SI**mulation of the **LO**ad response of power generating or process controlling **N**etwork structures". It is utilized for designing, evaluation and optimization of different types power plant and other thermodynamic processes. It allows the course of action of individual parts, segment gatherings, sub-frameworks and complete

frameworks inside closed or open cycles. Standard segments and programmable parts (EbsScript with client characterized conduct) can be utilized together empowering an exact simulation.

For the estimation, it utilizes a numerical “kernel of EBSILON”, a closed arrangement calculation dependent on a consecutive arrangement technique that exhibits great convergence properties. EBSILON calculates water/steam cycles, processes of combustion, gas turbine cycles and CHP processes. Fluid properties are predefined; steam properties depend on the IF67 tables or the IAPWS-IF97, and air/exhaust gas properties are obtained from c_p-polynomials.

(ii) Working Environment

The principal toolbars are shown on the menu bar. The standard toolbar permits the management of files and other standard functions of windows. Segment bar, for admittance to parts gathered by classifications, for example, turbines, heat exchanger, pumps, and so on. Ebsilon bar, for beginning simulations, error, and validations studies; profile bar, for off-design evaluation, permitting various profiles for various partload cases.

(iii) Object Types

Components and Pipes: Components are the fundamental structure blocks of a cycle, with different channels and outlets, everyone with a particular "fluid type". By altering the distinctive detail esteems, every part changes with the individual case. The components are connected with pipes for simulation.

Controllers: Controllers are segments utilized to accomplish a particular estimation of one parameter in a chosen area of the cycle. A controller looks at the mentioned value (reference value set by the client) and the genuine estimation of one parameter and iterates correcting a second

parameter till the reference value is reached. These are significant segments for the simulation and have been utilized in the modelling of the steam generator, gas turbine, and air preheater.

Macros are a predefined set of elements as well as lines with explicit execution, for example, the gas turbine structure in the gas turbine library.

EbsScript: EbsScript is a device for EBSILON that empowers users to utilize the input, output, and computation abilities automatically, and to consolidate them with the particular client computation. EbsScript utilizes PASCAL syntax and has access to all calculation parameters, detail values, attributes, and result values for all segments, lines, and profiles.

Display objects: Value Crosses, OLE Objects, Graphical and Text fields components can be utilized for showing results.

(iv) Design Mode

The Design mode is the actual design parameters model. The subsequent stages must be followed for the design of a specific cycle:

Adding parts: option of all segments is important for the model, choosing them from the Component bar.

Connecting parts: when the segments are arranged, the subsequent stage is to interface them. Every element has a few connections. The motivation behind these networks is shown in the properties window of the component. To associate segments, fitting lines must be chosen. Each sort of line has an alternate shading.

Specification of values: to describe the topology of the cycle. Specific values can be characterized in the segment properties window or straightforwardly on the lines with the segment "Measured Value input". An example of the input value component on the pipe.

Simulation and error study: After simulating, EBSILON show results and mistakes in the simulation. Error analysis advises about missing information, over-determination, and other sorts of mistakes that stop the simulation.

Showing results: Results are shown in various ways, straightforwardly in the segments or the lines, or by the utilization of cross values.

(v) Off-Design Mode

In off-design modelling, the process is displayed at first in nominal conditions, which means that all components are characterized by their design characteristics. The investigation of off-design conditions is permitted by Ebsilon to utilize this mode of operation. In addition, with the root profiles included it is conceivable to characterize a few off-design computations. Every part comprises predefined charlines. In off-design mode, the components are characterized by trademark lines known as charlines. For instance, the isentropic efficiency of the turbine in off-design relies on M1, the inlet mass flow rate to the component. Two dimensionless relationships are represented by the charlines for each component. In Ebsilon software, “ETA/ETAIN and M1/M1N” are used, where the relationship with N denotes the nominal condition and 1 is for the actual off-design value. These ratios vary according to the off-design requirements during the simulation process.

(vi) OEM-GTLib – The Gas Turbine Library

OEM-GTLib, created in participation with and dispersed by VTU Energy GmbH, contains countless gas turbine models. These are changed under genuine performance conduct and depend on legitimate producer information. Accordingly, one can choose the ideal gas turbine for one's capacity plant to study. The library contains gas turbine models from manufacturers such as from Alstom, Siemens, Rolls Royce, General Electric, Solar Turbines, Centrax, and Hitachi.

(vii) Ebsilon Structure and Solution

A power plant cycle consists of connecting pipes between the individual components. The simulation is complete, when, based on the physical laws, every pipe value of the base variables can be associated with pressure, specific enthalpy and mass flow rate. The dependent variables like temperature or power can be calculated from the base variables through a property state function T= T(p,h) of temperature depending on pressure and specific enthalpy and an algebraic correlation of power depending on mass flow rate and specific enthalpy.

The solution process of Ebsilon is a matrix solution. This requires the linearization of all dependencies. To take into account influences resulting from non-linearities, a Newton iteration is done afterward. The iteration is considered complete if the deviation from the previous iteration step is smaller than the specific precision value for all matrix cells. It is recommended to choose a value of 10^{-6} or 10^{-7} (Ebsilon, 2016).

This showed software is suitable for solving problems in power plants. In addition, the software is easy to use, does not require complex coding. The software helped to solve the complex system of equations that make up the model of the gas turbine power plant. It is built from the first principles of physics and conservation of mass and energy for all power plant processes. It can therefore be

used for modelling and simulating power plant conditions at different loads to a high degree of accuracy. Thus, this makes it useful in the modelling of Azura Edo Power Plant conditions.

3.5.2 MATLAB Software

MATLAB is a powerful mathematical tool for matrix calculation and almost any other mathematical function (MATLAB, 2017). MATLAB also can form windows applications with its programming language. In the analysis of thermodynamic and environmental computation, a graphical user interface is an end product. Different methods can be adopted using MATLAB as a model language. These different methods range from the use of a guide editor to the writing of MATLAB function programmed code. It involved the coding of M Files. The codes or scripts are saved with appropriate names in M Files. The saved M Files with be simulated and results are displayed on the command window.

It is an advanced equation-oriented modelling platform that has the ability for the modelling, simulation and optimization of highly complex processes. The software was chosen for the analysis part of this work because it is best suited for scriptwriting for mathematical computation and produces graphical results easily.

3.6 Thermodynamic Analysis Equations

The equations for the thermodynamic analysis are presented in this section.

3.6.1 Energy Analysis

The calculation of energy analysis of the Azura Edo Power Plant was based on the states shown in Figure 3.3 and Equations (3.1) to (3.21). The following assumptions were made:

i) Neglecting heat losses from components of the gas turbine power plant because the heat transfer from the surfaces of components is often small compared to power generated by the components.

ii) Neglecting potential and kinetic energy parts because it is assumed that there is no change in potential and kinetic energy between the inlet and outlet of each component of the power plant considered.

iii) The principle of ideal mixture was applied for all gases involved.

iv) Energy and mass are conserved, which means mass and energy are not destroyed for each component of the power plant considered.

v) The compressors and turbines are simulated using isentropic efficiencies provided for the power plant by the manufacturer.

The compressor discharged temperature was calculated using Equation (3.1). The exhaust gas temperature from the turbine can be determined by Equation (3.2). The pressure ratio was evaluated using Equations (3.1a) and (3.2a). These equations were obtained as provided in Cengel and Boles (2010); Ehyaei et al. (2011).

Compressor

$$T_2 = T_1\left[\left(\frac{r_{pc}^{\frac{\gamma-1}{\gamma}}-1}{\eta_c}\right)+1\right] \tag{3.1}$$

$$r_{p_c} = \frac{p_2}{p_1} \tag{3.1a}$$

Turbine

$$T_4 = T_3\left[1-\eta_T\left(1-\frac{1}{r_{p_t}^{\frac{\gamma_g-1}{\gamma_g}}}\right)\right] \tag{3.2}$$

$$r_{pt} = \frac{p_3}{p_4} \tag{3.2b}$$

Equations (3.4) to (3.21) used for energy analysis performance of the Azura Edo Power Plant were obtained from Rogers and Mayhew (1992); Cengel and Boles, (2010); Eastop and McConkey (2011).

The work done by compressor and turbine was evaluated using Equations (3.3) and (3.4) respectively.

$$W_C = \dot{m}_a c_{pa}\left(T_2 - T_1\right) \tag{3.3}$$

$$W_T = \dot{m}_g c_{pg}\left(T_3 - T_4\right) \tag{3.4}$$

The thermal power of the power plant was determined by applying Equation (3.5) or (3.6).

$$P_{themal} = W_T - W_C \tag{3.5}$$

$$P_{thermal} = \dot{m}_g * c_{pg}\left(T_3 - T_4\right) - \dot{m}_a c_{pa}\left(T_2 - T_1\right) \tag{3.6}$$

Mechanical losses

The lubricating oil is used to remove heat from bearing as friction losses and dissipate it into the oil cooler.

The mass flow rate of lube oil, $\dot{m}_{oil}$ $=V_{oil} * \rho_{oil}$ (3.7)

The heat removed from the bearing at the oil coolers, $P_{mech\ losses}$, which is the mechanical losses is given by Equation (3.8).

$$P_{mech\ losses} = \dot{m}_{oil} * c_{poil} * (T_{o2} - T_{01}) \tag{3.8}$$

where T_{o1} and T_{o2} are lube oil cooler exit and entry temperatures respectively.

Generator losses

Air is used to cool the generator; the heat is removed by air that is translated to generator losses. The heat absorbed by the air is cooled by water in the water coolers. Density (ρ_w) or the specific volume of cooling water (v_w) was obtained from the Thermodynamic table at a given temperature.

The mass flow rate of cooling water, $\dot{m}_w = \frac{V_w}{v_w}$ or $\rho_w * V_w$ (3.9)

The heat removed from the generator at the water cooler, $P_{gen\ losses,}$ which is the generator losses is given by Equation (3.10).

$$P_{gen\ loses} = \dot{m}_w * c_{pw} * (T_{w2} - T_{w1}) \quad (3.10)$$

where T_{w1} and T_{w2} are temperatures of water entering and leaving the generator air cooler respectively.

The heat supply by the fuel, gross thermal efficiency, and the heat from flue gas of the gas turbine were determined using Equations (3.11) to (3.13) respectively.

Heat supply, $HS = \dot{m}_f LHV$ (3.11)

Gross thermal efficiency $\eta_{thgr} = \frac{P_{net}}{\dot{m}_f LHV}$ (3.12)

Flue gas losses

Flue Gas Heat, $Q_{flue} = \dot{m}_g c_{pg} (T_4 - T_1)$ (3.13)

Power consumed by auxiliaries, $P_{aux,}$ which was estimated.

P_{aux} = Total power consumed by auxiliaries components (3.14)

The electrical power generated, P_{net} is given by Equation (3.15)

$P_{net} = P_{thermal} - P_{mech\ losses} - P_{gen\ losses} - P_{aux}$ (3.15)

The mechanical efficiency is expressed as

$$\eta_m = \frac{P_{thermal} - P_{\text{mech losses}}}{P_{thermal}} \tag{3.16}$$

The generator efficiency was computed using Equation (3.17).

$$\eta_g = \frac{P_{thermal} - P_{\text{mech losses}} - P_{aux}}{P_{thermal} - P_{\text{mech losses}}} \tag{3.17}$$

The net thermal efficiency was determined using Equation (3.18)

$$\eta_{net} = \frac{P_{net}}{\dot{m}_f * LHV} \tag{3.18}$$

The specific fuel consumption, heat rate, and work ratio of the gas turbine power plant were evaluated using Equations (3.19) to (3.21) respectively.

$$\text{Specific Fuel Consumption, } SFC = \frac{3600\dot{m}_f}{p_{net}} \tag{3.19}$$

$$\text{Heat Rate, } HR = LHV * SFC \tag{3.20}$$

$$\text{Work Ratio, } WR = \frac{P_{net}}{W_T} \tag{3.21}$$

3.6.2 Exergy Analysis

(a) Formulation of Exergy Balance Equation

The First and Second Laws of Thermodynamics can be applied to formulate the equations of general exergy balance for each component and the overall thermal system. The thermo-mechanical exergy stream might be separated into its mechanical and thermal segments (Ebadi and Gorji – Brandpy 2005) as expressed in Equation (3.22).

$$E_i^M - E_o^M = \left(E_i^P + E_o^P\right) + \left(E_i^T + E_o^T\right) \tag{3.22}$$

where i and o are the inlet and outlet component exergy flow stream respectively, M is the material element under study, T is the thermal property and P is the mechanical property.

The components of the thermal and mechanical exergy stream for an ideal gas with constant heat capacity at constant pressure are expressed as shown in Equations (3.23) and (3.24) respectively as stated in (Rogers and Mayhew, 1995; Kotas, 1995).

$$E^T = \dot{m}_a c_p \left[\left(T - T_{ref} \right) - T_{ref} In \frac{T}{T_{ref}} \right] \tag{3.23}$$

$$E^P = \dot{m} R T_{ref} In \frac{p}{p_{ref}} \tag{3.24}$$

The entropy for each state is given by Equation (3.25).

$$\dot{S}_1 = \dot{m} \left(c_p In \frac{T}{T_{ref}} - RIn \frac{p}{p_{ref}} \right) \tag{3.25}$$

With the disintegration characterized by Equation (3.22), the general exergy balance equation can be written as Equation (3.26) (Ebadi and Gorji – Brandpy 2005).

$$E^{CHE} + \left(\sum E_i^T - \sum E_o^T \right) + \left(\sum E_i^P - \sum E_o^P \right) + T_{ref} \left(\sum S_i - \sum S_o + \frac{Q_{cv}}{T_{ref}} \right) = E^W \tag{3.26}$$

where E^{CHE} represents the plant fuel exergy flow rate.

Q_{cv} represents the heat transfer component from the environment.

E^W is the Work done by the material component under study.

The thermal, mechanical, and entropy of the various states as shown in Figure 3.3 for air compressor, combustion chamber and gas turbine sections were determined using Equations (3.27) to (3.41) as stated in Barzegar et al. (2011); Amadi et al. (2008); Bejan et al. (1996) applying Equations (3.23) to (3.25). The results obtained from these equations will be used in various component analyses to determine their exergy work, thermal exergy and mechanical exergy quantities.

State 1(Entry into Compressor)

Equations (3.27) to (3.29) were used to determine the thermal exergy, mechanical exergy and entropy of the air entering into the compressor respectively.

$$E_1^T = \dot{m}_a c_{pa}\left[\left(T_1 - T_{ref}\right) - T_{ref} In \frac{T_1}{T_{ref}}\right] \tag{3.27}$$

$$E_1^p = \dot{m}_a R_a T_{ref} In \frac{p_1}{p_{ref}} \tag{3.28}$$

$$\dot{S}_1 = \dot{m}_a \left(c_{pa} In \frac{T_1}{T_{ref}} - R_a In \frac{p_1}{p_{ref}} \right) \tag{3.29}$$

State 2 (Entry into the Combustion Chamber or Compressor Exit)

The thermal exergy, mechanical exergy and entropy of the compressed air leaving the compressor were computed using Equations (3.30) to (3.32) respectively.

$$E_2^T = \dot{m}_a c_{pa}\left[\left(T_2 - T_{ref}\right) - T_{ref} In \frac{T_2}{T_{ref}}\right] \tag{3.30}$$

$$E_2^p = \dot{m}_a R_a T_{ref} In \frac{p_2}{p_{ref}} \tag{3.31}$$

$$\dot{S}_2 = \dot{m}_a \left(c_{pa} In \frac{T_2}{T_{ref}} - R_a In \frac{p_2}{p_{ref}} \right) \tag{3.32}$$

State f (Fuel inlet to Combustion Chamber)

Equations (3.33) to (3.35) were used to determine the thermal exergy, mechanical exergy and entropy of the fuel entering into the combustion chamber respectively.

$$E_f^T = \dot{m}_f c_{pf}\left[\left(T_f - T_{ref}\right) - T_{ref} In \frac{T_f}{T_{ref}}\right] \tag{3.33}$$

$$E_f^p = \dot{m}_f R_f T_{ref} In \frac{p_f}{p_{ref}} \tag{3.34}$$

$$\dot{S}_f = \dot{m}_f \left(c_{pf} In \frac{T_f}{T_{ref}} - R_f In \frac{p_f}{p_{ref}} \right) \tag{3.35}$$

State 3 (Entry into Gas Turbine)

The thermal exergy, mechanical exergy and entropy of the combustion gas entering into the gas turbine section were computed using Equations (3.36) to (3.38) respectively.

$$E_3^T = \dot{m}_g c_{pg} \left[\left(T_3 - T_{ref} \right) - T_{ref} In \frac{T_3}{T_{ref}} \right] \tag{3.36}$$

$$E_3^p = \dot{m}_g R_g T_{ref} In \frac{p_3}{p_{ref}} \tag{3.37}$$

$$\dot{S}_3 = \dot{m}_g \left(c_{pg} In \frac{T_3}{T_{ref}} - R_g In \frac{p_3}{p_{ref}} \right) \tag{3.38}$$

State 4 (Exit from Gas Turbine)

The thermal exergy, mechanical exergy and entropy of the burnt gas leaving the gas turbine section were evaluated using Equations (3.39) to (3.41) respectively.

$$E_4^T = \dot{m}_g c_{pg} \left[\left(T_4 - T_{ref} \right) - T_{ref} In \frac{T_4}{T_{ref}} \right] \tag{3.39}$$

$$E_4^p = \dot{m}_g R_g T_{ref} In \frac{p_4}{p_{ref}} \tag{3.40}$$

$$\dot{S}_4 = \dot{m}_g \left(c_{pg} In \frac{T_4}{T_{ref}} - R_g In \frac{p_4}{p_{ref}} \right) \tag{3.41}$$

(b) Components Analysis Equation for Azura Edo Power Plant

Each component of the Azura Edo Power Plant exergy balance equation was derived from the general exergy balance equation as provided in Equation (3.22) which also includes thermal and mechanical exergy terms. The following are air compressor, combustion chamber, and gas turbine exergy balance equations.

(i) Air Compressor

The exergy work done; thermal, mechanical exergy quantities of the compressor were determined by using Equations (3.42) to (3.44) respectively as expressed in Kotas (1995); Abam and Moses (2011).

$$W_{AC} = \left(E_1^T - E_2^T\right) + \left(E_1^p - E_2^p\right) + T_{ref}\left(\dot{S}_1 - \dot{S}_2\right) \tag{3.42}$$

$$E_{AC}^T = E_2^T - E_1^T \tag{3.43}$$

$$E_{AC}^p = E_2^p - E_1^p \tag{3.44}$$

(ii) Combustion Chamber

The chemical exergy of the fuel can be obtained using Equation (3.45) as expressed in Moran and Shapiro (2000) and Bejan (2012) for gaseous hydrocarbon fuel. Equation (3.45) was simplified to Equation (3.46) after substituting the values a and b of the fuel used. The chemical exergy or fuel exergy, thermal and mechanical exergy quantities was evaluated using Equations (3.46) to (3.48) respectively.

$$E^{CHE} = \dot{m}_f LHV\left(1.033 + \frac{0.0169b}{a} - \frac{0.0698}{a}\right) \tag{3.45}$$

where a and b are carbon and hydrogen atoms respectively.

$$E^{CHE} = 1.06\dot{m}_f LHV \tag{3.46}$$

$$E_{CC}^T = E_3^T - \left(E_2^T + E_f^T\right) \tag{3.47}$$

$$E_{CC}^{p} = E_{3}^{p} - \left(E_{2}^{p} + E_{f}^{p}\right) \tag{3.48}$$

The exergy balance equation for the combustion chamber is written as Equation (3.49) (Al-Doori, 2012).

$$E^{CHE} + \left(E_{2}^{p} + E_{f}^{p} - E_{3}^{p}\right) + \left(E_{2}^{T} + E_{f}^{T} - E_{3}^{T}\right) + T_{ref}\left(\dot{S}_{2} + \dot{S}_{f} - \dot{S}_{3}\right) + Q_{CC} = 0 \tag{3.49}$$

(iii) Gas Turbine

In the gas turbine section, Equations (3.50) to (3.52) were used to compute the exergy work done, thermal and mechanical exergy quantities respectively as stated in Bejan (2012).

$$W_{GT} = \left(E_{3}^{T} - E_{4}^{T}\right) + \left(E_{3}^{p} - E_{4}^{p}\right) + T_{ref}\left(\dot{S}_{3} - \dot{S}_{4}\right) \tag{3.50}$$

$$E_{GT}^{T} = E_{4}^{T} - E_{3}^{T} \tag{3.51}$$

$$E_{GT}^{p} = E_{4}^{p} - E_{3}^{p} \tag{3.52}$$

(c) Exergy Destruction

In contrast to energy, exergy is destroyed by irreversibilities in a system but not conserved. Irreversibilities in the system are categorized as internal and external irreversibilities. Unrestrained expansion, friction, chemical reaction, and mixing are major sources of internal irreversibilities, while the heat conversion as a result of difference in temperature gives rise to external irreversibilities. When the energy that is related to an energy or material stream is rejected to the surrounding it is referred to as exergy lost.

The exergy destroyed during each process in the component and for the overall plant was evaluated as stated in Equations (3.53) to (3.56) (Bejan 2012; Cengel and Boles, 2010).

For the compressor, Exergy destroyed, E_{DAC}

$$E_{DAC} = T_{ref}\left(\dot{S}_{2} - \dot{S}_{1}\right) \tag{3.53}$$

For the combustion chamber, E_{DCC}

$$E_{DCC} = E^{CHE} + \left(E_2^T + E_f^T - E_3^T\right) + \left(E_2^p + E_f^p - E_3^p\right) \tag{3.54}$$

For the Gas Turbine

$$E_{DGT} = T_{ref}\left(\dot{S}_4 - \dot{S}_3\right) \tag{3.55}$$

The overall plant exergy destroyed, E_{Dplant}

$$E_{Dplant} = E_{DAC} + E_{DCC} + E_{DGT} \tag{3.56}$$

Where E_{DAC}, E_{DCC} and E_{DGT} represent the exergy destroyed in the air compressor, combustor and GT respectively.

The exergy destruction efficiency is the ratio of the component exergy destroyed to the exergy supplied rate. So, the exergy destruction efficiency of the various components and the overall plant were determined using Equations (3.57) to (3.60).

(i) Air Compressor

$$\varepsilon_{DAC} = \frac{E_{DAC}}{W_{AC}} \tag{3.57}$$

(ii) Combustion Chamber

$$\varepsilon_{DCC} = \frac{E_{DCC}}{E^{CHE}} \tag{3.58}$$

(iii) Gas turbine

$$\varepsilon_{DGT} = \frac{E_{DGT}}{W_{GT}} \tag{3.59}$$

(iv) Overall Plant

$$\varepsilon_{Dplant} = \frac{E_{Dplant}}{E^{CHE}} \tag{3.60}$$

(d) Exergy Efficiency

The exergy efficiency of a system is defined as the proportion of exergy output (useful) to exergy input (supplied). The exergy efficiency of a system was computed as expressed in Equation (3.61) (Cengel & Boles 2010).

$$\varepsilon = \frac{\text{Useful exergy}}{\text{Exergy supplied}} = 1 - \frac{\text{Exergy destroyed}}{\text{Exergy supplied}} \tag{3.61}$$

Consequently, the exegetic efficiency of the gas turbine power plant is assessed for the different parts and the total plant as shown in Equations (3.62) to (3.65).

(i) Air Compressor

$$\varepsilon_{AC} = 1 - \frac{E_{DAC}}{W_{AC}} \tag{3.62}$$

(ii) Combustion Chamber

$$\varepsilon_{CC} = 1 - \frac{E_{DCC}}{E^{CHE}} \tag{3.63}$$

(iii) Gas Turbine

$$\varepsilon_{GT} = 1 - \frac{E_{DGT}}{W_{GT}} \tag{3.64}$$

(iv) Overall Plant, ε_{plant}

$$\varepsilon_{plant} = 1 - \frac{E_{Dplant}}{E^{CHE}} \tag{3.65}$$

The net exergy power (W_{plant}) and Second Law of Thermodynamics efficiency of the Azura Edo Power Plant were determined by applying Equations (3.66) and (3.67) respectively as stated in Abam and Moses (2011); Abam et al. (2012); Oyedepo et al. (2015); Cengel and Boles (2010).

$$W_{plant} = W_{GT} + W_{AC} \tag{3.66}$$

$$\eta_{SL} = \frac{W_{plant}}{E^{CHE}} \tag{3.67}$$

3.6.3 Improvement Potential

Exergy Improvement Potential of the Azura Edo Power Plant was determined using Equation (3.68) as expressed in Van Gool (1997) and Hammond (2004); Oyedepo et al. (2015).

$$E_{XIP} = (1-\varepsilon) I \tag{3.68}$$

Where E_{XIP} the exergy improvement potential, ε is the exergy efficiency and I is the exergy loss or destruction or irreversibility rate.

Consequently, the exergy improvement potential for the different components and the overall plant were evaluated using Equations (3.69) to (3.71b).

For Air Compressor

$$E_{XIPAC} = (1-\varepsilon_{AC}) I_{AC}, \text{ where } I_{AC} = E_{DAC} \tag{3.69}$$

For Combustion Chamber

$$E_{XIPCC} = (1-\varepsilon_{CC}) I_{CC}, \text{ where } I_{CC} = E_{DCC} \tag{3.70}$$

For Gas Turbine

$$E_{XIPGT} = (1-\varepsilon_{GT}) I_{GT}, \text{ where } I_{GT} = E_{DGT} \tag{3.71a}$$

For Overall Plant

$$E_{XIplant} = (1-\varepsilon_{plant}) I_{plant} \text{ where } I_{plant} = E_{Dplant} \tag{3.71b}$$

3.6.4 Depletion Number and Sustainability Index

The formula proposed by Connelly and Koshland (1997) and Chandramohan (2008) to calculate depletion number as shown in Equation (3.72) was used. It states that for the characterization of fuel consumption, the depletion number is a very useful factor to determine the degradation and lengthening of the fuel when used in power plant and other thermal processes. The relationship between the exergy efficiency and the depletion number is expressed in Equation (3.72).

$$D_p = \frac{E_{DCC}}{E_{xin}} \tag{3.72}$$

where E_{DCC} is the exergy destruction and E_{xin} is the exergy supplied by fuel consumption.

Additionally, the sustainability index (SI), which is the fuel resource sustainability is expressed as the reciprocal of the depletion number (Altayib, 2011; Oyedepo et al., 2015) as shown in Equation (3.73).

$$SI = \frac{1}{D_p} \tag{3.73}$$

3.7 Environmental Analysis

Environmental modeling is undertaken by using the generated work rate and the carbon dioxide emission rate from the Azura Edo Power Plant to the atmosphere as shown in this section. To evaluate the greenhouse gas emission parameters of the exhaust gases through the stack to the environment for Edo Azura Gas Turbine Power Plant, Equations (3.74) to (3.101) were used. The composition of fuel (natural gas) used to fire the Edo Azura Gas Turbine Power Plant is presented in Table 3.1.

Table 3.1: Composition and Property of the Fuel

S/N	Name of Constituent	Formula of Constituent	Molar fraction (Volumetric)(x_f)	Molar mass of Constituent (Mi) (kg/kmol)
1	Methane	CH_4	0.87721	16
2	Ethane	C_2H_4	0.03658	30
3	Propane	C_3H_8	0.03031	44
4	Normal –Butane	$C_4H_{10\text{-}N}$	0.003325	58
5	Iso – Butane	$C_4H_{10\text{-}I}$	0.003318	58
6	Normal – Pentane	$C_5H_{12\text{-}N}$	0.002157	72
7	Normal – Hexane	$C_6H_{14\text{-}N}$	0.000448	86
8	Iso – Pentane	$C_5H_{12\text{-}I}$	0.002352	72
9	Carbon dioxide	CO_2	0.02722	44
10	Nitrogen	N_2	0.01708	28

*Source: (Azura Edo, 2017)

The molar mass of fuel (M_f) was computed by combining Equations (3.74) and (3.75), and using the mole fraction and molar mass of fuel constituents in Table 3.1 (Rogers and Mayhew, 1992; Eastop and McConkey, 2011; Cengel and Boles, 2010).

$$M_f = \sum x_{fi} M_i \tag{3.74}$$

Equation (3.74) can be rewritten as Equation (3.75) according to each constituent that makes up the fuel.

$$\begin{aligned} M_f = &\left(x_{fCH_4} * M_{CH_4}\right) + \left(x_{fC_2H_6} * M_{C_2H_6}\right) + \left(x_{fC_3H_8} * M_{C_3H_8}\right) + \left(x_{fC_4H_{10-N}} * M_{C_4H_{10-N}}\right) + \left(x_{fC_4H_{10-I}} * M_{C_4H_{10-I}}\right) + \\ &\left(x_{fC_5H_{12-N}} * M_{C_5H_{12-N}}\right) + \left(x_{fC_6H_{14-N}} * M_{C_6H_{14-N}}\right) + \left(x_{fC_5H_{12-I}} * M_{C_5H_{12-I}}\right) + \left(x_{fCO_2} * M_{CO_2}\right) + \left(x_{fN_2} * M_{N_2}\right) \end{aligned} \tag{3.75}$$

The fuel molar flow rate, n_f in kmol/s was computed using Equation (3.76).

$$n_f = \frac{\dot{m}_f}{M_f} \tag{3.76}$$

where $\dot{m}_f$ is the fuel mass flow rate and M_f is fuel molar mass, which is 18.89079kg/kmol as computed from Equation (3.75).

The saturation pressure(p_s) of the water vapour in ambient air is the corresponding pressure at the compressor inlet temperature. The partial pressure, p_v and molar fraction (x_{aH_2O}) of water vapour in the air were obtained from Equations (3.77) and (3.78) respectively.

$$p_v = \phi * p_s \tag{3.77}$$

where ϕ is the relative humidity.

$$x_{aH_2O} = \frac{p_v}{p_{atm}} \tag{3.78}$$

The mole fraction of dry air x_{da} was evaluated using Equation (3.79).

$$x_{da} = 1 - x_{aH_2O} \tag{3.79}$$

Equations (3.80) to (3.82) were used to compute the molar fraction of carbon dioxide, x_{aCO_2}, nitrogen, x_{aN_2} and oxygen, x_{aO_2} in the air respectively.

$$x_{aCO_2} = x_{da} * n_{aCO_2} \tag{3.80}$$

$$x_{aN_2} = x_{da} * n_{aN_2} \tag{3.81}$$

$$x_{aO_2} = x_{da} * n_{aO_2} \tag{3.82}$$

where n_{aco2}, n_{aO2} and na_{N2} are the molar values for carbon dioxide, oxygen and nitrogen, which are 0.0003058, 0.20988789 and 0.78980632 respectively as obtained from Kanbur et al. (2017).

The molar mass of air, M_a in kg/kmol was computed using Equation (3.83).

$$M_a = (x_{aN_2} * M_{N_2}) + (x_{aO_2} * M_{O_2}) + (x_{aCO_2} * M_{CO_2}) + (x_{aH_2O} * M_{aH_2O}) \tag{3.83}$$

where the molar masses of M_{N2}, M_{O2}, M_{CO2} and M_{H2O} for nitrogen, oxygen, carbon dioxide and water vapour are 28, 32, 44 and 18 kg/kmol respectively.

The molar flow rate of air (n_a) in kmol/s was calculated using Equation (3.84).

$$n_a = \frac{\dot{m}_a}{M_a} \tag{3.84}$$

where, $\dot{m}_a$ is the mass flow rate of air as obtained from the Azura Edo Power Plant.

The fuel air ratio, λ was calculated using Equation (3.85).

$$\lambda = \frac{n_f}{n_a} \tag{3.85}$$

In the various computations, the air chemical compositions were assumed to be carbon dioxide, oxygen water vapour and nitrogen, and assuming all gases to be ideal gases (Bejan et al., 1996).

The relationship between the chemical contents of the fuel, air and exhaust gases are indicated in the combustion reaction that took place in the combustor as illustrated in Equation (3.86).

$$\lambda\begin{bmatrix} 0.87721CH_4 + \\ 0.03658C_2H_6 + \\ 0.03031C_3H_8 + \\ 0.003325C_4H_{10-N} + \\ 0.003318C_4H_{10-I} + \\ 0.002157C_5H_{12-N} + \\ 0.000448C_6H_{14-N} + \\ 0.002352C_5H_{12-I} + \\ 0.02722CO_2 + \\ 0.01708N_2 \end{bmatrix} + \begin{bmatrix} x_{aO_2}O_2 + \\ x_{aN_2}N_2 + \\ x_{aCO_2}CO_2 + \\ x_{aH_2O}H_2O \end{bmatrix} \rightarrow (1+\lambda)\begin{bmatrix} x_{pCO_2}CO_2 + \\ x_{pH_2O}H_2O + \\ x_{pO_2}O_2 + \\ x_{pN_2}N_2 \end{bmatrix} \tag{3.86}$$

where x_a is the molar fraction of the air components, x_p is the molar fraction of combustion products components, and λ is the fuel-air ratio of the power plant. The combustion equation was obtained from Bejan et al. (1996) where more details can be found.

Applying carbon, hydrogen, oxygen and nitrogen balances to solve the combustion reaction expressed in Equation (3.86), the molar fractions of carbon dioxide x_{pCO_2}, water vapour x_{pH_2O}, oxygen x_{pO_2} and nitrogen x_{pN_2} were respectively computed using Equations (3.87) to (3.90).

$$x_{pCO_2} = \frac{1.118765\lambda + x_{aCO_2}}{1+\lambda} \tag{3.87}$$

$$x_{pH_2O} = \frac{1.2022233\lambda + x_{aH_2O}}{1+\lambda} \tag{3.88}$$

$$x_{pO_2} = \frac{0.02722\lambda + x_{aO_2} + x_{aCO_2} + 0.5x_{aH_2O} - x_{pCO_2} - 0.5x_{pH_2O}}{1+\lambda} \tag{3.89}$$

$$x_{pN_2} = \frac{0.01708\lambda + x_{aN_2}}{1+\lambda} \tag{3.90}$$

The molar flow rate of the exhaust gases can be evaluated by applying Equation (3.91).

$$n_p = n_a * (1+\lambda) \tag{3.91}$$

The mass flow rates of the constituents of the products or exhaust gases were computed by using Equations (3.92) to (3.95) (Eastop and McConkey, 2011; Kanbur et al., 2017).

$$m_{pCO_2} = x_{pCO_2} * n_p * M_{CO_2} \tag{3.92}$$

$$m_{pO_2} = x_{pO_2} * n_p * M_{O_2} \tag{3.93}$$

$$m_{pH_2O} = x_{pH_2O} * n_p * M_{H_2O} \tag{3.94}$$

$$m_{pN_2} = x_{pN_2} * n_p * M_{N_2} \tag{3.95}$$

To validate the model used, the computed mass flow rate of the combustion products will be compared with the measured values from the power plant logbook. This was done because the value of CO_2 emission was not provided by the power plant operator. The amount of flue gas ought to be the same, that is why it was selected to be compared as a value of reference.

The measured mass flow rate of combustion products, m_g was evaluated using Equation (3.96).

$$\dot{m}_g = \dot{m}_a + \dot{m}_f \tag{3.96}$$

The computed exhaust mass flow rate of combustion products ($\dot{m}_{gc}$) using the combustion equation is expressed in Equation (3.97).

$$\dot{m}_{gc} = \dot{m}_{pCO_2} + \dot{m}_{pH_2O} + \dot{m}_{pO_2} + \dot{m}_{pN_2} \tag{3.97}$$

The deviation in mass flow rates of both is shown in Equation (3.98) and the percentage error was computed using Equation (3.99) as used in Amjady et al. (2011); Oyedepo et al. (2015); Azim and Farshid (2017); Abbaspour et al. (2021).

$$\Delta\dot{m}_g = \dot{m}_{gc} - \dot{m}_g \tag{3.98}$$

$$\%error = \frac{\Delta\dot{m}_g * 100\%}{\dot{m}_g} \tag{3.99}$$

The mass of carbon dioxide emission rate in terms of kg/kWh and annual mass of carbon dioxide discharged was computed by applying Equations (3.100) to (3.101) respectively (Barzegar Avval et al., 2011; Altayib, 2011; Kanbur et al., 2017).

$$\xi_{CO_2} = \frac{3600 * m_{pCO_2}}{P_{net}} \tag{3.100}$$

$$m_{pCO_2/yr} = m_{pCO_2} * LF * OPT \tag{3.101}$$

where LF and OPT are load factor and operation time for the Azura Edo Power Plant for one year respectively.

3.8 Modelling and Simulation of SGT5 – 2000E Gas Turbine Power Plant

The model of the installed turbine in Azura Edo Power Plant is the Siemens SGT5 – 2000E. The nominal conditions for the Model ISO and Azura Edo Guaranteed parameters are presented in Table 3.2. The model data used in the Ebsilon Professional for the SGT5 – 2000E model are in two categories. The ISO conditions are obtained from Siemens (2011), which form the root profile of the modelling. The other set of data are the Azura Edo guaranteed conditions as obtained from Azura (2017), which are values guaranteed by Siemens for the power plant. The power plant model structure executed in EBSILON Professional programming is shown in Figure 3.4. The principal model data are recorded in Table 3.2

Table 3.2: Nominal Conditions for ISO and Azura Edo SGT5 - 2000E Gas Turbine Power Plant

ISO Design condition		
S/N	Parameters	Design values
1	Power (MW)	166
2	Heat Rate(kJ/kWh)	10375
3	Thermal Efficiency (%)	34.7
4	Turbine Exhaust Temperature (^{0}C)	541
5	Exhaust mass flow rate (kg/s)	525
6	Pressure Ratio (r_p)	12
7	Ambient air temperature (^{0}C)	15
8	Ambient air pressure (bar)	1.013
9	Relative Humidity (%)	60
Azura Edo Guarantee Condition		
S/N	Parameters	Values
1	Power (MW)	153
2	Heat Rate(kJ/kWh)	10528
3	Ambient air temperature (^{0}C)	26
4	Ambient air pressure (bar)	1.013

3.8.1 General and Component Assumptions

The assumptions made in the modelling of the power plant are as follows:

(i) The simulations are performed at a steady state, which means that the mass and other parameters within the various components and the boundary do not vary with time. Quasi steady state is assumed for compressor inlet air temperature because it depends on time which was assumed to steady at every hour.

(ii) Neglecting the transient impact caused by start-up and shut down during operation because the data obtained were recorded at times when the power plant are fully in operation without fault.

(iii) The pressure drop in Ebsilon was considered for each component nominal pressure drops as obtained from the power plant. This was done in order to ensure that the pressures of the various fluids were more realistic.

3.8.2 Building the Model with Ebsilon

Ebsilon professional software was used in modelling the SGT5 -2000E gas turbine model in this work. After opening the Ebsilon software installed on the computer, the first thing that was done when building the SGT5 – 2000E model was to create a new Ebsilon project. This was carried out by clicking on the Ebsilon menu bar user interface and selecting "New". The project was then saved under a suitable name. The next step was selecting all components such as air compressor, combustion chamber, gas turbine and generator. The components were then linked together by clicking the outer of one component to the inlet of another component, like compressor outlet to combustion chamber inlet in that order for all components. The air compressor, gas turbine and generator are connected by the shaft. The complete model set is shown in Figure 3.4. The parameters are inputted accordingly at various components. The model was simulated, if an error occurred, all error codes will be attended to until the model was successfully simulated.

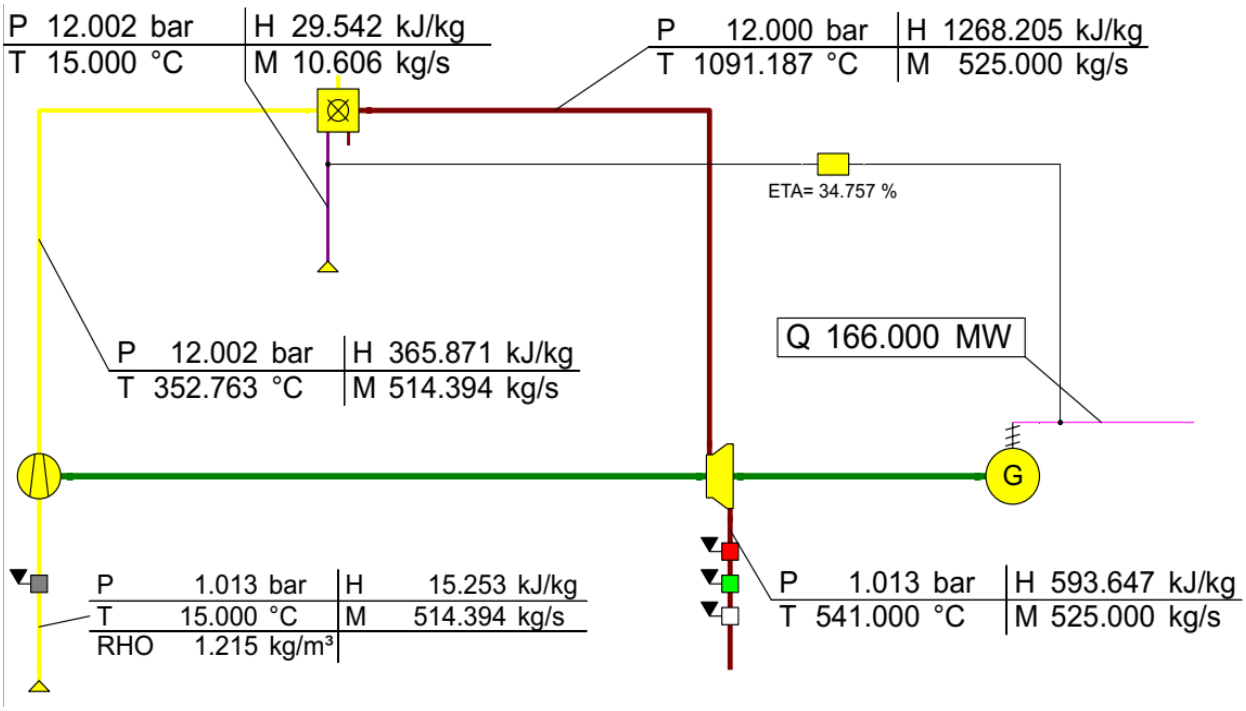

Figure 3.4: Topology of ISO SGT5 – 2000E based on the Fixed Exhaust Data

This was done for power plant first “mapped out” in the Ebsilon Professional Software to establish the consistency of the power plant data and compare it with the ISO design parameters of the plant. The outcome of this simulation gives a complete mapping of the SGT5 – 2000 E into Ebsilon which allows Ebsilon to simulate various conditions. This allows the identification of problems where there are mismatches of the design data with the power plant.

The Azura Edo Power Plant (SGT5 – 2000E Turbine model) comprises an air compressor, a combustion chamber, a gas turbine, and a generator, which was modelled by selecting and connecting the components mentioned together as shown in Figure 3.4. The ISO conditions of 1.013bar pressure and 15^0C temperature for ambient air were used to establish the design performance outcomes of the SGT5 – 2000E Turbine. The values of ambient air temperature and pressure, pressure ratio, exhaust mass flow rate and temperature from Table 3.2 were used to perform the modelling of the ISO SGT5 – 2000E Turbine. The “general input value” was utilized to set the nominal mass flow rate and temperature of the flue gas, whereas the pressure ratio was set in the gas turbine component. The isentropic efficiencies of the compressor and turbine of 90% and 85% respectively obtained from the power plant manual were used. This was done because the air and fuel mass flow rates were not provided, which will be obtained after the model simulation. The mechanical and generator efficiency of 99% and 98.5% respectively which were obtained after series of iteration processes, were used for the modelling. The composition and LHV of the fuel were inputted accordingly. After inputting all data and performing the model simulation, the mass flow rates of air and fuel are attained for the nominal conditions in the gas turbine.

Then, the values of air and fuel mass flow rates obtained were used to carry out the simulation again without the exhaust temperature and mass flow rate. When the initial results for exit conditions were obtained, the nominal condition for the gas turbine was achieved. This explanation

is illustrated in Figure 3.5. This was done to enable the mass flow rate of air and mass flow rate of fuel that enter the compressor and combustion chamber respectively to determine the gas turbine performance under different input conditions and part load. This formed the root profile for this model, which made it possible to input the new parameters of air for off-design conditions using the “boundary value input”. The values for Azura Edo guaranteed conditions were obtained from the nominal SGT5 – 2000E parameters. This was done because the Azura Edo guaranteed data are different from the ISO data in terms of ambient temperature and power output and heat rate. Some results obtained from modelling of the Azura Edo Power Plant for the guarantee condition using Ebsilon are presented in Figure 3.6.

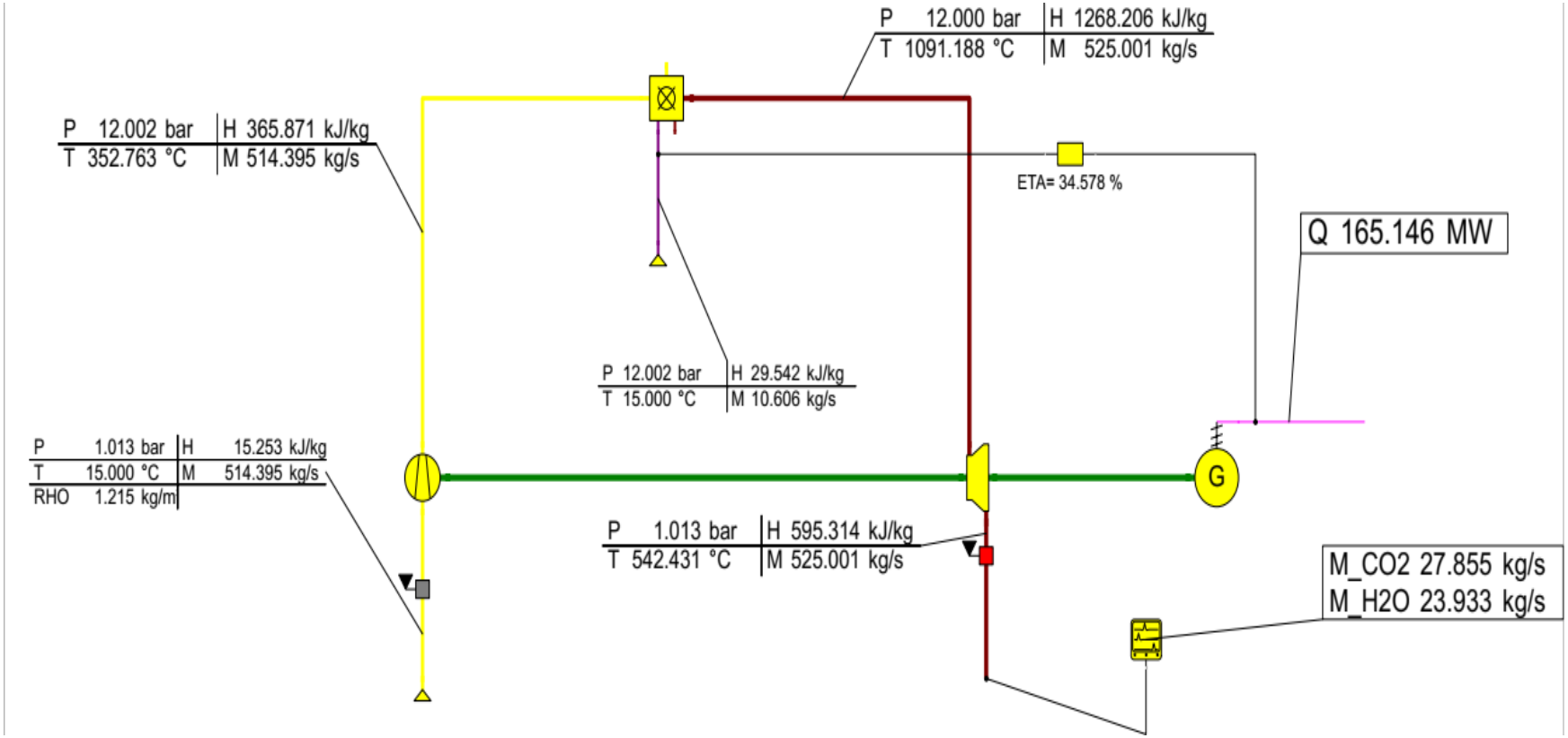

Figure 3.5: Topology of SGT5 – 2000E for ISO Design Condition

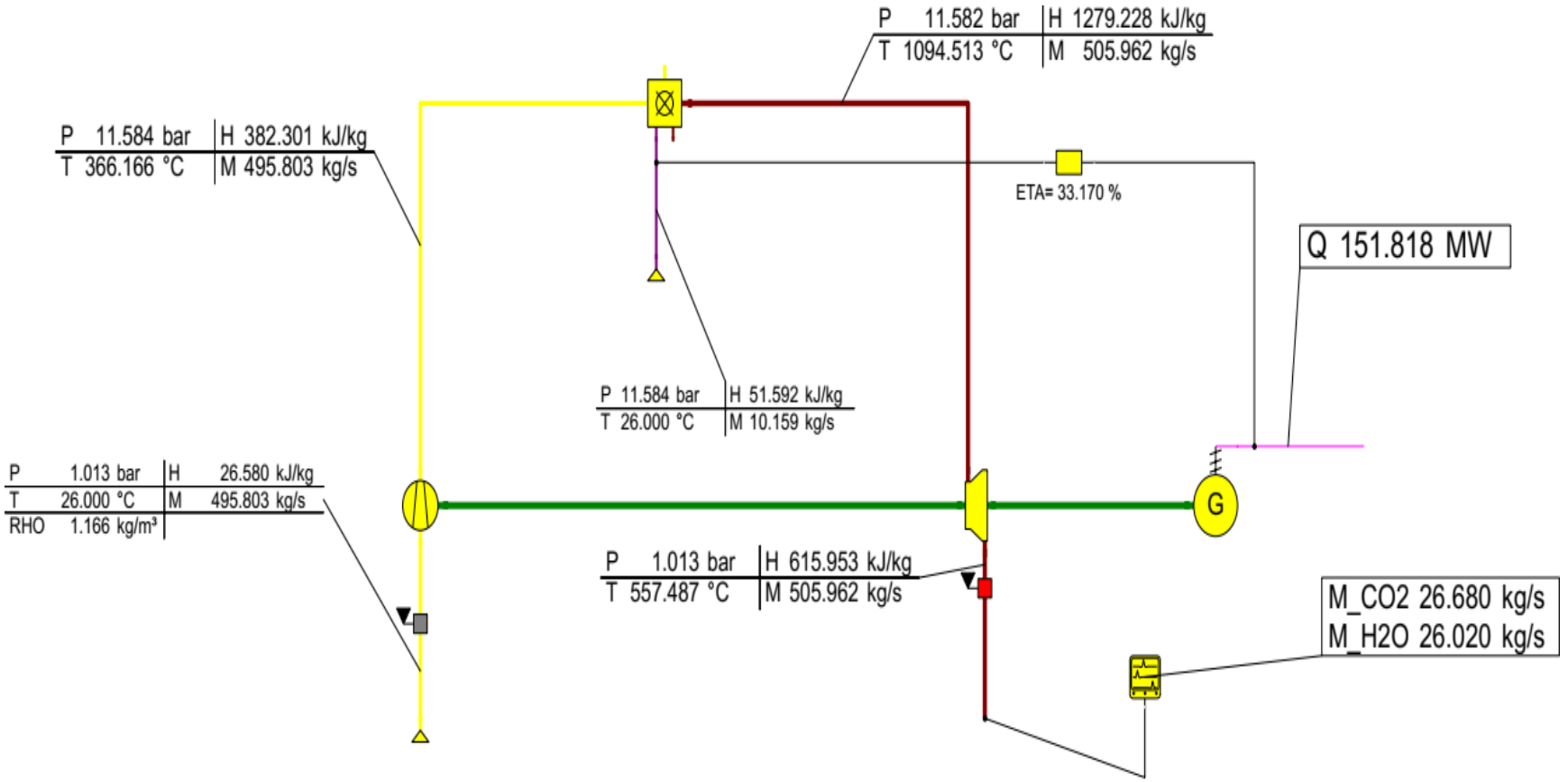

Figure 3.6: Topology of Azura Edo SGT5 – 2000E for Guarantee Condition

3.8 3 The SGT5 – 2000E Gas Turbine in Off-design Modelling

When the gas turbine is operating in the design condition, it is also referred to as nominal condition or ISO condition as the case may be or 100% off-design condition. When the power plant operates at any condition different from nominal specifications it is known as off-design condition. The off-design conditions can be experienced when there are changes in ambient air conditions such as temperature and humidity, or when the power output generated by the turbine is less or more than the design power output. The off-design model will be carried out by changing air ambient temperature and when the power output is different from nominal condition.

The analysis of variation of power output and thermal efficiency with ambient air temperature was modelled using the Ebsilon Professional Software for the Azura Edo Power Plant. Figure 3.7 presents the simulated outcome of the Azura Edo Power plant at 26 ^{0}C ambient air temperature.

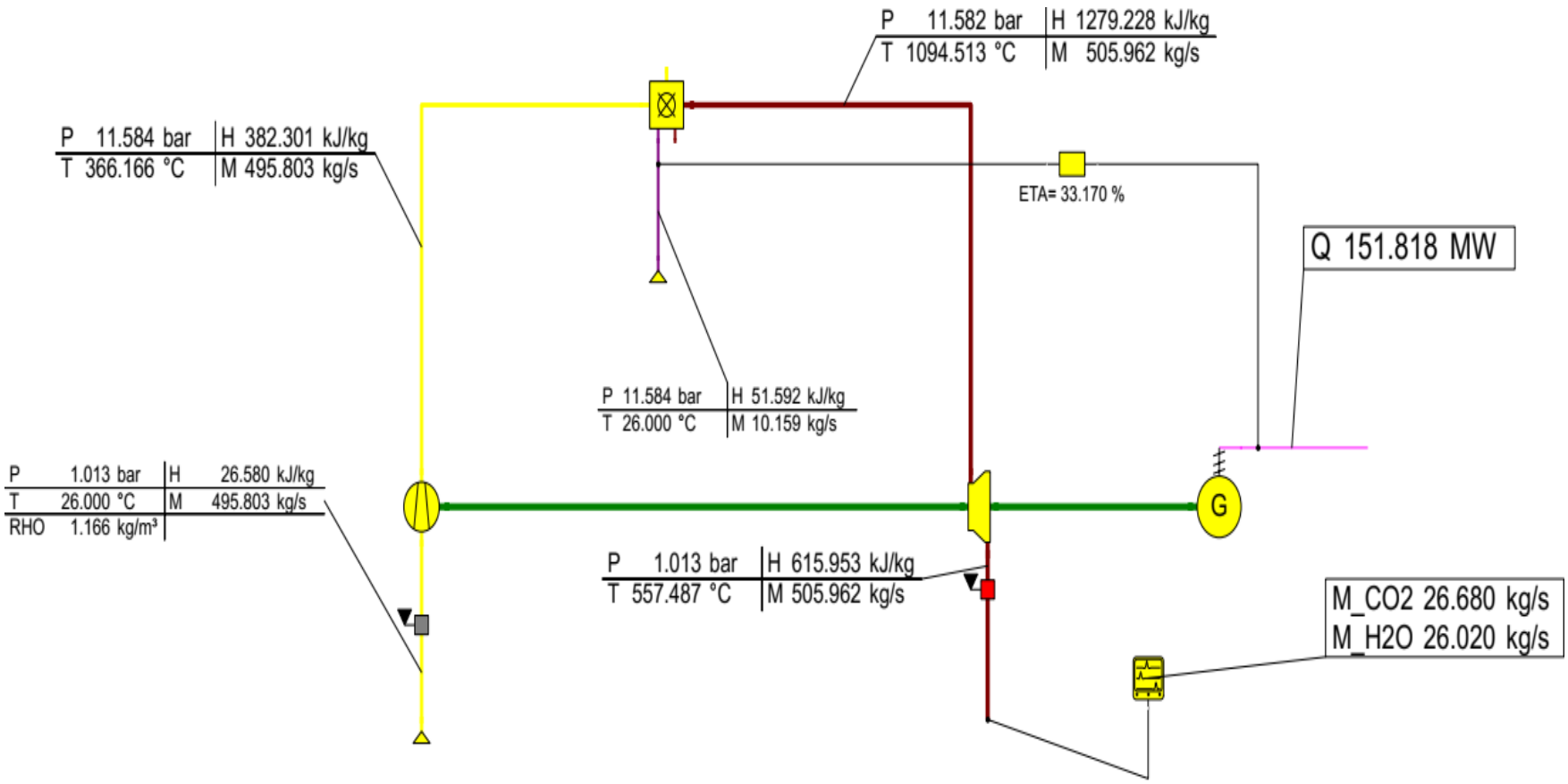

Figure 3.7: Topology of Azura Edo SGT5 – 2000E for Off-Design Conditions

3.8.4 Variation of Ambient Air Temperature

The performances of power plants are affected by changes in ambient conditions. The variations of thermodynamic performance that occur are due to changes in the air properties entering the air compressor like relative humidity and temperature. For this research, the variation of relative humidity (φ) with temperature was obtained using Equation (3.104). This equation was determined by using the data curve fit from data obtained in Azura EIA (2013) as explained in Appendix III. Additionally, the change in temperature affects the density (ρ) of air inversely, and the density of air is proportional to its mass flow rate. Accordingly, the mass airflow rate into the compressor will be reduced at high ambient air temperature since the compressor volume flow rate is fixed. This implies that gas turbines that operate in hotter weather conditions generate lower power output because of the low mass flow of air induced. Consequently, it is important to study the effect of ambient air temperature on the gas turbine output parameters. The various ambient air density and mass flow rates were calculated using Equations (3.102) and (3.103) respectively for different ambient air temperatures.

$$\rho_i = \rho_N \frac{T_N}{T_i} \tag{3.102}$$

$$\dot{m}_i = \dot{m}_N \frac{\rho_i}{\rho_N} \tag{3.103}$$

$$\phi = -0.0408 \times \left(T_1 - 273.15\right)^3 + 3.1218 \times \left(T_1 - 273.15\right)^2 - 80.238 \times \left(T_1 - 273.15\right) + 774.44 \tag{3.104}$$

where T_N, ρ_N, and $\dot{m}_N$ are ambient air absolute temperature, density and air mass flow rate at nominal or design condition respectively; T_i, ρ_i and $\dot{m}_i$ are ambient air absolute temperature, density and air mass flow rate at off-design conditions respectively; T_1 and ϕ are ambient air temperature and relative humidity respectively.

The mass flow rate of fuel will be computed by Ebsilon software according to the air ratio entered. In Ebsilon, the parameter that helps to control the maximum temperature obtained from the gas turbine cycle is represented by “ALAM” and is known as air ratio. For a given amount of fuel, the ratio of the actual mass flow rate of air to the stoichiometric mass flow rate of air is defined as the air ratio.

When the air ratio is changed, the combustion chamber will take in less or more fuel. The turbine inlet temperature of the cycle will also change. If the air ratio is increased more air will be accepted about close to the stoichiometric air, which will result in the reduction of turbine inlet and exhaust temperatures. However, the gas turbine inlet and exhaust temperatures will be increased when the air ratio is reduced.

3.8.5 Variation of Partload

When an amount of power delivered is lower or higher than the nominal power, which is enough for satisfying the demand, it is termed as partload operation by the gas turbine. This happens when the load demand is different from the nominal load. A controller will be introduced to take care of the load adjusting accordingly as needed. The off-design model for the partload variation is shown in Figure 3.8. Once the correct load is inputted in the controller the air ratio will be adjusted accordingly. The Ebsilon will then calculate the amount of air and fuel flow rates needed to generate the corresponding power. Partload of 40 – 110% of the nominal load condition was considered for this analysis. GT partload is controlled by using the “GT load level controller” to regulate the exhaust mass flow rate in the GT combustor and the range 40-110%.was used for the load variation analysis.

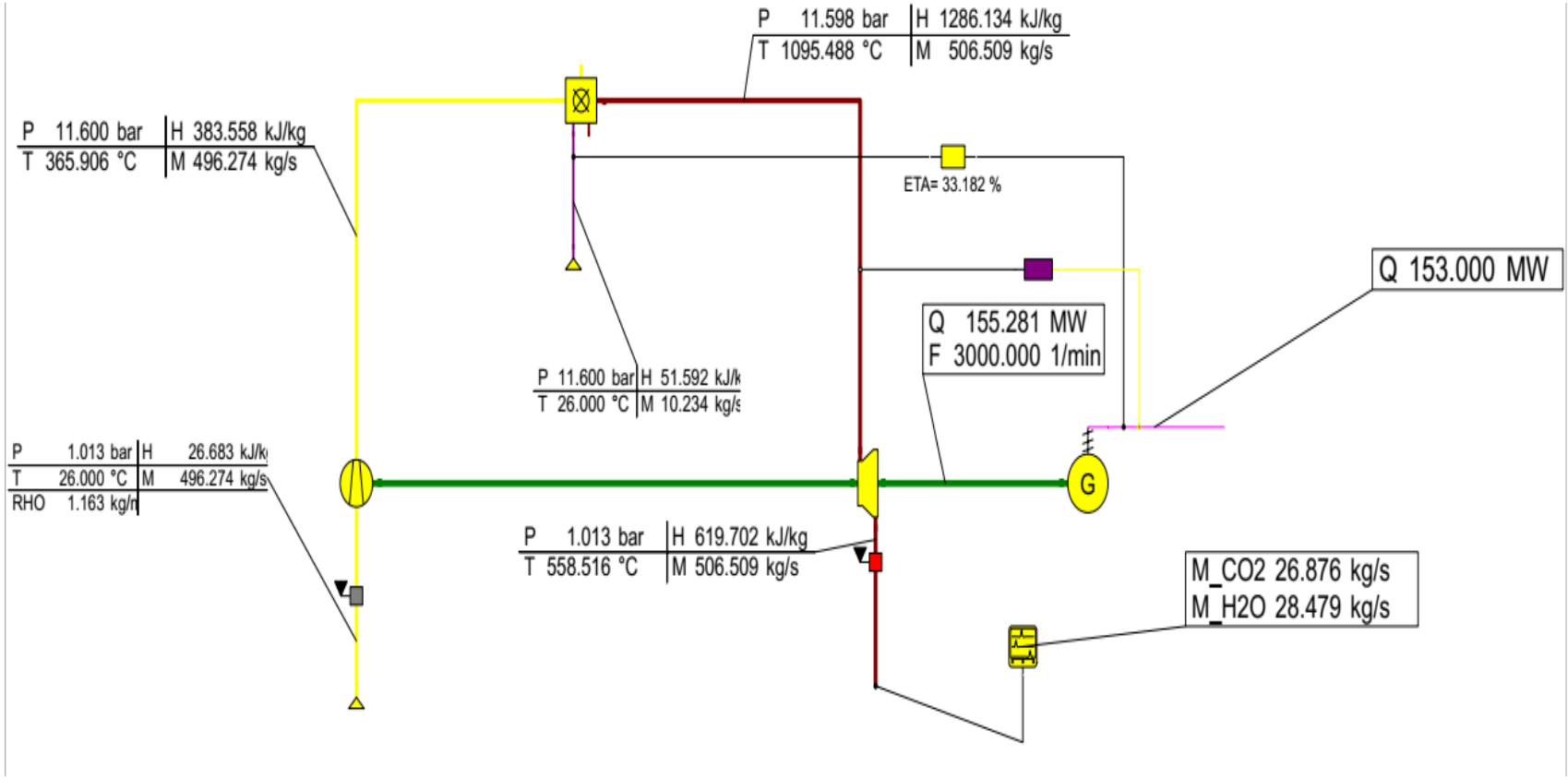

Figure 3.8: Topology of Azura Edo SGT5 – 2000E for Part Load Analysis

3.8.6 Variation of Efficiency in Components

The pressure ratio and power output of gas turbine change during off-design operations. The compressors and turbines' isentropic efficiencies are also affected. The isentropic efficiencies of the compressor and turbine vary directly to their mass flow rates. Normally, the designed or default isentropic efficiencies are used for design conditions simulation, while for off-design simulation the isentropic efficiencies will vary according to the actual mass flow rate. Tables 3.3 and 3.4 show the correction data for the compressor and turbine to take care of the variation between isentropic efficiencies and mass flow rates for off-design modelling and simulation. The isentropic efficiency values are denoted by ETAI as shown in Tables 3.3 and 3.4. Table 3.3 shows the variation of the ratio of mass flow of air at off-design to the mass flow of air at design with ratio of the isentropic efficiency of the compressor at off–design to isentropic efficiency of compressor at design for air compressor. Table 3.4 shows the variation of the ratio of the exhaust mass flow at off-design to the mass flow of exhaust at design with the ratio of the isentropic efficiency of turbine off-design to isentropic efficiency of gas turbine isentropic efficiency for design condition.

Table 3.3: Variation of Compressor Isentropic Efficiency with Mass flow Rate of Air

$\dot{m}/\dot{m}_N$	$ETAI/ETAI_N$
0	0
0.4	0.9
1	1
1.2	1.1

Table 3.4: Variation of Turbine Isentropic Efficiency with Mass flow Rate of Exhaust Gas

$\dot{m}/\dot{m}_N$	$ETAI/ETAI_N$
0	0.85
0.4	0.9
0.7	0.95
1	1
1.2	1.1

3.9 Ebsilon Model Validation

The model built is used for monitoring existing gas turbine power plant performance, the values obtained will be compared with the ISO and Azura Edo SGT5 – 2000E data. The power generated, exhaust mass flow rate, turbine exhaust temperature, and heat rate will be used for ISO condition validation, the power generated and heat rate will be used to validate the Azura Edo guarantee condition. The operating data from the three GTs will be used for the line operating validation for the model to show how the model mimic the actual operation of the power plant. Equation (3.105) was utilized to compute the percentage error in the model (Miguez Da Rocha, 2010; Amjady et al., 2011; Wallentinen, 2016; Azim and Farshid, 2017; Matjanov, 2020; Abbaspour et al., 2021).

$$\%\text{ModelError} = \frac{\left(\text{Actual data - Model data}\right)*100\%}{\text{Actual data}} \tag{3.105}$$

3.10 Performance Simulation with MATLAB

The thermodynamic and environmental performance of Azura Edo Power plant is estimated by component-wise modelling followed by a system simulation. A flow–sheet computer program "MATLAB R2017a software" is used for the analysis simulation. It is designed to be suited for the steady-state energy, exergy and environmental analysis of the Azura Edo Power Plant.

A MATLAB script was used for the energy, exergy, exergy improvement potential and carbon dioxide emission performance calculation of Azura Edo Power Plant. The MATLAB interference was written in this work to allow "hand-off" computation and generation of appropriate graphs as shown in Appendix I. The MATLAB scripts generated from Equations (3.3) to (3.101) employed in this study simulated the performance of the Azura Edo Power Plant.

3.11 Preliminary Analyses of Ways to Enhance the Plant Performance

To enhance the thermodynamic efficiency and environmental performance of the Edo Azura Gas Power Plant, preliminary studies of inlet air cooling incorporation and combined cycle operation were carried out. These preliminary studies were considered because their inclusion require little modifications and there are provisions for their incorporation into the existing Azura Edo Power Plant. The performances of the integrated models will be compared with the simple open cycle gas turbine power plant. The outcomes of the integration studies will help provide useful information for the Azura Edo Power Plant upgrade.

3.11.1 Energy Cost Analysis of Integrating Inlet Air Cooling System

Model Description

The schematic diagram of an integrated air intake cooling model for Azura Edo Power Plant is presented in Figure 3.9. The model consists of a pump that supplies treated water to the cooling chamber, which cools the air that flows into the air compressor.

It consists of a cooling tower, pump, spray cooler, compressor, combustion chamber, turbine, and generator. The cold water from the water treatment plant enters the cooler chamber, where it contacts the air entering the plant and reduces its dry bulb temperature to a value close to its initial wet-bulb temperature. The water from the sump of the spray cooler is returned to the cooling tower where it is cooled to ensure the continuation of the process.

The advantages of utilizing the evaporative cooling system as outlined by Al- Ibrahim and Varham (2010) include basic and dependable design and operation, low unit capital cost, low operational expenses, no restriction on schedule or length of inlet cooling process, low parasitic power consumption as well as fast delivery and installation. However, the disadvantages include

the demand for a large amount of treated water and high costs of maintenance that arise from water treatment and scaling.

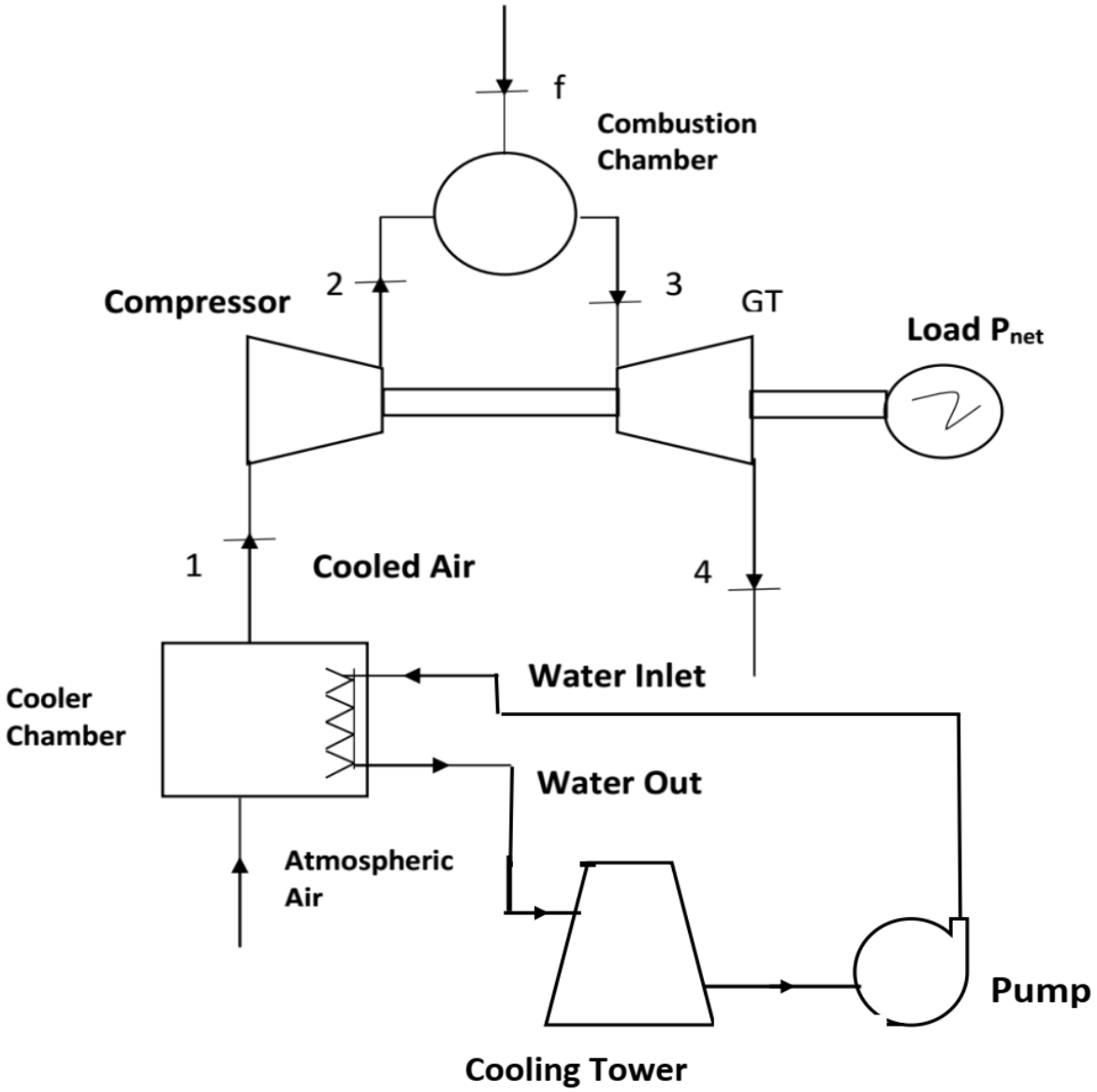

Figure 3.9: Schematic Diagram of Incorporation of an Intake Air – Cooling System

The energy cost study was carried out based on the ambient air being cooled from average ambient temperature (T_{av}) close to its wet-bulb temperature (T_1), using an evaporative cooling system

before entering the compressor. Equation (3.106) was used to determine the fuel saving per annum (FSPA) based on the different net thermal efficiency of cooling and without cooling system as stated in Rogers and Mayhew (1992); Salami (2004).

$$FSPA_{cooling} = \left(\frac{1}{\eta_{av}} - \frac{1}{\eta_o} \right) * power * OPT * \frac{LF}{LHV} * \frac{\text{Cost of fuel}}{mass / therm} \tag{3.106}$$

The water vapour saturation pressure (p_s) can be taken from Rogers and Mayhew (1995) at T_{av}. The water vapour partial pressure can be computed using Equation (3.77). The moisture content of air was calculated by applying Equation (3.107).

$$\omega = \frac{0.622 p_v}{p - p_v} \tag{3.107}$$

The specific heat capacity of moist air at constant pressure (c_{pma}) was computed by Equation (3.108) as stated in Jones (1985).

$$c_{pma} = c_{pda} + \omega c_{ps} \tag{3.108}$$

where c_{pda} and c_{ps} are specific heat capacities at constant pressure for dry air (1.005kJ/kgK) and water vapour (1.88kJ/kgK) respectively.

The cooling load (Qc) was determined using Equation (3.109) as stated in Cengel and Boles (2010).

$$Q_c = \dot{m}_a * c_{pma} * \left(T_{av} - T_1 \right) \tag{3.109}$$

Equations (3.110) – (3.112) were utilized to evaluate the different costs, for example, capital incremental installation cost, operation and maintenance cost.

$$\text{Capital cost, Cc} = Q_c * \text{unit incremental cost of cooling} \tag{3.110}$$

where, unit capital cost for incorporating the inlet air cooling system is US $468/kW (El-Shazly et al., 2016).

The operating and maintenance cost (OMC) is assumed to be 10% of the capital cost per annum (Yazdi et al., 2020).

Operation and maintenance cost, $OMC = 0.1 * Cc$ (3.111)

Total Cost, $TC = Cc + OMC$ (3.112)

The profit obtained as a result of income obtained from FSPA was determined utilizing Equation (3.108).

Profit, $Pt = FSPA_{cooling} - TC$ (3.113)

The reduction of GHG emission regarding carbon dioxide obtained by incorporating an intake air cooling system was assessed utilizing Equations (3.114) and (3.116) in MW/h and $kgCO_2/yr$ respectively as stated in Arsalis and Alexandrou (2014); Kanbur et al. (2017). The values of ξ_{co2} and m_{pco2}/year for with cooling and without cooling systems were determined from the environmental model at T_1 and T_{av} ambient air temperatures.

$$\xi_{CO_2(saving)} = \xi_{CO_2(\text{without cooling})} - \xi_{CO_2(\text{with cooling})} \quad (3.114)$$

$$m_{pCO_2/yr(saving)} = m_{pCO_2/yr(\text{without cooling})} - m_{pCO_2/yr(\text{with cooling})} \quad (3.115)$$

$$ER_{cooling} = \left(1 - \frac{\xi_{CO_2(cooling)}}{\xi_{CO_2(without\ cooling)}}\right) \quad (3.116)$$

where "ER denotes the emission reduction as a result of comparison between the without and with cooling systems" as stated in Kanbur et al. (2017).

The proposed air inlet cooling system using an evaporative cooler for Azura Edo Power Plant was modelled with Ebsilon software and the results are presented in Figure 3.10.

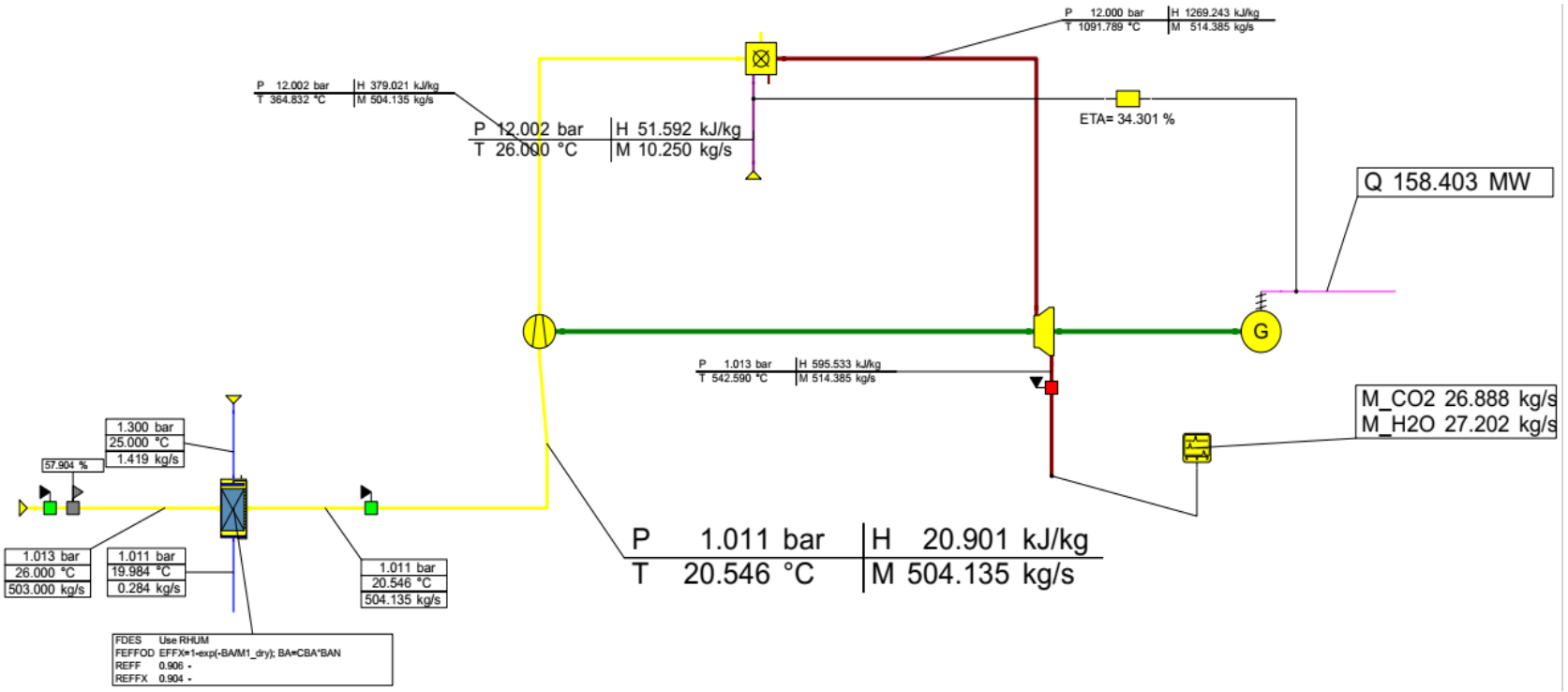

Figure 3.10: Topology of an Air Inlet Cooling System Model

3.11.2 Energy Cost Analysis of Integrating Heat Recovery Steam Generator

(a) Model description of the combined cycle

In this analysis, the topping cycle (Brayton cycle) and the bottoming cycle (Rankine cycle) were utilized for the combined cycle power plant model. Figure 3.11 represents the schematic diagram of the proposed model. The gas turbine main components considered for the analysis are a compressor, combustion chamber, gas turbine, and generator; while the HRSG, steam turbine, condenser, feed pump and generator were the components used for Rankine Cycle.

The air flows into the compressor. It is compressed and flows into the combustor. In the combustion chamber, fuel (natural gas) is supplied, which burns with compressed air to increase its temperature. The burnt gases flow into the gas turbine when they are expanded to generate power. The flue gases flow into the Heat Recovery Steam Generator (HRSG) before exiting the plant to the environment. The flue gases from the gas turbine flowing through the HRSG is used to generate steam that circulates in the bottom cycle. The steam is expanded in the steam turbine to produce electrical power; it then passes to the condenser after which the feed pump pumps it back to the HRSG.

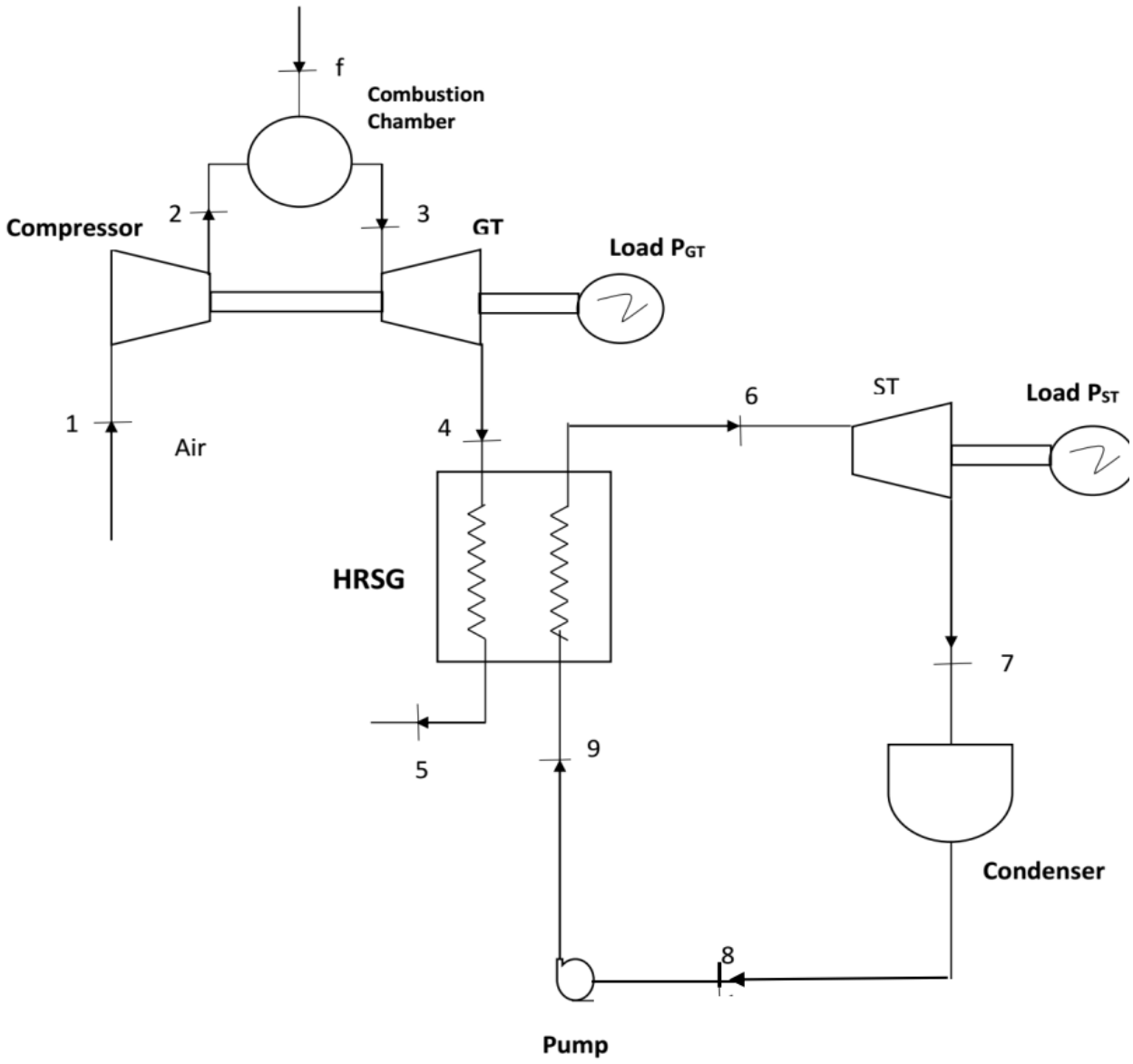

Figure 3.11: The Schematic Diagram of the Combined Cycle Model

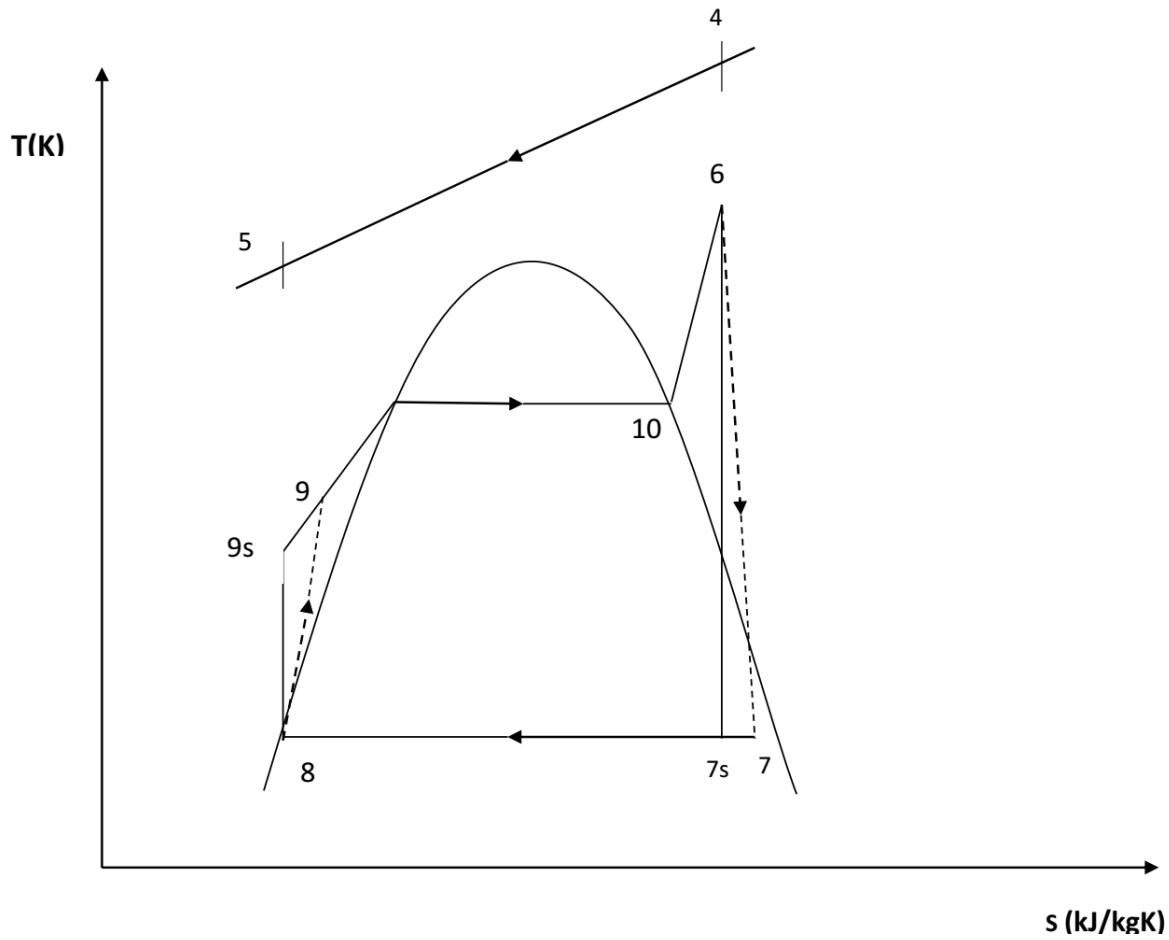

Figure 3.12: T-s Diagram of Combined Cycle Model

(b) Model analysis

The evaluation of the Rankine cycle will be carried out by applying Equations (3.117) to (3.129) for the combined cycle model utilizing the gas turbine outcome parameters. The performance of the open simple gas turbine and combined cycle model will be compared in terms of their thermal efficiencies.

Figure 3.12 represents the temperature-specific entropy (T-s) diagram of the model. The energy balance for water and gas in each stream of the HRSG is used to determine the water and gas properties. The states indicated in Figures 3.11 and 3.12 were applied in Equations (3.117) to

(3.122) as expressed in Rogers and Mayhew (1992); Cengel and Boles (2010) to determine the model performance.

The gas turbine's available heat through exhaust gases was evaluated by utilizing Equation (3.117).

$$Q_s = \dot{m}_g * c_{pg} * (T_4 - T_5) * \eta_{th} \tag{3.117}$$

where η_{th} is the HRSG heat transfer efficiency from the exhaust gas to steam, 90% was assumed.

The specific enthalpies of states 6 – 10 can be obtained from corresponding pressure and temperature tables by Rogers and Mayhew (1995). The steam temperature according to Fisk and VanHousen (1996) is typically 10 ^{0}C (or more) lower than the turbine exhaust gas temperature for effective heat transfer between exhaust gas and steam. A typical pinch temperature difference ranges from 8 ^{0}C to 15 ^{0}C (Buecker, 2002; Pooneh, 2012), which is the difference between the temperature of the flue gas and temperature of the evaporator steam outlet at that point in the Heat Recovery Steam Generator. The steam temperature and pressure were selected based on this condition. The energy balance between the water and exhaust gas properties was utilized to evaluate the mass flow rate of steam (m_s) from the HRSG as expressed in Equation (3.118).

$$\dot{m}_s = \frac{Q_s}{h_6 - h_9} \tag{3.118}$$

The power output of the steam turbine was calculated by applying Equation (3.119).

$$P_{ST} = \dot{m}_s (h_6 - h_7) \tag{3.119}$$

The pump power input was calculated by applying Equation (3.120).

$$P_{89} = 100\dot{m}_s * v_{f8} * (p_9 - p_8) \tag{3.120}$$

The Rankine cycle net power output was computed as expressed in Equation (3.121).

$$p_{STnet} = \left(P_{ST} - P_{89}\right) * \eta_{mech} * \eta_{gen} - P_{STaux} \tag{3.121}$$

The combined cycle power plant model's overall thermal efficiency was determined using Equation (3.122).

$$\eta_{combined} = \frac{P_{STnet} + P_{GT}}{\dot{m}_f * LHV} \tag{3.122}$$

Equation (3.123) was utilized to calculate the fuel saving per annum (FSPA) as given by Rogers and Mayhew (1992); Salami (2004).

$$FSPA_{combined} = \left(\frac{1}{\eta_{GT}} - \frac{1}{\eta_{overall}}\right) * \left(P_{GT} + P_{STnet}\right) * OPT * \frac{LF}{LHV} * \frac{\text{Cost of fuel}}{mass / therm} \tag{3.123}$$

The unit capital cost of implementing the Rankine cycle in the combined cycle is $550/kW (Frey and Zhu, 2012)

$$\text{Capital cost (combined)} = P_{STnet} * \text{unit incremental power cost} \tag{3.124}$$

Assume operation and maintenance cost of 10% per annum (Kehlhofer et al., 2009)

$$\text{Operation and Maintenance cost, } OMC_{combined} = 0.1 * Cc(\text{combined}) \tag{3.125}$$

$$\text{Total cost, } TC_{combined} = Cc_{combined} + OMC_{combined} \tag{3.126}$$

Assuming simple linear calculation and other conditions are the same.

$$\text{Cost Recovery Period} = \frac{TC}{FSPA_{combined}} \tag{3.127}$$

The environmental analysis was carried out to compare the simple cycle with the combined cycle. The emission rate and emission reduction of carbon dioxide computation were performed using Equations (3.128) to (3.130) as stated in Arsalis and Alexandrou (2014); Kanbur et al. (2017).

$$\xi_{CO_2(GT)} = \frac{\dot{m}_{Co_2}}{P_{net(GT)}} \tag{3.128}$$

$$\xi_{CO_2(combined)} = \frac{\dot{m}_{Co_2}}{P_{net(combned)}} \tag{3.129}$$

$$ER_{combined} = \left(1 - \frac{\xi_{CO_2(combined)}}{\xi co_{2(GT)}}\right) \tag{3.130}$$

Where ξ_{CO_2} (GT) and ξ_{CO_2} (combined) are carbon dioxide emission rates for the simple and combined cycles respectively obtained from the environmental analysis section. “ER denotes the emission reduction as a result of comparison between the simple cycle and combined cycle” as stated in Kanbur et al. (2017).

The proposed combined cycle power plant model was also developed in Ebsilon software using various pressures for HRSG. The single pressure, double pressure, and triple pressure HRSG Models in Ebsilon software are illustrated in Figures 3.13 to 3.15 respectively. The performance of the different pressure HRSGs were evaluated using Equations (3.123) to (3.130). A recommendation will be made based on the outcome of their performances.

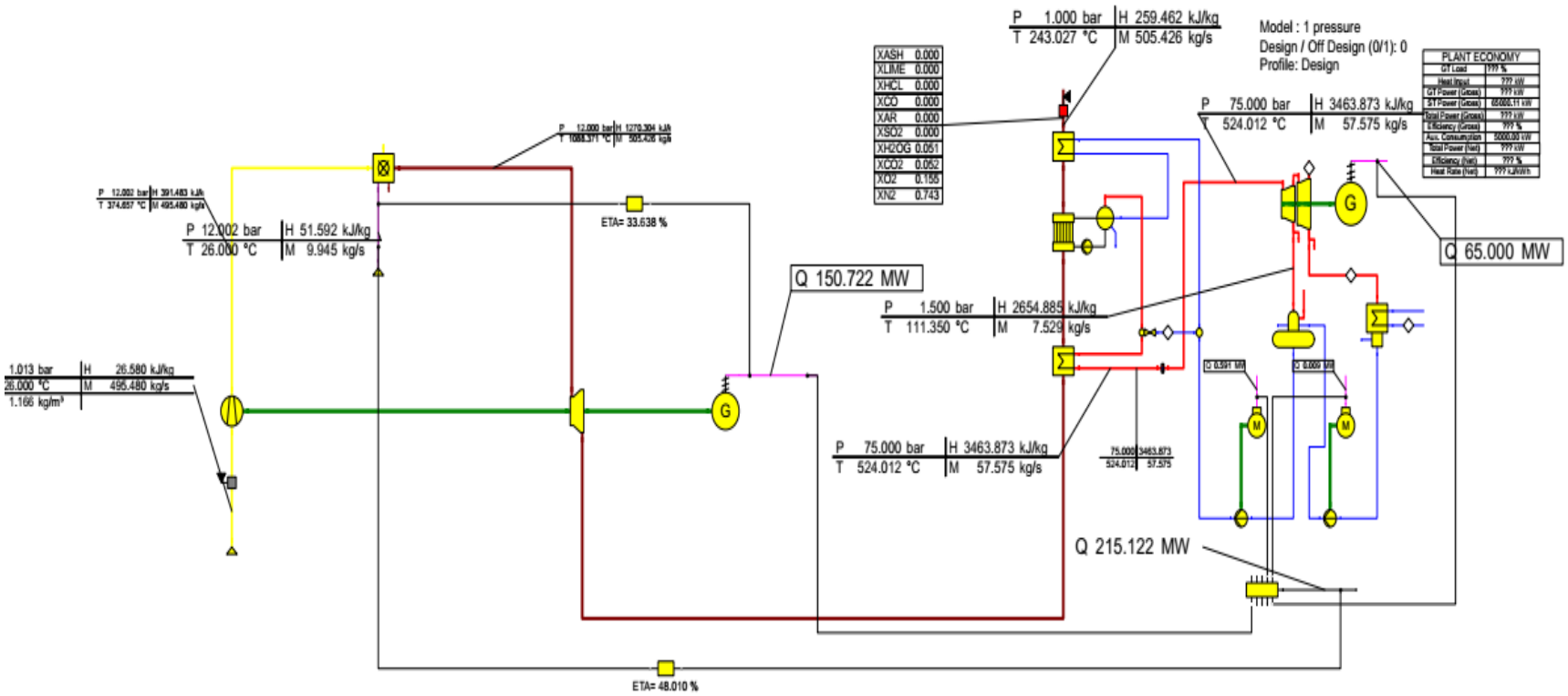

Figure 3.13: Topology of a Single Pressure HRSG Combined Cycle Power Plant Model

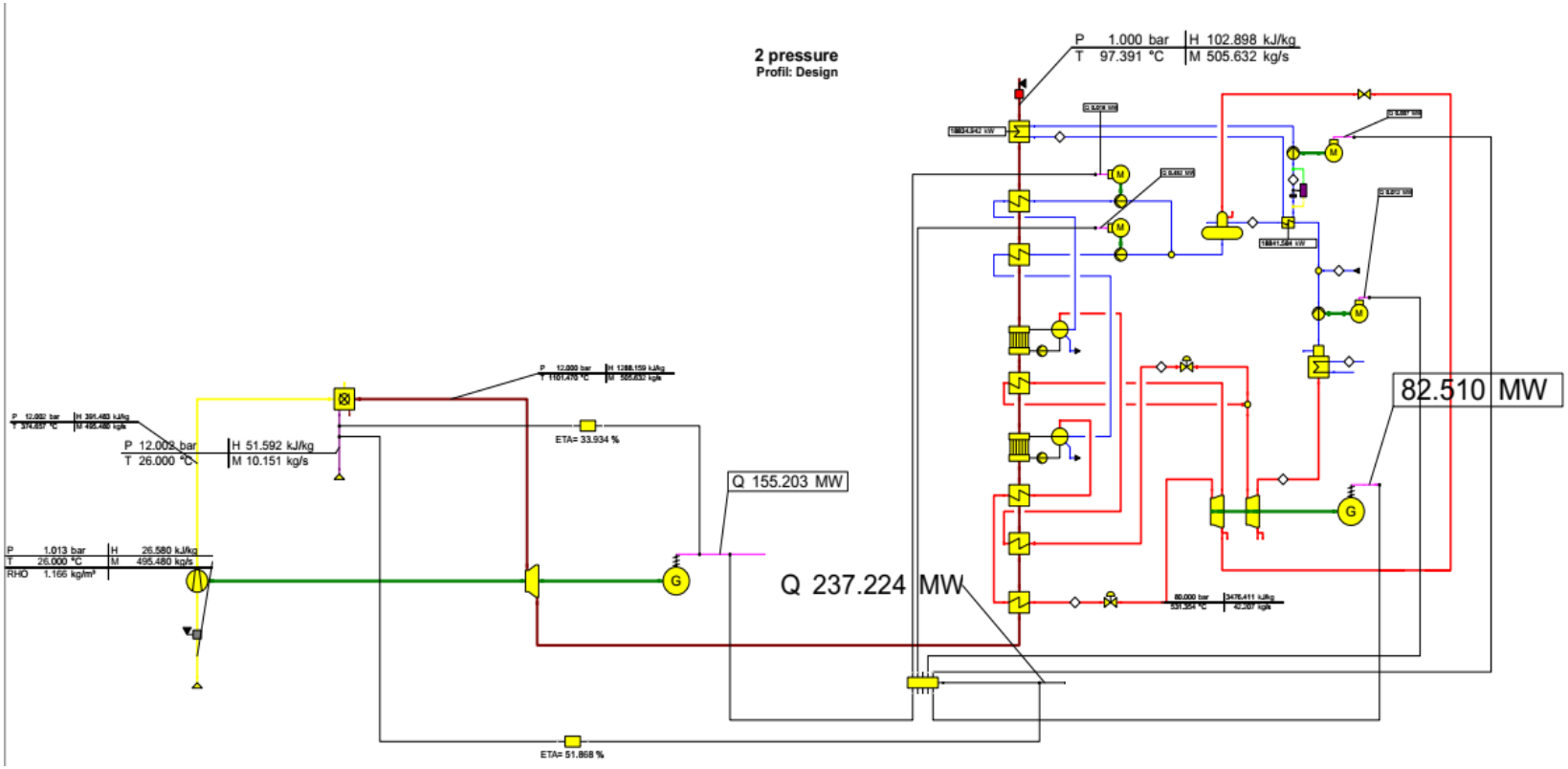

Figure 3.14: Topology of a Double Pressure HRSG Combined Cycle Power Plant Model

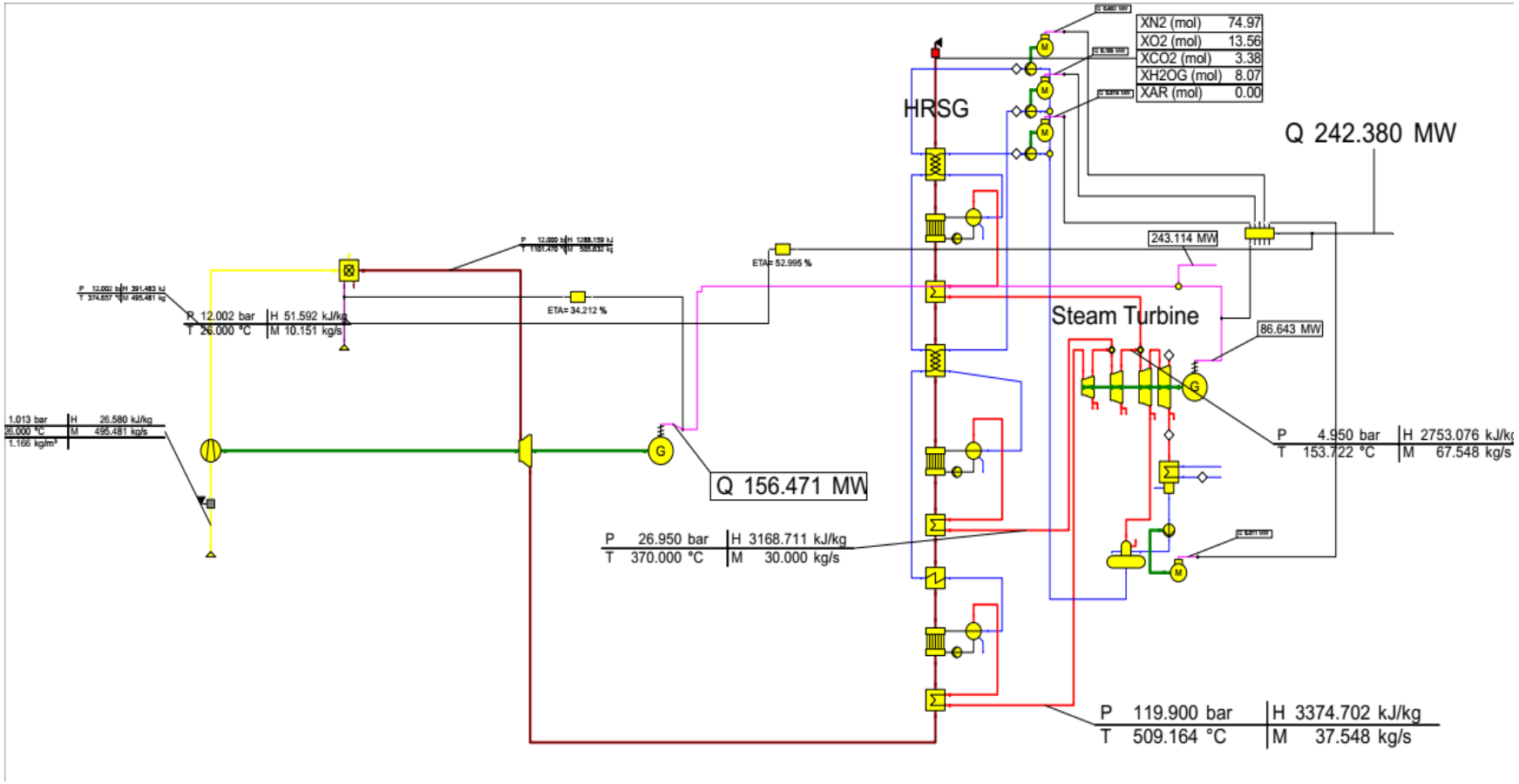

Figure 3.15: Topology of a Triple Pressure HRSG Combined Cycle Power Plant Mode

CHAPTER FOUR

RESULTS AND DISCUSSION

4.1 Presentation of Results

The operating data collected for December 2017 to December 2020, which was the period of study for GT11, GT12 and GT13 are presented respectively in Tables A11 to A13 of Appendix II. The parameters such as temperatures, pressures, mass flow rates, power output were recorded at full loads. Also, the average operating data for the three GT units are presented in Appendix II. All the results obtained in this study are presented in the section.

4.1.1 Simulation for the Gas Turbine Power Units

In this research work, Ebsilon Professional 11.4 was used for the modeling and simulation of SGT5 – 2000E. The validation and analysis of results for the performance simulation of SGT5 - 2000E for design and off-design conditions are presented in the section.

Model Validation

The validation results of the SGT5 – 2000E model for both ISO and Azura Edo guaranteed conditions developed in Ebsilon are presented in Table 4.1. Equation (3.105) was used to compute the percentage error or deviation between the design data and model data. This was carried out to ensure that the model is consistent with the ISO design data, which form the root profile of the model.

Table 4.1: Results of Model Validation for ISO Design and Azura Edo Guarantee Data

	ISO Design condition				
S/N	Parameters	Design	Model	Diff	%Error
1	Power (MW)	166	165.128	0.872	0.525301
2	Heat Rate(kJ/kWh)	10375	10411.55	-36.5452	-0.35224
3	Thermal Efficiency (%)	34.7	34.577	0.123	0.354467
4	Turbine Exhaust Temperature (^{0}C)	541	542.389	-1.389	-0.25675
5	Exhaust mass flow rate (kg/s)	525	525	0	0
	Azura Edo Guarantee Condition				
S/N	Parameters	Design	Model	Diff	%Error
1	Power (MW)	10528	10858	-330	-3.1345
2	Heat Rate(kJ/kWh)	153	151.645	1.355	0.885621

Ambient Temperature Variation

The ambient temperature ranging from 15 ^{0}C to 35 ^{0}C was utilized in the Ebsilon Model developed to evaluate the power plant performance. The variation of density and the air mass flow rate for various ambient temperatures were determined using Equations (3.102) and (3.103) and the outcome is presented in Table 4.2. The relative humidity values obtained using Equation (3.104) are illustrated in Table 4.3.

Table 4.2: Model Results for Density and Air Mass Flow Rate for Various Ambient Air Temperatures

T (^{0}C)	T (K)	Density (kg/m^3)	$\dot{m}_a$ kg/s)
15	288.15	1.215	514.395
26	299.15	1.170323	495.4803
21	294.15	1.190217	503.9025
22	295.15	1.186184	502.1952
23	296.15	1.182179	500.4995
24	297.15	1.1782	498.8151
25	298.15	1.174249	497.1421
26	299.15	1.170323	495.4803
27	300.15	1.166424	493.8295
28	301.15	1.162551	492.1897
29	302.15	1.158703	490.5607
30	303.15	1.154881	488.9425
31	304.15	1.151084	487.3349
32	305.15	1.147312	485.7379
33	306.15	1.143564	484.1513
34	307.15	1.139841	482.575
35	308.15	1.136142	481.009

Table 4.3: Temperature and Relative Humidity Relationship for Azura Edo Power Plant Location

S/N	T(^{0}C)	ϕ (%)
1	20	92
2	21	88.307
3	22	85.7168
4	23	83.9846
5	24	82.8656
6	25	82.115
7	26	81.488
8	27	80.7398
9	28	79.6256
10	29	77.9006
11	30	75.32
12	31	71.639
13	32	66.6128
14	33	59.9966
15	34	51.5456
16	35	41.015

The various values of relative humidity and air mass flow rates in Tables 4.2 and 4.3 were used in off-design modelling for ambient air temperature as described in Section 3.8.4 and the model performance results are showed in Table C1 of Appendix V. The turbine inlet and exhaust temperature evolution with ambient air for off-design conditions are shown in Figure 4.1.

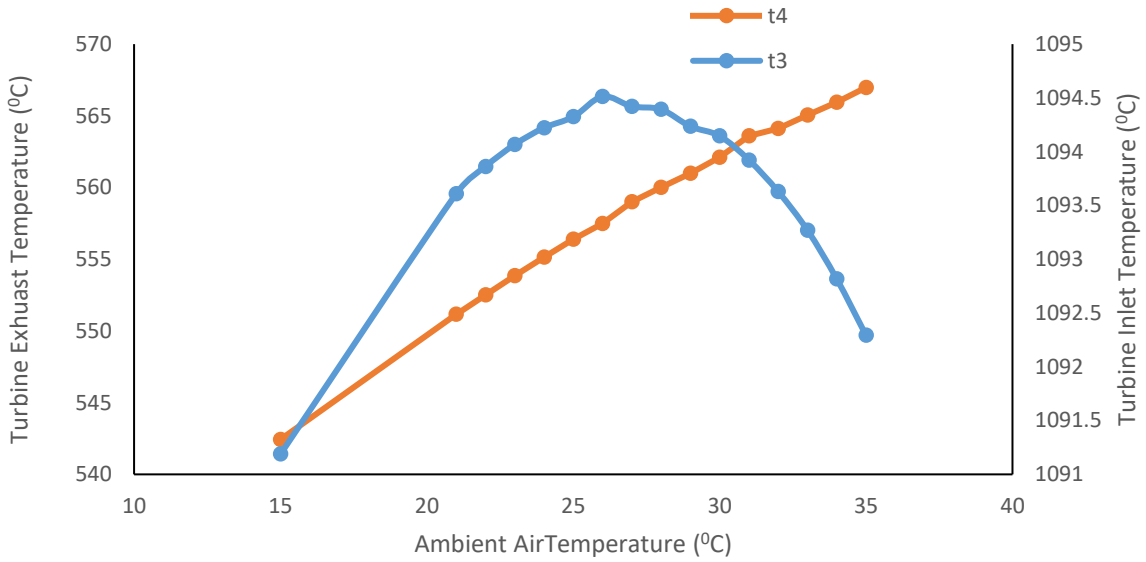

Figure 4.1: Model Variation of Turbine Inlet and Exhaust temperatures with ambient air temperature

Partload Performance

The various values obtained from the 40% to 110% partload off-design condition that was discussed in Section 3.8.5 are shown in Table 4.4. Figure 4.2 presents the variation of the mass flow rate and gas turbine temperature ratios with power part load ratio.

Table 4.4: Model Results for Partload Variation off – Design

S/N	Part Load (%)	$\dot{m}_a$ (kg/s)	$\dot{m}_f$ (kg/s)	$\dot{m}_g$ (kg/s)	AR	t_4 (^{0} C)	t_3 (^{0} C)	p_3 (bar)	η_{th} (%)	P_{net} (MW)	$\dot{m}_{co2}$	p_2 (bar)	r_{pc}	r_{pt}
1	110	495.37	11.073	506.449	2.86	593.68	1152.13	11.83	33.736	168.3	29.06	11.84	11.68	11.68
2	100	496.274	10.234	506.509	3.1	558.52	1095.49	11.60	33.182	153	26.88	11.60	11.45	11.45
3	90	494.846	9.415	504.261	3.36	526.38	1041.90	11.32	32.462	137.7	24.74	11.32	11.17	11.17
4	80	496.186	8.573	504.759	3.7	489.37	981.76	11.07	31.689	122.4	22.55	11.07	10.93	10.93
5	70	496.334	7.739	504.073	4.1	453.39	922.58	10.80	30.719	107.1	20.38	10.80	10.66	10.66
6	60	496.638	6.902	503.54	4.6	416.42	861.72	10.51	29.521	91.8	18.2	10.51	10.38	10.37
7	50	496.186	6.065	502.251	5.23	379.30	799.77	10.20	27.251	76.5	16.02	10.20	10.07	10.06
8	40	495.249	5.224	500.473	6.06	341.41	736.01	9.86	26.1	61.2	13.83	9.86	9.73	9.73

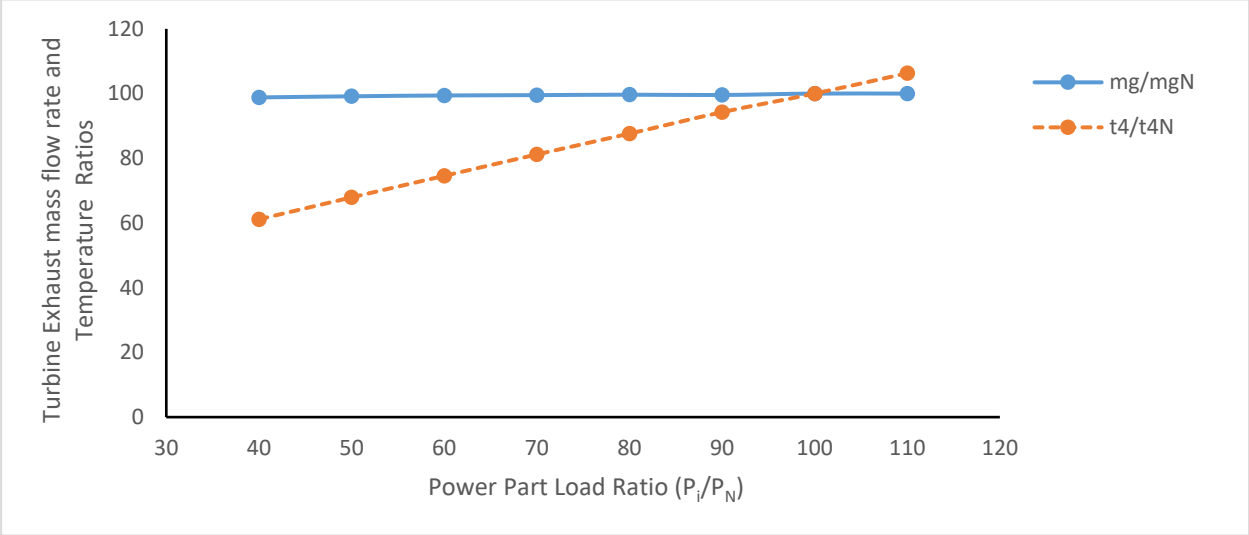

Figure 4.2: Variation of the Gas Turbine Exhaust Mass Flow Rate and Exhaust Temperature Ratios with Power Load Ratio

Comparison of Model Data with Actual Operating Data

As mentioned in Section 3.9, the model validation was done in two ways. The first was presented in Section 4.1.1 for the ISO design and Azura Edo guaranteed conditions. The second is presented in this section, for the validation of the model results with actual operating data from the Azura Edo Power plant. The compressor exit, turbine inlet and exhaust temperatures, air, fuel, and exhaust mass flow rates, and net power out from GT11, GT12 and GT13 at various states were compared with model data. The variations of the operating and model data with ambient air

temperature for the various GT units are presented in Figures 4.3 to 4.9. The summary of the resulting errors between model data and operating data for various parameters and GT units is presented in Table 4.5.

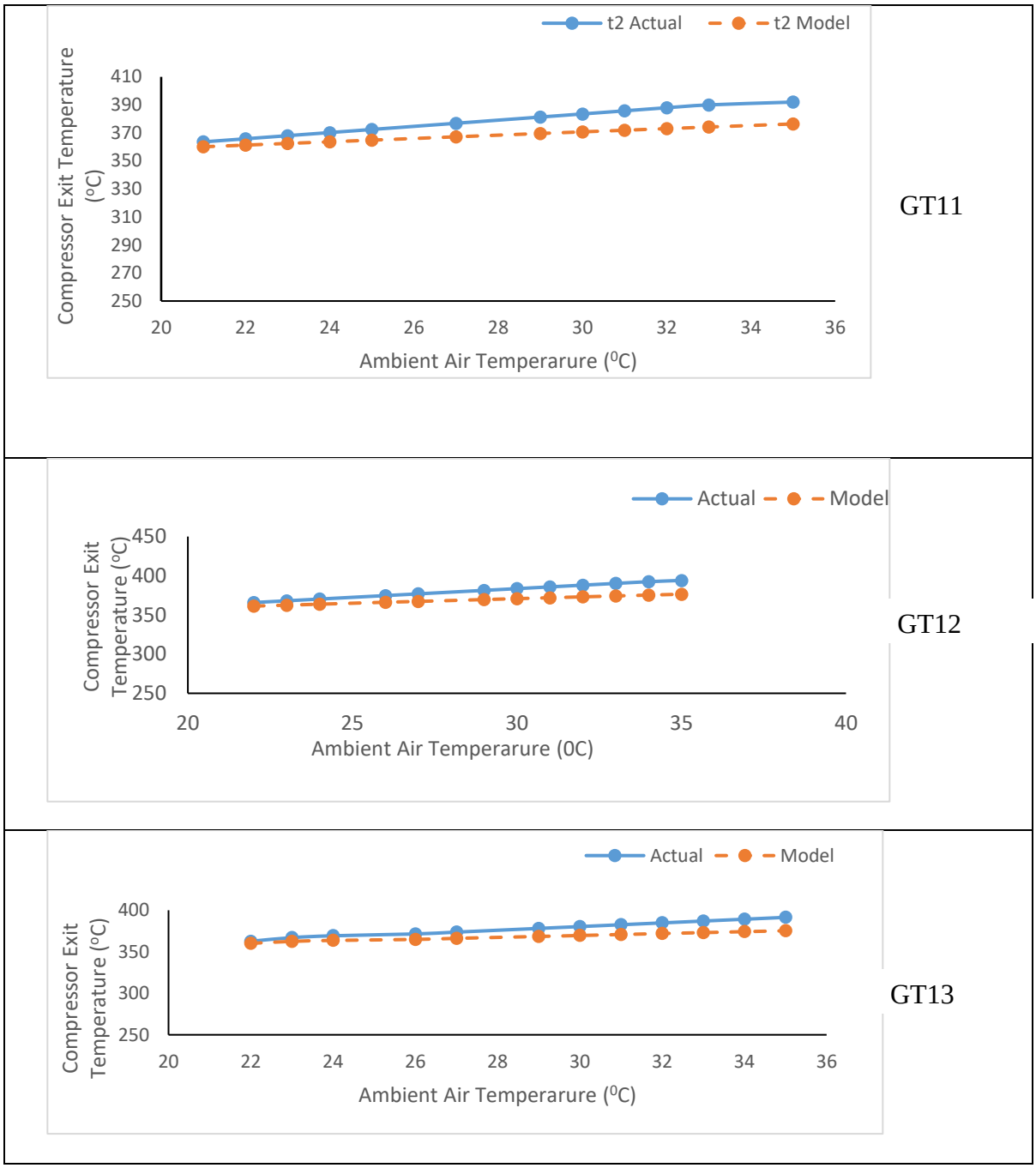

Figure 4.3: Model Validation for Variation in Compressor Exit Temperature with Ambient Air Temperature for the GTs

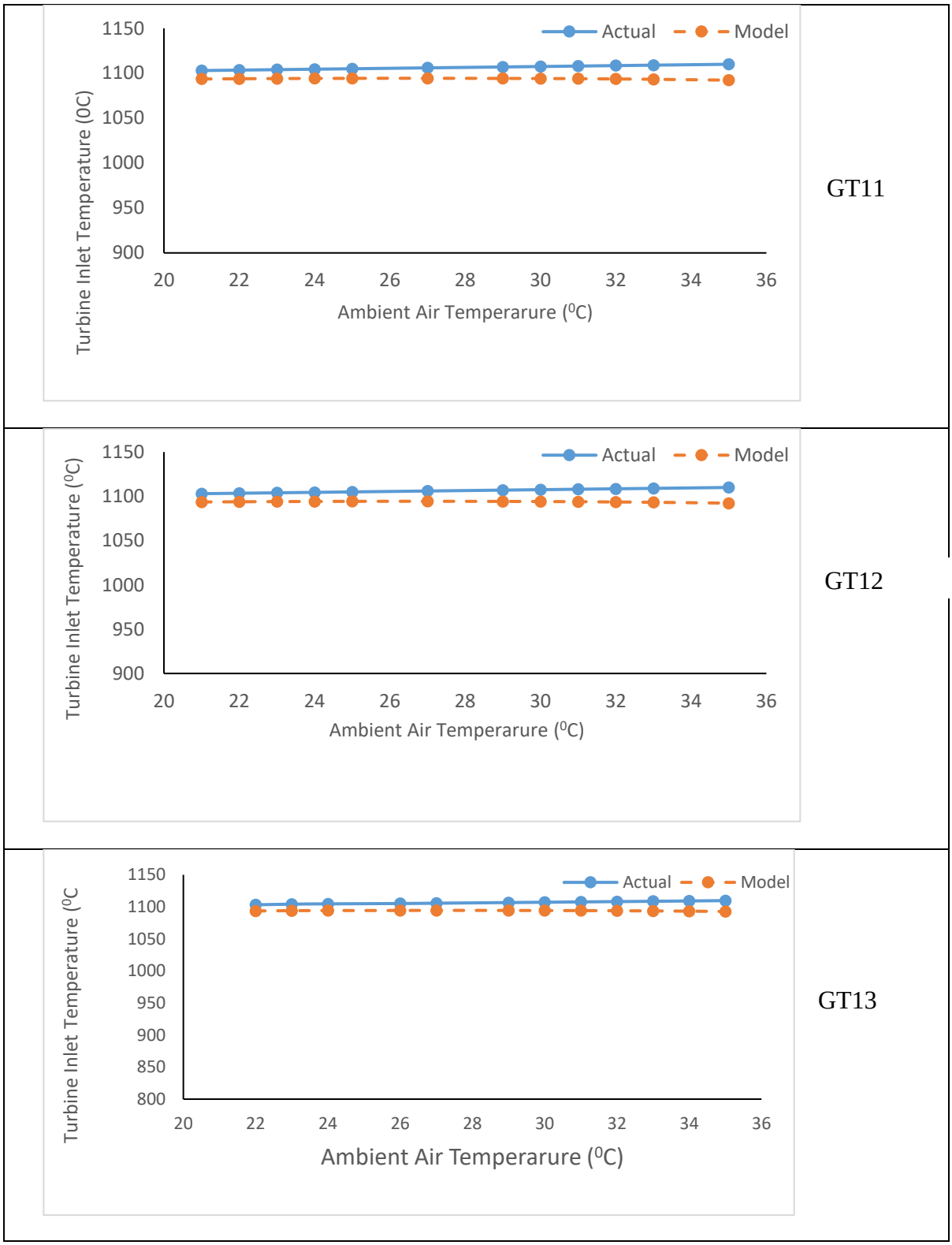

Figure 4.4: Model Validation for Variation in Turbine Inlet Temperature with Ambient Air Temperature for the GTs

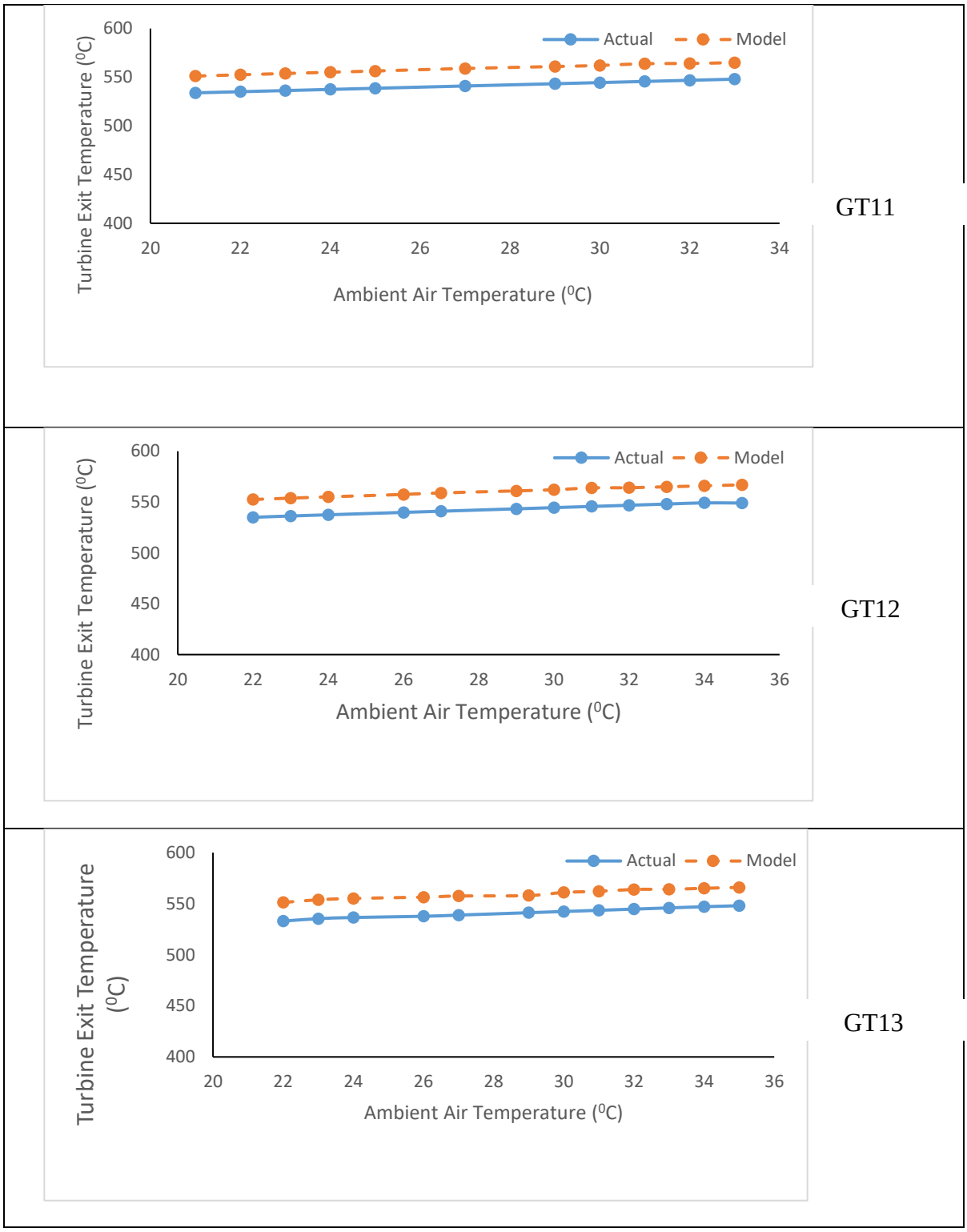

Figure 4.5: Model Validation for Variation in Turbine Exhaust temperature with Ambient air Temperature for the GTs

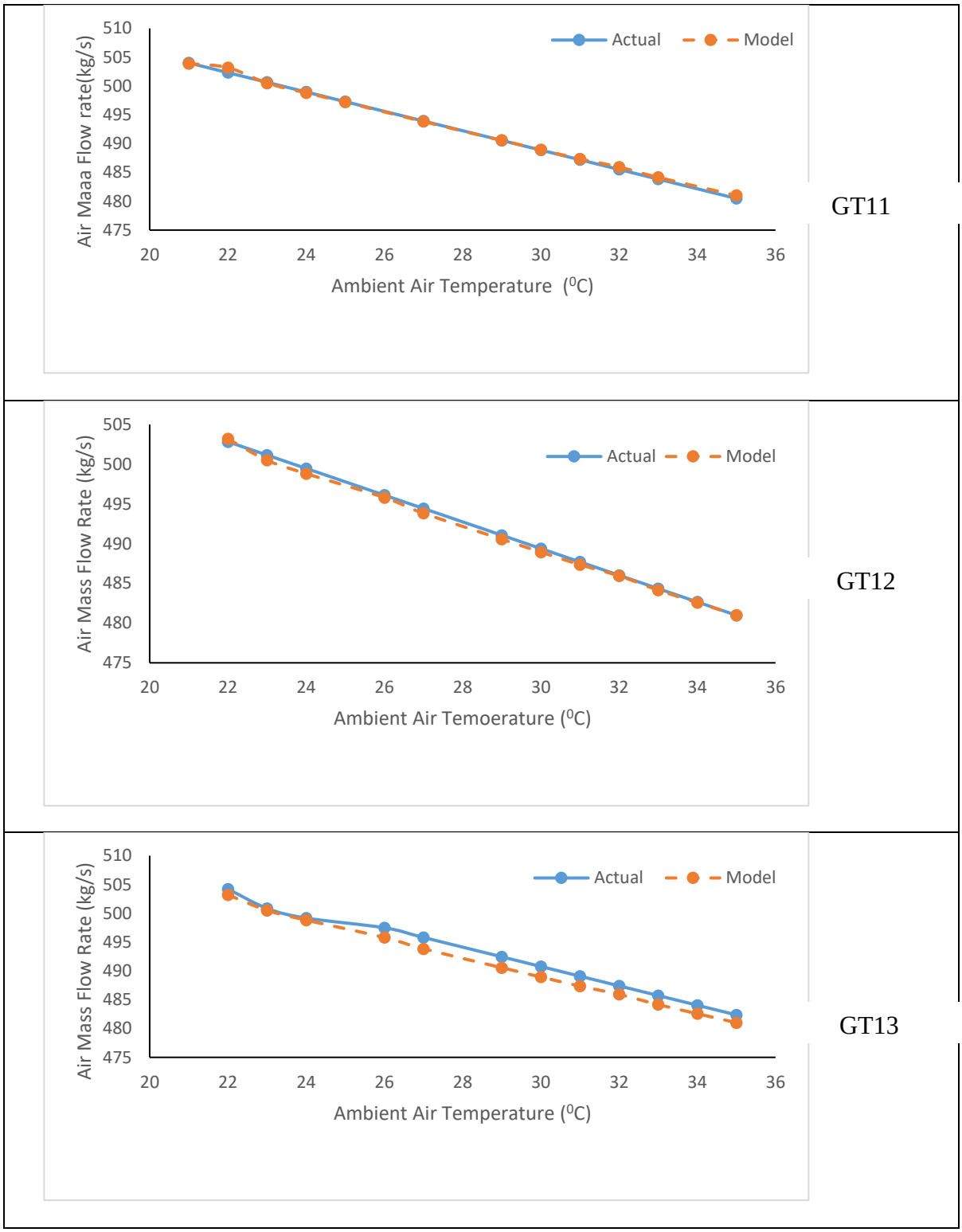

Figure 4.6: Model Validation for Variation in Air Mass Flow Rate with Ambient Air Temperature for the GTs

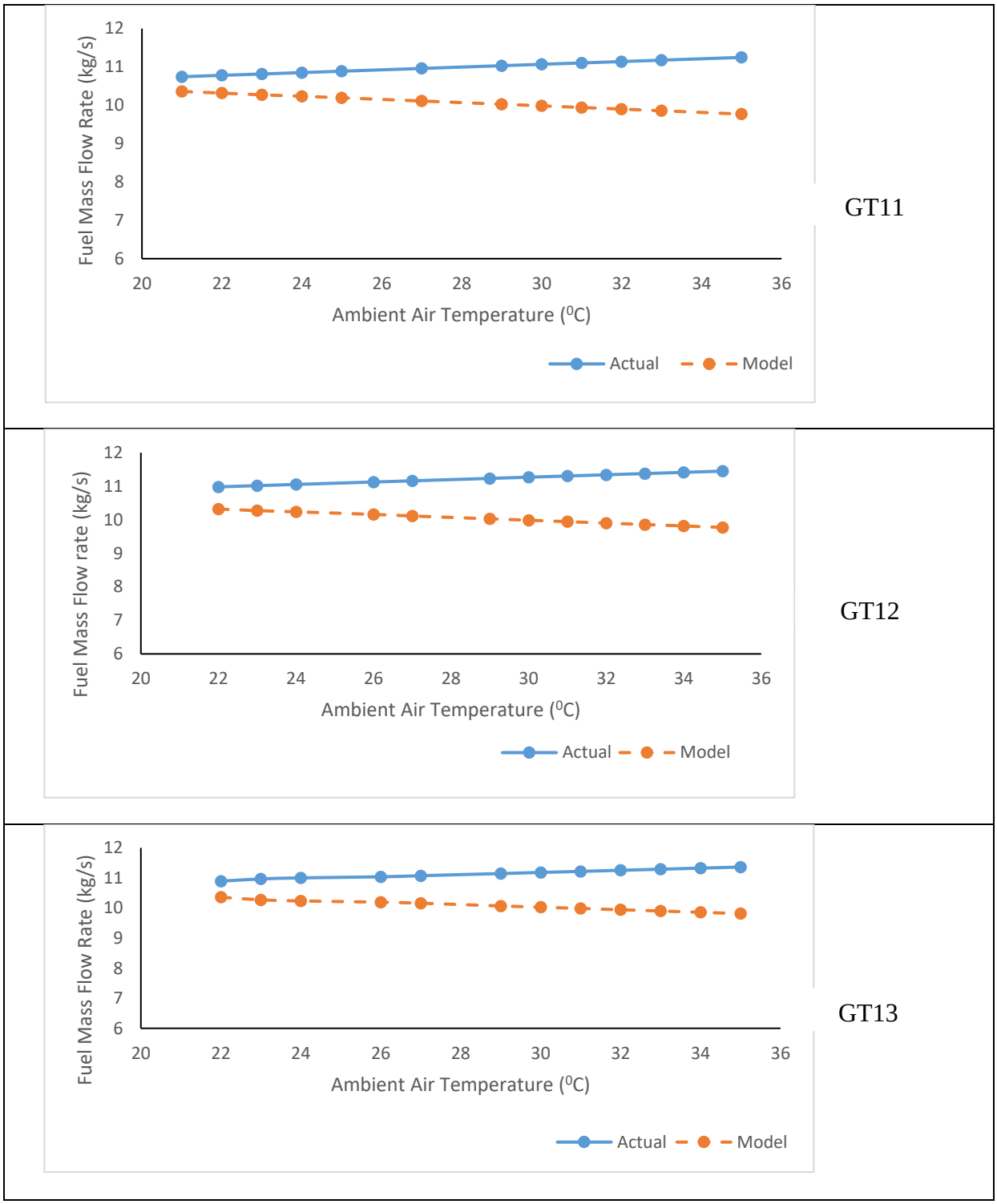

Figure 4.7: Model Validation for Variation in Fuel Mass Flow Rate with Ambient Air Temperature for the GTs

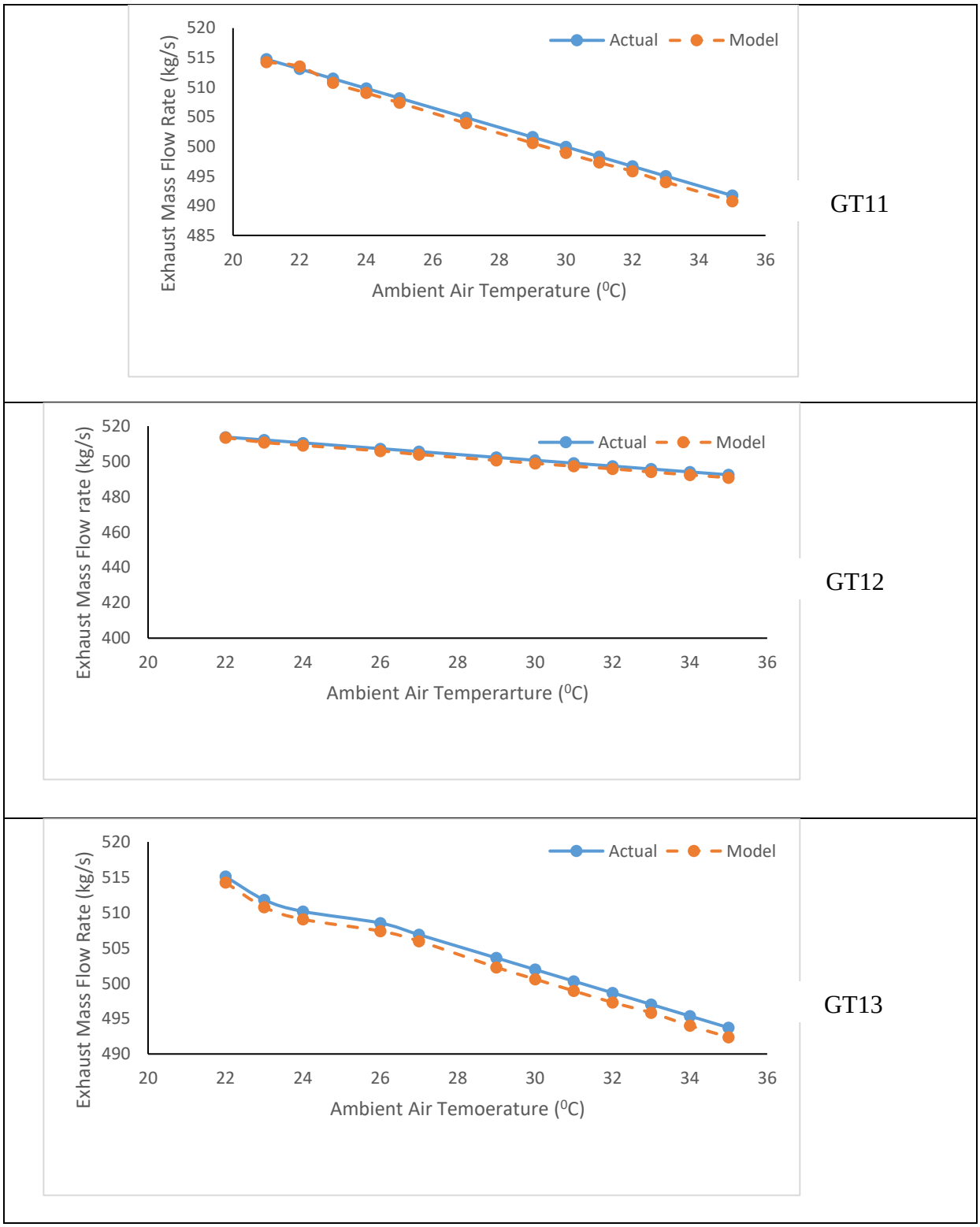

Figure 4.8: Model Validation for Variation in Exhaust Mass Flow Rate with Ambient Air Temperature for the GTs

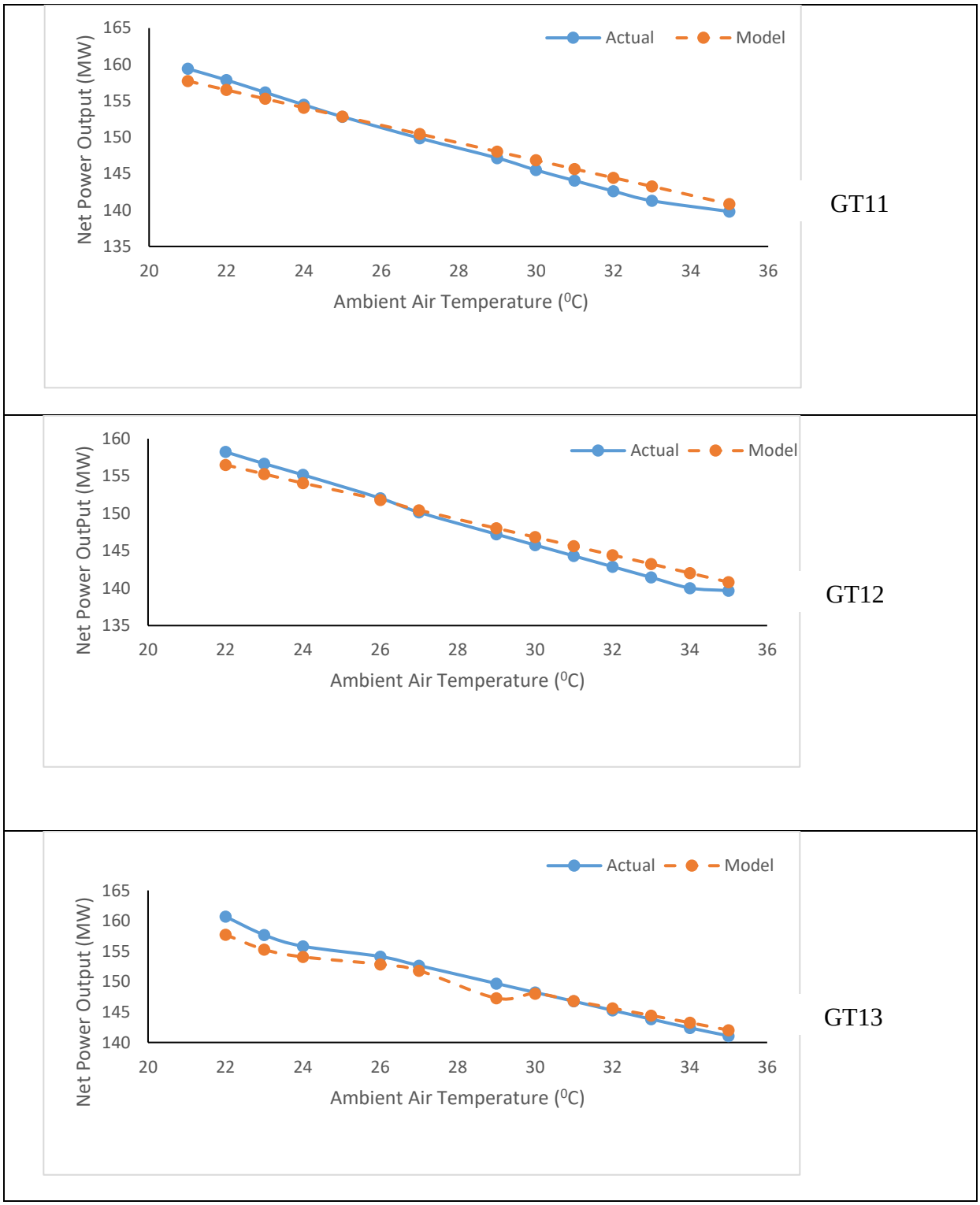

Figure 4.9: Model Validation for Variation in Net Power Output with Ambient Air Temperature for the GTs

Table 4.5: Model Validation Results for GT11, GT12 and GT13

% Error																					
	T_2			T_3			T_4			m_a			m_f			m_g			P_{net}		
S/N	GT11	GT12	GT13	GT11	GT12	GT13	GT11	GT12	GT13	GT11	GT12	GT13	GT11	GT12	GT13	GT11	GT12	GT13	GT11	GT12	GT13
1	0.96	1.23	0.69	0.85	0.92	0.87	-3.22	-3.27	-3.42	0.02	-0.07	0.20	3.58	6.03	4.91	0.10	0.06	0.16	1.06	1.10	1.85
2	1.234	1.50	1.24	0.87	0.94	0.92	-3.25	-3.27	-3.46	-0.17	0.13	0.07	4.29	6.75	6.33	-0.08	0.27	0.20	0.86	0.88	1.52
3	1.504	1.78	1.51	0.90	0.98	0.95	-3.27	-3.29	-3.48	0.03	0.13	0.07	5.03	7.39	6.97	0.14	0.29	0.22	0.56	0.71	1.13
4	1.777	2.27	1.78	0.93	1.04	0.98	-3.29	-3.27	-3.49	0.03	0.06	0.34	5.69	8.67	7.65	0.15	0.25	0.22	0.26	0.15	0.83
5	2.047	2.57	2.01	0.97	1.09	1.01	-3.30	-3.33	-3.46	0.02	0.12	0.40	6.37	9.40	8.26	0.16	0.33	0.18	-0.02	-0.19	0.54
6	2.567	3.08	2.57	1.05	1.20	1.11	-3.33	-3.25	-3.10	0.02	0.10	0.38	7.75	10.73	9.66	0.19	0.34	0.26	-0.39	-0.54	1.62
7	3.079	3.33	2.82	1.15	1.25	1.17	-3.25	-3.23	-3.44	0.00	0.09	0.37	9.11	11.39	10.33	0.20	0.34	0.27	-0.60	-0.73	0.14
8	3.333	3.59	3.08	1.21	1.32	1.22	-3.23	-3.34	-3.42	-0.01	0.07	0.35	9.78	12.05	10.99	0.21	0.34	0.28	-0.93	-0.91	-0.04
9	3.589	3.84	3.34	1.27	1.39	1.29	-3.34	-3.15	-3.53	-0.03	0.02	0.30	10.46	12.70	11.66	0.20	0.31	0.27	-1.11	-1.08	-0.24
10	3.845	4.10	3.60	1.34	1.463	1.36	-3.15	-3.11	-3.34	-0.09	0.04	0.32	11.13	13.35	12.31	0.17	0.35	0.24	-1.29	-1.27	-0.41
11	4.055	4.36	3.85	1.42	1.548	1.44	-3.11	-3.05	-3.29	-0.06	0.02	0.30	11.80	14.00	12.97	0.20	0.34	0.27	-1.40	-1.43	-0.60
12	3.977	4.46	4.11	1.60	1.64	1.52	-3.09	-3.27	-3.27	-0.11	-0.01	0.28	13.14	14.66	13.62	0.19	0.34	0.27	-0.73	-0.82	-0.67
AVG	**2.66**	**3.01**	**2.55**	**1.13**	**1.23**	**1.15**	**-3.24**	**-3.24**	**-3.39**	**-0.03**	**0.06**	**0.28**	**8.18**	**10.59**	**9.64**	**0.15**	**0.30**	**0.24**	**-0.31**	**-0.34**	**0.47**

4.1.2 Energy Analysis

The evaluation of the various gas turbine unit's performance parameters was done by applying Equations (3.1) to (3.21) using data from Tables A11 to A13 and some design data as stated in Section 3.4. Computer scripts developed from MATLAB programming language were used to simulate the energy performance of the various gas turbine units. The MATLAB codes used are presented in Appendix I. The results of the energy analysis are presented in Tables C2 to C4 and Figures 4.10 to 4.13. Figure 4.10 shows the variation of net thermal efficiency and net power output with ambient air temperature and pressure ratio for the three GT units. The variation of specific fuel consumption and work ratio with ambient air temperature and pressure ratio for the three GT units are shown in Figure 4.11. The variation heat rate with ambient air temperature and pressure ratio for various gas turbine units are presented in Figures 4.12. The energy flow diagram, which is also known as the Sankey diagram for GT11 is presented in Figure 4.13. The performance parameters for GT11, GT12, GT13 are illustrated in Table 4.6.

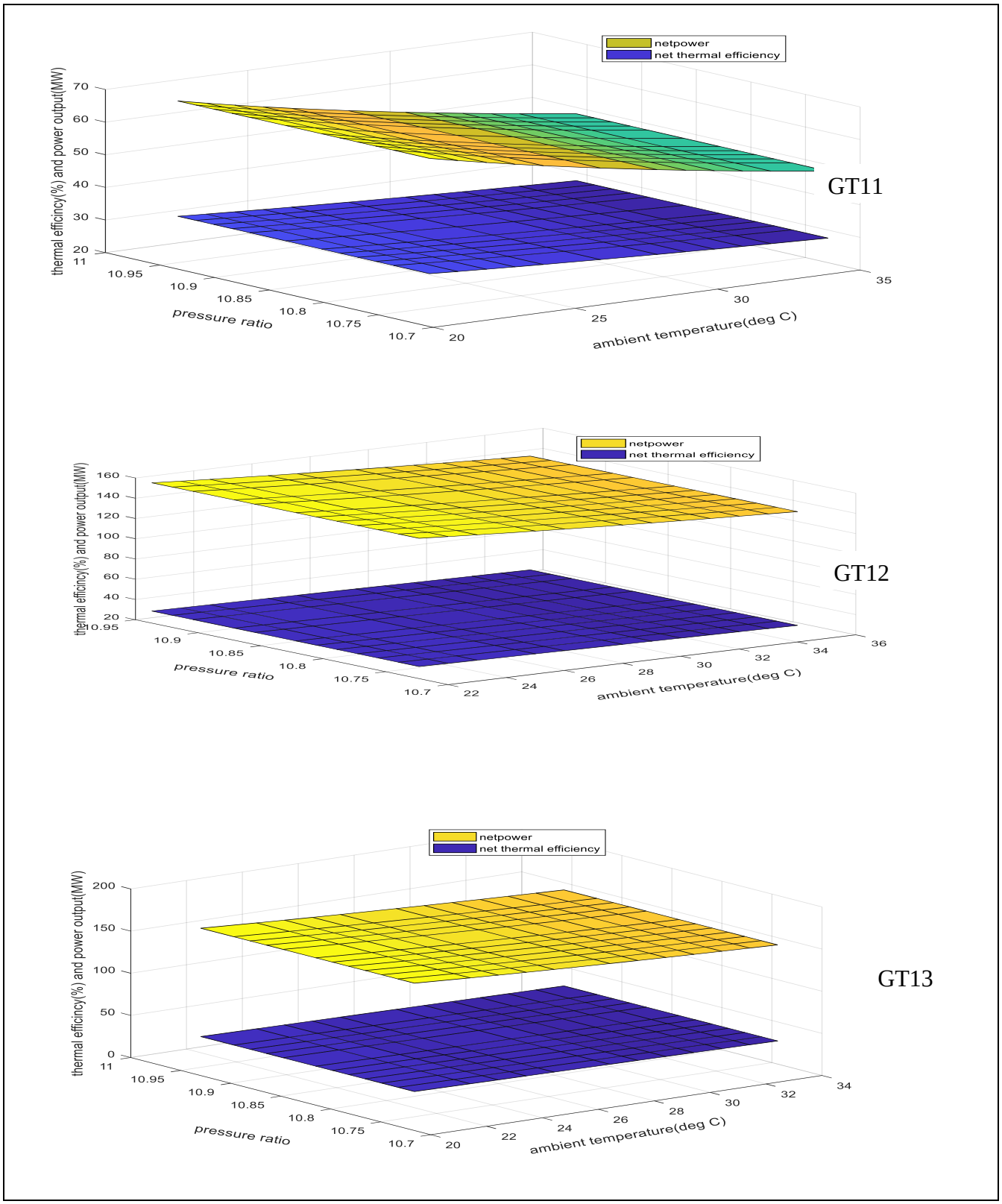

Figure 4.10: Variation of Power Output and Net Thermal Efficiency with Ambient Temperature and Compressor Pressure Ratio for GT11, GT12 and GT13.

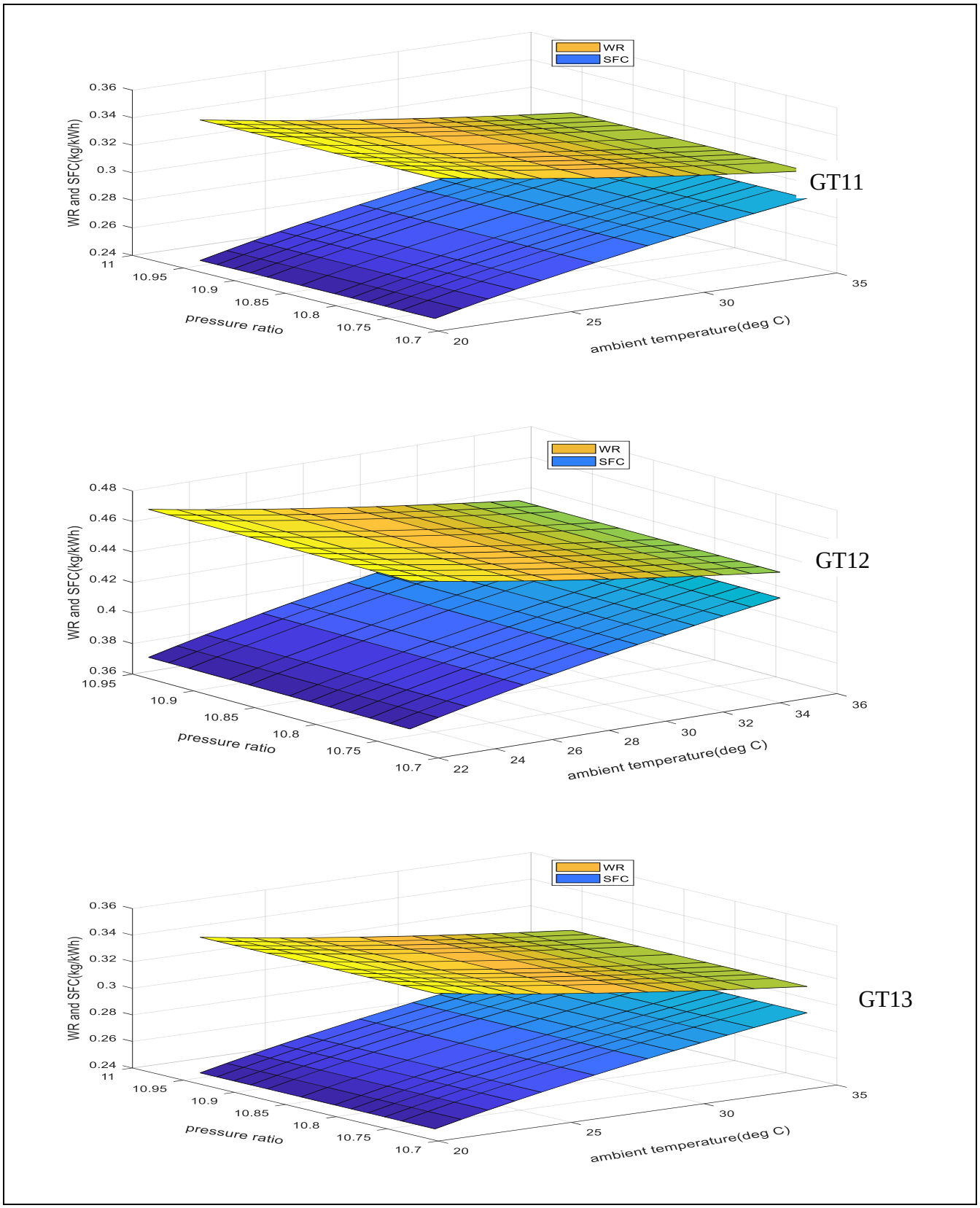

Figure 4.11: Variation of Work Ratio and Specific Fuel Consumption with Ambient Temperature and Compressor Pressure Ratio for GT11, GT12 and GT13

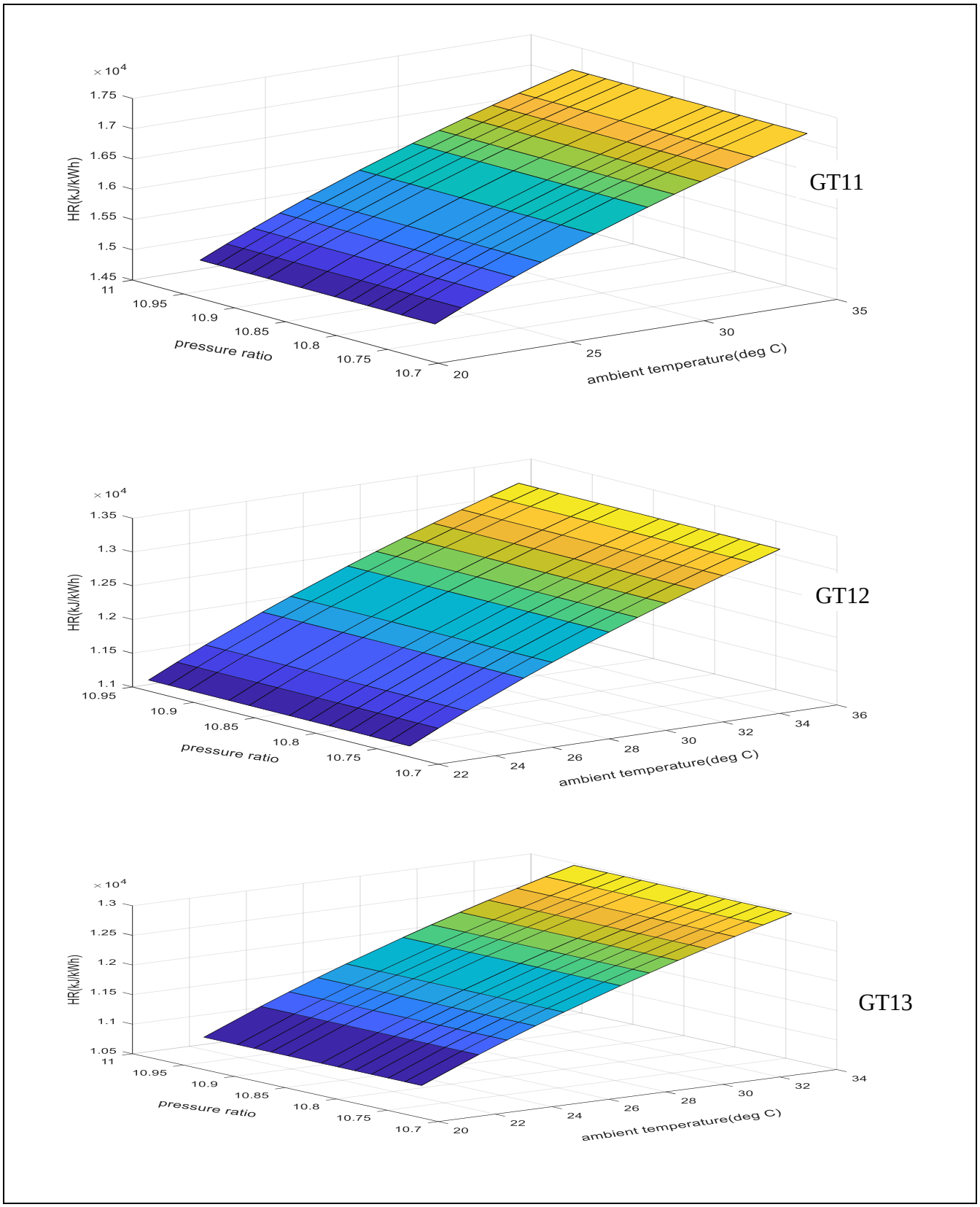

Figure 4.12: Variation of Heat Rate with Ambient Temperature and Compressor Pressure Ratio for GT11, GT12 and GT13

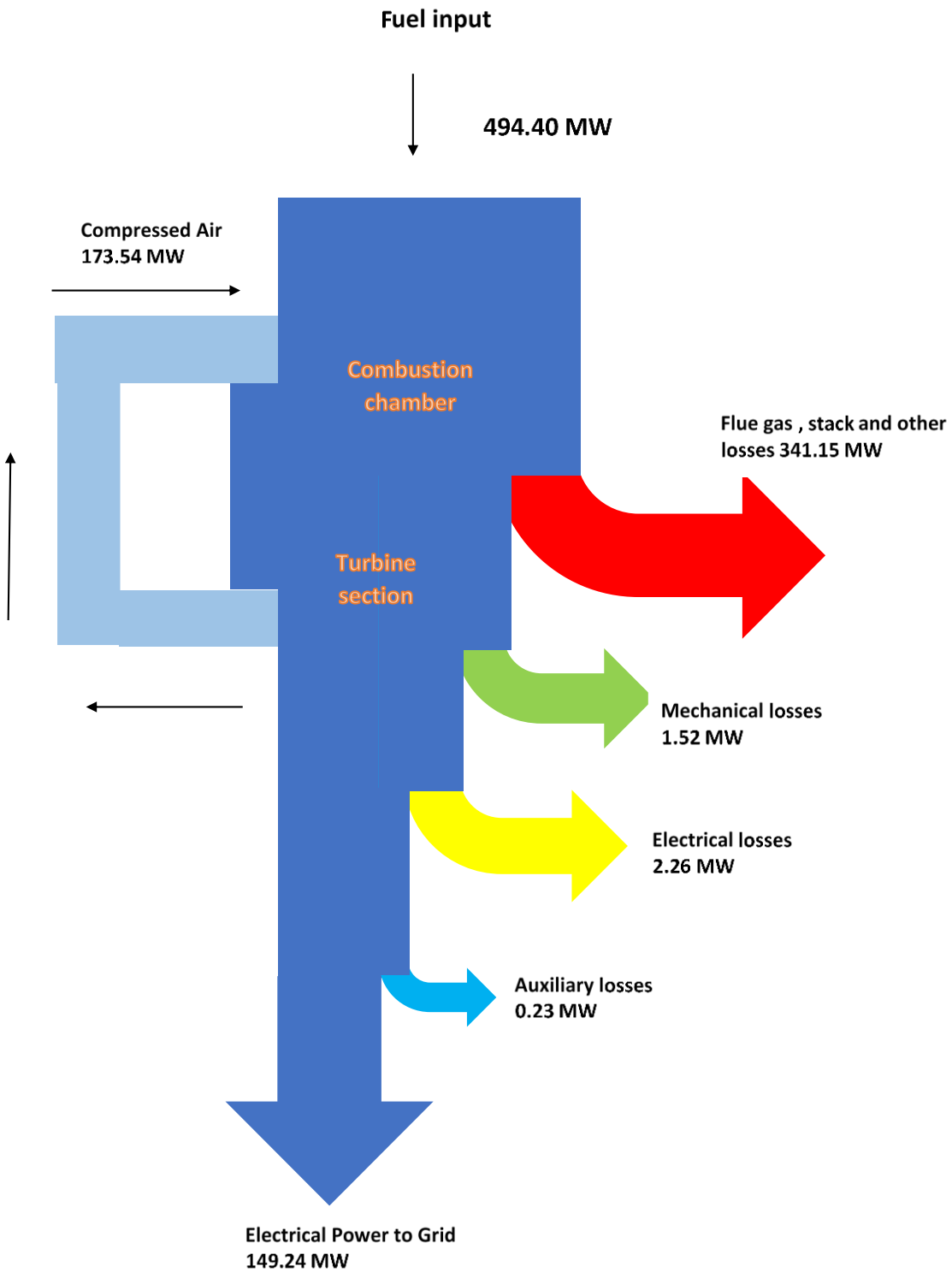

Figure 4.13: Energy flow diagram for GT11

Table 4.6: Average Performance Results for the Various Gas Turbine Units

S/N	**Parameters**	**GT11**	**GT12**	**GT13**	**AVG**
1	$T_1(^0C)$	27.67	28.83	28.00	28.17
2	r_p	10.85	10.82	10.84	10.84
3	P_c (MW)	173.54	173.82	173.24	173.53
4	P_t(MW)	326.56	325.65	326.98	326.40
5	$P_{thermal}$(MW)	153.02	151.84	153.74	152.87
6	HS(MW)	494.40	505.29	501.69	500.46
7	η_{thgr}(%)	30.98	30.07	30.67	30.57
8	Q_{flue}(MW)	297.31	296.65	296.66	296.87
9	mechloss(MW)	1.52	1.56	1.58	1.55
10	genloss(MW)	2.26	2.25	2.30	2.27
11	auxPower(MW)	0.23	0.23	0.23	0.23
12	η_{mech}(%)	99.01	98.97	98.97	98.98
13	η_{gen}(%)	98.50	98.50	98.48	98.49
14	P_{net}(MW)	149.24	147.80	149.86	148.97
15	η_{net} (%)	30.21	29.27	29.89	29.79
16	SFC(kg/kWh)	0.266	0.274	0.268	0.269
17	HR(kJ/kWh)	11956.06	12336.32	12077.93	12123.44
18	WR	0.457	0.454	0.458	0.456
19	%flue gas	60.16	58.73	59.15	59.35

4.1.3 Exergy Analysis

The recorded data from the power plant as presented in Tables A11 to A13 like pressure, temperatures that were converted to absolute temperatures, and mass flow rates with other properties such as specific capacity at constant pressure (c_p) and the gas constant (R) are shown in Section 3.4 of Chapter 3. The data were used to evaluate the exergy flow rates at the inlet and exit of each component applying Equations (3.22) to (3.67). These parameters were utilized as input data to computer code (MATLAB) developed to perform the simulation of each component and overall plant performance of the Azura Edo Power Station. The MATLAB scripts used for the exergy analysis of all three GT units are presented in Appendix 1.

The exergy appraisal outcomes of the GT units were computed based on the collated data from Tables A11 to A13. Thus, each state exergy was determined using state 1 as a reference state and in conjunction with the T- s diagram of the Azura Edo Power Plant illustrated in Figure 3.3. The results are presented in Tables 4.7 to 4.12.

The net flow rates of different exergies traversing the boundary of each component of the GT power plant at average working data of the rated condition are presented in Tables 4.7, 4.8 and 4.9 for GT11, GT12, and GT13 respectively. Products exergy flow rates are represented by positive values and the exergy rates of fuel or resources are indicated by negative values to determine resultant of exergy summation. As explained in Ebadi and Gorgi – Brandpy (2005), "the product of a component corresponds to the added exergy, while the resource is the consumed exergy". For each component, the summation of the exergy flow rate of resources, products, and destruction is equal to zero, the zero-sum obtained shows that exergy balances were accurately satisfied.

Table 4.7: Rated Exergy Condition for GT11

state	ṁ (kg/s)	T (K)	P (bar)	E^{CHE} (MW)	E^{T} (MW)	E^{p} (MW)	Ṡ(MW/K)
1	492.81	300.82	1.0101	0	0	0	0
2	492.81	651.52	10.96	0	62.2838	101.4131	0.045525
f	10.98	333.15	24.00	524.06	0.02789	4.721861	0.00304
3	503.79	1379.48	10.74	0	358.9442	103.8703	0.535598
4	503.79	814.92	1.020	0	123.9645	0.432854	0.575063

Table 4.8: Rated Exergy Condition for GT12

state	ṁ (kg/s)	T (K)	P (bar)	E^{CHE} (MW)	E^{T} (MW)	E^{p} (MW)	Ṡ (MW/K)
1	492.81	301.98	1.0118	0	0	0	0
2	492.81	654.10	10.95	0	62.54112	101.7082	0.045902
f	10.98	333.15	24	524.06	0.025864	4.737631	0.002976
3	503.79	1380.57	10.73	0	358.403	104.1716	0.534142
4	503.79	816.29	1.0218	0	123.7904	0.433823	0.573786

4.9: Rated Exergy Condition for GT13

state	ṁ (kg/s)	T (K)	P (bar)	E^{CHE} (MW)	E^{T} (MW)	E^{p} (MW)	Ṡ (MW/K)
1	492.45	301.15	1.0122	0	0	0	0
2	492.45	651.26	10.97	0	62.98684	101.4276	0.044841
f	11.15	333.15	24	531.79	0.027637	4.79354	0.003074
3	503.59	1379.85	10.76	0	358.6645	103.9199	0.534967
4	503.59	814.31	1.0222	0	123.4989	0.432307	0.573744

Table 4.10: Results of Exergy Analysis for GT11

components	W(MW)	E^{CHE} (MW)	E^{T} (MW)	E^{P} (MW)	E_D (MW)	ε (%)	ε_D (%)
AC	-177.392	0	62.2838	101.4131	13.69473	92.28	7.72
CC	0	524.06	296.6325	-2.26468	229.6971	56.17	43.83
GT	326.5454	0	-234.98	-103.437	11.8717	96.36	3.64
Total P	149.1534	524.06	123.9366	-4.28901	255.2635	51.29	48.71

Table 4.11: Results of Exergy Analysis for GT12

components	W(MW)	E^{CHE} (MW)	E^{T} (MW)	E^{P} (MW)	E_D (MW)	ε (%)	ε_D (%)
AC	-178.111	0	62.54112	101.7082	13.86163	92.22	7.78
CC	0	524.06	295.8361	-2.27423	230.503	56.02	43.98
GT	326.3785	0	-234.613	-103.738	11.97193	96.33	3.67
Total P	148.2676	524.06	123.7645	-4.30381	256.3366	51.09	48.91

Table 4.12: Results of Exergy Analysis for GT13

Components	W(MW)	E^{CHE} (MW)	E^{T} (MW)	E^{P} (MW)	E_D (MW)	ε (%)	ε_D (%)
AC	-177.918	0	62.98684	101.4276	13.50401	92.41	7.59
CC	0	531.79	295.65	-2.30131	238.4454	55.16	44.84
GT	326.9754	0	-235.166	-103.488	11.6778	96.43	3.57
Total P	149.0574	531.79	123.4712	-4.36123	263.6272	50.43	49.57

Tables 4.10 to 4.12 present results of the net exergy flow rates crossing the boundary of each component of the plant as well as exergy destruction, exergy efficiency and exergy destruction efficiency. The average exergy efficiency and exergy destruction efficiency for GT11, GT12 and GT13 are presented in Figures 4.14 and 4.15 respectively. The Second Law of Thermodynamics efficiency for the three GTs are presented in Table 4.13. Figure 4.17 shows the comparison of the

First and Second Laws of Thermodynamics efficiencies. The variation of the plant operating parameters such as exergy efficiency and exergy destruction efficiency with ambient air temperature are presented in Figures 4.17 and 4.18.

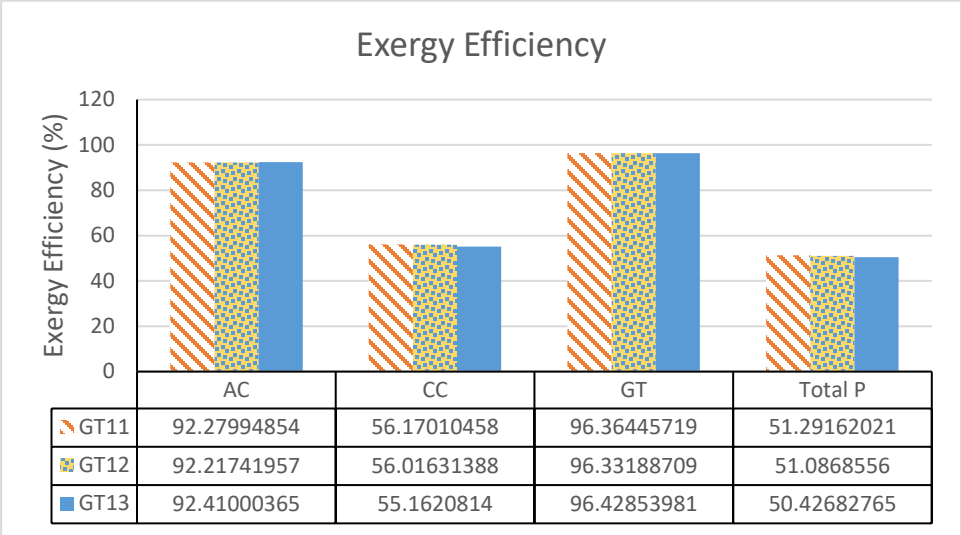

	AC	CC	GT	Total P
GT11	92.27994854	56.17010458	96.36445719	51.29162021
GT12	92.21741957	56.01631388	96.33188709	51.0868556
GT13	92.41000365	55.1620814	96.42853981	50.42682765

Figure 4.14: Exergy Efficiency of Components and Total Plant for all the Three Gas Turbine Units

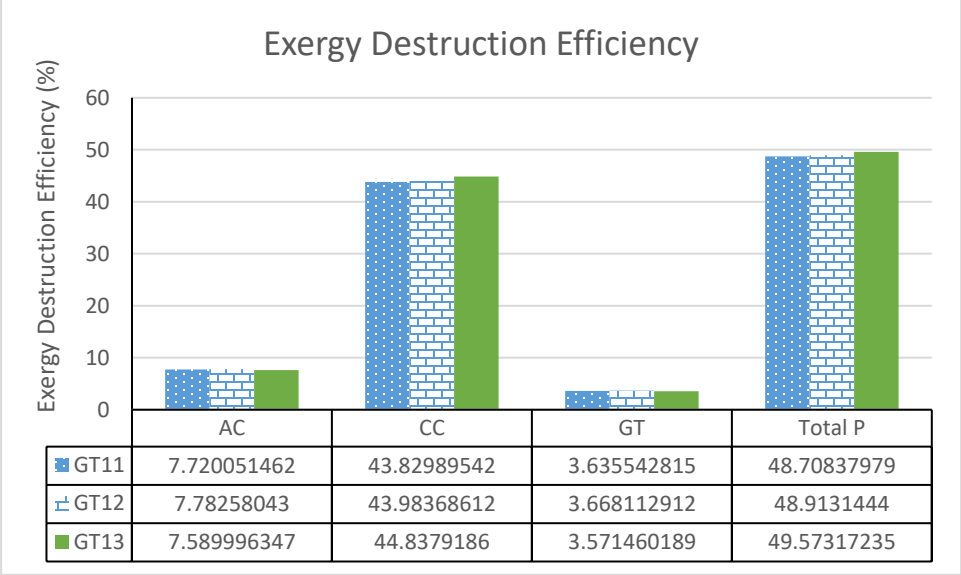

	AC	CC	GT	Total P
GT11	7.720051462	43.82989542	3.635542815	48.70837979
GT12	7.78258043	43.98368612	3.668112912	48.9131444
GT13	7.589996347	44.8379186	3.571460189	49.57317235

Figure 4.15: Exergy Destruction Efficiency of Components and Total Plant for all the Three Gas Turbine Units

Table 4.13: Second Law of Thermodynamics Efficiency for the Three Units

S/N	UNIT	η_{SL} (%)
1	GT11	28.46
2	GT12	28.29
3	GT13	28.03
Average		28.26

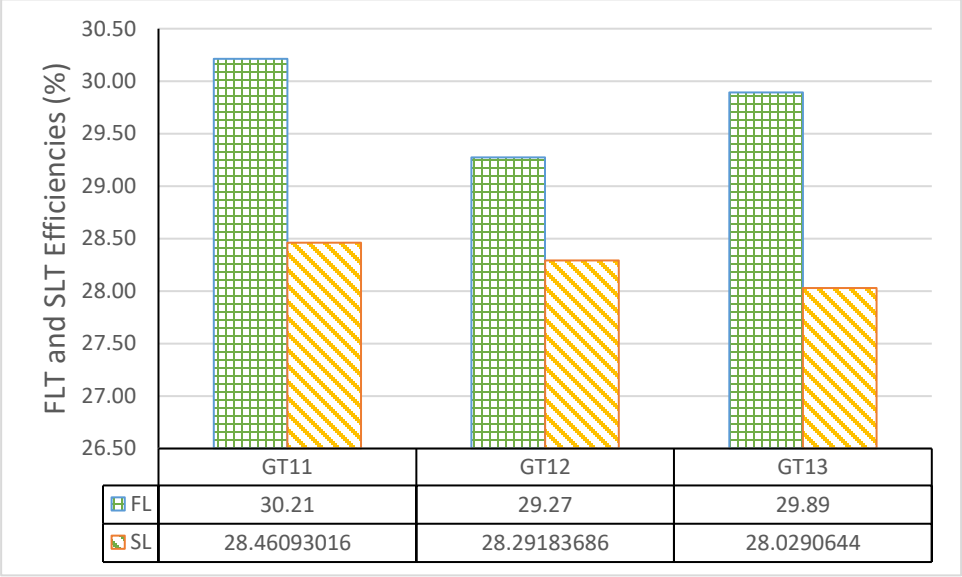

Figure 4.16: First and Second Laws of Thermodynamics Efficiency for Various Units

The variation of exergy and exergy destruction efficiencies with ambient air temperature for the combustion chamber and total plant of the three GTs are presented in Figures 4.19 and 4.20 respectively. The variation of the Second Law of Thermodynamics efficiency with ambient air temperature for GT11, GT12 and GT13 is illustrated in Figure 4.21. The exergy balance diagram for GT11 is presented in Figure 4.22.

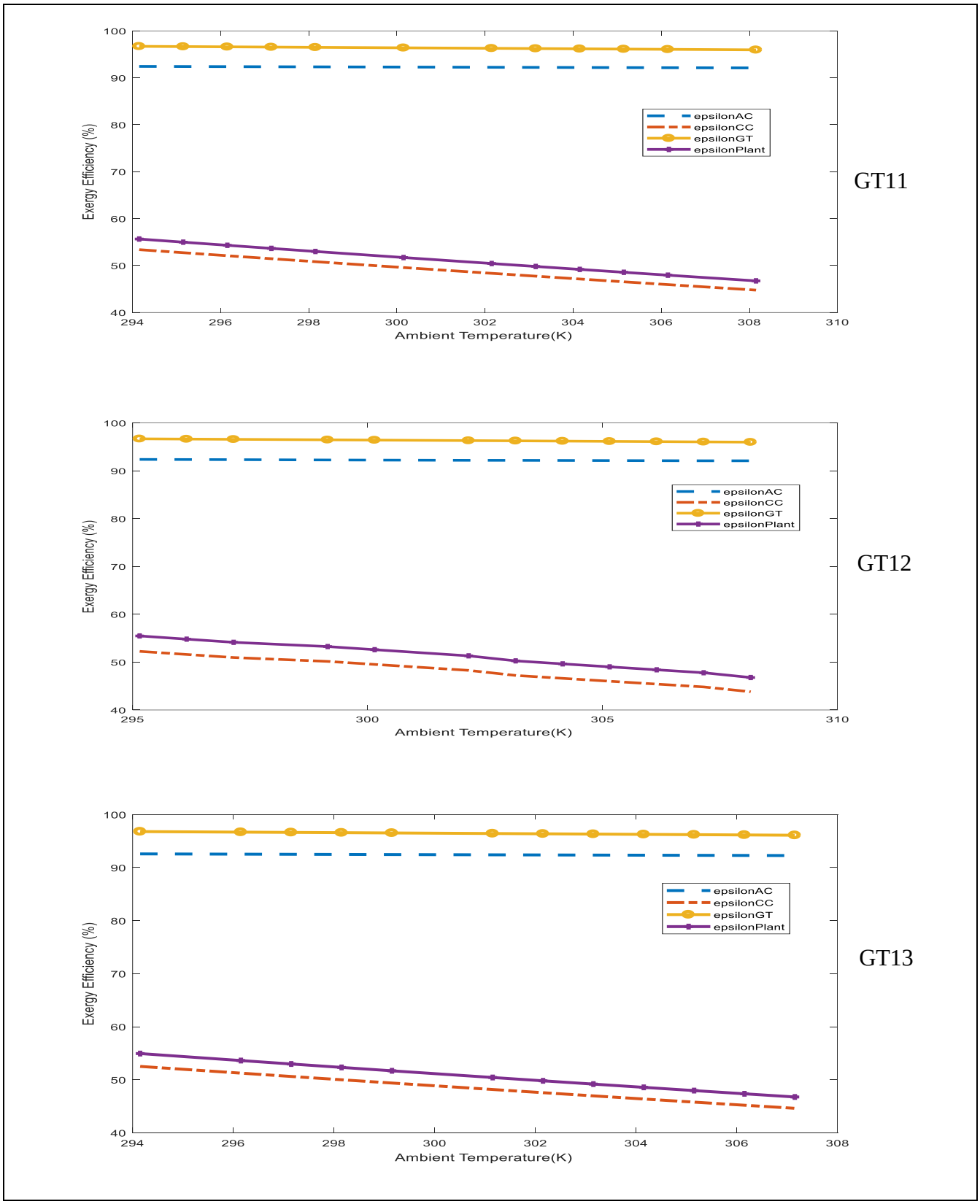

Figure 4.17: Variation of Exergy Efficiency with Ambient Air Temperature for GT11, GT12 and GT13

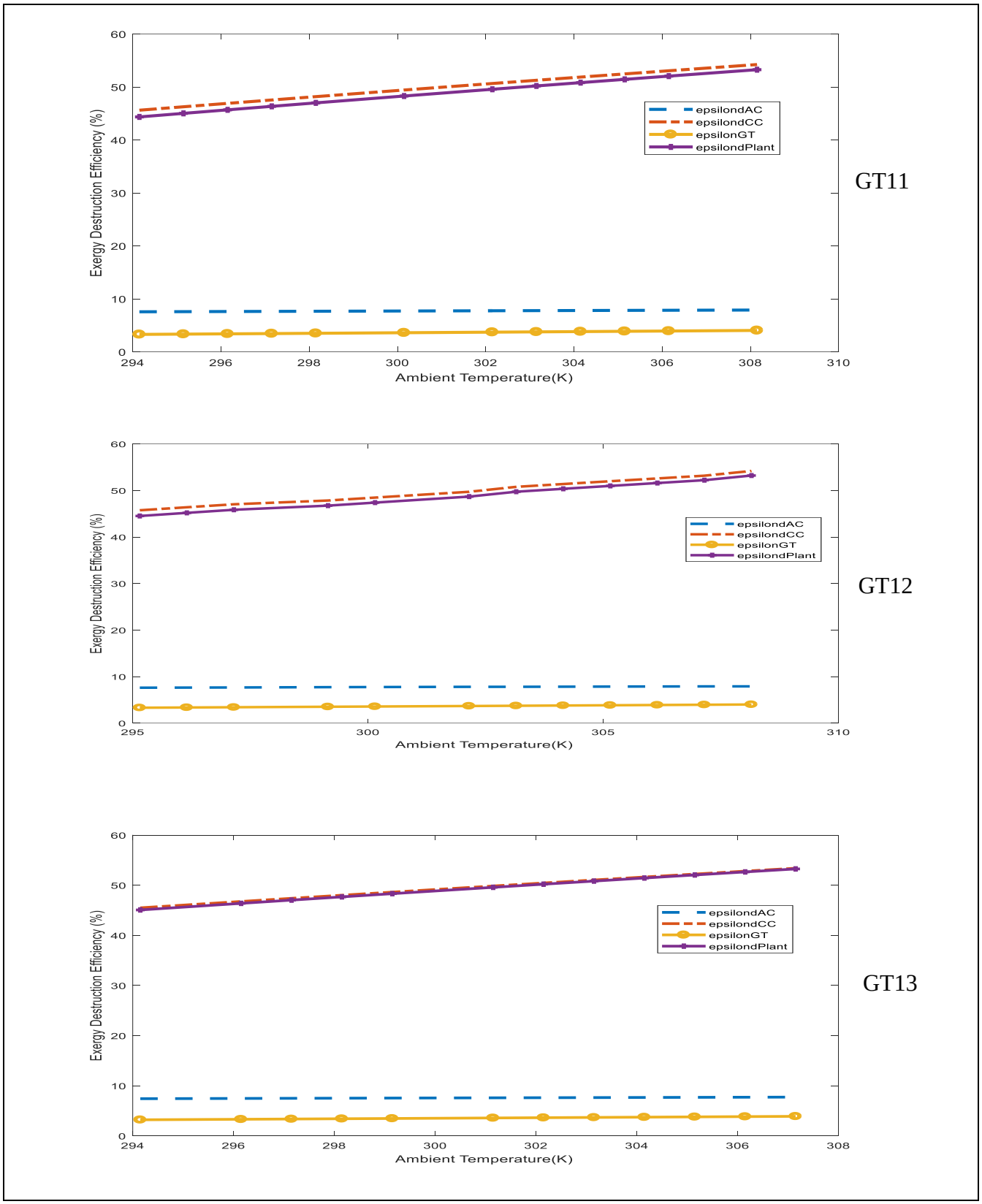

Figure 4.18: Variation of Exergy Destruction Efficiency with Ambient Air Temperature for GT11, GT12 and GT13

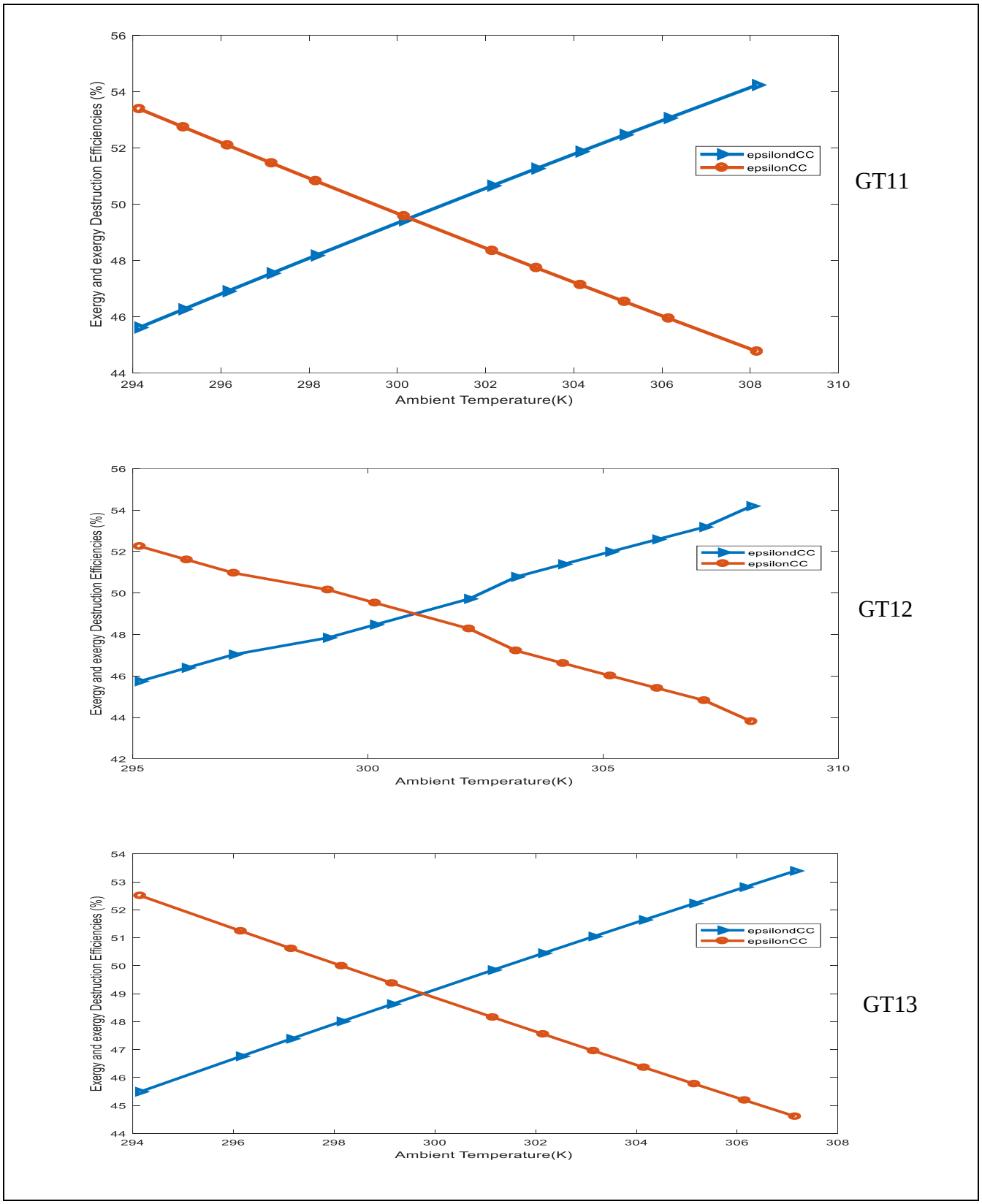

Figure 4.19: Variation of Exergy Efficiency and Exergy Destruction Efficiency of CC with Ambient Air Temperature for GT11, GT12 and GT13

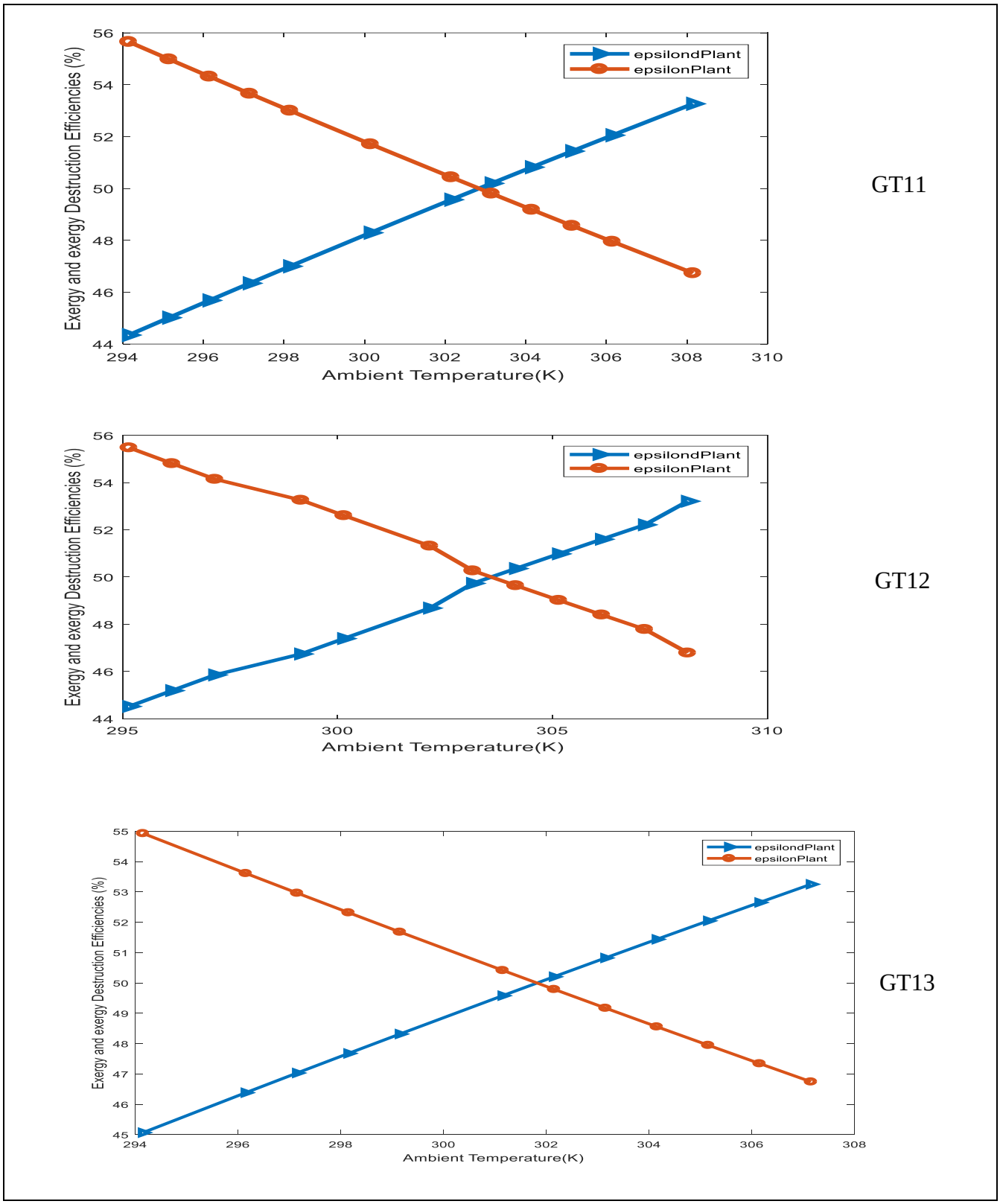

Figure 4.20: Variation of Exergy Efficiency and Exergy Destruction Efficiency of the Total Plant with Ambient Air Temperature for GT11, GT12 and GT13

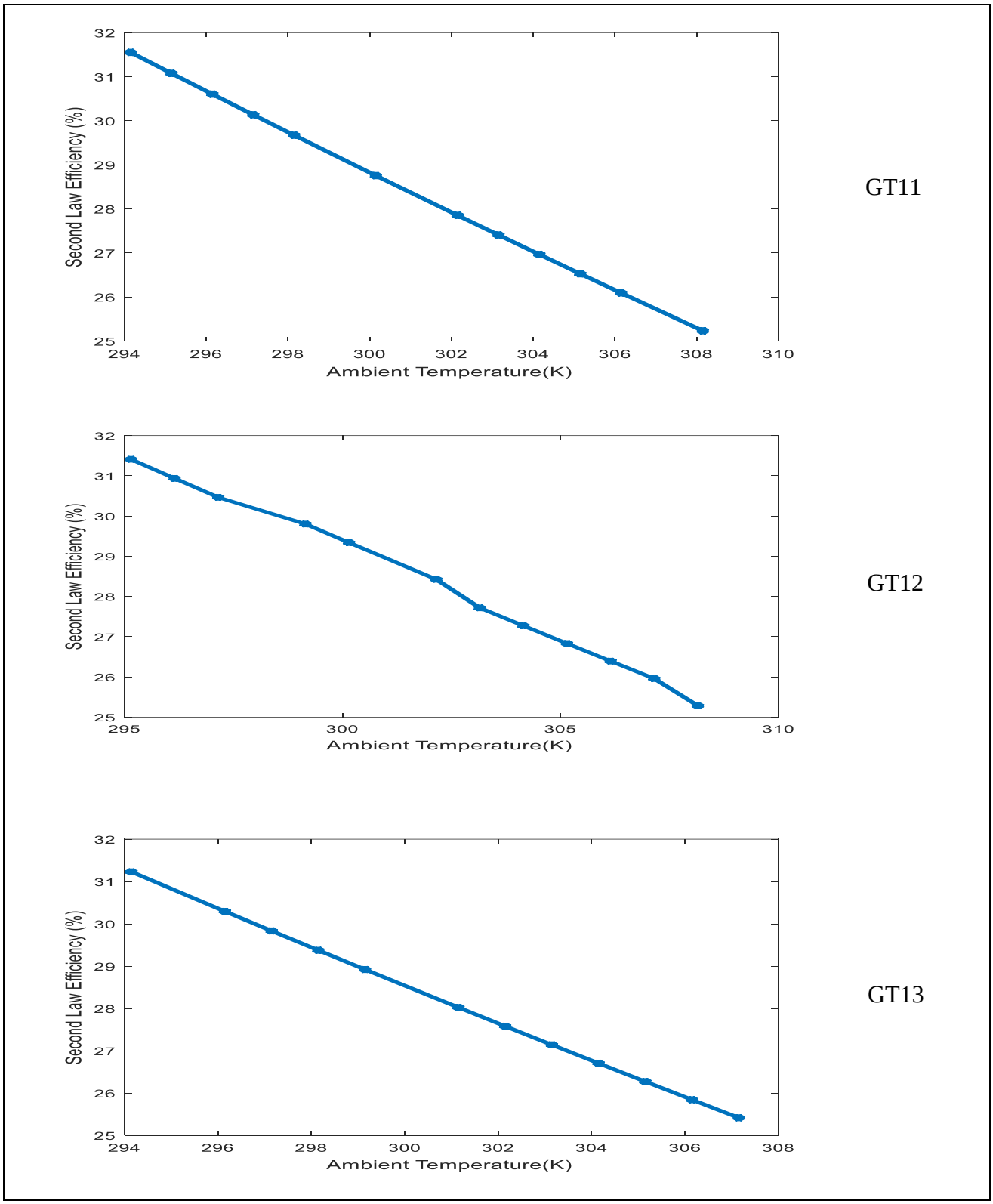

Figure 4.21: Variation of Second Law of Thermodynamics Efficiency with Ambient Air Temperature for GT11, GT12 and GT13

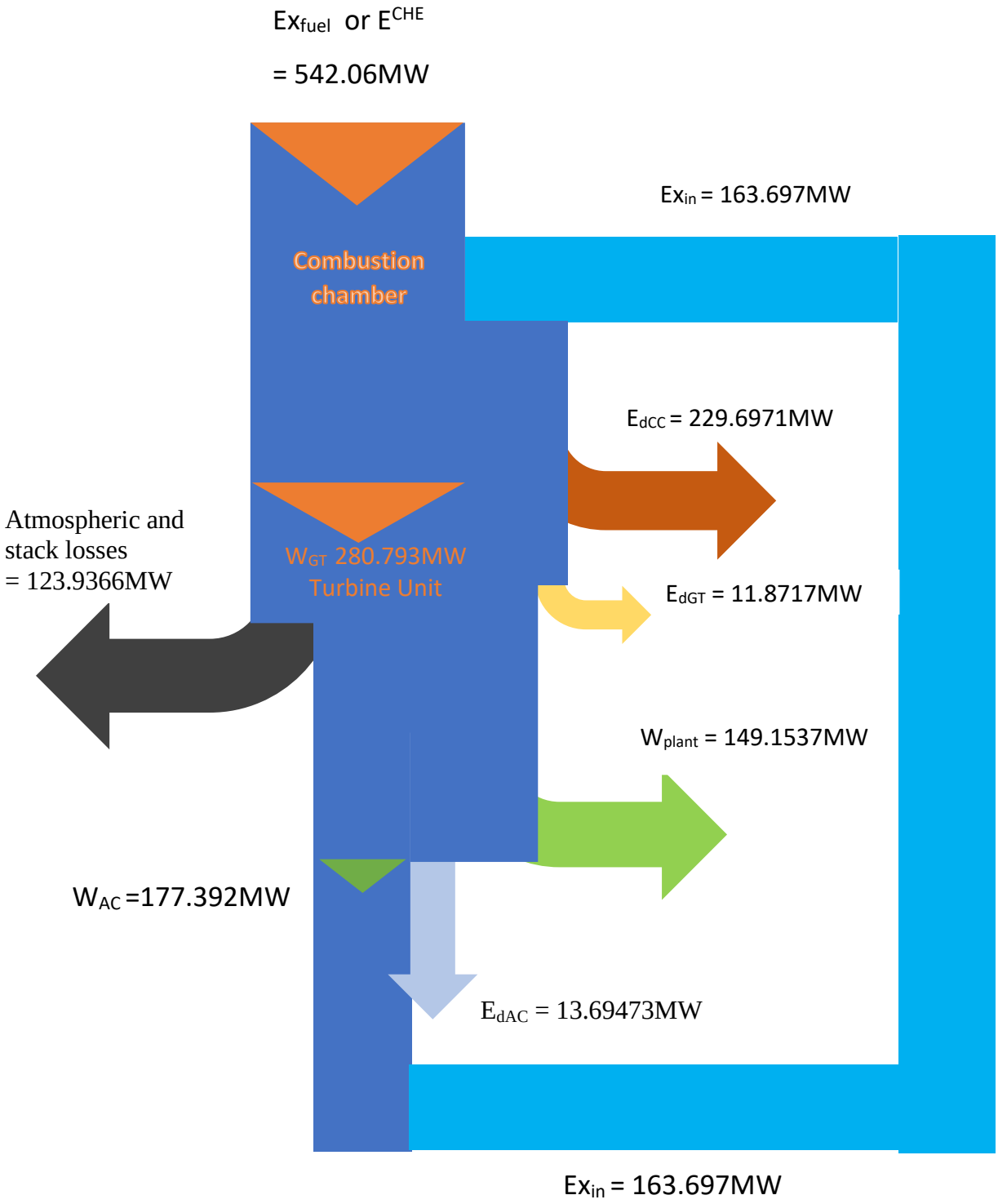

Figure 4.22: Exergy Balance (Sankey) Diagram for GT11 of Azura Edo Power Plant

4.1.4 Exergy Improvement Potential, Sustainability Index and Depletion Number of Fuel

Equations (3.68) to (3.72) in Sections 3.6.3 and 3.6.4 were applied to evaluate the Azura Edo Power Plant improvement potential, depletion number and sustainability index of the fuel using some exergy performance data as shown in the equations. MATLAB programme was used to simulate the improvement potential, depletion and sustainability of the various GT units as shown in Appendix I. The exergy improvement potential results for the various gas turbine units are illustrated in Figure 4.23. The sustainability index and depletion number of the fuel average results for the three GT units are presented in Figure 4.24. The variation of sustainability index and depletion of the fuel with ambient air temperature are illustrated in Figure 4.25.

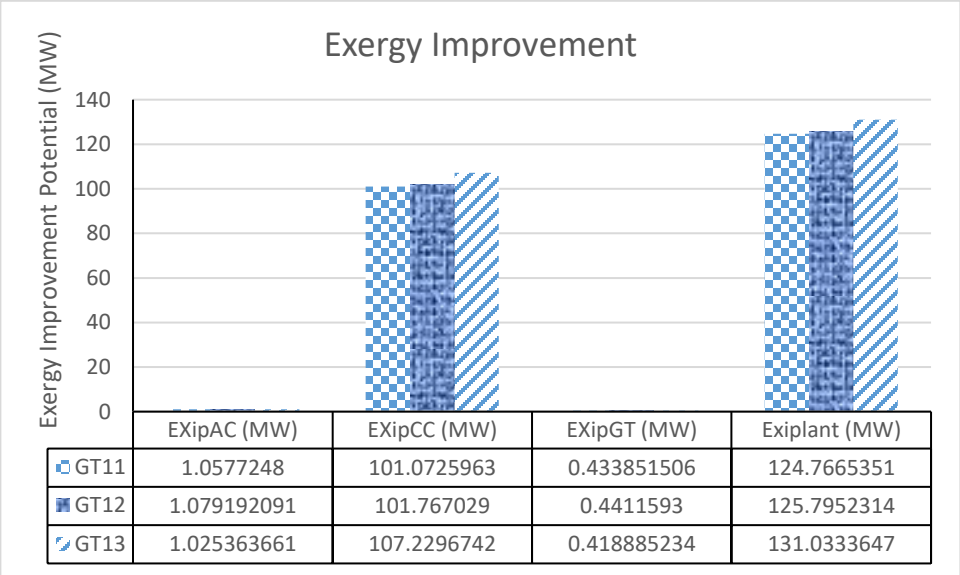

	EXipAC (MW)	EXipCC (MW)	EXipGT (MW)	Exiplant (MW)
GT11	1.0577248	101.0725963	0.433851506	124.7665351
GT12	1.079192091	101.767029	0.4411593	125.7952314
GT13	1.025363661	107.2296742	0.418885234	131.0333647

Figure 4.23: Exergy Improvement Potential for the Azura Edo Power Plant

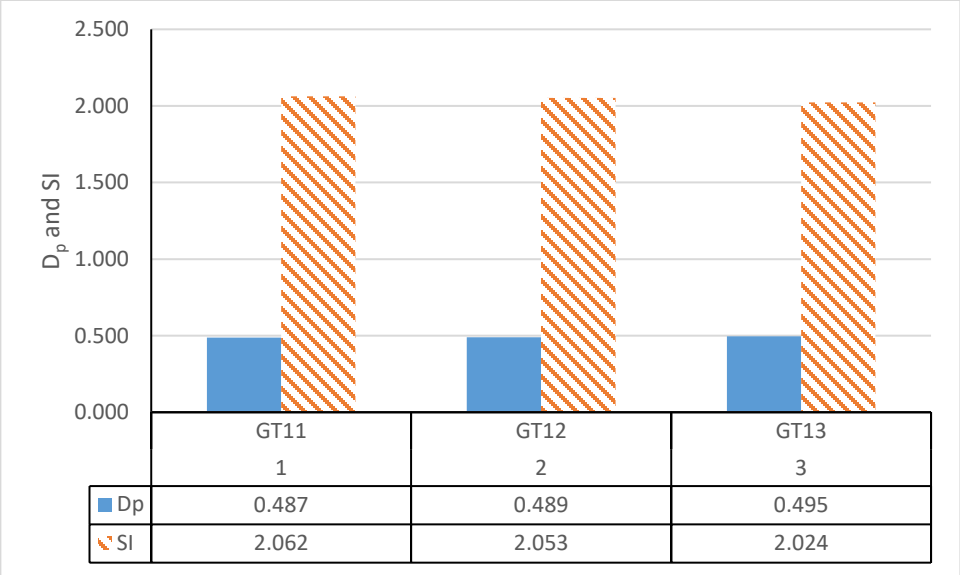

Figure 4.24: Summary of Depletion Number and Sustainability Index of Fuel for the Three GT Units

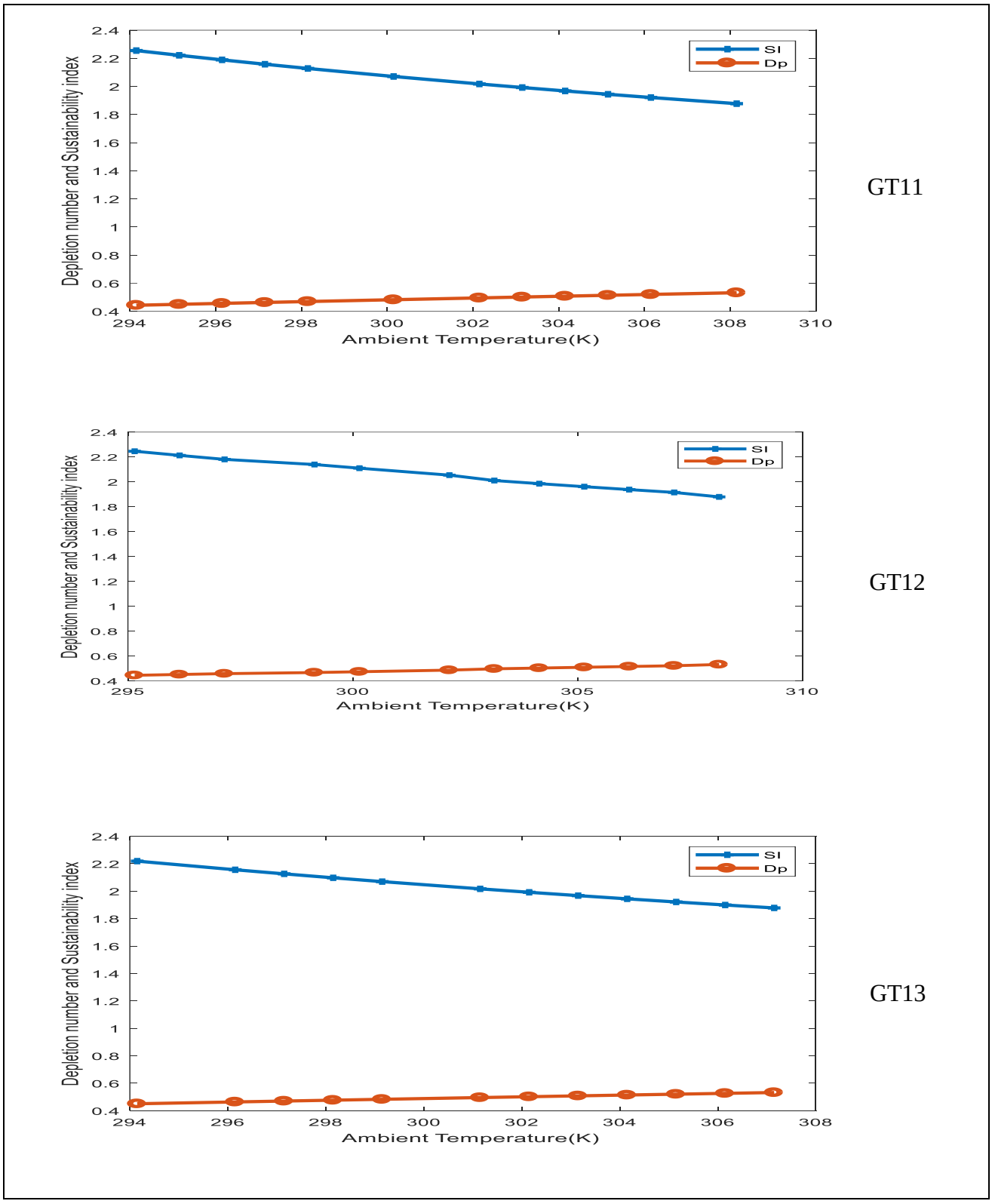

Figure 4.25: Variation of Sustainability Index and Depletion Number with Ambient Air Temperature for GT11, GT12 and GT13

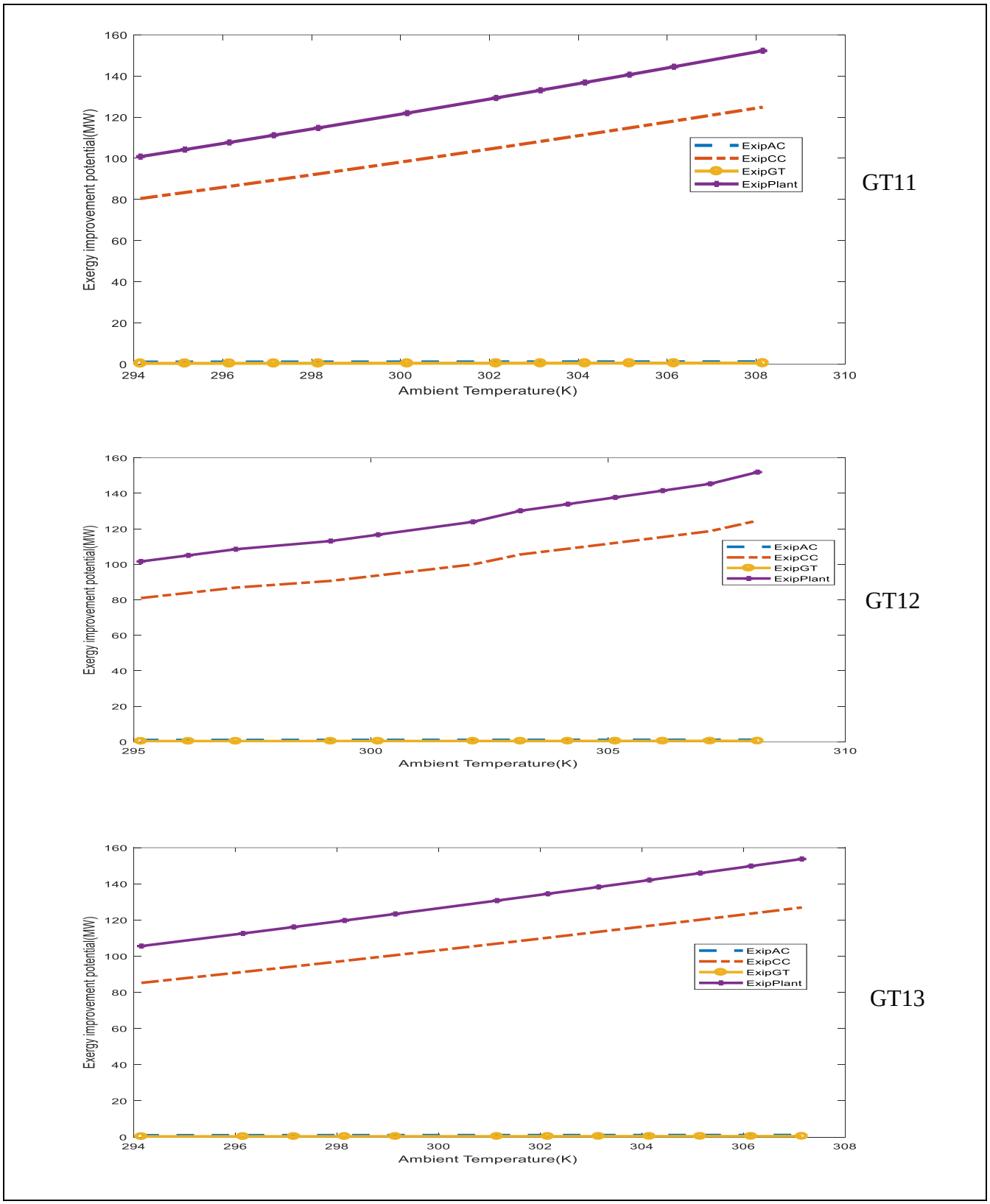

Figure 4.26: Variation of Improvement Potential with Ambient Air Temperature for GT11, GT12 and GT13

4.1.5 Environmental Analysis

The environmental variables evaluated were CO_2 emission in kg/MWh of electricity generated and the mass of CO_2 emitted annually for various GTs units. MATLAB script was developed as shown in Appendix I for simulation by applying Equations (3.74) to (3.101) and using corresponding data from Tables A11 to A13. The average results of the CO_2 emission in $kgCO_2$/MWh and the annual mass of CO_2 emitted obtained from the environmental analysis of Azura Edo Power Plant units are presented in Table 4.14. The variation of CO_2 rate emitted in kg/MWh and mass of CO_2 emitted per year with ambient air temperature are presented in Figures 4.27 and 4.29 respectively. Figure 4.28 illustrates the variation of CO_2 in kg/MWh with net thermal efficiency for the three GT units. The difference in results between the computed and actual exhaust mass flow rates using the environmental model are presented in Table 4.15.

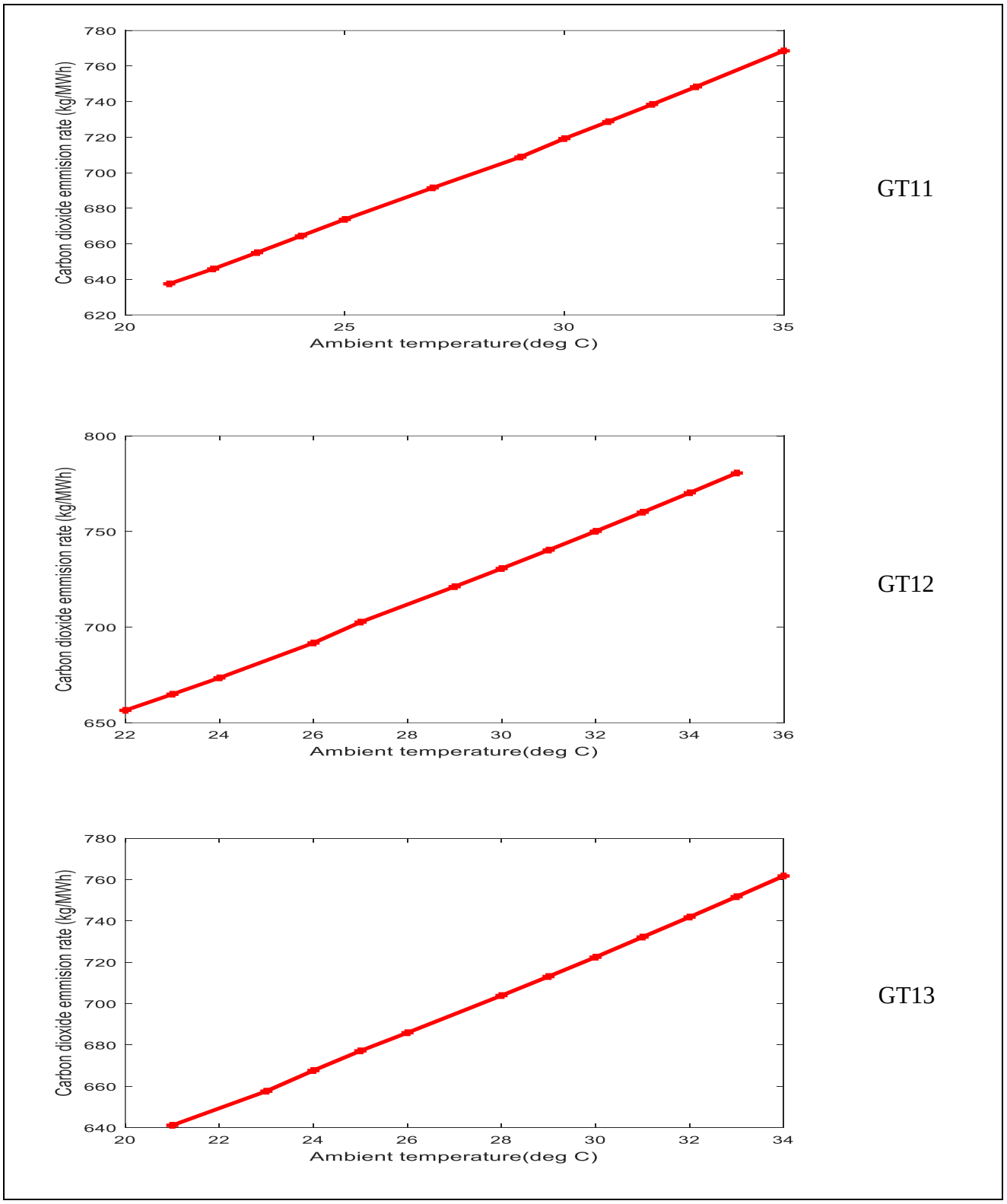

Figure 4.27: Variation of Carbon Dioxide Rate Emitted in (kg/MWh) with Ambient Air Temperature for GT11, GT12 and GT13

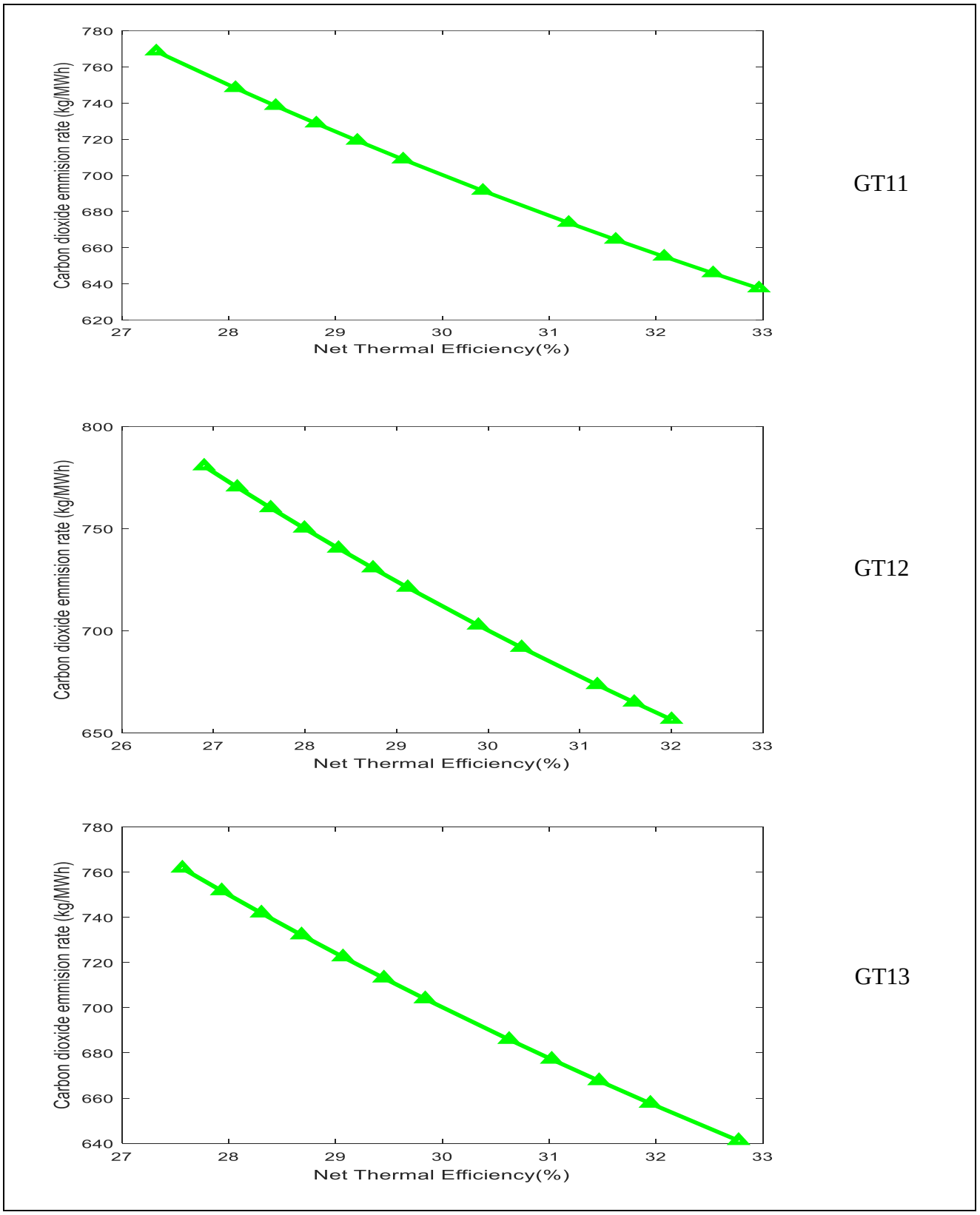

Figure 4.28: Variation of Carbon Dioxide Rate (kg/MWh) with Net Thermal Efficiency for GT12, GT12 and GT13

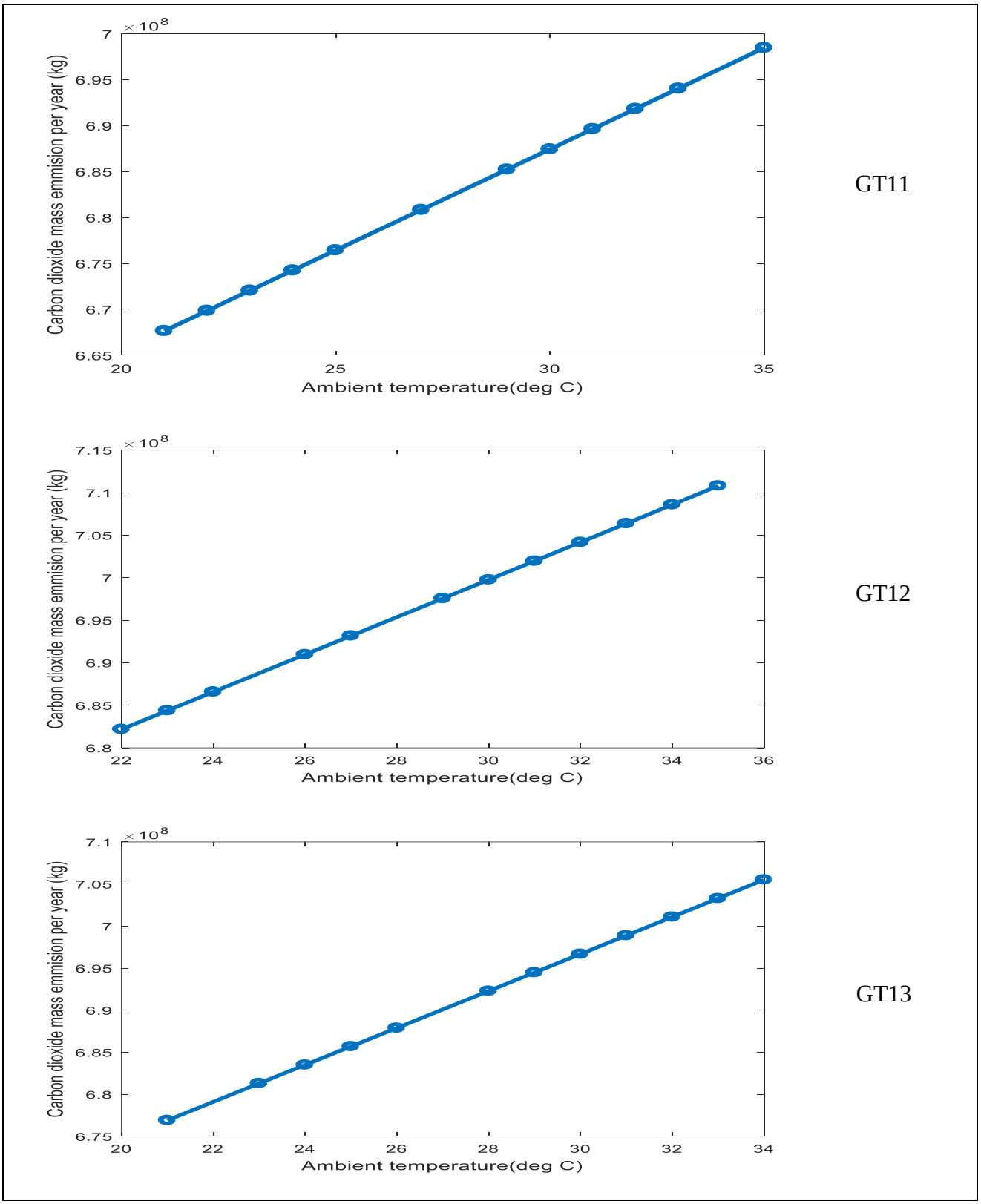

Figure 4.29: Variation of Mass of Carbon Dioxide Emitted Annually with Ambient Air Temperature for GT11, GT12 and GT13

Table 4.14: Average Results Values of CO_2 Emission for GT11, GT12 and GT13

	GT11	GT12	GT13	Total	**Average**
T_1 (^{0}C)	27.67	28.83	28		
ξ_{CO_2} ($kgCO_2/MWh$)	698.34	720.20	704.69	2123.23	**707.74**
$m_{pCO2/yr}$ (kg)	682,310,721.95	697,208,581.77	692,288,165.79	2,071,807,469.51	**690,602,489.84**

Table 4.15: Environmental Model Validation Error Results Comparing Model and Actual Exhaust Mass Flow Rate for GT11, GT12 and GT13

% Error			
S/N	GT11	GT12	GT13
1	0.68625	0.70693	0.69628
2	0.69380	0.71508	0.71205
3	0.70186	0.72368	0.72062
4	0.71035	0.74163	0.72950
5	0.71914	0.75056	0.73852
6	0.73689	0.76684	0.75593
7	0.75297	0.77341	0.76367
8	0.75947	0.77829	0.77022
9	0.76430	0.78093	0.77509
10	0.76694	0.78071	0.77773
11	0.76676	0.77693	0.77753
12	0.75513	0.76883	0.77377
Average	**0.73449**	**0.75532**	**0.74924**

The comparison of carbon dioxide emission rate and intensity for model and actual power plant performance are presented in Figures 4.30 and 4.31 respectively.

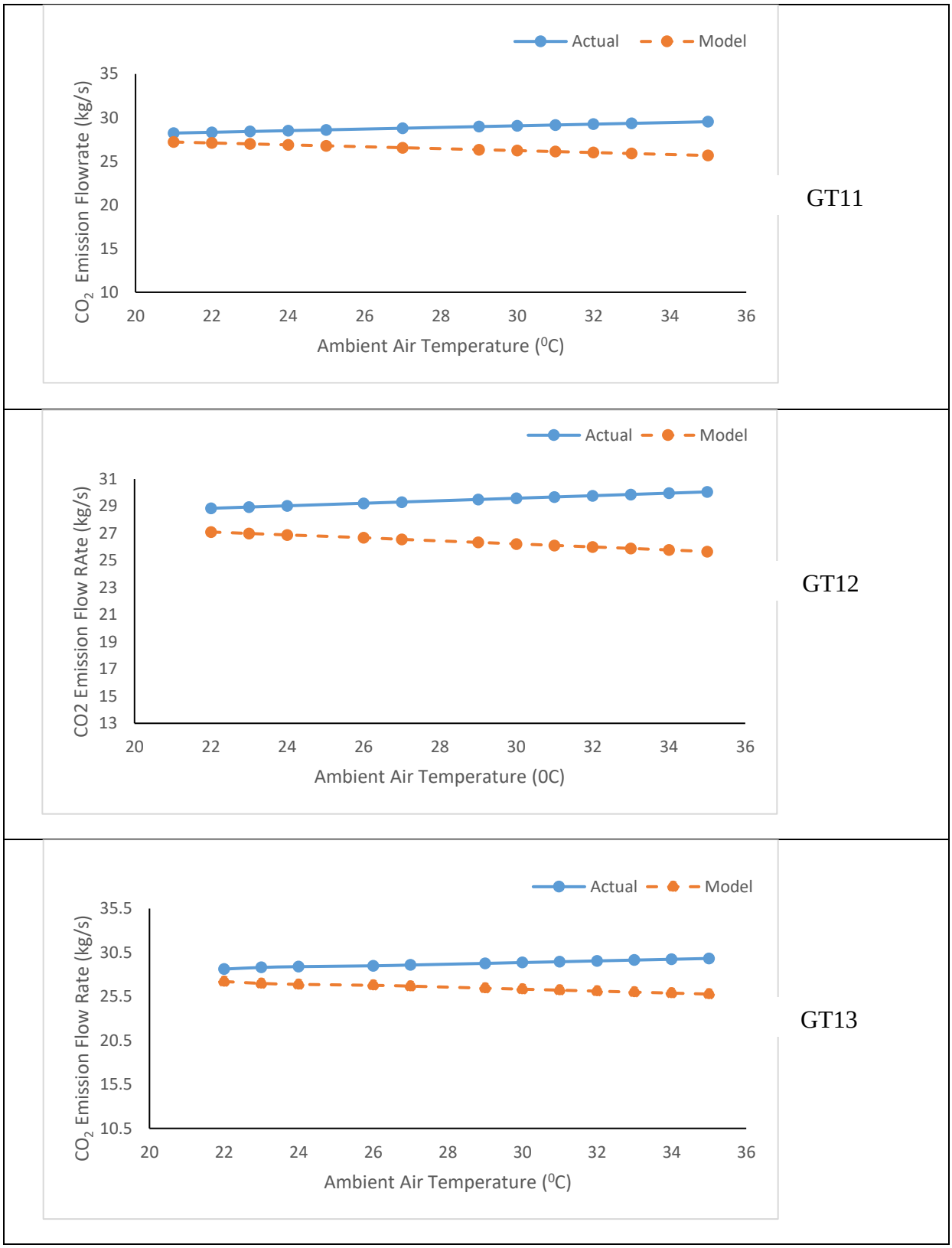

Figure 4.30: Model Validation for Variation in m_{co2} with Ambient Air Temperature for the GTs

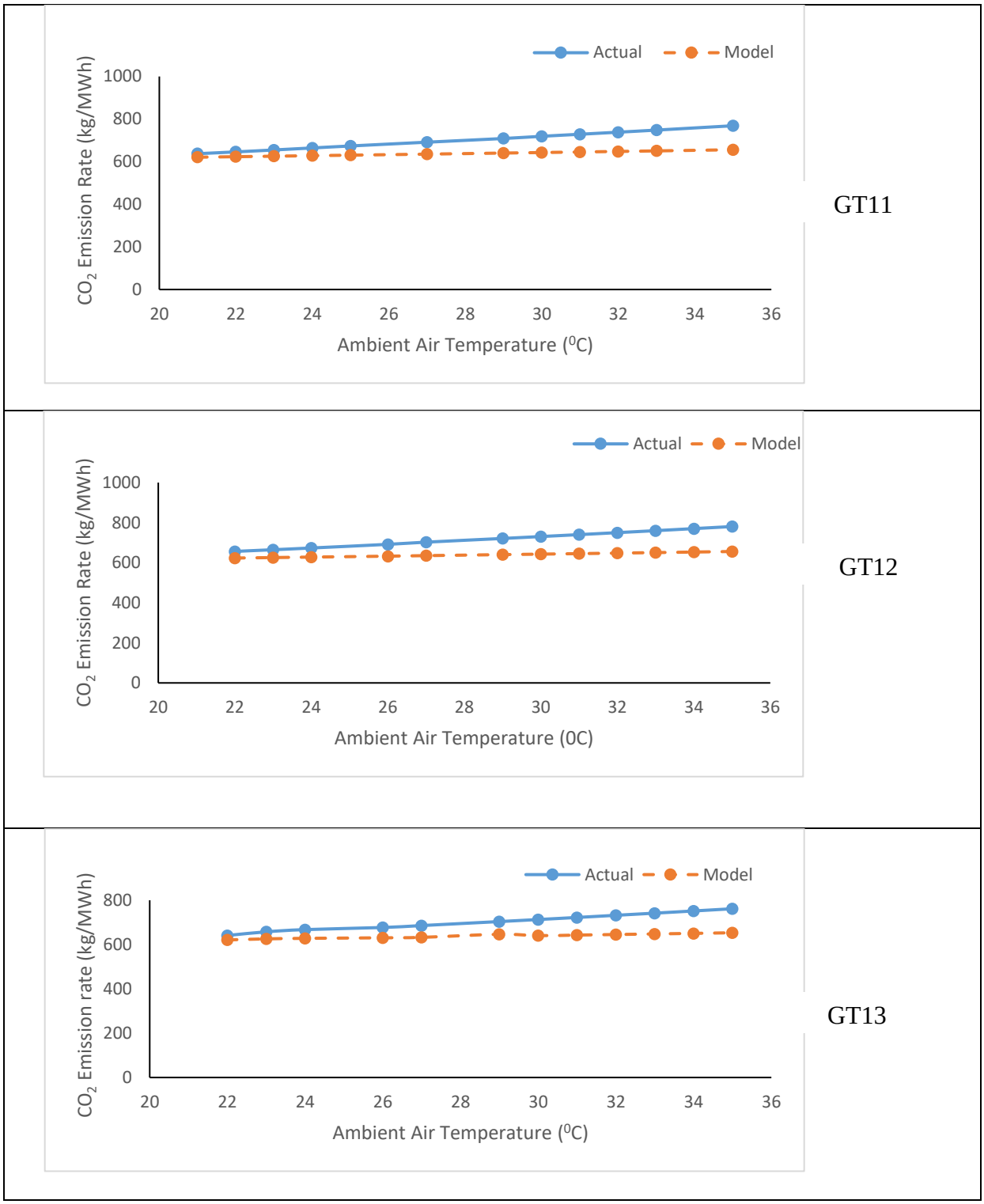

Figure 4.31: Model Validation for Variation in ξco_2 with Ambient Air Temperature for the GTs

4.1.6 Preliminary Analysis of Azura Edo Power Plant Improvement

The results obtained from this research have shown that Azura Edo Power Plant performance is affected by ambient air temperature and the exhaust gas can be used to carry out combined cycle power plant operation. In order to determine the economic implications of the modification to the power plant, energy cost analysis was carried out for the air intake cooling system and combined cycle system integration. The preliminaries of energy cost for the air intake cooling system and combined cycle system results are presented in this section.

Inlet Air Cooling System

The performance of the Azura Edo Power plant was influenced by ambient air temperature occurring at its location. Also, the mean monthly ambient air temperature occurred more at 27 ^{0}C to 35 ^{0} C as obtained from Table A10 in Appendix 11. Hence, this led to the investigation of incorporating an air intake cooling system to enhance its performance. The data used for the integration of the air intake cooling model were obtained from Figure 3.10. Also, the average performance parameters of GT11 considered with and without the incorporation of an air intake cooling system in the study are shown in Table 4.16. The financial benefit from the efficiency improvement of integrating the inlet air cooling system was evaluated using the FSPA technique by utilizing Equations (3.106) to (3.113). The impact of CO_2 was also determined by utilizing Equations (3.114) to (3.116) to ascertain if its integration is environmentally friendly.

Equations (3.106) to (3.113) were used to calculate the FSPA, Qc, Capital cost, OMC, TC, Profit and Recovery period for integrating the inlet air cooling system utilizing data from Tables 4.16 and 4.17. The results of the energy cost analysis for the model are given in Table 4.18. The results of CO_2 emission rates for without cooling and with inlet air cooling system are presented in Figures 4.32 and 4.33.

Table 4.16**:** GT11 Performance Data for without and with Inlet Air Cooling System

S/N	**Parameters**	**Without cooling**	**With cooling**
1	Compressor Inlet air temperature (^{0}C)	27.67	20.546
2	Net power output (MW)	149.24	158.403
3	Thermal efficiency (%)	30.21	34.301
4	Fuel mass flow rate (kg/s)	10.98	10.25
5	Air mass flow rate (kg/s)	492.81	504.135

Table 4.17**:** Other Plant Parameters

S/N	**Parameters**	**Values**
1	Load factor (%)	75.00
2	Operational Time in a year (days)	365
3	Cost of fuel ($/kg)	0.1232
4	Relative Humidity (ϕ)	0.74

Table 4.18: Evaporative Inlet Air Cooling Model Results

S/N	Parameters	Value
1	Fuel savings per annum ($)	2,980,829.79
2	Cooling energy cost ($/kW)	468
3	Capital Cost, CC ($)	1,541,775.08
4	Operation and Maintenance Cost, OMC ($)	154,177.51
5	Total cost, TC ($)	1,695,952.59
6	Profit per annum ($)	1,284,877.20
7	Savings in power (MW)	11.863
8	Payback period (yr)	0.569
9	Emission Reduction, ER	0.102

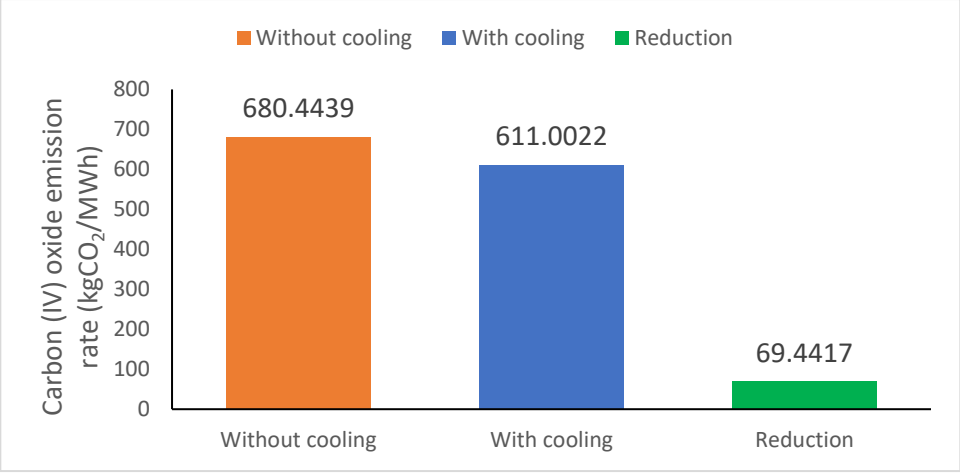

Figure 4.32**:** Carbon Dioxide Emission Rate in kgCO_2 per MWh for without Cooling and with Cooling System Incorporation

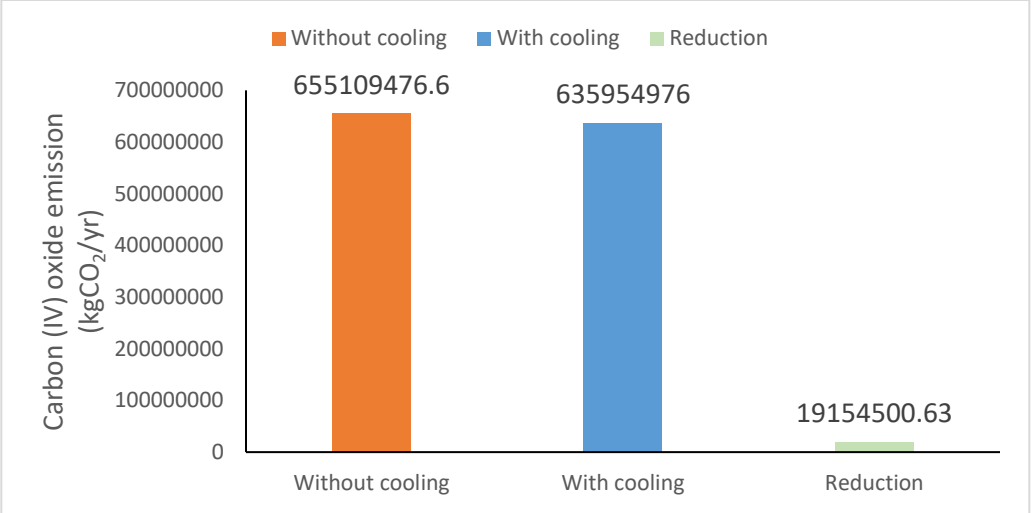

Figure 4.33**:** Mass of Carbon Dioxide Emission in $kgCO_2$ per year for without Cooling and with Cooling System Incorporation

Combined Cycle Model

Table 4.19 which contains data taken from the thermal performance of GT11 were used to analyse the gas turbine section of the proposed steam and gas power plant. The stack temperature of 170 ^{0}C was utilized for the study to circumvent deterioration owing to water vapour condensation in the products of combustion. The data used for the steam cycle study are provided in Table 4.20, which depended on the corresponding values from the gas turbine operating performance.

Equations (3.117) to (3.123) were fundamental mathematical equations that Ebsilon software employed in the combined cycle power plant model. The different pressure level combined cycle was developed using Ebsilon software and the simulation results of the model are presented in Table 4.20. Equations (3.123) to (3.127) were used to determine the energy cost analysis utilizing data from Tables 4.19 and 4.20, and the results obtained are presented in Table 4.21. The results of CO2 emission rates for the simple and combined cycle model are presented in Figure 4.34.

Table 4.19: Edo Azura GT11 Gas Turbine Performance Data

S/N	Parameters	Unit	Single Pressure	Double Pressure	Triple Pressure
1	Gas Turbine Exhaust, t_4	^{0}C	544.012	551.354	555.977
2	Stack Temperature, ts	^{o}C	170	170	170
3	Exhaust Gas mass flow rate, $\dot{m}_g$	kg/s	505.426	505.362	505.362
4	Fuel mass flow rate, $\dot{m}_f$	kg/s	9.945	10.151	10.151
5	Specific Heat capacity of Exhaust Gas, c_{pg}	kJ/kgK	1.148	1.148	1.148
6	Gas Turbine Power, P_{GTnet}	(MWe)	150.722	155.203	152.568
7	Gas Turbine, η_{GTnet}	(%)	33.638	33.934	33.358
8	Operational Time, OPT	s	31,536,000	31,536,000	31,536,000
9	Load Factor, LF	%	75	75	75
10	Cost of Fuel per Therm	$	2.5	2.5	2.5
11	Mass per Therm	kg	20.3	20.3	20.3

Table 4.20: Steam Cycle Parameters

S/N	Parameters	Single Pressure	Double Pressure	Triple Pressure
1	Steam Turbine (MWe)	65	82.51	76.348
2	Net Combined Power (MWe)	215.122	237.224	227.776
3	HRSG Steam Outlet Temperature (^{0}C)	524.012	531.354	392.968
4	High Pressure (bar)	75	80	119.973
5	Intermediate Pressure (bar)			26.991
6	Low Pressure (bar)		5	4.98
7	Condenser Pressure (bar)	0.05	0.05	0.05
8	Combined Efficiency (%)	48.01	51.868	49.802
9	Turbine Isentropic Efficiency, η_{ST}	85 %	85 %	85 %
10	Pump Isentropic Efficiency, η_p	92 %	92 %	92 %
11	Mechanical Efficiency, η_m	99 %	99 %	99 %
12	Generator Efficiency, η_g	97 %	97 %	97 %
13	Auxiliary Consumption Power	$0.05P_{ST}$	$0.05P_{ST}$	$0.05P_{ST}$

Table 4.21: Performance Results of the Combined Cycle Model

S/N	Parameters	Single Pressure HRSG	Double Pressure HRSG	Triple Pressure HRSG
1	Steam Turbine Net Power Output, PSTnet (MW)	65	82.51	76.348
2	Combined Cycle net Thermal Efficiency, $\eta_{combined}$ (%)	48.01	51.868	49.802
3	Fuel Savings Per annum, FSPA combined ($)	12394560.82	15642076.72	14590219.35
4	Savings in Power (MW)	65	82.51	76.348
5	Capital Cost, CC ($)	35750000	45380500	41991400
6	Operational and Maintenance Cost, OMC ($)	3575000	4538050	4199140
7	Total Cost, TC ($)	39325000	49918550	46190540
8	Pay Back Period (year)	3.173	3.191	3.166
9	Emission Reduction, ER	0.2994	0.3458	0.3302

The results of the CO_2 emission rate in $kgCO_2/MWh$ for both simple gas turbine and 3 models combined power cycle models, and reduction in CO_2 emission using Equations (3.127) to (3.129) are presented in Figure 4.38.

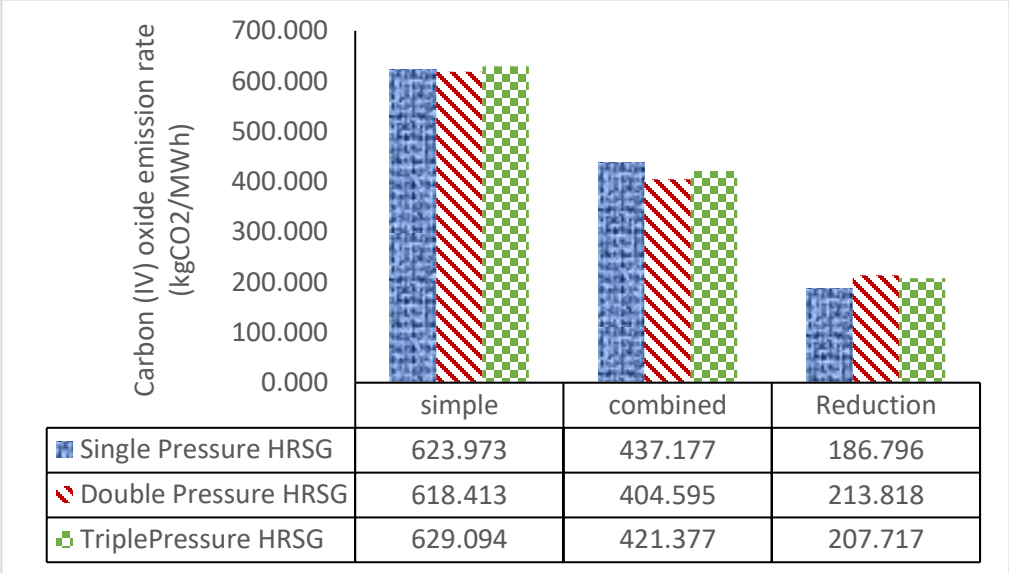

Figure 4.34: CO_2 Emission Rates for Simple and Combined Cycle Models

4.2 Discussion of Results

All the results presented in Section 4.1 are discussed in this section.

4.2.1 Results of Simulation for the Gas Turbine Power Units

The validation and analysis of results of SGT5 -2000E for design and off-design conditions using EBSILON software are discussed in the section.

Model Validation

As presented in Table 4.1, the percentage errors between the ISO and model data are 0.525%, -0.352%, 0,354%, -0.257% and 0% for net power output, heat rate, net thermal efficiency, turbine exhaust temperature and turbine exhaust mass flow rate respectively. For Azura Edo Power Plant guarantee data and model comparison, the error recorded is -3.135% and 0.886% for net power output and heat rate respectively. The results obtained from the model validation revealed that the model data are found to be in good agreement with the ISO and Azura Edo Power Plant guarantee data. These validation results are also in the same range as the works of Miguez Da Rocha (2010), Wallentinen (2016) and Matjanov (2020) which employed Ebsilon Professional in their work. Since the results of the model are consistent with the ISO and Azura Edo parameters, the off-design conditions results will be presented and be compared with operating parameters from the Azura Edo Power Plant. This is expected to show how the model mimics the actual operation of the power plant.

Ambient Temperature Variation

As the ambient air temperature increases and the air mass flow rate reduces, the compressor pressure ratio decreases as shown in Table C1. Also, as a result of the gas turbine allowing capacity and the decrease in air and fuel mass flow rates, the pressure, p_3 at the turbine inlet is lowered due to the increase in ambient air temperature. This results in a lower expansion pressure

ratio, and the net power output is reduced. It was also observed in Table C1 that as the ambient air temperature increased from 15 ^{0}C to 35 ^{0}C, the net power generated decreases from 165.146 to 140.816MW, the net thermal efficiency from 34.578 to 31.577%, the specific fuel consumption increases from 0.232 to 0.250 kg/kWh, the heat rate increases from 10411.24 to 11258.09 kJ/kWh, the mass of carbon dioxide emitted reduces from 27.855 to 25.66kg/s, and the carbon dioxide emission rate increases from 607.21 to 656.01 kg/kWh.

As observed in Figure 4.1, as the ambient air temperature increases, the turbine inlet temperature increases to a peak value of 1094.513 ^{0}C at 26 ^{0}C ambient air temperature and starts decreasing until it gets to a value of 1092.30 ^{0}C at 35 ^{0}C. The turbine exhaust temperature increases as the ambient temperature rises as shown in Figure 4.1, this is due to the decrease in expansion pressure ratio.

The model results have shown that the gas turbine generates more power at lower ambient temperature conditions. This is because of the large mass of gas that was expanded in the turbine at a higher-pressure ratio. Consequently, this makes the gas turbine generate more power at low ambient air temperature than at high ambient air temperature.

Partload Variation

In Table 4.4, it was observed that as the partload reduces, mass flow rates of fuel and exhaust gas, the turbine inlet and exhaust temperatures, net thermal efficiency, compression and expansion pressure ratios, and mass of carbon dioxide emitted decrease. The air ratio (AR) increases as the partload decreases.

As shown in Figure 4.2, the percentage of exhaust mass flow rate with the nominal value was almost constant with a change in partload. This shows that partload variation has little effect on

the exhaust mass flow rate of the gas turbine power plant. The percentage change in the turbine exhaust temperature increased as the partload increases. This means the higher the partload, the higher the exhaust temperature and this will be favourable when utilizing the exhaust temperature for further processes like HRSG at high partload.

Comparison of Model Data with Actual Operating Data

In Figures 4.3 to 4.5, it was observed that the model values for compressor exit, turbine inlet and exhaust temperatures were close to the actual operating data, with the three parameters increasing linearly as ambient air temperature increases for the three turbine units. The difference noticed was as a result of differences in pressure ratio observed for the model and actual data as shown in Tables A11 to A13 and C1 of Appendix V. The model and operating values for air and exhaust mass flow rates decrease with an increase in ambient air temperature and slight differences between them was observed as shown in Figures 4.6 and 4.8 in GT11, GT12 and GT13. The comparison between the model and operating values for fuel flow rate as shown in Figure 4.7 revealed that model data decreases slightly while the operating data increases as ambient air temperature increases. The high mass flow rate of fuel in the operating data could be attributed to the fact that the power plant needed more fuel to meet up power generated at a low-pressure ratio value compared to the corresponding model value with a higher-pressure ratio. As shown in Figure 4.9, both the model and operating data for net power output decrease as ambient air temperature increases. It was observed that for net power output, the model and operating data values were close. This also shows that the mass flow rate of fuel plays an important role in power generation.

Table 4.5 indicates the average error between the model and operating values for compressor exit, turbine inlet and exhaust temperatures, air, fuel and exhaust mass flow rates and net power output are 2.56 to 3.01, 1.13 to 1.23, -3.39 to -3.34, -0.03 to 0.28, 8.18 to 10.59, 0.15 to 0.30 and -0.34

to 0.47 respectively for the three GT units. The moderate deviations observed in turbine inlet and exhaust temperatures, mass flow rates of fuel, and net power output generated are indications of the difference in pressure ratios ranging from 0.376 to 0.703 for compressor and 0.583 to 0.911 for turbine between the model and actual data as shown in Table C5 of Appendix V. Also, it indicates some additional uncertainty in the modelling of the SGT5 – 2000E gas turbine on the same principle. The validation results are in good agreement with the results ranging from 3% to 14.5% obtained from Miguez Da Rocha (2010) and Wallentinen (2016) that used the same software for their study.

4.2.2 Energy Analysis

The actual data obtained from the power plant for the net power output of 139.80 to 159.41MW, 139.67 to 158.24MW and 141.08 to 160.70MW with ambient air temperature variations from 21 to 35 ^{0} C, 22 to 35 ^{0}C and 21 to 34 ^{0}C for GT11, GT12 and GT13 respectively are shown in Tables C2 to C4. The designed data for net power output for each of the GTs is 153MW at 26 ^{0}C. From the manufacturer's catalog, SGT5 – 2000E is designed for a net power output of 166MW at 15 ^{0}C, 1.013bar and 60% relative humidity, which is the International Standard Organization (ISO) weather data specification for rating gas turbines. The compressor pressure ratio for the designed net power output is 12:1, the pressure ratio obtained for the operating data range from 10.72 – 10.96 for the GT units. The low-pressure ratios obtained are responsible for the lower net power output compared to the designed net power output. The manufacturer of the Azura Edo Power Plant guaranteed net power output of 153MW at 26 ^{0}C per GT unit is based on the average ambient air temperature of the location. The average net power output for the three gas turbine units is 148.97MW for the period of study. This was an good performance but slightly lower than the guarantee net power output of 153MW, which was due to the difference in ambient air

temperature of 28.17 ^{0}C as shown in Table 4.6 for actual data compared to the guaranteed value of 26 ^{0}C and compressor pressure ratio of 10.72 to 10.96 compared to design compressor ratio of 12 and other unforeseen uncertainty. To enhance the net power output performance of the Azura Edo Power Plant, lowering the compressor air inlet temperature and ways to increase the compressor pressure ratio should be considered.

Figure 4.10 presents the variation of net power output and net thermal efficiency with ambient air temperature and compressor pressure ratio for GT11, GT12, and GT13. It was observed that in all the three units that the net power output and net thermal efficiency decrease as ambient air temperature increases and increase with compressor pressure ratio. This variation agrees with the results obtained in Kanbur et al. (2017). The highest net thermal efficiency obtained was 32.96% at an ambient temperature of 21 ^{0}C and 159.41MW net power output for GT11. The lowest net thermal efficiency of 27.11% was obtained at an ambient air temperature of 35 ^{0}C and 139.671MW net power output for GT12 as shown in Tables C2 to C4. Thus, this revealed that the net power output and net thermal efficiency are influenced by the changes in ambient air temperature and compressor pressure ratio. This is as a result of mass flow rate being proportional to the density of the air intake to the compressor, which shows that as density increases, the efficiency and power output increase as stated in Wood (1981) and Brooks (2000); and also increased compressor pressure ratio favours increase in efficiency and power output. The average net thermal efficiency and net power output for Azura Edo Power Plant are 29.79% and 148.97MW at an ambient air temperature of 28.17 ^{0}C as shown in Table 4.6.

The specific fuel consumption of all three GTs increases as the ambient air temperature increases and decreases with an increased pressure ratio as shown in Figure 4.11. Also, it was observed in Figure 4.11 that the work ratio decreases with increase in ambient air temperature and increases

with increase in the compressor pressure ratio. These changes agree with the results discussed in El – Shazly et al. (2016) and Brooks (2000). Specific fuel consumption means the rate of fuel consumed for a unit of power generated. The analysis shows that more fuel was burnt at high ambient air temperature and low compressor pressure ratio. Thus, reducing the compressor air inlet temperature and increasing the compressor pressure ratio will enhance efficient fuel usage in the power plant. The power plant will be susceptible to more irreversibility at high ambient air temperature and low-pressure ratio because the reduction in work ratio reduces the power plant effectiveness. The average specific fuel consumption and work ratio for the Azura Edo Power Plant are 0.269kg/kWh and 0.456 respectively as shown in Table 4.6.

Figure 4.12 presents the variation of heat rate with ambient air temperature and compressor pressure ratio for the three GT units. As illustrated in Figure 4.12, as the ambient air temperature increases the heat rate (HR) increases, while the heat rate decreases with an increase in compressor pressure ratio. The results obtained are in accord with the results obtained in El – Shazly et al. (2016) and Brooks (2000). Heat rate is an important decision parameter in the design feasibility and performance evaluation of a power plant, the cost of running a power plant can be reduced by lowering its heat rate (Bishoyi and Sudhakar, 2017). This shows that high ambient air temperature and the low-pressure ratio will increase the cost of power production. From Table 4.6, the average net heat rate for the station was 12,123.44 kJ/kWh, which is higher than the guaranteed net heat rate of 10,528 kJ/kWh. Thus, there is a need to reduce the net heat rate to improve the Azura Edo Power Plant performance by reducing the compressor inlet air temperature. Also, the results obtained revealed that for a 1 ^{0}C rise in ambient air temperature, there are drops of 1.16% in net power output and 1.58% net thermal efficiency, a 1.58% increase in SFC and HR, and a 0.64% decrease in WR.

From Table 4.6, the average flue gas loss was 296.87MW, which amounts to about 59.35% of fuel energy input into the power plant. The heat lost by the flue gases to the Azura Edo Power Plant surroundings occurred at an average exhaust temperature of 541.97 ^{0}C. This turbine exhaust temperature is high enough to raise steam for a combined cycle power plant, which means that the power plant can be operated as a combined power plant as proposed.

The Sankey diagram for GT11 was presented in Figure 4.13. This shows the energy supplied by the fuel, various losses such as flue gas losses, mechanical losses, generator losses and auxiliary losses, energy consumed by the compressor and net power output to the grid. The flue gas and other stack losses have the highest loss of 341.15MW, followed by generator losses of 2.26MW, mechanical losses of 1.52MW and the lowest was auxiliary losses of 0.23MW. It also provides the value of the net power output of 149.29MW and 173.54MW as power consumed by the compressor. It indicates the diagrammatic representation of the energy balance of GT11 at a glance.

The mechanical losses as shown in Tables C2 to C4 for the GT units were moderately consistent and were not depend on power output. This can be ascribed to the way that the turbine speeds are steady regardless of power output since frictional losses correspond to turbine speed as stated in Ighodaro (2006). Additionally, the generator losses rely upon the influence factor at which the electricity is being produced. The least generator losses will take place when the power factor is near unity. The auxiliary's losses were steady and they occur regardless of the electrical power generated.

4.2.3 Exergy Analysis

The exergy flow rates of the various Azura Edo Power Plant GTs were found to range from 148.27 to 149.15MW as shown in Tables 4.10 to 4.12. The fuel exergy flow rates in the combustion

chamber for GT11, GT12 and GT13 were 524.06, 524.06 and 531.79MW respectively. The total exergy destruction was evaluated to be 255.26 MW, 255.34 MW and 263.63MW for GT11, GT12 and GT13 respectively. The results indicate that exergy destruction in the combustion chamber is more than exergy output in the power plant. The high exergy destruction observed was a result of the high irreversibility that occurred due to the large temperature difference between the combustion chamber and the working fluid (Ibrahim et al., 2017). As shown in Figure 4.14, the gas turbine section is found to have the highest exergy efficiency of 96.36, 96.33 and 96.43% for GT11, GT12 and GT13 respectively. The combustion chamber has the least exergetic efficiency of 56.17, 56.02 and 55.16% for GT11, GT12 and GT13 respectively. The air compressor and the total plant exergy efficiency ranged from 92.22 to 92.41% and 50.43 to 51.29% respectively. Thus, the combustion chamber experienced the highest degradation of energy and irreversibility among the components studied.

The exergy destruction efficiency for the various components and total plant for the three GTs presented in Figure 4.15 revealed that the largest exergy destruction efficiency took place in the combustor, which is 44.84% in GT13. The least exergy destruction efficiency of 3.57% occurred in the turbine section of GT13. It was seen that the highest exergy destruction efficiency in the overall plant was 49.57% in GT13 of the inlet exergy flow in the Azura Edo Power Plant as illustrated in Figure 4.15. The results of exergy efficiency and exergy destruction efficiency largely agree with those of Al-Doori (2012); Oyedepo et al. (2015); Ibrahim et al. (2017) but different from work of Ofudu and Abam (2002) that stated that the highest exergy destruction took place in the gas turbine.

Figures 4.17 and 4.18 compared the exergy efficiency and exergy destruction efficiency of each of the components and the total plant for various ambient air temperatures ranging from 21 to 35

^{0}C for the three GTs in the Azura Edo Power Plant. The exergy efficiency of the combustion chamber and the overall plant was observed to reduce notably with a rise in the ambient air temperature, whereas a slight increase was observed in the compressor and turbine with the rise in ambient air temperature. The exergy destruction efficiency increases with an increase in ambient temperature for the combustion chamber and overall plant, no changes were observed for air compressor and gas turbine units. These revealed that when the Azura Edo Power Plant operates at various ambient air temperatures, more exergy loss occurred at high ambient air temperatures than at low ambient air temperatures. The results of the variation of exergy and exergy destruction efficiencies with ambient air temperature agreed with those obtained by Ibrahim et al. (2017).

The variation of exergy efficiency and exergy destruction efficiency of the combustion chamber and total plant with ambient temperatures are presented in Figures 4.19 and 4.20 respectively for various GT units. For the combustion chamber, the optimum ambient temperature for better performance was determined to be 300, 301 and 300K for GT11, GT12 and GT13 respectively as shown in Figure 4.19. From Figure 4.20, 303, 304, and 302K ambient air temperature were obtained for the total plant as the optimum ambient air temperature for GT11, GT12 and GT13 respectively. These optimum ambient air temperatures were obtained based on the points of intersection between exergy and exergy destruction efficiencies for the combustion chamber and overall plant. These values obtained are higher than the ones obtained in Ibrahim et al. (2017) of 281 to 283.15K because of the high ambient air temperature data recorded at the power plant location used for this study. The inlet air cooling system should be used to reduce the optimum compressor air inlet temperature in order to enhance the performance of the Azura Edo Power Plant.

The summary of the Second Law efficiencies for three GTs presented in Table 4.13 shows that GT11 has the highest value of 28.46% and the lowest is for GT12 with 28.03%; and station average of 28.26%. Figure 4.16 compared the net thermal efficiency using the First Law of Thermodynamics with the Second Law of Thermodynamics efficiencies. It was observed that all the values of the Second Law efficiencies for the three GTs were lower than corresponding net thermal efficiencies. This indicates that the Second Law efficiency caters for more irreversibility or loss of energy quality in the power plant than the First Law.

It was also observed that Second Law efficiency decreases with an increase in ambient air temperature for the three GT units as shown in Figure 4.21. This illustrates high degradation of energy in the performance of the Edo Azura Power Plant at high ambient air temperature. Thus, the air temperature entering the compressor needs to be reduced in order to increase the Azura Edo Power Plant Second Law efficiency.

4.2.4 Exergy Improvement Potential, Sustainability Index and Depletion of Fuel

As presented in Figure 4.23, the total exergy improvement potential of the gas turbine plant ranges from 124.77MW to 131.03MW for various units. The combustion chamber has the largest exergy improvement potential, which varies from 101.07MW to 107.23MW for the three GT units. The air compressor is next, with values ranging from 1.025MW to 1.079MW and the least occurred in the gas turbine section with values ranging from 0.419MW to 0.441MW for various units. The high exergy improvement potential obtained in the combustor is because of irreversibility related to combustion and a huge difference in temperature values between the air entering the combustor and the temperature of combustion products. The massive losses imply that a lot of exergy present in fuel with the potential to generate power was wasted.

Figure 4.26 compares the variation of exergy improvement potential with ambient air temperature for the various components and total plant of the three GT units. It was observed there is an increase in exergy improvement potential with ambient air temperature in CC and total plant, while little changes occurred in the air compressor and turbine sections. This means that at low ambient air temperature less improvement will be required in the combustion chamber section.

The combustion chamber's exergy improvement potential can be managed by preheating its inlet air, which will reduce heat loss and extra fuel flowing into the combustor. Also, this will be achieved because the temperature of the air flowing into the combustor will be increased, thereby reducing the temperature difference between the combustor inlet air and flame temperature. These outcomes have shown that the combustion chamber section of the Azura Edo Power Plant needs more attention for improvement.

As shown in Figure 4.24, the highest sustainability of 2.062 and the lowest depletion number of 0.487 for the fuel were obtained for GT11. While the lowest sustainability index of 2.024 and the highest depletion number of 0.495 were observed for GT13. The station average sustainability index and depletion number of the fuel are 2.046 and 0.490 respectively. These values obtained in this work agree with those obtained by Oyedepo et al. (2015). The sustainability index decreases with an increase in ambient air temperature, while the depletion number of the fuel increases with ambient air temperature as shown in Figure 4.25. Thus, this revealed that low ambient air temperature favours sustainability and reduces the depletion of fuel utilization.

4.2.5 Environmental Analysis

The average emission of CO_2 for the various gas turbine units varies from 698.34 to 720.20 $kgCO_2/MWh$ during the period of this study as presented in Table 4.14. The GT12 has the highest value and GT11 has the lowest value. The power plant average of 707.74$kgCO_2/MWh$ is in the range value of 214 -720$kgCO_2/MWh$ obtained from various studies as mentioned by Robert et al. (2020). The average value is on the high side of the mentioned range, which means CO_2 capture technology such as post combustion carbon capture will be encouraged to reduce the emission rate. The average mass of CO_2 emitted annually shown in Table 4.14 ranges from 682,310,721.95 kg to 697,208,581.77 kg with a station average of 690,602,489.84 kg. Again, GT11 has the lowest rate and the highest value is from GT12. The total annual mass of CO_2 emitted for the Azura Edo Power Plant was 2,071,807.46951 tCO_2/yr, which is lower than the design value of 2,178,000 tCO_2/yr. Also, the station average is less than the guaranteed value of 726,000,000 $kgCO_2$ annually. The results obtained indicate that the Azura Edo Power Plant has a fairly high carbon dioxide emission rate. The values obtained are higher than the International Finance Council (IFC) performance standard recommendation of 100,000,000 $kgCO_2/yr$ as stated in Azura EIA (2013). So, there is a need to reduce the quantity of CO_2 emissions from the power plant by carbon capture technology as earlier mentioned.

As seen in Figures 4.27 and 4.29, the carbon dioxide emission rate in kg/MWh and annual emission increases with ambient air temperature. Thus, at high ambient air temperature more CO_2 was emitted, so the inlet air cooling system will be required to reduce CO_2 emission in Azura Edo Power Plant. Figure 4.28 is a plot of the CO_2 emission rate against net thermal efficiency. for the three GT units. It was observed that the CO_2 emission rate in kg/kWh decreases as the net thermal efficiency increases. This indicates that improved net thermal

efficiency will reduce CO_2 emission in kg/MWh, which agrees with the works of Steen (2000) and Memon et al. (2013).

The actual mass flow rate (m_g) of the combustion products from various gas turbine units were compared with the computed values (m_{gc}) to validate the environmental model. The percentage of error values obtained from the model validation is presented in Table 4.15. The comparison of computed values and actual values from the power plant reveals that the difference in percentage error ranges from 0.68625% to 0.78093%. GT11, GT12 and GT13 have an average percentage error of 0.734, 0.755 and 0.750% respectively. The percentage error obtained validates the environmental model used since the results of the computed value agree closely with the actual operating data of the Azura Edo Power Plant.

From Figure 4.30, the emission of CO_2 decreases for actual data and increases for model data with an increase in ambient air temperature. The variation was due to the difference in the mass flow rate of fuel used for model and operating values because the mass flow rate of fuel is also a parameter in determining the mass of CO_2 emitted (Kang et al., 2011). The emission of CO_2 rates for both model and operating data are presented in Figure 4.31 shows that both increase as ambient air temperature increases. The comparison results for emission rate for model and operating data with change in ambient air temperature are close. So, this indicates good potency between the developed model and actual data performances.

This research work has shown that the Azura Edo Power Plant's net thermal efficiency can be improved in two ways. By enhancing the most ineffective components such as reducing the temperature of the air flowing into the compressor and using the least sufficient flow rate of fuel

and achieve optimal combustion. Also, the reduction in the net CO_2 emission rate will be achieved by improving the overall plant thermal efficiency.

4.2.6 Preliminary Analysis on Azura Edo Power Plant Improvement

Inlet Cooling System

Table 4.18 shows the outcomes for FSPA, energy cooling cost, profit, payback and ER for the cooling model. From the results obtained, it was seen that the energy cost study for the retrofitted model for the Azura Edo Power Plant, a profit of $1,284,877.20 was realized for the first year of the proposed retrofit for GT11. As it were, for the three gas turbine units, the impact of integrating an intake cooling model gave a net yearly profit of $3,854,631.60. This outcome shows that the model is economically feasible because the expenses can be recovered within the first year of operation. This concurs with the investigation carried out by Yazdi et al. (2015) and Ehyaei et al (2012) of the economic feasibility of the inlet air cooling arrangement in gas turbine power plants.

There is an inclination in the energy industry to lower emitted GHG, for example, CO_2. The emission of CO_2 evaluation model was done utilizing Equations (3.114) to (3.116). The air and fuel mass flow rates obtained from the power plant as presented in Tables 4.17 and 4.18 were utilized in the calculation with other data stated in the Environmental Model section. The values of CO_2 emission obtained for the scenarios of the incorporation of an intake cooling system and without an installation are shown in Figures 4.32 and 4.33.

Figure 4.32 shows that the emission of CO_2 in units of $kgCO_2$ per MWh for without and with cooling system are 680.4439 and 611.0022 respectively. Incorporating the inlet air cooling system, led to a reduction in GHG emission of 69.4417 $kgCO_2$ per MWh. Once more, in Figure 4.33 it is seen that the emission of GHG per year for the “Without” and “With” inlet air cooling

systems are 655,109,476.6kgCO_2 and 635,954,976.0kgCO_2 respectively. In essence, the reduction in CO_2 emitted per year for integrating the air intake cooling model is 19,154,500.6 kgCO_2 for one gas turbine unit (GT11). The reduction occurred as a result of the inlet air cooling model consuming less fuel and generating more power. Hence, the reduction in CO_2 emitted for the three gas turbine units is 57,463,501.80 kg. In addition, the emission reduction (ER) value of 0.102 was obtained for comparing the CO_2 emission rates for the without cooling and with cooling inlet air cooling systems. This again showed that the impact of integrating compressor inlet air cooling system into Azura Edo Power Plant has environmental advantages in light of the fact that less quantity of CO_2 will be released into the atmosphere. The profit earned is extra revenue which can be utilized for pay rates and different costs of operating the power plant. The reduction in the emission of GHG kgCO_2 of fuel by inlet air cooling system integration will help to improve the environmental conditions of the power plant surroundings.

Combined Cycle Model

From Table 4.21, the retrofitted GT11 with various HRSG pressure steam cycle models by using waste heat from the unit, the efficiency has been improved from 33.638% to 48.01%, 33.934% to 51.868% and 33.358% to 49.802% for single, double and triple HRSG pressures models respectively. The efficiency enhancement will make the combined cycle power plant suitable for generating base load. Also, as shown in Table 4.21, the additional power of 65MW, 82.51MW and 76.348MW for electricity and fuel saving per year for GT11 of $12,394,560.82, $15,642,076.72 and $14,590,219.35 for utilizing HRSG with single, double and triple pressures respectively. The payback period or cost recovery period for integrating the single, double and triple HRSG pressure steam cycle components to form a combined cycle power plant was evaluated to be 3.173, 3.191 and 3.166 years respectively. A normal thermal power plant has an

active life ranging from 25 to 30 years. In other words, the energy cost analysis indicates that the incorporation of the steam cycle components is economically viable.

As shown in Figure 4.34, the benefits of the reduction in CO_2 emission for combined cycle model application utilizing single, double and triple HRSG pressures are 186.796 $kgCO_2$/MWh, 213.818 $kgCO_2$/MWh and 207.717 $kgCO_2$/MWh respectively. The values of emission reduction (ER) comparing both simple and combined cycles are 0.2994, 0.3458 and 0.3302 for single, double and triple HRSG pressure respectively as shown in Table 4.21. Also, the model has reduced the emission rate close to the international standard of 404 $kgCO_2$/MWh (Ong et al., 2011), 407.5 $kgCO_2$/MWh (Hondo, 2005). The reduction of CO_2 emission rate was due to the fact that the combined cycle produced more power than the simple cycle for the same amount of fuel consumed. Thus, this indicates that the combined cycle model is environmentally viable. Further, the utilization of waste heat from the Azura Edo Power Plant will assist to lower the quantity of heat released to its environment, subsequently assisting with reducing its environmental pollution as expressed by Pilavachi (2000).

The comparison of utilizing the single, double and triple HRSG pressures for steam cycle integration in Azura Edo Power Plant to evaluate the various pressure level combined cycle models was carried out. Based on the outcomes achieved for the steam cycle power output, combined cycle thermal efficiency, payback period, and CO_2 emission reduction the double HRSG pressure concept was selected to be the best option. Thus, the double HRSG pressure scheme is recommended for optimal operation of the combined cycle power plant for the Azura Edo Power Plant.

4.3 Findings

The findings from the study were as follows:

(i) The results obtained from model validation showed that the model data are found to be in good agreement with the ISO and Azura Edo guaranteed data for both design and off-design conditions.

(ii) The study has shown that from the energy analysis performance the Azura Edo Power Plant achieved 97.37% of its guaranteed performance within the period considered.

(iii) The results from exergy analysis revealed that the combustion chamber has the lowest exergy efficiency of 55.16% and the highest exergy destruction efficiency of 44.84%.

(iv) The combustion chamber has the highest exergy improvement potential and the average depletion number and sustainability index values obtained were 0.490 and 2.046 respectively for the power plant.

(v) The emission of CO_2 from the Azura Edo Power Plant was found to be lower than the guaranteed value but still higher than International Finance Council (IFC) standard.

(vi) The study has indicated that ambient air temperature influenced the thermodynamic and environmental performance of the power plant.

(vii) The integration of air inlet cooling and combined cycle models will enhance the power plant's performance and reduction in its CO_2 emission rate.

CHAPTER FIVE

CONCLUSION AND RECOMMENDATION

5.1 Conclusion

In this study, the thermodynamic and environmental analyses of the Azura Edo Power Plant have been carried out using the data from the power plant. A review of previously conducted works revealed that there was a need to carry out performance analysis of various plants from time to time. It was observed that energy, exergy and environmental analyses carried out previously provided information about power plant performance and made suggestions for their performance improvement.

The design and off-design condition of the Azura Edo Power Plant were modelled employing Ebsilon Software. The results obtained from model validation showed that the model data was found to be in good agreement with the ISO and Azura Edo guaranteed data for both design and off-design conditions. MATLAB codes were generated for the energy, exergy and environmental analyses for the Azura Edo Power Plant operational data. The results obtained from the energy analysis showed that the average plant net thermal efficiency was 29.79% at an ambient air temperature of 28.17 ^{0}C and net power out of 148.97MW. Also, the SFC, HR and WR were 0.269kg/kWh, 12123.44kJ/kWh and 0.456 respectively. The flue gas loss is about 59.35% of the fuel energy input. It was also observed from the energy analysis that the ambient air temperature and pressure ratio affected the power plant performance.

The exergy analysis showed that the highest exergy efficiency occurred in the gas turbine section and the lowest occurred in the combustion chamber. Also, the highest exergy destruction efficiency occurred in the combustion chamber and the least took place in the turbine. Furthermore, the ambient air temperature affects the exergy and exergy destruction efficiencies

of various components and the total plant. The optimum ambient air temperatures of 27.487 ^{0}C and 30.15 ^{0}C were obtained when the combustion chamber and total plant exergy and exergy destruction efficiencies were considered. The components that have the highest and lowest exergy improvement potential were the combustion chamber and the turbine respectively. The average depletion number and sustainability index values obtained were 0.490 and 2.046 respectively. The exergy improvement potential, depletion of fuel, and plant sustainability were observed to be affected by the ambient air temperature.

The CO_2 emission rates obtained were within the range of the designed data. Also, the study showed that the emission of CO_2 was affected by the ambient air temperature and net thermal efficiency. Based on the preliminary analysis results, incorporations of the inlet cooling system, and combined cycle components are suggested. The results obtained revealed that the various preliminary analyses are useful in improving the performance and environmental impact of the Azura Edo Power Plant. The information obtained from this study will help the energy manager and engineer in running the Azura Edo Power Plant for the effective utilization of available fuel and enhance its performance.

5.2 Recommendation

This study showed that the Azura Edo Power Plant performance was good, further performance study will be required from time to time for proper performance monitoring. More work on other inlet air cooling systems such as mechanical chiller and vapour absorption chiller model incorporation to Azura Edo Power Plant should be carried out. Further study on carbon capture techniques, can be considered to reduce the carbon dioxide emission from the power plant.

5.3 Contribution to Knowledge

The research work has contributed to knowledge as follows:

(i) A steady-state adiabatic model has been developed for the Azura Edo Power Plant for predicting its performance.

(ii) The study has developed a procedure for determining CO_2 emission for Azura Edo Power Plant.

(iii) The study has shown that integrating inlet air cooling and combined cycle components will lead to the improvement of the plant performance.

REFERENCES

Abam, D. P. S., and Moses N. N. (2011). Computer simulation of a gas turbine performance. Global J. Res. Eng. 11:37–44.

Abam, F. I., I. U. Ugot, and D. I. Igbong. (2012). Performance analysis and components irreversiblities of a (25 MW) gas turbine power plant modeled with a spray cooler. Am. J. Eng. Appl. Sci. 5:35–41.

Abbaspour H, Ehyaei M.A., Ahmadi A., Panahi M., Abdalisousan A., Mirzohosseini A. (2021), Energy, exergy, economic, exergoenvironmental and environmental (5E) analyses of the cogeneration plant to produce electrical power and urea, Energy Conversion and Management 235: 113951. https://doi.org/10.1016/j.enconman.2021.113951.

Ahmad, P., A. H. Barzegar, A. Ghaffarizadeh, and M. H. Saidi. (2010). Thermoeconomic-environmental multi-objective optimization of a gas turbine power plant with preheater using evolutionary algorithm. Int. J. Energy Res. 35:389–403.

Ahmadi M.H, Ahmadi M.A, Pourfayaz F, Hosseinzade H, Acıkkalp E, Tlili I, Feidt M, (2016), Designing a powered combined otto and stirling cycle power plant through multi-objective optimization approach, Renew. Sustain. Energy Rev 62:585 -595.

Ahmadi M.H., Nazari M.A., Sadeghzadeh M., Pourfayaz F., Ghazvini M., Ming T., Meyer J.P., and Aharifpur M. (2018), Thermodynamic and Economic Analysis of Performance Evaluation of all the Thermal Power Plants: A Review, Energy Science and Engineering 2018, 1 – 36.

Ahmadi P, Dincer I, Rosen MA (2011), Exergy, exergoeconomic and environmental analyses and evolutionary algorithm based multi-objective optimization of combined cycle power plants. Energy 36 (10):5886–98.

Ahmadi P, Dincer I, Rosen MA (2013), Thermodynamic modeling and multi-objective evolutionary-based optimization of a new multigeneration energy system. Energy Convers Manage 76:282–300.

Ahmadi, P. and Dincer I. (2010). Exergo- environmental analysis and optimization of a cogeneration plant system using Multimodal Genetic Algorithm (MGA). Energy 35:5161–5172.

Ahmadi, P., Rosen M. A., and Dincer. I. (2011). Greenhouse gas emission and exergo-environmental analyses of a trigeneration energy system. Int. J. Greenhouse Gas Control 5:1540–1549.

Al-Doori W.H.A (2012), Exergy Analysis of Gas Turbine Performance with Effect Cycle Temperatures, IJRRAS 13 (2): 549 – 556.

Alhazmy M.M, Jassim R.K, Zaki G.M (2006): Performance Enhancement of Gas Turbines by Inlet Air – Cooling in Hot and Humid Climates International Journal of Energy Research 30: 777 – 797

Al-Ibrahim A, Varnham A (2010), A Review of Inlet Air – Cooling Technologies for Enhancing the Performance of Combustion Turbines in Saudi Arabia, Applied Thermal Engineering, Volume 30, pp 1879 – 1888.

Aliu S.A and Ochornma P.I (2018), Exergoeconomic Analysis of Ihovbor Gas Power Plant, *Nigerian Journal of Technology (NIJOTECH) Vol. 37, No. 4, pp.* 927 – 935. http://dx.doi.org/10.4314/njt.v37i4.10.

Aljundi, I. H. (2009). Energy and exergy analysis of a steam power plant in Jordan. Appl. Therm. Eng. 29:324–328.

Allam, R. J., Palmer, M. R., Brown Jr, G. W., Fetvedt, J., Freed, D., Nomoto, H. and Jones Jr, C. (2013). High efficiency and low cost of electricity generation from fossil fuels while eliminating atmospheric emissions, including carbon dioxide. *Energy Procedia*, *37*, 1135-1149.

Allam, R.J., Palmer, M.R., Brown Jr, G.W., Fetvedt, J., Freed, D., Nomoto, H., Itoh, M., Okita, N. and Jones Jr, C., (2013). High efficiency and low cost of electricity generation from fossil fuels while eliminating atmospheric emissions, including carbon dioxide. *Energy Procedia*, *37*, pp.1135-1149.

Allen, R. P., and Kovacik, J. M. (1984). Gas turbine cogeneration—principles and practice.

Almansoori M.H and Dadachi Z.E (2018), Exergy Efficiency and Environmental Impact of Electricity of a 620MW – Natural Gas Combined Cycle, Journal of Power and Energy Engineering 6, 1 – 21.

Altayib, K. (2011). Energy, exergy and exergoeconomic analyses of gas-turbine based systems. M.Sc. thesis, University of Ontario Institute of Technology.

Ameri M, Nabati H, Keshtgar A. (2004): Gas Turbine Power Augmentation Using Fog Inlet Cooling System. Proceedings ESDA 04 7th Biennial Conference of Engineering Systems design and Analysis. Manchester UK. ESDA 2004 – 58101.

Ameri M, Shahbazian H.R, Nabizadeh M. (2007): Comparison of Evaporative Inlet Air Cooling Systems to Enhance the Gas Turbine Generated Power, Int. J. Energy Res 31: 483 – 503.

Aminov Z, Nakagoshi N, Xuan T.D, Higashi O, Alikulov K (2016), Evaluation of the energy efficiency of combined cycle gas turbine. Case study of Tashkent thermal power plant, Uzbekistan, Applied Thermal Engineering 103: 501–509.

Amjady A. Keynia F and Zareipour H (2011), Short Term wind Power Forecasting Using Ridgetel Neural Network. Electrical Power Systems Research, Vol. 81, pp 581 – 595.

Amrollahi, Z., Ertesvag, I. and Bolland. O. (2011). Thermodynamic analysis on post- combustion CO_2 capture of natural- gas fired power plant. Int. J. Greenhouse Gas Control 5:422–426.

Angelis-Dimakis, A., Biberacher, M., Dominguez, J., Fiorese, G., Gadocha, S., Gnansounou, E., Guariso, G., Kartalidis, A., Panichelli, L., Pinedo, I. and Robba, M. (2011). Methods and tools to evaluate the availability of renewable energy sources. *Renewable and Sustainable Energy Reviews*, *15*(2), pp.1182-1200.

Ankit K., Ankit S., Abhishek K.S., Remendra R., and Bijan K.M (2017), Thermodynamic Analysis of Gas Turbine Power Plant, International Journal of Innovative Research in Engineering & Management (IJIREM), Vol.4, Issue 3(May) pp 648 – 654.

Anthony G.W.G., McHugh J, Schiesser W. E. (2015), An Introductory Global CO_2 Model, World Scientific Publishing Co.

Arsalis A. and Alexandrou A. (2014), A Thermodynamic Modelling and Exergy Analysis of a Decentralized Liquified Natural Gas – Fueled Combined - Cooling Heating – and – Power Plant, J. Nat. Gas Sci. Eng, 21: 209 – 220. https://doi.org/10.1016/j.jngse.2014.08.009.

ASHARE (2008), 2008 Handbook HVAC systems and Equipment, S.I. Edition. Chapter 17.

Attala, L., Facchini, B., and Ferrara, G.(2001), Thermoeconomic Optimization Method as Design Tool in Gas-Steam Combined Plant Realization," Journal of Energy Conversion and Managment, Vol. 42, No. 1, (July), pp. 2163 – 2172.

Awaludin M., Miswandi, Adhy P., Iwan K., and Rommy (2016), Exergy Analysis of Gas Turbine Power Plant 20MW in Pekanbaru – Indonesia, International Journal of Technology 5 921 – 927.

Azim H and Farshid K (2017), Different Techniques for Prediction of Wind Power Generation, In: Renewable Energy Systems, Edited by Sandip A. Kale, Chapter 5, pp 85 – 99, Nova Science Publisher Inc.

Azura Edo (2017), Testing Manual for Azura Edo Power Plant.

Azura EIA (2013), Azura Edo Independent Power Project Environmental Impact Assessment Vol. 1: Final Report January 2013, Prepared by Environmental Resources Management. www.erm.com.

Baakeem, S.S., Orfi, J. and Al-Ansary, H., (2018), Performance improvement of gas turbine power plants by utilizing turbine inlet air-cooling (TIAC) technologies in Riyadh, Saudi Arabia. *Applied Thermal Engineering*, *138*, pp.417-432.

Babaelahi M, Rafat E and Mofidipour E (2019), Emergy-based economic and environmental analysis and multi-objective optimization of a two-cascade solar gas turbine power plant, Sustainable Production and Consumption 20 (2019) 165–177.

Baes C F, Goeller H E, Olson J S and Rotty R M. (1977), Carbon dioxide and climate: The uncontrolled experiment. American Scientist.65:310-320.

Balkrishna, M. C. (2009). Energy and exergy analysis of a captive steam power plant. Proceedings of International Conference of Energy and Environmental, ISSN: 2070 – 3740

Balli, O., 2017. Advanced exergy analyses of an aircraft turboprop engine (TPE). *Energy*, *124*, pp.599-612.

Barzegar Avval H, Ahmadi P, Ghaffarizadeh AR, Saidi MH (2011), Thermo-economic-environmental multiobjective optimization of a gas turbine power plant with preheater using evolutionary algorithm. Int J Energy Res 35(5):389–403.

Başoğul Y. (2019), Environmental assessment of a binary geothermal sourced power plant accompanied by exergy analysis, Energy Conversion and Management 195: 492–501.

Bejan A (2012), Advanced Engineering Thermodynamics, 3rd edition, John Wiley & Sons, Inc, Hoboken, New Jersey.

Bejan A., Tsatsaronis G., Moran MJ (1996), Thermal Design and Optimization, Wiley, New York.

Bishoyi, D. and Sudhakar, K., (2017), Modeling and performance simulation of 100 MW PTC based solar thermal power plant in Udaipur India. *Case studies in thermal engineering*, *10*, pp.216-226.

Blumberg T, Assar M, Morosuk T, Tsatsaronis G (2017), Comparative exergoeconomic evaluation of the latest generation of combined-cycle power plants. Energy Convers Manage; 153:616–26.

Boait P, Advani V, Gammon R (2015). Estimation of demand diversity and daily demand profile for off-grid electrification in developing countries. Energy Sustain Develop 29:135–41.

Bolatturk A, Kanoglu M, Coskun A (2007). Thermodynamic evaluation of first and second law performance of evaporative cooling schemes for regenerative gas turbines. Energy Explor Exploit 25(3):227–46. https://doi.org/10.1260/014459807782009196.

Bontempo R, Manna M (2019), Work and efficiency optimization of advanced gas turbine cycles, Energy Conversion and Management 195: 1255–1279.

Boonmasa S, Namprakai P., Muangapoh T. (2006), Performance Improvement of the Combined Cycle Power Plant by Intake Air Cooling Using an Absorption Chiller, Energy, 31 (12): 2036 – 2046.

Boyce, M.P. (2012), Combined cycle power plants. In *Combined Cycle Systems for Near-Zero Emission Power Generation* Woodhead Publishing. pp. 1-43.

Brink J.C (2003), Modelling Cost – effectiveness of Interrelated Emission Reduction Strategies - the case of Agriculture in Europe, Ph. D Thesis, Wageringen University, Dissertation No. 3337, Netherland.

Brooks F.J (2000): GE Gas Turbine Performance Characteristics, GE Power systems, New York

Buchgeister, J. (2010). Exergoenvironmental analysis – a new approach to support the design for environment of chemical processes? Chem. Eng. Technol. 33:593–602.

Buecker B (2002), Basics of Boiler & HRSG Design, Penn Well Corporation, Tulsea, Oklahoman, U.S.A.

Carapellucci, R., Giordano, L., and Vaccarelli, M. (2016). The use of biomass to reduce power derating in combined cycle power plants retrofitted with post-combustion CO_2 capture. *Energy conversion and management*, *107*, 52-59.

Carneiro M.L.N.M and Gomes M. S. P (2019), Energy, exergy, environmental and economic analysis of hybrid waste-toenergy plants, Energy Conversion and Management 179 :397–417

Carranza-Sánchez Y and Oliveira Jr. S. (2015), Exergy analysis of offshore primary petroleum processing plant with CO_2 capture. Energy 88:46–56.

Cengel Y.A and Boles, M.A (2010), Thermodynamics an Engineering Approach. 7th Edn: Mc Graw-Hill, New York, pp: 1024.

Chandramohan, S. (2008). First and second law analysis of organic Rankine cycle. Ph.D. thesis, Mississippi State University.

Chavan, B. L., and Rasal, G. B. (2010). Sequestered Standing Carbon Stock in Selective Tree Species Grown in University Campus at Aurangabad, Maharashtra, India. International Journal of Engineering Science and Technology, 2, 3003-3007

Chen B, Guo Q, Chen Y, Sun H (2020), An Economic Dispatch Model for Combined Heat and Power Systems Considering the Characteristics of Heat Recovery Steam Generators, Electrical Power and Energy Systems 118: 105775, pp 1 -9.

Chen X (2017). Operation and scheduling optimization of a multi-energy complementary combined heat and power system [dissertation]. Zhejiang: Zhejiang University;

Chmielniak T, Monka P, Pilarz P(2016), Investigation of a combined gas-steam system with flue gas recirculation. Chem Process Eng – Inzynieria Chemicznai Procesowa 37(2):305–16. https://doi.org/10.1515/cpe-2016-0025.

Colera M, Soria A, Ballester J, (2019), A numerical scheme for the thermodynamic analysis of gas turbines, Applied Thermal Engineering 147: 521–536

Colmenar-Santosa A., Gómez-Camazóna D., Rosales-Asensiob E., Blanes-Peiró J. (2018), Technological improvements in energetic efficiency and sustainability in existing combined-cycle gas turbine (CCGT) power plants, Applied Energy 223: 30–51.

Colonna, P., Casati, E., Trapp, C., Mathijssen, T., Larjola, J., Turunen-Saaresti, T., and Uusitalo, A. (2015). Organic Rankine cycle power systems: from the concept to current technology, applications, and an outlook to the future. *Journal of Engineering for Gas Turbines and Power*, *137*(10).

Connelly, L., and Koshland. C. P. (1997). Two aspects of consumption: using an energy based measure of degradation to advance the theory and implementation of industrial ecology. Resour. Conserv. Recycl. 19:199–217.

Coplan CO. (2005), Exergy Analysis of Combined Cycle Cogeneration Systems (M. Sc Thesis), Department of Mechanical Engineering, Middle East Technical University, Ankara, Turkey.

De Olivera M.E.D, Vaughan B.E and Rykiel Jr E.J (2005), Ethanol as Fuel: Energy, Carbon Dioxide Balances, and Ecological Footprint, Bio Science 55: 593 – 602.

De Sa, A. and Al Zubaidy, S., 2011. Gas turbine performance at varying ambient temperature. *Applied Thermal Engineering*, *31*(14-15), pp.2735-2739.

Delgado-Torres A.M (2018), Effect of ideal gas model with temperature-independent heat capacities on thermodynamic and performance analysis of open-cycle gas turbines, Energy Conversion and Management 176:256–273

Dell R.M and Rand D.A.J(2004), Clean Energy, Royal Society of Chemistry, Chapter 1: Energy Production and Use, pp. 1–31.

Demibas F, Bozbas K, Balat M (2004), Carbon Dioxide Emission Trends and Environmental Problems in Turkey, Energy Explor Exploit 22: 355 – 65.

Demirbas A (2006), Hazardous Emission, Global Climate and Environmental Precautions, Energy Sources B 1: 75 – 84.

Dey, S. and Dhal, G.C., (2019). Materials progress in the control of CO and CO_2 emission at ambient conditions: an overview. *Materials Science for Energy Technologies*, *2*(3), pp.607-623.

Diesel and Gas Turbine Worldwide (2004): Kawasaki's L20 A in Combined Cycle Operation, pp 61 – 63.

Dincer I and Rosen MA (2007). Exergy, Energy, Environment and Sustainable Development, Exergy Hand Book, 1st edition, Elsevier, UK.

Dincer, I., and Rosen M. A. (2003). Thermoeconomic analysis of power plants: an application to a coal- fired electrical generating station. Energy Convers. Manage. 44:2743–2761.

Dincer, I., and Rosen M. A. (2013). Exergy, energy, environmental and sustainable development. Elsevier, Oxford, U.K. Pp. 257–276

Dincer, I., and. Rosen. M. A (1999). Exergy analysis of waste emissions. Int. J. Energy Res. 23:1153–1163.

Duran MD, Vald es M, Rovira A, Rincon E (2013). A methodology for the geometric design of heat recovery steam generators applying genetic algorithms. Appl Therm Eng 52:77 – 83.

Eastop T.D and McConkey A (2011), Applied Thermodynamics for Engineering Technologists, 5th ed. (8th Impression), Dorling Kindersley, New Delhi, India.

Ebadi M.J and Gorji – Brandpy M. (2005): Exergetic Analysis of Gas Turbine Plant, International Journal of Exergy, Vol. 2, No. 1. pp.31 – 39.

Ebsilon (2016), Ebsilon Professional Software, STEAG Energy Services GmH, Germany.

Edgerton, R. H. (1992). Available energy and environmental economics. D.C. Heath, Toronto, Canada.

Ehsana, A., and Yilmazoglub M. Z. (2011). Design and exergy analysis of a thermal power plant using different types of Turkish lignite. Int. J. Thermodyn. 14:125–133.

Ehyaei M.A, Tahani M., Ahmadi P. and Esfandiari M. (2015): Optimization of Fog Inlet Air Cooling System for Combined Cycle Power Plant Using Genetic Algorithm, Applied Thermal Engineering, 76; 449 – 461.

Ehyaei, M. A. and Mozafari, A., (2010), Energy, Economic and Environmental (3E) Analysis of a Micro Gas Turbine Employed for *on-site* Combined Heat and Power Production, *Int. J. Energy and Buildings*, *42:* 2, pp. 259-264

Ehyaei, M. A., Mozafari, A., & Alibiglou, M. H. (2011). Exergy, economic & environmental (3E) analyses of inlet fogging for gas turbine power plant. *Energy*, *36*(12), 6851-6861.

Ehyaei, M.A.; Hakimzadeh, S.; Enadi, N.; Ahmadi, P. (2012): Exergy, economic and environment (3E) analysis of absorption chiller inlet air cooler used in gas turbine power plants. *Int. J. Energy Res. 36*: 486–498.

EIA (1999), Analysis of the climate change technology initiative, EIA, DOE, April 99, SR/OIAF/99-01, p. 68

El Hadik, A. A. (1990). The Impact of Atmospheric Conditions on Gas Turbine Performance. ASME. *J. Eng. Gas Turbines Power*. October; 112(4): 590–596. https://doi.org/10.1115/1.2906210

El-Shazly A.A, Elhelw M., Sorour M.M, El-Maghany W.M (2016), Gas Turbine Performance Enhancement Utilizing Different Integrated Turbine Inlet Cooling Techniques, Alexandria Engineering Journal 55: 1903 – 1914.

Energy Technology Perspectives (2014), Harnessing Electricity's Potential, International Energy Agency.

Ersayin E, Ozgener L. (2015), Performance analysis of combined cycle power plants: a case study. Renew Sustain Energy Rev 43:832–42.

Fagbenle, R. L., Oguaka A. B. C., and Olakoyejo O. T. (2007). A thermodynamic analysis of a biogas- fired integrated gasification steam injected gas turbine (BIG/STIG) plant. Elsevier Appl. Therm. Eng. 27:2220–2225.

Farrell W (1988). Air cycle thermodynamic conversion system. New York, USA Patent US Patent 4.751.814A.

Feng, X., Fu, B., Lu, N., Zeng, Y., and Wu, B. (2013). How ecological restoration alters ecosystem services: an analysis of carbon sequestration in China's Loess Plateau. *Scientific reports*, *3*, 2846.

Fisk RW and VanHousen R.L (1996), Cogeneration Application Consideration, GE Power Generation, New York.

Fout T, Murphy JT (2009) DOE/NETL's Carbon Capture R&D Program for existing coal-fired power plants

Frey H.C and Zhu Y. (2012), Techno – Economic Analysis of Combined Cycle Systems for Near-Zero Emission Power Generation, Woodhead Publishing series in Environmental Energy, 306 -328.

Gacitua, L., Gallegos, P., Henriquez-Auba, R., Lorca, A., Negrete-Pincetic, M., Olivares, D., Valenzuela, A. and Wenzel, G. (2018). A comprehensive review on expansion planning: Models and tools for energy policy analysis. *Renewable and Sustainable Energy Reviews*, *98*, pp.346-360.

Gadalla M and Saghafifar M (2017). Energy and exergy analyses of pulse combustor integration in air bottoming cycle power plants. Appl Therm. Eng 121:674–87.

Ganapathy, T. K., Murugesan, N. A. and. Gakkar R. P (2009). Exergy analysis of operating lignite fired thermal power plants. J. Eng. Sci. Technol. Rev. 2:123–130.

Ganjehkaviri, A., Jaafar, M. M., and Hosseini, S. E. (2015). Optimization and the effect of steam turbine outlet quality on the output power of a combined cycle power plant. *Energy Conversion and Management*, *89*, 231-243.

Garcia Sanchez-Cervera I. (2010), Energetic Optimization of a Steam Cycle Power Plant for an Efficient Operation of a Post-combustion CO_2 Capture Plant, Master Thesis, E 302 - Institut fur Energietechnik und Thermodynamik, Technische Universit¨ at Wien Fakult¨ at fur Maschinenwesen und Betriebswissenschaften von, Madrid Spain.

Gas Turbine world (2008), GTW Handbook, Vol 26, Pequot Publication, Inc, South Port, U.S.A

Ghaem Sigarchian S, Malmquist A, Martin V (2018), The choice of operating strategy for a complex polygeneration system: A case study for a residential building in Italy. Energy Convers Manage 163:278–91.

Gimelli A and Sannino R (2018), A multi-variable multi-objective methodology for experimental data and thermodynamic analysis validation: An application to micro gas turbines, Applied Thermal Engineering 134: 501–512.

Gogoi T (2014). A combined cycle plant with air and fuel recuperator for captive power application, part 1: Performance analysis and comparison with non-recuperated and gas turbine cycle with only air recuperator. Energy Convers Manage 79:771–7. https://doi.org/10.1016/j.enconman.2013.10.028.

Grant, D., Jorgenson, A.K. and Longhofer, W., (2016), How organizational and global factors condition the effects of energy efficiency on CO_2 emission rebounds among the world's power plants. *Energy Policy*, *94*, pp.89-93.

Hammond, G. P. 2004. Engineering sustainability: thermodynamics, energy systems, and the environment. Int. J. Energy Res. 28:613–639.

Haseli Y, Dincer I, Naterer GF (2008). Thermodynamic modeling of a gas turbine cycle combined with a solid oxide fuel cell. Int J Hydrogen Energy 33 (20):5811–22.

Hendriksa C, de Vissera E, Jansenb D, Carbob M, Ruijg G J, Davison J (2009), Capture of CO_2 from Medium-scale Emission Sources, Energy Procedia 1: 1497–1504.

Hoffmann S, Barlett M, Finkenrith M, Evulet A, and Ursin T.P (2008), Performance and Cost Analysis of Advanced Gas Turbine Cycles with Precombustion CO_2 capture, AMSE GT2008 -51207, ASME Turbo Expo 2008 Power for land, Sea, and Air, June 9, 2008, Berlin Germany.

Hondo H. (2005), Life Cycle GHG Emission Analysis of Power Generation Sytems: Japan Case, Energy 30: 2042 – 2056. Doi: 10161j.energy2004.07.020.

Horlock J.H (2003), Advance Gas Turbine Cycles, Elsevier Sci. Ltd, UK.

Hosseini, R., Beshkani, A. and Soltani, M., (2007). Performance improvement of gas turbines of Fars (Iran) combined cycle power plant by intake air cooling using a media evaporative cooler. *Energy Conversion and Management*, *48*(4), pp.1055-1064.

Howes, R., Skea, J., and Whelan, B. (2013). *Clean and competitive: motivating environmental performance in industry*. Routledge.

Ibrahim T.K, Basrawi F., Awad O.I, Abdullah A.N., Najafi G., Mamat R., and Hagos F.Y (2017), Thermal Performance of Gas Turbine Power Plant Based on Exergy Analysis, Applied Thermal Engineering 115: 977 – 985.

Ibrahim, T.K. and Mohammed, M.N. (2015). Thermodynamic evaluation of the performance of a combined cycle power plant. *International journal of energy science and engineering 1*, No.2, pp 60 – 70.

Ibrahim, T.K., Basrawi, F., Awad, O.I., Abdullah, A.N., Najafi, G., Mamat, R. and Hagos, F.Y., 2017. Thermal performance of gas turbine power plant based on exergy analysis. *Applied thermal engineering*, *115*, pp.977-985.

IEA (2015). Energy and Climate Change, World Energy Outlook Special Report. International Energy Agency; p. 1–200.

IEA (2017). Outlook for Natural Gas, in World Energy Outlook 2017. International Energy Agency; p. 449–60.

Ighodaro O. O (2006), Performance Appraisal of Delta IV Power Station, Ughelli, M. Eng Thesis, Department of Mechanical Engineering, University of Benin, Nigeria.

Ighodaro, O. O., and Aburime B. A. (2011). Exergetic appraisal of Delta IV power station, Ughelli. J. Emerg. Trends Eng. Appl. Sci. 2:216–218.

Ighodaro O.O and Osikhuemhe M (2019), Thermo-Economic Analysis of a Heat Recovery Steam Generator Combined Cycle, *Nigerian Journal of Technology (NIJOTECH) Vol. 38, No. 2, pp.* 342 – 347. http://dx.doi.org/10.4314/njt.v38i2.10

International Energy Agency (IEA) (2016), World Energy Outlook, < https://www. iea.org/weo/ > (Accessed on 04 September 2018).

IPCC (2014). Climate Change 2014: Mitigation of Climate Change, in Working Group III Contribution to the Fifth Assessment Report of the Intergovernmental Panel on Climate Change, UN. p. 1454.

IPCC (2015) Climate change 2014: mitigation of climate change, Vol 3. Cambridge University Press, Cambridge and New York

Islam S, Dincer I, Yilbas BS (2018), Development, analysis and assessment of solar energy based multigeneration system with thermoelectric generator. Energy Convers Manage 156:746–56.

Janusz Kotowicz J and Brzeczek M (2018), Analysis of increasing efficiency of modern combined cycle power plant: A case study, Energy 153: 90 – 99.

Jarre M, Noussan M, Poggio A (2016). Operational analysis of natural gas combined cycle CHP plants: Energy performance and pollutant emissions. Appl Therm Eng 100:304–14.

Jassim RK, Zaki GM, Alhazmy MM (2009) Energy and Exergy Analyses of Reverse Brayton Refrigerator for Gas Turbine Power Boosting, International Journal of Exergy 6 (2): 143 – 165.

Jaszczur M.and Dudek M. (2019), Thermodynamic analysis of a gas turbine combined cycle integration with a high temperature nuclear reactor, E3S Web of Conferences **113**, *SUPEHR19 Volume 1 pp 1- 6.* https://doi.org/10.1051/e3sconf/201911302019

Jaszczur, M., Dudek, M., Rosen, M.A. and Kolenda, Z., (2020), An analysis of integration of a power plant with a lignite superheated steam drying unit. *Journal of Cleaner Production*, *243*, p.118635.

Kalina J (2017). Analysis of alternative configurations of heat recovery process in small and medium scale combined cycle power plants. Energy Convers Manage 152:13–21.

Kanbur B.B, Xiang L., Dubey S., Choo F.H., and Duan F. (2017), Thermoeconomic and Environmental Assessments of a Combined Cycle for the Small Scale LNG Cold Utilization, Applied Energy Vol. 204, pp 1148 – 1162.

Kang, C.A., Brandt, A.R. and Durlofsky, L.J., (2011), Optimal operation of an integrated energy system including fossil fuel power generation, CO_2 capture and wind. *Energy*, *36*(12), pp.6806-6820.

Karaali R and Ztrk TT (2015). Thermoeconomic optimization of gas turbine cogeneration plants. Energy 80:474–85.

Karapekmez A and Dincer I (2020), Comparative efficiency and environmental impact assessments of a solar assisted combined cycle with various fuels, Applied Thermal Engineering 164

Kaviri AG, Jaafar MNM, Lazim TM (2012). Modeling and multi-objective exergy based optimization of a combined cycle power plant using a genetic algorithm. Energy Convers Manage 58:94–103.

Kaviri AG, Jaafar MNM, Lazim TM (2012). Modeling and multi-objective exergy based optimization of a combined cycle power plant using a genetic algorithm. Energy Convers Manage 58:94–103.

Kaviri, A. G., Jaafar, M. N. M., Lazim, T. M., and Barzegaravval, H. (2013). Exergoenvironmental optimization of heat recovery steam generators in combined cycle power plant through energy and exergy analysis. *Energy Conversion and Management*, *67*, 27-33.

Kayadelen H and Ust Y (2017). Thermodynamic, environmental and economic performance optimization of simple, regenerative, stig and rstig gas turbine cycles. Energy 121:751–71. https://doi.org/10.1016/j.energy.2017.01.060.

Kehlhofer, R., Rukes, B., Hannemann, F. and Stirnimann, F (2009). *Combined-cycle gas & steam turbine power plants*. PennWell Books, LLC.

Khan M.N and Tlili I (2018), Innovative thermodynamic parametric investigation of gas and steam bottoming cycles with heat exchanger and heat recovery steam generator: energy and exergy analysis, Energy Rep. 4 (November) 497–506. https://doi.org/10.1016/j.egyr.2018.07.007.

Khan M.N and Tlili l. (2019), New approach for enhancing the performance of gas turbine cycle: A comparative study, Results in Engineering 2: 100008.

Khan M.N, Tlili I, Khan W.A (2017), Thermodynamic optimization of new combined gas/steam power cycles with HRSG and heat exchanger, Arabian J. Sci. Eng. 42 (11): 4547–4558. https://doi.org/10.1007/s13369-017-2549-4.

Khosravi A, Gorji-Bandpy M., and Fazelpour F. (2014), Optimization of a Gas Turbine Cycle Generic and PSO Algorithm, Journal of Middle East Applied Science and Technology (JMEAST), Issue 21, pp 706 -711.

Kiameh P (2012), Power Generation Handbook, 2nd edition, The Mcgraw -Hall companies.

Kırlı, M.S. and Fahrioğlu, M., (2019). Sustainable development of Turkey: Deployment of geothermal resources for carbon capture, utilization, and storage. *Energy Sources, Part A: Recovery, Utilization, and Environmental Effects*, *41*(14), pp.1739-1751.

Kopac, M and Hilalci, A., (2007), Effect of Ambient Temperature on the Efficiency of the Regenerative and Reheat Catalagzi Power Plant in Turkey, *Applied Thermal Engineering, 27* 8-9, pp. 1377-1385

Kotas, T. J. (1995). The exergy method of thermal plant analysis. Krieger Publishing Company, Malabar, FL.

Kotowicz J, Bartela Ł(2011) . The influence of the legal and economical environment and the profile of activities on the optimal design features of a natural-gas-fired combined heat and power plant. Energy 36:328–38.

Kumar K. (2017), A Critical Review on Energy, Exergy, Exergoeconomic and Economic (4-E) Analysis of Thermal Power Plants, Engineering Science and Technology International Journal 20: 283 – 292.

Kumari A (2015), Investigation of Parameters Affecting Exergy and Emission Performance of Basic and Intercooled Gas Turbine Cycles, Energy 90: 525 – 536.

Kurt H, Recebli Z, Gedik E (2009), Performance analysis of open cycle gas turbines. Int J Energy Res 2009;33(3):285–94.

Lebele – Alawa B.T and Jo – Appah V. (2015), Thermodynamic Performance Analysis of a Gas Turbine in an Equatorial Rain Forest Environment, Journal of Power and Energy Engineering 3, 11 – 23. http://dx.doi.org/10.4236/jpee2015:31002.

Leung DYC, Caramanna G, Mercedes Maroto-Valer M (2014). An overview of current status of carbon dioxide capture and storage technologies. Renew Sustain Energy Rev 39:426–43.

Li, K., and Lin, B. (2015), Impacts of urbanization and industrialization on energy consumption/CO_2 emissions: does the level of development matter, *Renewable and Sustainable Energy Reviews*, *52*, 1107-1122.

Liszka M, Ziebik A(2009). Economic optimization of the combined cycle integrated with multi-product gasification system. Energy Convers Manage 50:309–18.

Lombardi L (2003), Life Cycle Assessment Comparison of Technical Solution for CO_2 Emission Reduction in Power Generation, Energy Convers Manage 44: 93 -108.

Lotfalipour, M. R., Falahi, M. A., and Ashena, M. (2010). Economic growth, CO_2 emissions, and fossil fuels consumption in Iran. *Energy*, *35*(12), 5115-5120.

Mach K and Mastrandrea M (2014) Climate change 2014: impacts, adaptation, and vulnerability, vol 1. Cambridge University Press, New York

Mahmood F.G and Mahdi D.D (2009), A New Approach for Enhancing Performance of a Gas Turbine (Case Study: Khangiran Refinery), Applied Energy, 86: 2750 – 2759.

Mahto D and Pal S (2013), Thermodynamics and Thermo-Economic Analysis of Simple Combined Cycle with Inlet Fogging, Applied Thermal Engineering 51: 413 -424.

Mancarella p and Chicco G (2009), Global and local emission impact assessment of distributed cogeneration systems with partial-load models, Applied Energy, Volume 86, Issue 10, Pp 2096-2106, https://doi.org/10.1016/j.apenergy.2008.12.026.

Matjanov E. (2020), Gas turbine efficiency enhancement using absorption chiller. Case study for Tashkent CHP, Energy 192 (2020) 116625.

MATLAB (2017), App Building. The MathWorks Inc., 3 Apple Hill Drive, Natick, M.A 01760 - 2098

McPherson E.G (1998), Atmospheric Carbon Dioxide Reduction by Sacramento's Urban Forest, Journal of Arboriculture 25 (4): 215 – 223.

Meher – Homji C.B and Mee T.R (1999), Gas Turbine Power Augmentation by Fogging of Inlet Air, in: Proceeding of 28th Turbo Machinery Symposium,Turbo Machinery Laboratory pp. 92 – 113.

Memon A.G, Memon R.A, Harijan K and Uquili M.A (2014), Thermo – Environmental Analysis of an Open Cycle Gas Turbine Power Plant with Regression Modelling and Optimization, Journal of the Energy Institute 87: 81 – 85.

Memon AG, Harijan K, Uqaili MA, Memon RA (2013), Thermo-environmental and economic analysis of simple and regenerative gas turbine cycles with regression modeling and optimization. Energy Convers Manage 76:852–64.

Miguez Da Rocha A. (2010), Analysis on Solar Retrofit in Combined Cycle Power Plants, Master Thesis, - Institut fur Energietechnik und Thermodynamik, Technische Universit¨ at Wien Fakult¨ at fur Maschinenwesen und Betriebswissenschaften von, Madrid Spain.

Mikkelsen M, Jorgensen M, Krebs F.C (2010), Synthesis and characterization of zwitterionic carbon dioxide fixing reagents, Int. J. Greenh. Gas Control 4: 452 - 458.

Mishra, S., Sharma, A. and Kumari, A., (2020), Response surface methodology based optimization of air-film blade cooled gas turbine cycle for thermal performance prediction. *Applied Thermal Engineering*, *164*, p.114425.

Mohammadi K,, Saghafifar M. and McGowan J.G (2018), Thermo-economic evaluation of modifications to a gas power plant with an air bottoming combined cycle, Energy Conversion and Management 172: 619–644

Mohammadi, K., McGowan, J.G., Saghafifar, M., (2019), Thermoeconomic analysis of multi-stage recuperative Brayton power cycles: Part I-hybridization with a solar power tower system. Energy Convers. Manag. 185, 898–919.

Moran MJ and Shapiro.H. N. (2000), Fundamentals of Engineering Thermodynamics, 4rd edition, John Wiley and Sons, New York.

Moran, M. J., and Sciubba E. (1994). Exergy analysis: principles and practice. J. Eng. Gas Turbines Power 116:285–290.

Mousafarash A (2016). Exergy and exergoenvironmental analysis of a CCHP system based on a parallel flow double-effect absorption chiller. Int J Chem Eng. https://doi. org/10.1155/2016/2370305.

Mousavi, B., Lopez, N.S.A., Biona, J.B.M., Chiu, A.S. and Blesl, M., (2017). Driving forces of Iran's CO_2 emissions from energy consumption: an LMDI decomposition approach. *Applied energy*, *206*, pp.804-814.

Mukherjee, A., Okolie, J.A., Abdelrasoul, A., Niu, C. and Dalai, A.K., (2019), Review of post-combustion carbon dioxide capture technologies using activated carbon. *Journal of Environmental Sciences*, *83*, pp.46-63.

Nascimento Silva F. C., Flórez-Orrego D., De Oliveira Junior S. (2019), Exergy assessment and energy integration of advanced gas turbine cycles on an offshore petroleum production platform, Energy Conversion and Management 197:111846.

Nazari N, Heidarnejad P, Porkhial S (2016). Multi-objective optimization of a combined steam-organic Rankine cycle based on exergy and exergo-economic analysis for waste heat recovery

Nazari S, Shahhoseini O, Sohrabi-Kashani A, Davari S, Paydar R, Delavar-Moghadam z (2010), Experimental determination and analysis of CO_2, SO_2 and NO_x emission factors in Iran's thermal power plants, Energy 35:2992 - 98

NERC (2020), Power Generation in Nigeria, www.nerc.gov.ng, accessed on 31st March, 2021.

Neserian M.M, Farahat S.and Sarhaddi F. (2016), Exergoeconomic Analysis and Genetic Algorithm Power Optimization of an Irreversible Regenerative Brayton Cycle, Energy Equipment and Systems, Vol.4, No. 2, pp 189 – 203.

Noh Y, and Chang D (2019), Methodology of exergy-based economic analysis incorporating safety investment cost for comparative evaluation in process plant design, Energy 182: 864 - 880

Nordstrom L. (2005): Construction of a Simulator for the Siemens Gas Turbine SGT – 600, Linkoping University, Linkoping.

Ofodu, J. C., and Abam D. P. S. (2002). Exergy analysis of Afam thermal power plant. NSE Tech. Trans. 37:14–28.

Oladipo1 K, Felix A.A, Bango O, Chukwuemeka O, Olawale F (2018), Power Sector Reform in Nigeria: Challenges and Solutions. IOP Conf. Series: Materials Science and Engineering 413:012037 doi:10.1088/1757-899X/413/1/012037

Olatomiwa, L., Mekhilef, S., and Ohunakin, O. S. (2016). Hybrid renewable power supply for rural health clinics (RHC) in six geo-political zones of Nigeria. *Sustainable Energy Technologies and Assessments*, *13*, 1-12.

Olausson, M. (2017). *Thermodynamic and Economic Evaluation of a 1000MWth Chemical Looping Combustion Power Plant* (Master's thesis). Chalmers University of Technology Goteborg, Sweden.

Olivenza-Len D, Medina A, Calvo Hernndez A (2015), Thermodynamic modeling of a hybrid solar gas-turbine power plant. Energy Convers Manage 93:435–47. https://doi.org/10.1016/j.enconman.2015.01.027.

Ong H, Mahlia T, and Masjuki H (2011), A review on energy scenario and sustainable energy in Malaysia, Renewable and Sustainable Energy Reviews 15 639-47

Otunuya O. and Emeka U.P (2017), Optimal Operating Parameters of 100MW Delta IV Ughelli Gas Turbine Power Plant Unit, International Journal of Enery and Power Engineering Vol. 6, No. 5, pp 68 – 74.

Owusu, P. A., and Asumadu-Sarkodie, S. (2016). A review of renewable energy sources, sustainability issues and climate change mitigation. *Cogent Engineering*, *3*(1), 1167990.

Oyedepo S.O, Fagbenle R.O, Adefila S.S and Alam M.M (2015), Thermodynamic and Thermoenvironomic Modelling and Analysis of Selected Gas Turbine Power Plants in Nigeria, Energy Science and Engineering 3 (5): 423 – 442.

Park S.R, Pandey A.K, Tyagi V.V and Tyagi S.K (2014), Energy and Exergy Analysis of Typical Renewable Systems, Renew. Sustain. Energy Rev. 30: 105 – 123.

Pattanayak L (2015). Thermodynamic modeling and exergy analysis of gas turbine cycle for different boundary conditions. Int J Power Electron Drive Syst 6(2):205–15. https://doi.org/10.11591/ijpeds.v6.i2.pp205-215.

Pilavachi P.A (2000), Power Generation with Gas Turbine Systems and Combined Heat and Power, Applied Thermal Engineering 20, (15) 1421 – 1429.

Pilavachi, P.A., (2000), Power generation with gas turbine systems and combined heat and power. *Applied Thermal Engineering*, *20*(15-16), pp.1421-1429.

Polyzakis AL, Koroneos C, Xydis G (2008), Optimum gas turbine cycle for combined cycle power plant. Energy Convers Manage 49(4):551–63.

Pooneh A (2012), Development of a Framework for Thermoeconomic Optimization of Simple and Combined Gas – Turbine Cycles, Ph. D Thesis, School of Engineering, Cranfield University, England.

Raghuvanshi, S.P., Chandra, A. and Raghav, A.K. (2006). Carbon dioxide emissions from coal based power generation in India. *Energy Conversion and Management*, *47*(4), pp.427-441.

Rahman M.M, Ibrahim T.K, and Abdalla A.N (2011), Thermodynamic Performance of a Gas – Turbine Power – Plant, International Journal of Physical Sciences, Vol 6 (14) pp 3539 – 3550. DOI: 105897/IJPS11.272

Rahman M.M, Ibrahim T.K, Tab M.Y, Noor M.M, Kadingama K., Baker R A (2010), Thermal Analysis of Open – Cycle Regenerator Gas - Turbine Power Plant, WASET 66: 94 – 99.

Rahman MM, Ibrahim TK, Kadirgama K, Mamat R, Bakar RA. (2011), Influence of operation conditions and ambient temperature on performance of gas turbine power plant. Adv Mater Res, 189-193.

Rahman, M. M., Salehin, S., Ahmed, S. S. U., and Islam, A. S. (2017). Environmental impact assessment of different renewable energy resources: a recent development. In *Clean Energy for Sustainable Development* (pp. 29-71). Academic Press.

Rajkumar, S. C. and Ashok K. (2009). Energy and exergy analysis of non-reheat thermal power plant. Proceedings of International Conference of Energy and Environmental.

Rashidi, M. Aghagoli, M., A. and Ali. M. (2014). Thermodynamic analysis of a steam power plant with double reheat and feed water heaters. Adv. Mech. Eng. 2014:1–12.

Robert F, Dan T, Katherine C, Harmen S D, Johannes E, Oliver F, Shinichiro F, Gunnar L, Joeri R and Steven J D, (2020), Early retirement of power plants in climate mitigation scenarios, *Environ. Res. Lett.* 15 (2020) 094064.

Robert F, Dan T., Katherine C, Harmen S.D, Johannes E, Oliver F, Shinichiro F, Gunnar L, Joeri R and Steven J.D (2020), Early Retirement of Power Plants in Climate Mitigation Scenarios, Environmental Research Letters 15: 094064. http://doi.org/10.1088/1748-9326/ab96d3.

Robertson D.S. (2006), Health Effects of Increase in Concentration of Carbon Dioxide in the Atmosphere, Current Science 90, 1607 – 1609.

Rocco, M.V., Colombo, E. and Sciubba, E. (2014), Advances in exergy analysis: a novel assessment of the Extended Exergy Accounting method. *Applied Energy*, *113*, pp.1405-1420.

Rogers G.F.C and.Mayhew Y.R (1992), Engineering Thermodynamics. Work and Heat Transfer, 4th ed., Pearson Education Ltd, England.

Rogers GFC and Mayhew YR (1992), Engineering Thermodynamics, Work and Heat Transfer, 4th Edition, Pearson Education Ltd, Britain

Rogers GFC and Mayhew YR (1995), Thermodynamic and Transport Properties of Fluids, 5th Edition, Oxford Basic Blackwell Publishers, Britain.

Rovira A (2005). Desarrollo de un modelo para la caracterizacin termoeconmica de ciclos combinados de turbina de gas y de vapor en condiciones de carga variable Phd. Thesis Universidad Politécnica de Madrid.

Saghafifar M, Poullikkas A (2017). Comparative analysis of power augmentation in ABC power plants. Int J Sustain Energy 36:47–60.

Saghafifar M. and Gadalla, M., (2016). Thermo-economic analysis of air bottoming cycle hybridization using heliostat field collector: A comparative analysis. Energy 112, 698–714.

Sahu MK (2017), Sanjay. Comparative exergoeconomics of power utilities: air-cooled gas turbine cycle and combined cycle configurations. Energy 139:42–51.

Salami L.A (2004): Thermal Power Engineering 1, Lecture Note, Department of Mechanical Engineering, University of Benin.

Saravanamuttoo H, Roger GFC, Cohen H, Straznicky PV (2009) Gas Turbine Theory, 6th edition, Pearson Education Ltd, England.

Schivley, G., Azevedo, I., and Samaras, C. (2018). Assessing the evolution of power sector carbon intensity in the United States. *Environmental Research Letters*, *13*(6), 064018.

Selveira J.L, Tuna C.E, Lamas W.Q, and Castro Villela I.A (2010), A contribution for Thermoeconomic Modelling: A Methodology Proposal, App. Therm. Eng. 30: 1734 – 1740.

Seyyedi, S. MAjam, H. and Farahat. S. (2011). Thermoenvironomic optimization of gas turbine cycles with air preheat. Proc. Inst. Mech. Eng. Part A: J. Power and Energy 225:12–23.

Shahbaz, M., Loganathan, N., Sbia, R., and Afza, T. (2015). The effect of urbanization, affluence and trade openness on energy consumption: A time series analysis in Malaysia. *Renewable and Sustainable Energy Reviews*, *47*, 683-693.

Shahsavari, A. and Akbari, M., (2018), Potential of solar energy in developing countries for reducing energy-related emissions. *Renewable and Sustainable Energy Reviews, 90,* pp.275-291.

Shamoushaki M and Ehyaei M.A (2018), Exergy, Economic, And Environmental (3e) Analysis of A Gas Turbine Power Plant and Optimization By Mopso Algorithm, Thermal Science, Vol. 22, No. 6A, pp. 2641-2651

Shengya H, Yuandan W, Yaodong Z and Lijun Y (2017), Performance analysis of the combined supercritical CO_2 recompression and regenerative cycle used in waste heat recovery of marine gas turbine", Energy Convers. Manag. 151: 73–85.

Siemens A.G (2011), Gas Turbine SGT5 – 2000E Brochure, Energy Sector, Freyeslebenstrasse 1, 91058 Erlangen, Germany.

Siemens A.G (2018), Azura Edo Power Plant – Powering Nigeria Future, Power and Gas Division, Johannesburg, South Africa.

Simon K., Christopher S. and Martin S. (2013), Successful Power Limit Increase of SGT5 – 2000E, Gas Turbine on the Basis of Si3D Blading, Russia Power 2013, Moscow Russia. www.siemens.com/energy accessed on 10/10/2018.

Smith K.A, Ball T., Conen F., Dabbie K.E, Massheder J., and Ray A. (2003), Exchange of Greenhouse Gases between Soil and Atmosphere: Interactions of Soil Physical Factors and Biological Process, European Journal of Soil Science 54, 779 – 791. http://dx.doi.org10.1146j365-23892003.00567x.

Soltani, S., Mahmoudi, S.M.S., Yari, M. and Rosen, M.A., (2013), Thermodynamic analyses of an externally fired gas turbine combined cycle integrated with a biomass gasification plant. *Energy Conversion and Management*, *70*, pp.107-115.

Sonibare M.A., Ogunwande I.A., Walker T.M., Setzer W.N., Soladoye M.O. and Essien E. (2006), *Volatile constituents of* Ficus exasperata *Vahl leaves*. Nat. Prod. Comm., **1**, 763–765.

Stangeland A. (2007), A Model of CO_2 Capture Potential, International Journal of Greehouse Gas Control 1, (4), 418 – 429. http://dx.doi.org10.101016/si750-5836(07)000874.

Stechel E.B. and Miller J.E. (2013), Re-energizing CO_2 to fuels with the sun: issues of efficiency, scale, and economics, J. Co2 Util. 1: 28 - 36.

Steen, M. (2000). *Greenhouse gas emissions from fossil fuel fired power generation systems*. Institute for Advanced Materials, Joint Research Centre, European Commission.

Thundiyil, K.A., (2003), *Rising temperatures and expanding megacities: improving air quality in Mexico City through Urban Heat Island mitigation* (Doctoral dissertation, Massachusetts Institute of Technology).

Tlili I (2015), Renewable energy in Saudi Arabia: current status and future potentials, Environ. Dev. Sustain. 17 (4):859–886.

Tlili, I., and S. A. Musmar. (2013), Thermodynamic Evaluation of a Second Order Simulation for Yoke Ross Stirling Engine. *Energy Conversion and Management* 68: 149–160. doi: 10.1016/j.enconman.2013.01.005

Valdes, M., Duran, M. D., and Rovira, A. (2003), Thermoeconomic Optimization of Combined Cycle Gas Turbine Power Plants Using Genetic Algorithms," Journal of Applied Thermal Engineering, Vol. 23, No. 1, pp. 2169 - 2182.

Van Gool, W. 1997. Energy policy fairy tales and factualities. Pp. 93–105 in O. D. D. Soares, A. Martins da Cruz, G. Costa Pereira, I. M. R. T. Soares and A. J. P. S. Reis, eds. Innovation and technology-strategies and policies. Kluwer, Dordrecht.

Vélez, F., Segovia, J. J., Martín, M. C., Antolín, G., Chejne, F., and Quijano, A. (2012). A technical, economical and market review of organic Rankine cycles for the conversion of low-grade heat for power generation. *Renewable and Sustainable Energy Reviews*, *16*(6), 4175-4189.

Wallentinsen B.S (2016), Concentrated Solar Power Gas Turbine Hybrid with Thermal Storage, Master Thesis in Mechanical Engineering, Department of Energy and Process Engineering Norwegian University of Science and Technology.

Wang J., Lu Z., Li M, Lior N, Li W. (2019), Energy, exergy, exergoeconomic and environmental (4E) analysis of a distributed generation solar-assisted CCHP (combined cooling, heating and power) gas turbine system, Energy 175:1246 – 1258.

WBG (2017), Nigeria: The Azura-Edo Independent Power Plant, Multilateral Development Banks' Collaboration: Infrastructure Investment Project Briefs. https://library.pppknowledgelab.org/documents/4691/download. Accessed on 12th April, 2021.

Wicks F (1991). The thermodynamic theory and design of an ideal fuel burning engine. In: Intersociety energy conversion engineering conference, vol. 2, Boston, p. 474-481.

Wildenborg T and Lokhorst A (2005), Introduction on CO_2 Geological Storage – Classification of Storage Options, Oil and Gas Techol Rev IFP 60: 513 – 5.

Wojcik J. D. and Wang J. (2018), Feasibility study of Combined Cycle Gas Turbine (CCGT) power plant integration with Adiabatic Compressed Air Energy Storage (ACAES). Applied Energy, 221, pp. 477-489. doi:10.1016/j.apenergy.2018.03.089

Wood B. (1981): Gas Turbine, Kempe's Engineers Year – Book, Vol. 1, Morgan – Grampian Book Publishing Co.Ltd, 30 Calderwood Street, London SE6QH Chapter F4 pp 8.

Wright R.T and Boorse D (2011), Environmental Science: Toward a Sustainable Future (11th ed.) Upper Saddle River, NJ: Prentice Hall.

Xue L, Wang W, and Huang Z (2007), Investigation on performance of cycle combined Brayton and ambient pressure gas turbine, in: K. Cen, Y. Chi, F. Wang (Eds.), Challenges of Power Engineering and Environment, Springer, Berlin, Heidelberg.

Yang C, Yang Z and Cai R (2009), Analytical Method for Evaluation of Gas Turbine Inlet Air Cooling in Combined Cycle Power Plant, Applied Energy 86: 848 – 856

Yazdi M.R.M, Ehyaei M.A, Rosen M.A (2015), Exergy, Economic and Environmental Analyses of Gas Turbine Inlet Air Cooling with a Heat Pump Using a Novel System Configuration, Sustainability 7: 14259 – 14286.

Yazdi, M.R.M., Ommi, F., Ehyaei, M.A. and Rosen, M.A (2020). Comparison of gas turbine inlet air cooling systems for several climates in Iran using energy, exergy, economic, and environmental (4E) analyses. *Energy Conversion and Management*, *216*, p.112944.

Yu J, Corripio A.B, Harrison O.P and Copeland R.J (2003), Analysis of the Sorbent Energy Transfer System (SETS) for Power Generation and CO_2 Capture, Adv. Environ 7: 333 – 45.

Zeitoun, O. (2021), Two-Stage Evaporative Inlet Air Gas Turbine Cooling. Energies 14: 1382. https://doi.org/10.3390/en14051382

Zhang Q, Li H, Mclellan B (2014). An integrated scenario analysis for future zero-carbon energy system. Energy Proc 61:2801–4.

Ziółkowskia P, Kowalczykb T, Lemańskib M, Badurb J (2019), On energy, exergy, and environmental aspects of a combined gas-steam cycle for heat and power generation undergoing a process of retrofitting by steam injection, Energy Conversion and Management 192: 374–384

Zohuri, B. and McDaniel, P. (2017), Combined *cycle driven efficiency for next generation nuclear power plants: An innovative design approach*. Springer.

Zyrkowski M and Zymelka P (2019), Modelling of Flexible Boiler Operation in Coal Fired Power Plant, Earth and Environmental Science 214: 012074. Pp 1-7.

APPENDIX I

MATLAB SCRIPTS

ENERGY ANALYSIS

GT 11

```
% Energy Analyss for GT11
A=xlsread('GT11energy.xlsx');
% compressor inlet temperature t1 in deg C, the same ambient temperature
t1 = A(:,1);
% compressor exit temperature,in deg C t2
t2 = A(:,2);
% compressor inlet pressure in bar, p2
p1 = A(:,12);
% compressor discharge pressure in bar, p2
p2 = A(:,3);
% turbine inlet temperature, t3 in deg C
t3 = A(:,4);
% turbine exit temperature, t4 in deg C
t4 = A(:,5);
% mass flow rate of air, ma in kg/s
ma = A(:,6);
% mass flow rate of fuel, mf in kg/s
mf = A(:,7);
% inlet temperatur e of cooling water in deg C
tw1 = A(:,8);
% outlet temperature of cooling water in deg C
tw2 = A(:,9);
% inlet temperature of cooling oil in deg C
to1 = A(:,10);
% outlet temperature of cooling oil in deg C
to2 = A(:,11);
% Lower Heating Value, LHV in kJ/kg
LHV = 45011;
% specific capacity of air at constant pressure,cpa in kJ/kgK
cpa = 1.005;
% specific capacity of exhuast gas at constant pressure,cpg in kJ/kgK
cpg = 1.148;
% mass flow rate of cooling oil, mo in kg/s
mo = 22;
% specific capacity of cooling oil at constant pressure,cpo in kJ/kgK
cpo = 2.001;
% mass flow rate of cooling water, mw in kg/s
mw = 38.2;
% specific capacity of cooling water at constant pressure,cpw in kJ/kgK
cpw = 4.182;
% mass flow rate of Exhuast gas, mg
mg = ma + mf;
% Compressor Power, Wc in MW
wc = ma*cpa.*(t2 - t1)/1000;
% Turbine Power, Wt in MW
wt = mg*cpg.*(t3 - t4)/1000;
% Net Thermal Power Pth in MW
```

```
Pth = (wt - wc);
% Heat supply in MW
HS = mf.*LHV/1000;
% Gross Thermal Efficiency,etathg in (%)
etathg = (Pth.*100)/HS;
% Flue gas losses to the atmosphere, Qflue in MW
Qflue = mg*cpg.*(t4 - t1)/1000;
% Mechanical Losses, Pmech in MW
Pmech = mo*cpo.*(to2 - to1)/1000;
% Generator Losses, Pgen in MW
Pgen = mw*cpw.*(tw2 - tw1)/1000;
% Power consumed by Auxillaries in MW
Paux = 0.23;
% Mechanical Efficiency, etamech in (%)
etamech = (Pth -Pmech).*100/Pth;
% Generator Efficiency, etageg in (%)
etagen = (Pth - Pmech - Pgen).*100/(Pth - Pmech);
% net power or Electrical Power Generated, Pnet in MW
Pnet = Pth - Pmech - Pgen - Paux;
% Net Thermal Efficiency, etanet in (%)
etanet = (100*Pnet)/HS;
% Net specific fuel consumption, SFC in kg/kWh
SFC = 3600*mf./(1000*Pnet);
% Net Heat rate, HR in kJ/kWh
HR = SFC.*LHV;
% Net Work ratio, WR
WR = Pnet./wt;
% Percentage of Flue gases emitted to the amosphere etaflue
etaflue = Qflue.*100/HS;
% pressure ratio, PR
PR = p2./p1;
[t1,PR]=meshgrid(t1,PR);
Pnet= (-39.79*log(t1))+189.52;
figure (1)
surf(t1,PR,Pnet)
hold on
etanet=  (-10.75*log(t1))+65.764;
surf(t1,PR,etanet)
xlabel('ambient temperature(deg C)');
ylabel('pressure ratio');
zlabel('thermal efficincy(%) and power output(MW)');
legend('netpower','net thermal efficiency');
figure (2)
WR= (-0.067*log(t1))+0.547;
surf(t1,PR,WR)
hold on
SFC= (0.0941*log(t1))-0.0456;
surf(t1,PR,SFC)
xlabel('ambient temperature(deg C)');
ylabel('pressure ratio');
zlabel('WR and SFC(kg/kWh)');
legend('WR','SFC');
figure (3)
HR= (4235.1*log(t1))+2049.5;
surf(t1,PR,HR)
xlabel('ambient temperature(deg C)');
ylabel('pressure ratio');
```

```
zlabel('HR(kJ/kWh)');
figure (4)
etaflue= (-10.2*log(t1))+93.883;
surf(t1,PR,etaflue)
xlabel('ambient temperature(deg C)');
ylabel('pressure ratio');
zlabel('percentage of flue gas');
```

GT12

```
% Energy Analyss for GT12
D=xlsread('GT12energy.xlsx');
% compressor inlet temperature t1 in deg C, the same ambient temperature
t1 = D(:,1);
% compressor exit temperature,in deg C t2
t2 = D(:,2);
% compressor inlet pressure in bar, p1
p1 = D(:,12);
% compressor discharge pressure in bar, p2
p2 = D(:,3);
% turbine inlet temperature, t3 in deg C
t3 = D(:,4);
% turbine exit temperature, t4 in deg C
t4 = D(:,5);
% mass flow rate of air, ma in kg/s
ma = D(:,6);
% mass flow rate of fuel, mf in kg/s
mf = D(:,7);
% inlet temperature of cooling water in deg C
tw1 = D(:,8);
% outlet temperature of cooling water in deg C
tw2 = D(:,9);
% inlet temperature of cooling oil in deg C
to1 = D(:,10);
% outlet temperature of cooling oil in deg C
to2 = D(:,11);
% Lower Heating Value, LHV in kJ/kg
LHV = 45011;
% specific capacity of air at constant pressure,cpa in kJ/kgK
cpa = 1.005;
% specific capacity of exhuast gas at constant pressure,cpg in kJ/kgK
cpg = 1.148;
% mass flow rate of cooling oil, mo in kg/s
mo = 22;
% specific capacity of cooling oil at constant pressure,cpo in kJ/kgK
cpo = 2.001;
% mass flow rate of cooling water, mw in kg/s
mw = 38.2;
% specific capacity of cooling water at constant pressure,cpw in kJ/kgK
cpw = 4.182;
% mass flow rate of Exhuast gas, mg
mg = ma + mf;
% Compressor Power, Wc in MW
wc = ma*cpa.*(t2 - t1)/1000;
% Turbine Power, Wt in MW
wt = mg*cpg.*(t3 - t4)/1000;
```

```
% Net Thermal Power Pth in MW
Pth = (wt - wc);
% Heat supply in MW
HS = mf.*LHV/1000;
% Gross Thermal Efficiency,etathg in (%)
etathg = (Pth.*100)/HS;
% Flue gas losses to the atmosphere, Qflue in MW
Qflue = mg*cpg.*(t4 - t1)/1000;
% Mechanical Losses, Pmech in MW
Pmech = mo*cpo.*(to2 - to1)/1000;
% Generator Losses, Pgen in MW
Pgen = mw*cpw.*(tw2 - tw1)/1000;
% Power consumed by Auxillaries in MW
Paux = 0.23;
% Mechanical Efficiency, etamech in (%)
etamech = (Pth -Pmech).*100/Pth;
% Generator Efficiency, etageg in (%)
etagen = (Pth - Pmech - Pgen).*100/(Pth - Pmech);
% net power or Electrical Power Generated, Pnet in MW
Pnet = Pth - Pmech - Pgen - Paux;
% Net Thermal Efficiency, etanet in (%)
etanet = (100*Pnet)/HS;
% Net specific fuel consumption, SFC in kg/kWh
SFC = 3600*mf./(1000*Pnet);
% Net Heat rate, HR in kJ/kWh
HR = SFC.*LHV;
% Net Work ratio, WR
WR = Pnet./wt;
% Percentage of Flue gases emitted to the amosphere etaflue
etaflue = Qflue.*100/HS;
% pressure ratio, PR
PR = p2./p1;
[t1,PR]=meshgrid(t1,PR);
Pnet= (-41.66*log(t1))+287.37;
figure (1)
surf(t1,PR,Pnet)
hold on
etanet= (-0.389*t1)+40.489;
surf(t1,PR,etanet)
xlabel('ambient temperature(deg C)');
ylabel('pressure ratio');
zlabel('thermal efficincy(%) and power output(MW)');
legend('netpower','net thermal efficiency');
figure (2)
WR= (-0.072*log(t1))+0.6934;
surf(t1,PR,WR)
hold on
SFC= (0.1006*log(t1))+0.0629;
surf(t1,PR,SFC)
xlabel('ambient temperature(deg C)');
ylabel('pressure ratio');
zlabel('WR and SFC(kg/kWh)');
legend('WR','SFC');
figure (3)
HR= (4526.91*log(t1))-2830.8;
surf(t1,PR,HR)
xlabel('ambient temperature(deg C)');
```

```
ylabel('pressure ratio');
zlabel('HR(kJ/kWh)');
figure (4)
etaflue= (-10.22*log(t1))+92.981;
surf(t1,PR,etaflue)
xlabel('ambient temperature(deg C)');
ylabel('pressure ratio');
zlabel('percentage of flue gas');
```

GT13

```
% Energy Analyss for GT11
E=xlsread('GT13energy.xlsx');
% compressor inlet temperature t1 in deg C, the same ambient temperature
t1 = E(:,1);
% compressor exit temperature,in deg C t2
t2 = E(:,2);
% compressor inlet pressure in bar, p1
p1 = E(:,12);
% compressor discharge pressure in bar, p2
p2 = E(:,3);
% turbine inlet temperature, t3 in deg C
t3 = E(:,4);
% turbine exit temperature, t4 in deg C
t4 = E(:,5);
% mass flow rate of air, ma in kg/s
ma = E(:,6);
% mass flow rate of fuel, mf in kg/s
mf = E(:,7);
% inlet temperature of cooling water in deg C
tw1 = E(:,8);
% outlet temperature of cooling water in deg C
tw2 = E(:,9);
% inlet temperature of cooling oil in deg C
to1 = E(:,10);
% outlet temperature of cooling oil in deg C
to2 = E(:,11);
% Lower Heating Value, LHV in kJ/kg
LHV = 45011;
% specific capacity of air at constant pressure,cpa in kJ/kgK
cpa = 1.005;
% specific capacity of exhuast gas at constant pressure,cpg in kJ/kgK
cpg = 1.148;
% mass flow rate of cooling oil, mo in kg/s
mo = 22;
% specific capacity of cooling oil at constant pressure,cpo in kJ/kgK
cpo = 2.001;
% mass flow rate of cooling water, mw in kg/s
mw = 38.2;
% specific capacity of cooling water at constant pressure,cpw in kJ/kgK
cpw = 4.182;
% mass flow rate of Exhuast gas, mg
mg = ma + mf;
% Compressor Power, Wc in MW
wc = ma*cpa.*(t2 - t1)/1000;
```

```
% Turbine Power, Wt in MW
wt = mg*cpg.*(t3 - t4)/1000;
% Net Thermal Power Pth in MW
Pth = (wt - wc);
% Heat supply in MW
HS = mf.*LHV/1000;
% Gross Thermal Efficiency,etathg in (%)
etathg = (Pth.*100)/HS;
% Flue gas losses to the atmosphere, Qflue in MW
Qflue = mg*cpg.*(t4 - t1)/1000;
% Mechanical Losses, Pmech in MW
Pmech = mo*cpo.*(to2 - to1)/1000;
% Generator Losses, Pgen in MW
Pgen = mw*cpw.*(tw2 - tw1)/1000;
% Power consumed by Auxillaries in MW
Paux = 0.23;
% Mechanical Efficiency, etamech in (%)
etamech = (Pth -Pmech).*100/Pth;
% Generator Efficiency, etageg in (%)
etagen = (Pth - Pmech - Pgen).*100/(Pth - Pmech);
% net power or Electrical Power Generated, Pnet in MW
Pnet = Pth - Pmech - Pgen - Paux;
% Net Thermal Efficiency, etanet in (%)
etanet = (100*Pnet)/HS;
% Net specific fuel consumption, SFC in kg/kWh
SFC = 3600*mf./(1000*Pnet);
% Net Heat rate, HR in kJ/kWh
HR = SFC.*LHV;
% Net Work ratio, WR
WR = Pnet./wt;
% Percentage of Flue gases emitted to the amosphere etaflue
etaflue = Qflue.*100/HS;
% pressure ratio, PR
PR = p2./p1;
[t1,PR]=meshgrid(t1,PR);
Pnet= (-41.13*log(t1))+286.46;
figure (1)
surf(t1,PR,Pnet)
hold on
etanet= (-0.3984*t1)+41.045;
surf(t1,PR,etanet)
xlabel('ambient temperature(deg C)');
ylabel('pressure ratio');
zlabel('thermal efficincy(%) and power output(MW)');
legend('netpower','net thermal efficiency');
figure (2)
WR= (-0.07*log(t1))+0.6907;
surf(t1,PR,WR)
hold on
SFC= (0.0963*log(t1))-0.0514;
surf(t1,PR,SFC)
xlabel('ambient temperature(deg C)');
ylabel('pressure ratio');
zlabel('WR and SFC(kg/kWh)');
legend('WR','SFC');
figure (3)
HR= (4333*log(t1))-2314.3;
```

```
surf(t1,PR,HR)
xlabel('ambient temperature(deg C)');
ylabel('pressure ratio');
zlabel('HR(kJ/kWh)');
figure (4)
etaflue= (-9.954*log(t1))+92.212;
surf(t1,PR,etaflue)
xlabel('ambient temperature(deg C)');
ylabel('pressure ratio');
zlabel('percentage of flue gas');
```

EXERGY, IMPROVEMENT POTENTIAL, SUSTAINABILITY AND DEPLETION OF FUEL ANALYSIS

GT11

```
% Exergy Analyss for GT11
B=xlsread('GT11Exergy.xlsx');
T1 = B(:,1);
T2 = B(:,2);
T3 = B(:,9);
T4 = B(:,10);
Tf = 333;
ma = B(:,11);
mf = B(:,12);
mg = ma + mf;
p1 = 1.013;
p2 =B(:,4);
pf = 24;
p3 = B(:,7);
p4 = B(:,8);
cpa = 1.005;
cpf = 1.54;
cpg = 1.148;
Ra = 0.287;
Rf = 0.451;
Rg = 0.29;
Tref = B(:,1);
pref = 1.013;
Eche = (1.06*45011*mf)/1000;
ET1 =(ma.*cpa.*((T1-Tref)-(Tref.*log(T1/Tref))))/1000;
EP1 = (ma.*Ra.*Tref.*log(p1/pref))/1000;
S1 = (ma.*cpa.*(log(T1/Tref)-Ra*log(p1/pref)))/1000;
ET2 =(ma.*cpa.*((T2-Tref)-(Tref.*log(T2/Tref))))/1000;
EP2 = (ma.*Ra.*Tref.*log(p2/pref))/1000;
S2 = (ma.*cpa.*(log(T2/Tref)-Ra*log(p2/pref)))/1000;
ETf =(mf.*cpf.*((Tf-Tref)-(Tref.*log(Tf/Tref))))/1000;
EPf = (mf.*Rf.*Tref.*log(pf/pref))/1000;
Sf = (mf.*cpf.*(log(Tf/Tref)-Rf*log(pf/pref)))/1000;
ET3 =(mg.*cpg.*((T3-Tref)-(Tref.*log(T3/Tref))))/1000;
EP3 = (mg.*Rg.*Tref.*log(p3/pref))/1000;
S3 = (mg.*cpg.*(log(T3/Tref)-Rg*log(p3/pref)))/1000;
ET4 =(mg.*cpg.*((T4-Tref)-(Tref.*log(T4/Tref))))/1000;
EP4 = (mg.*Rg.*Tref.*log(p4/pref))/1000;
```

```
S4 = (mg.*cpg.*(log(T4/Tref)-Rg*log(p4/pref)))/1000;
% component analysis
% Air Compressor
Wac =(ET1-ET2)+(EP1-EP2)+Tref.*(S1-S2);
ETac = ET2 - ET1;
EPac = EP2 - EP1;
% Combuustion Chamber
ETcc = ET3 - (ET2+ET1);
EPcc = EP3 - (EP2+EP1);
Qcc = Eche +(ET2+ETf-ET3)+(EP2+EPf-EP3)+Tref.*(S2+Sf-S3);
% Gas Turbine
Wgt =(ET3-ET4)+(EP3-EP4)+Tref.*(S3-S4);
ETgt = ET4 - ET3;
EPgt = EP4 - EP3;
% Exergy Desruction
% Air Compressor
EDac = Tref.*(S2-S1);
% Combustion Chamber
EDcc = Eche +(ET2+ETf-ET3)+(EP2+EPf-EP3);
% Gas Turbine
EDgt = Tref.*(S4-S3);
% Total exergy destruction in the plant
EDplant = EDac + EDcc + EDgt;
% Exergy desruction efficiency
% air compressor
epsilonDac =(EDac./(-Wac))*100;
%Combustion Chamber
epsilonDcc = (EDcc./Eche)*100;
% Gas Turbine
epsilonDgt = (EDgt./Wgt)*100;
% Overall Plant
epsilonDplant = (EDplant./Eche)*100;
% Exergy  efficiency
% air compressor
epsilonAc =(1-(EDac./-Wac))*100;
%Combustion Chamber
epsilonCc = (1-(EDcc./Eche))*100;
% Gas Turbine
epsilonGt = (1 - (EDgt./Wgt))*100;
% Overall Plant
epsilonPlant = (1- (EDplant./Eche))*100;
% Net exergy power
Wplant = Wac + Wgt;
% Second Law efficiency
etaSL = (Wplant./Eche)*100;
% improvement potential
% Air compressor
Exiac = (1-epsilonAc/100).*EDac;
%Combustion Chamber
Exicc = (1-epsilonCc/100).*EDcc;
% Gas Turbine
Exigt = (1-epsilonGt/100).*EDgt;
% Overall Plant
Exiplant = (1-epsilonPlant/100).*EDplant;
% depletion number
Dp = EDcc./Eche;
% Sustainability index
```

```
SI = 1./Dp;
% graph of Ambient Temperature against Exergy Efficiency
figure (1)
plot(T1,epsilonAc,'--',T1,epsilonCc,'-.',T1,epsilonGt,'-
o',T1,epsilonPlant,'-+''linewidth',3)
legend('epsilonAc','epsilonCc','epsilonGt','epsilonPlant')
% graph of Ambient Temperature against Exergy Destruction Efficiency
figure (2)
plot(T1,epsilonDac,'--',T1,epsilonDcc,'-.',T1,epsilonDgt,'-
o',T1,epsilonDplant,'-+')
legend('epsilonDac','epsilonDcc','epsilonDgt','epsilonDplant')
% graph of Ambient Temperature against Second Law Efficiency
figure (3)
plot(T1,etaSL)
% graph of Ambient Temperature against Depletion number and
Sustainability index
figure (4)
plot (T1,SI,'-+',T1,Dp,'-o')
legend('SI','Dp')
% graph of Ambient Temperature against Exergy improvement potential
figure (5)
plot(T1,Exiac,'--',T1,Exicc,'-.',T1,Exigt,'-o',T1,Exiplant,'-+')
legend('Exiac','Exicc','Exigt','Exiplant')
% graph of Ambient Temperature against Exergy Efficiency Exergy exergy
detruction for CC
figure (6)
plot(T1,epsilonDcc,'->',T1,epsilonCc,'-o')
legend('epsilonDcc','epsilonCc')
% graph of Ambient Temperature against Exergy Efficiency Exergy exergy
% detruction for Plant
figure (7)
plot(T1,epsilonDplant,'->',T1,epsilonlant,'-o')
legend('epsilonDplant','epsilonPlant')
disp (Wac)
mean(Wac)
```

GT12

```
% Exergy Analyss for GT12
B=xlsread('GT12Exergy.xlsx');
T1 = B(:,1);
T2 = B(:,2);
T3 = B(:,9);
T4 = B(:,10);
Tf = 333;
ma = B(:,11);
mf = B(:,12);
mg = ma + mf;
p1 = 1.013;
p2 =B(:,4);
pf = 24;
p3 = B(:,7);
p4 = B(:,8);
cpa = 1.005;
cpf = 1.54;
cpg = 1.148;
Ra = 0.287;
```

```
Rf = 0.451;
Rg = 0.29;
Tref = B(:,1);
pref = 1.013;
Eche = (1.06*45011*mf)/1000;
ET1 =(ma.*cpa.*((T1-Tref)-(Tref.*log(T1/Tref))))/1000;
EP1 = (ma.*Ra.*Tref.*log(p1/pref))/1000;
S1 = (ma.*cpa.*(log(T1/Tref)-Ra*log(p1/pref)))/1000;
ET2 =(ma.*cpa.*((T2-Tref)-(Tref.*log(T2/Tref))))/1000;
EP2 = (ma.*Ra.*Tref.*log(p2/pref))/1000;
S2 = (ma.*cpa.*(log(T2/Tref)-Ra*log(p2/pref)))/1000;
ETf =(mf.*cpf.*((Tf-Tref)-(Tref.*log(Tf/Tref))))/1000;
EPf = (mf.*Rf.*Tref.*log(pf/pref))/1000;
Sf = (mf.*cpf.*(log(Tf/Tref)-Rf*log(pf/pref)))/1000;
ET3 =(mg.*cpg.*((T3-Tref)-(Tref.*log(T3/Tref))))/1000;
EP3 = (mg.*Rg.*Tref.*log(p3/pref))/1000;
S3 = (mg.*cpg.*(log(T3/Tref)-Rg*log(p3/pref)))/1000;
ET4 =(mg.*cpg.*((T4-Tref)-(Tref.*log(T4/Tref))))/1000;
EP4 = (mg.*Rg.*Tref.*log(p4/pref))/1000;
S4 = (mg.*cpg.*(log(T4/Tref)-Rg*log(p4/pref)))/1000;
% component analysis
% Air Compressor
Wac =(ET1-ET2)+(EP1-EP2)+Tref.*(S1-S2);
ETac = ET2 - ET1;
EPac = EP2 - EP1;
% Combuustion Chamber
ETcc = ET3 - (ET2+ET1);
EPcc = EP3 - (EP2+EP1);
Qcc = Eche +(ET2+ETf-ET3)+(EP2+EPf-EP3)+Tref.*(S2+Sf-S3);
% Gas Turbine
Wgt =(ET3-ET4)+(EP3-EP4)+Tref.*(S3-S4);
ETgt = ET4 - ET3;
EPgt = EP4 - EP3;
% Exergy Desruction
% Air Compressor
EDac = Tref.*(S2-S1);
% Combustion Chamber
EDcc = Eche +(ET2+ETf-ET3)+(EP2+EPf-EP3);
% Gas Turbine
EDgt = Tref.*(S4-S3);
% Total exergy destruction in the plant
EDplant = EDac + EDcc + EDgt;
% Exergy desruction efficiency
% air compressor
epsilonDac =(EDac./(-Wac))*100;
%Combustion Chamber
epsilonDcc = (EDcc./Eche)*100;
% Gas Turbine
epsilonDgt = (EDgt./Wgt)*100;
% Overall Plant
epsilonDplant = (EDplant./Eche)*100;
% Exergy  efficiency
% air compressor
epsilonAc =(1-(EDac./-Wac))*100;
%Combustion Chamber
epsilonCc = (1-(EDcc./Eche))*100;
% Gas Turbine
```

```
epsilonGt = (1 - (EDgt./Wgt))*100;
% Overall Plant
epsilonPlant = (1- (EDplant./Eche))*100;
% Net exergy power
Wplant = Wac + Wgt;
% Second Law efficiency
etaSL = (Wplant./Eche)*100;
% improvement potential
% Air compressor
Exiac = (1-epsilonAc/100).*EDac;
%Combustion Chamber
Exicc = (1-epsilonCc/100).*EDcc;
% Gas Turbine
Exigt = (1-epsilonGt/100).*EDgt;
% Overall Plant
Exiplant = (1-epsilonPlant/100).*EDplant;
% depletion number
Dp = EDcc./Eche;
% Sustainability index
SI = 1./Dp;
% graph of Ambient Temperature against Exergy Efficiency
figure (1)
plot(T1,epsilonAc,'--',T1,epsilonCc,'-.',T1,epsilonGt,'-
o',T1,epsilonPlant,'-+''linewidth',3)
legend('epsilonAc','epsilonCc','epsilonGt','epsilonPlant')
% graph of Ambient Temperature against Exergy Destruction Efficiency
figure (2)
plot(T1,epsilonDac,'--',T1,epsilonDcc,'-.',T1,epsilonDgt,'-
o',T1,epsilonDplant,'-+')
legend('epsilonDac','epsilonDcc','epsilonDgt','epsilonDplant')
% graph of Ambient Temperature against Second Law Efficiency
figure (3)
plot(T1,etaSL)
% graph of Ambient Temperature against Depletion number and
Sustainability index
figure (4)
plot (T1,SI,'-+',T1,Dp,'-o')
legend('SI','Dp')
% graph of Ambient Temperature against Exergy improvement potential
figure (5)
plot(T1,Exiac,'--',T1,Exicc,'-.',T1,Exigt,'-o',T1,Exiplant,'-+')
legend('Exiac','Exicc','Exigt','Exiplant')
% graph of Ambient Temperature against Exergy Efficiency Exergy exergy
detruction for CC
figure (6)
plot(T1,epsilonDcc,'->',T1,epsilonCc,'-o')
legend('epsilonDcc','epsilonCc')
% graph of Ambient Temperature against Exergy Efficiency Exergy exergy
% detruction for Plant
figure (7)
plot(T1,epsilonDplant,'->',T1,epsilonlant,'-o')
legend('epsilonDplant','epsilonPlant')
disp (Wac)
mean(Wac)
```

GT13

```
% Exergy Analyss for GT13
B=xlsread('GT13Exergy.xlsx');
T1 = B(:,1);
T2 = B(:,2);
T3 = B(:,9);
T4 = B(:,10);
Tf = 333;
ma = B(:,11);
mf = B(:,12);
mg = ma + mf;
p1 = 1.013;
p2 =B(:,4);
pf = 24;
p3 = B(:,7);
p4 = B(:,8);
cpa = 1.005;
cpf = 1.54;
cpg = 1.148;
Ra = 0.287;
Rf = 0.451;
Rg = 0.29;
Tref = B(:,1);
pref = 1.013;
Eche = (1.06*45011*mf)/1000;
ET1 =(ma.*cpa.*((T1-Tref)-(Tref.*log(T1/Tref))))/1000;
EP1 = (ma.*Ra.*Tref.*log(p1/pref))/1000;
S1 = (ma.*cpa.*(log(T1/Tref)-Ra*log(p1/pref)))/1000;
ET2 =(ma.*cpa.*((T2-Tref)-(Tref.*log(T2/Tref))))/1000;
EP2 = (ma.*Ra.*Tref.*log(p2/pref))/1000;
S2 = (ma.*cpa.*(log(T2/Tref)-Ra*log(p2/pref)))/1000;
ETf =(mf.*cpf.*((Tf-Tref)-(Tref.*log(Tf/Tref))))/1000;
EPf = (mf.*Rf.*Tref.*log(pf/pref))/1000;
Sf = (mf.*cpf.*(log(Tf/Tref)-Rf*log(pf/pref)))/1000;
ET3 =(mg.*cpg.*((T3-Tref)-(Tref.*log(T3/Tref))))/1000;
EP3 = (mg.*Rg.*Tref.*log(p3/pref))/1000;
S3 = (mg.*cpg.*(log(T3/Tref)-Rg*log(p3/pref)))/1000;
ET4 =(mg.*cpg.*((T4-Tref)-(Tref.*log(T4/Tref))))/1000;
EP4 = (mg.*Rg.*Tref.*log(p4/pref))/1000;
S4 = (mg.*cpg.*(log(T4/Tref)-Rg*log(p4/pref)))/1000;
% component analysis
% Air Compressor
Wac =(ET1-ET2)+(EP1-EP2)+Tref.*(S1-S2);
ETac = ET2 - ET1;
EPac = EP2 - EP1;
% Combuustion Chamber
ETcc = ET3 - (ET2+ET1);
EPcc = EP3 - (EP2+EP1);
Qcc = Eche +(ET2+ETf-ET3)+(EP2+EPf-EP3)+Tref.*(S2+Sf-S3);
% Gas Turbine
Wgt =(ET3-ET4)+(EP3-EP4)+Tref.*(S3-S4);
ETgt = ET4 - ET3;
EPgt = EP4 - EP3;
% Exergy Desruction
% Air Compressor
EDac = Tref.*(S2-S1);
% Combustion Chamber
```

```
EDcc = Eche +(ET2+ETf-ET3)+(EP2+EPf-EP3);
% Gas Turbine
EDgt = Tref.*(S4-S3);
% Total exergy destruction in the plant
EDplant = EDac + EDcc + EDgt;
% Exergy desruction efficiency
% air compressor
epsilonDac =(EDac./(-Wac))*100;
%Combustion Chamber
epsilonDcc = (EDcc./Eche)*100;
% Gas Turbine
epsilonDgt = (EDgt./Wgt)*100;
% Overall Plant
epsilonDplant = (EDplant./Eche)*100;
% Exergy  efficiency
% air compressor
epsilonAc =(1-(EDac./-Wac))*100;
%Combustion Chamber
epsilonCc = (1-(EDcc./Eche))*100;
% Gas Turbine
epsilonGt = (1 - (EDgt./Wgt))*100;
% Overall Plant
epsilonPlant = (1- (EDplant./Eche))*100;
% Net exergy power
Wplant = Wac + Wgt;
% Second Law efficiency
etaSL = (Wplant./Eche)*100;
% improvement potential
% Air compressor
Exiac = (1-epsilonAc/100).*EDac;
%Combustion Chamber
Exicc = (1-epsilonCc/100).*EDcc;
% Gas Turbine
Exigt = (1-epsilonGt/100).*EDgt;
% Overall Plant
Exiplant = (1-epsilonPlant/100).*EDplant;
% depletion number
Dp = EDcc./Eche;
% Sustainability index
SI = 1./Dp;
% graph of Ambient Temperature against Exergy Efficiency
figure (1)
plot(T1,epsilonAc,'--',T1,epsilonCc,'-.',T1,epsilonGt,'-
o',T1,epsilonPlant,'-+''linewidth',3)
legend('epsilonAc','epsilonCc','epsilonGt','epsilonPlant')
% graph of Ambient Temperature against Exergy Destruction Efficiency
figure (2)
plot(T1,epsilonDac,'--',T1,epsilonDcc,'-.',T1,epsilonDgt,'-
o',T1,epsilonDplant,'-+')
legend('epsilonDac','epsilonDcc','epsilonDgt','epsilonDplant')
% graph of Ambient Temperature against Second Law Efficiency
figure (3)
plot(T1,etaSL)
%  graph  of  Ambient  Temperature  against  Depletion  number  and
Sustainability index
figure (4)
plot (T1,SI,'-+',T1,Dp,'-o')
```

```
legend('SI','Dp')
% graph of Ambient Temperature against Exergy improvement potential
figure (5)
plot(T1,Exiac,'--',T1,Exicc,'-.',T1,Exigt,'-o',T1,Exiplant,'-+')
legend('Exiac','Exicc','Exigt','Exiplant')
% graph of Ambient Temperature against Exergy Efficiency Exergy exergy
detruction for CC
figure (6)
plot(T1,epsilonDcc,'->',T1,epsilonCc,'-o')
legend('epsilonDcc','epsilonCc')
% graph of Ambient Temperature against Exergy Efficiency Exergy exergy
% detruction for Plant
figure (7)
plot(T1,epsilonDplant,'->',T1,epsilonlant,'-o')
legend('epsilonDplant','epsilonPlant')
disp (Wac)
mean(Wac)
```

ENVIRONMENTAL ANALYSIS

GT11

```
% carbon dioxide emission analysis for GT11
% input parameters
C =xlsread('GT11Emissiondata.xlsx');
Tamb = C(:,1);
RH= (-0.0408*(Tamb)^3)+(3.1218*(Tamb)^2)-(80.238*Tamb)+774.44;
Tamb2 = Tamb - (273.15);
% molar mass of fuel kg/kmol
Mf = 18.89079;
% mass flow rate (kg/s) and molar flow rate of fuel (kmol/s)
mf = C(:,3);
nf = mf./Mf;
% Saturation pressure of water kPa
Psat = (.195.*Tamb2)-1.4219;
% Partial pressure of water vapour kPa
Pp = Psat.*RH;
Pmpa = Pp./101.325;
% molar fraction of water vapour
xh2o_a = Pmpa;
% molar fraction of dry air
dry_a = 1-xh2o_a;
% chemical contents ratio of gas in the air
n2 = 0.78980632;
o2 = 0.20988787;
co2 = 0.0003058;
% molar fraction of chemical contents in the air
xn2_a = dry_a.*n2;
xo2_a = dry_a.*o2;
xco2_a = dry_a.*co2;
% molar mass of air constituents kg/kmol
Mn2 = 28;
Mo2 = 32;
Mco2 = 44;
Mh2o = 18;
% moalr mass of air kg/kmol
```

```
Ma = (Mn2.*xn2_a)+(Mo2.*xo2_a)+(Mco2.*xco2_a)+(Mh2o.*xh2o_a);
% mass flow rate of air (kg/s) and molar flow rate of air (kmol/s)
ma = C(:,2);
na = ma./Ma;
% fuel air ratio
lambda = nf./na;
% molar fraction of gasses in combustion products
xco2_p =(1.118765.*lambda + xco2_a)/(1+lambda);
xh2o_p = (1.2022233.*lambda +xh2o_a)/(1+lambda);
a = (0.02722.*lambda);
b = xo2_a + xco2_a;
c = xh2o_a./2;
d = xco2_p + xh2o_p./2;
xo2_p = (a + b + c - d)./(1+lambda);
xn2_p = (0.01708.*lambda + xn2_a)/(1+lambda);
% molar flow rate of gas product
np = na.*(1 + lambda);
% mass flow rate of each constituent of the product
mco2 = Mco2*xco2_p.*np;
mo2 = Mo2*xo2_p.*np;
mh2o = Mh2o*xh2o_p.*np;
mn2 = Mn2.*xn2_p.*np;
% measured mass flow rate of product
mpm = ma + mf;
%  calculated mass flow rate of product
mpc = (mco2 + mh2o + mo2 + mn2);
% deviation in mass flow of product
detam = mpm - mpc;
% percentage Error
error = 100*detam./mpm;
% net power
Pnet = C(:,4);
% masss of carbon dioxide per MWh
xico2 = 3600.*mco2./Pnet;
disp(mco2)
disp(xico2)
disp(error)
figure(1)
plot(Tamb2,xico2,'r-','linewidth',3)
Eff = C(:,5);
figure(2)
plot(Eff,xico2,'g-','linewidth',3)
figure (3)
plot(Tamb2,xico2,'o-',Tamb2,Eff,'b-','linewidth',3)
```

GT12

```
% carbon dioxide emission analysis for GT12
% input parameters
C =xlsread('GT12Emissiondata.xlsx');
Tamb = C(:,1);
Tamb2 = Tamb - (273.15);
RH= (-0.0408*(Tamb2)^3)+(3.1218*(Tamb2)^2)-(80.238*Tamb2)+774.44;
% molar mass of fuel kg/kmol
Mf = 18.89079;
% mass flow rate (kg/s) and molar flow rate of fuel (kmol/s)
```

```
mf = C(:,3);
nf = mf./Mf;
% Saturation pressure of water kPa
Psat = (.195.*Tamb2)-1.4219;
% Partial pressure of water vapour kPa
Pp = Psat.*RH;
Pmpa = Pp./101.325;
% molar fraction of water vapour
xh2o_a = Pmpa;
% molar fraction of dry air
dry_a = 1-xh2o_a;
% chemical contents ratio of gas in the air
n2 = 0.78980632;
o2 = 0.20988787;
co2 = 0.0003058;
% molar fraction of chemical contents in the air
xn2_a = dry_a.*n2;
xo2_a = dry_a.*o2;
xco2_a = dry_a.*co2;
% molar mass of air constituents kg/kmol
Mn2 = 28;
Mo2 = 32;
Mco2 = 44;
Mh2o = 18;
% moalr mass of air kg/kmol
Ma = (Mn2.*xn2_a)+(Mo2.*xo2_a)+(Mco2.*xco2_a)+(Mh2o.*xh2o_a);
% mass flow rate of air (kg/s) and molar flow rate of air (kmol/s)
ma = C(:,2);
na = ma./Ma;
% fuel air ratio
lambda = nf./na;
% molar fraction of gasses in combustion products
xco2_p =(1.118765.*lambda + xco2_a)/(1+lambda);
xh2o_p = (1.2022233.*lambda +xh2o_a)/(1+lambda);
a = (0.02722.*lambda);
b = xo2_a + xco2_a;
c = xh2o_a./2;
d = xco2_p + xh2o_p./2;
xo2_p = (a + b + c - d)./(1+lambda);
xn2_p = (0.01708.*lambda + xn2_a)/(1+lambda);
% molar flow rate of gas product
np = na.*(1 + lambda);
% mass flow rate of each constituent of the product
mco2 = Mco2*xco2_p.*np;
mo2 = Mo2*xo2_p.*np;
mh2o = Mh2o*xh2o_p.*np;
mn2 = Mn2.*xn2_p.*np;
% measured mass flow rate of product
mpm = ma + mf;
%  calculated mass flow rate of product
mpc = (mco2 + mh2o + mo2 + mn2);
% deviation in mass flow of product
detam = mpm - mpc;
% percentage Error
error = 100*detam./mpm;
% net power
Pnet = C(:,4);
```

```
% masss of carbon dioxide per MWh
xico2 = 3600.*mco2./Pnet;
disp(mco2)
disp(xico2)
disp(error)
figure(1)
plot(Tamb2,xico2,'r-','linewidth',3)
Eff = C(:,5);
figure(2)
plot(Eff,xico2,'g-','linewidth',3)
figure (3)
plot(Tamb2,xico2,'o-',Tamb2,Eff,'b-','linewidth',3)
```

GT13

```
% carbon dioxide emission analysis for GT11
% input parameters
C =xlsread('Emissiondata.xlsx');
Tamb = C(:,1);
Tamb2 = Tamb - (273.15);
RH= (-0.0408*(Tamb2)^3)+(3.1218*(Tamb2)^2)-(80.238*Tamb2)+774.44;
% molar mass of fuel kg/kmol
Mf = 18.89079;
% mass flow rate (kg/s) and molar flow rate of fuel (kmol/s)
mf = C(:,3);
nf = mf./Mf;
% Saturation pressure of water kPa
Psat = (.195.*Tamb2)-1.4219;
% Partial pressure of water vapour kPa
Pp = Psat.*RH;
Pmpa = Pp./101.325;
% molar fraction of water vapour
xh2o_a = Pmpa;
% molar fraction of dry air
dry_a = 1-xh2o_a;
% chemical contents ratio of gas in the air
n2 = 0.78980632;
o2 = 0.20988787;
co2 = 0.0003058;
% molar fraction of chemical contents in the air
xn2_a = dry_a.*n2;
xo2_a = dry_a.*o2;
xco2_a = dry_a.*co2;
% molar mass of air constituents kg/kmol
Mn2 = 28;
Mo2 = 32;
Mco2 = 44;
Mh2o = 18;
% moalr mass of air kg/kmol
Ma = (Mn2.*xn2_a)+(Mo2.*xo2_a)+(Mco2.*xco2_a)+(Mh2o.*xh2o_a);
% mass flow rate of air (kg/s) and molar flow rate of air (kmol/s)
ma = C(:,2);
na = ma./Ma;
% fuel air ratio
lambda = nf./na;
```

```
% molar fraction of gasses in combustion products
xco2_p =(1.118765.*lambda + xco2_a)/(1+lambda);
xh2o_p = (1.2022233.*lambda +xh2o_a)/(1+lambda);
a = (0.02722.*lambda);
b = xo2_a + xco2_a;
c = xh2o_a./2;
d = xco2_p + xh2o_p./2;
xo2_p = (a + b + c - d)./(1+lambda);
xn2_p = (0.01708.*lambda + xn2_a)/(1+lambda);
% molar flow rate of gas product
np = na.*(1 + lambda);
% mass flow rate of each constituent of the product
mco2 = Mco2*xco2_p.*np;
mo2 = Mo2*xo2_p.*np;
mh2o = Mh2o*xh2o_p.*np;
mn2 = Mn2.*xn2_p.*np;
% measured mass flow rate of product
mpm = ma + mf;
%  calculated mass flow rate of product
mpc = (mco2 + mh2o + mo2 + mn2);
% deviation in mass flow of product
detam = mpm - mpc;
% percentage Error
error = 100*detam./mpm;
% net power
Pnet = C(:,4);
% masss of carbon dioxide per MWh
xico2 = 3600.*mco2./Pnet;
disp(mco2)
disp(xico2)
disp(error)
figure(1)
plot(Tamb2,xico2,'r-','linewidth',3)
Eff = C(:,5);
figure(2)
plot(Eff,xico2,'g-','linewidth',3)
figure (3)
plot(Tamb2,xico2,'o-',Tamb2,Eff,'b-','linewidth',3)
```

GT13

```
% carbon dioxide emission analysis for GT13
% input parameters
C =xlsread('GT13Emissiondata.xlsx');
Tamb = C(:,1);
Tamb2 = Tamb - (273.15);
RH= (-0.0408*(Tamb2)^3)+(3.1218*(Tamb2)^2)-(80.238*Tamb2)+774.44;
% molar mass of fuel kg/kmol
Mf = 18.89079;
% mass flow rate (kg/s) and molar flow rate of fuel (kmol/s)
mf = C(:,3);
nf = mf./Mf;
% Saturation pressure of water kPa
Psat = (.195.*Tamb2)-1.4219;
% Partial pressure of water vapour kPa
Pp = Psat.*RH;
Pmpa = Pp./101.325;
```

```
% molar fraction of water vapour
xh2o_a = Pmpa;
% molar fraction of dry air
dry_a = 1-xh2o_a;
% chemical contents ratio of gas in the air
n2 = 0.78980632;
o2 = 0.20988787;
co2 = 0.0003058;
% molar fraction of chemical contents in the air
xn2_a = dry_a.*n2;
xo2_a = dry_a.*o2;
xco2_a = dry_a.*co2;
% molar mass of air constituents kg/kmol
Mn2 = 28;
Mo2 = 32;
Mco2 = 44;
Mh2o = 18;
% moalr mass of air kg/kmol
Ma = (Mn2.*xn2_a)+(Mo2.*xo2_a)+(Mco2.*xco2_a)+(Mh2o.*xh2o_a);
% mass flow rate of air (kg/s) and molar flow rate of air (kmol/s)
ma = C(:,2);
na = ma./Ma;
% fuel air ratio
lambda = nf./na;
% molar fraction of gasses in combustion products
xco2_p =(1.118765.*lambda + xco2_a)/(1+lambda);
xh2o_p = (1.2022233.*lambda +xh2o_a)/(1+lambda);
a = (0.02722.*lambda);
b = xo2_a + xco2_a;
c = xh2o_a./2;
d = xco2_p + xh2o_p./2;
xo2_p = (a + b + c - d)./(1+lambda);
xn2_p = (0.01708.*lambda + xn2_a)/(1+lambda);
% molar flow rate of gas product
np = na.*(1 + lambda);
% mass flow rate of each constituent of the product
mco2 = Mco2*xco2_p.*np;
mo2 = Mo2*xo2_p.*np;
mh2o = Mh2o*xh2o_p.*np;
mn2 = Mn2.*xn2_p.*np;
% measured mass flow rate of product
mpm = ma + mf;
%  calculated mass flow rate of product
mpc = (mco2 + mh2o + mo2 + mn2);
% deviation in mass flow of product
detam = mpm - mpc;
% percentage Error
error = 100*detam./mpm;
% net power
Pnet = C(:,4);
% masss of carbon dioxide per MWh
xico2 = 3600.*mco2./Pnet;
disp(mco2)
disp(xico2)
disp(error)
figure(1)
plot(Tamb2,xico2,'r-','linewidth',3)
```

```
Eff = C(:,5);
figure(2)
plot(Eff,xico2,'g-','linewidth',3)
figure (3)
plot(Tamb2,xico2,'o-',Tamb2,Eff,'b-','linewidth',3)
```

APPENDIX II

AVERAGE OPERATING DATA FOR THE THREE GT UNITS

Table A1: GT11 Average Operating Data for 2018

Item	Jan	Feb	Mar	Apr	May	June	July	Aug	Sep	Oct	Nov	Dec
t_{o1} (^{0}C)	42	42	42	43	43	44	44	45	44	44	43	42
t_{02}(^{0}C)	77	77	77	78	77	77	77	77	77	77	77	77
t_{w1}(^{0}C)	36	36	36	36	37	38	38	39	37	37	36	36
t_{w2}(^{0}C)	51	51	51	51	51	51	51	51	51	51	51	51
$t_{1(}$^{0}C)	26.4	27	27.5	27	27	25.6	25	24	25	26	27	27
t_2(^{0}C)	375.4	376.7	377.8	376.7	376.7	373.7	372.5	370.3	372.5	374.6	376.7	376.7
t_3(^{0}C)	1106	1106	1106	1106	1106	1105	1105	1105	1105	1106	1106	1106
t_4(^{0}C)	540.3	541.0	541.5	541.0	541.0	539.3	538.6	537.5	538.6	539.8	541.0	541.0
p_1(bar)	1.0086	1.0087	1.0088	1.0087	1.0087	1.0086	1.0085	1.0084	1.0085	1.0086	1.0087	1.0087
p_2(bar)	10.98	10.97	10.96	10.97	10.97	10.99	11.00	11.02	11.00	10.99	10.97	10.97
$\dot{m}_a$(kg/s)	494.93	493.93	493.09	493.93	493.93	496.28	497.29	498.97	497.29	495.61	493.93	493.93
$\dot{m}_f$(kg/s)	10.94	10.96	10.98	10.96	10.96	10.91	10.89	10.85	10.89	10.92	10.96	10.96
P_{net}(MW)	149.00	148.21	147.50	148.21	148.20	150.25	151.13	152.58	151.13	149.67	148.21	148.21

Table A2: GT11 Average Operating Data for 2019

Item	Jan	Feb	Mar	Apr	May	June	July	Aug	Sep	Oct	Nov	Dec
t_{o1} (^{0}C)	43	42	42	42	44	44	44	44	44	44	43	43
t_{02}(^{0}C)	78	77	77	77	77	77	77	77	77	77	77	78
t_{w1}(^{0}C)	36	35	36	36	37	38	38	39	37	36	36	36
t_{w2}(^{0}C)	51	51	51	51	51	51	51	51	51	51	51	51
$t_{1(}$^{0}C)	24	29	33	26.67	26	25	24.67	23	29	29.8	31	27
t_2(^{0}C)	370.3	381	389.5	376	374.6	372.5	371.7	368.2	381	382.7	385.2	376.7
t_3(^{0}C)	1105	1107	1109	1106	1106	1105	1105	1104	1107	1107	1108	1106
t_4(^{0}C)	537.5	543.3	547.9	540.6	539.8	538.6	538.3	536.3	543.3	544.2	545.6	541
p_1(bar)	1.008	1.009	1.009	1.009	1.009	1.009	1.008	1.008	1.009	1.009	1.009	1.009
p_2(bar)	11.02	10.94	10.88	10.97	10.99	11	11	11.03	10.94	10.93	10.91	10.97
$\dot{m}_a$(kg/s)	499	490.6	483.8	494.5	495.6	497.3	497.8	500.6	490.6	489.2	487.2	493.9
$\dot{m}_f$(kg/s)	10.85	11.03	11.18	10.95	10.92	10.89	10.88	10.82	11.03	11.06	11.1	10.96
P_{net}(MW)	152.6	145.3	139.5	148.7	149.7	151.1	151.6	154	145.3	144.1	142.4	148.2

Table A3: GT11 Average Operating Data for 2020

Item	Jan	Feb	Mar	Apr	May	June	July	Aug	Sep	Oct	Noiv	Dec
t_{o1} (^{0}C)	42	42	42	43	43	44	44	44	44	44	42	42
t_{02}(^{0}C)	78	77	77	77	77	77	77	77	77	77	77	78
t_{w1}(^{0}C)	35	35	36	36	37	38	38	39	37	36	36	35
t_{w2}(^{0}C)	51	51	51	51	51	51	51	51	51	51	51	51
$t_{1(}$^{0}C)	27.5	29	29.5	29	27.5	27	25.5	24.5	26	26.5	27.5	28
t_2(^{0}C)	377.8	381	382	381	377.8	376.7	373.5	371.4	374.6	375.6	377.8	378.8
t_3(^{0}C)	1106	1107	1107	1107	1106	1106	1105	1105	1106	1106	1106	1107
t_4(^{0}C)	541.5	543.3	543.9	543.3	541.5	541	539.2	538.1	539.8	540.4	541.5	542.1
p_1(bar)	1.009	1.009	1.009	1.009	1.009	1.009	1.009	1.008	1.009	1.009	1.009	1.009
p_2(bar)	10.96	10.94	10.93	10.94	10.96	10.97	10.99	11.01	10.99	10.98	10.96	10.96
$\dot{m}_a$(kg/s)	493.1	490.6	489.7	490.6	493.1	493.9	496.4	498.1	495.6	494.8	493.1	492.2
$\dot{m}_f$(kg/s)	10.98	11.03	11.05	11.03	10.98	10.96	10.91	10.87	10.92	10.94	10.98	11
P_{net}(MW)	147.5	145.3	144.6	145.3	147.5	148.2	150.4	151.9	149.7	148.9	147.5	146.8

Table A4: GT12 Average Operating Data for 2018

Item	Jan	Feb	Mar	Apr	May	June	July	Aug	Sep	Oct	Noiv	Dec
t_{o1} (^{0}C)	NA	41	42	42	42	43	43	44	43	43	42	41
t_{02}(^{0}C)	NA	77	78	77	77	77	77	77	77	77	77	77
t_{w1}(^{0}C)	NA	36	36	37	38	39	38	39	37	36	36	36
t_{w2}(^{0}C)	NA	51	51	51	51	51	51	51	52	51	51	51
$t_{1(}$^{0}C)	NA	29	29	28	27.5	26.64	25.5	25	26	27.5	28	31
t_2(^{0}C)	NA	381.3	381.3	379.1	378.0	376.1	373.6	372.5	374.7	378.0	379.1	385.7
t_3(^{0}C)	NA	1107.5	1107.5	1107.0	1106.8	1106.3	1105.8	1105.5	1106.0	1106.8	1107.0	1108.5
t_4(^{0}C)	NA	543.2	543.2	542.1	541.5	540.5	539.2	538.7	539.8	541.5	542.1	545.5
p_1(bar)	NA	1.0133	1.0133	1.0131	1.0130	1.0128	1.0126	1.0125	1.0127	1.0130	1.0131	1.0137
p_2(bar)	NA	10.95	10.95	10.97	10.97	10.99	11.00	11.01	11.00	10.97	10.97	10.92
$\dot{m}_a$(kg/s)	NA	491.07	491.07	492.75	493.59	495.03	496.95	497.79	496.11	493.59	492.75	487.70
$\dot{m}_f$(kg/s)	NA	11.23	11.23	11.20	11.18	11.15	11.11	11.09	11.12	11.18	11.20	11.30
P_{net}(MW)	NA	147.6	147.6	149.0	149.8	151.1	152.8	153.5	152.0	149.8	149.0	144.6

Table A5: GT12 Average Operating Data for 2019

t_{o1} (^{0}C)	Jan	Feb	Mar	Apr	May	June	July	Aug	Sep	Oct	Noiv	Dec
t_{02}(^{0}C)	42	41	41	42	43	43	43	44	43	43	42	42
t_{w1}(^{0}C)	78	77	78	77	77	77	77	77	77	77	77	78
t_{w2}(^{0}C)	36	36	36	36	38	39	38	39	37	36	36	36
$t_{1(}$^{0}C)	51	51	52	51	51	51	51	51	52	51	51	51
t_2(^{0}C)	29	28	33	28.2	24.43	25.67	24.33	25	23.97	25	29	32
t_3(^{0}C)	381.3	379.1	390.1	379.5	371.2	373.9	371	372.5	370.2	372.5	381.3	387.9
t_4(^{0}C)	1108	1107	1110	1107	1105	1106	1105	1106	1105	1106	1108	1109
p_1(bar)	543.2	542.1	547.8	542.3	538	539.4	537.9	538.7	537.5	538.7	543.2	546.6
p_2(bar)	1.013	1.013	1.014	1.013	1.012	1.013	1.012	1.013	1.012	1.013	1.013	1.014
$\dot{m}_a$(kg/s)	10.95	10.97	10.89	10.96	11.02	11	11.02	11.01	11.03	11.01	10.95	10.91
$\dot{m}_f$(kg/s)	491.1	492.7	484.3	492.4	498.7	496.7	498.9	497.8	499.5	497.8	491.1	486
P_{net}(MW)	11.23	11.2	11.38	11.2	11.07	11.11	11.06	11.09	11.05	11.09	11.23	11.34
t_{o1} (^{0}C)	147.6	149	141.6	148.7	154.3	152.5	154.5	153.5	155	153.5	147.6	143.1

Table A6: GT12 Average Operating Data for 2020

Item	Jan	Feb	Mar	Apr	May	June	July	Aug	Sep	Oct	Noiv	Dec
t_{o1} (^{0}C)	41	41	42	42	42	43	43	43	43	43	42	41
t_{02}(^{0}C)	77	77	78	77	77	77	77	77	77	77	77	77
t_{w1}(^{0}C)	36	36	36	37	38	38	38	39	38	37	36	36
t_{w2}(^{0}C)	51	51	51	51	51	51	51	51	52	51	51	51
$t_{1(}$^{0}C)	29	29.5	29.5	29.5	28	26.5	25.5	25	26	27	28.5	29
t_2(^{0}C)	381.3	382.4	382.4	382.4	379.1	375.8	373.6	372.5	374.7	376.9	380.2	381.3
t_3(^{0}C)	1108	1108	1108	1108	1107	1106	1106	1106	1106	1107	1107	1108
t_4(^{0}C)	543.2	543.8	543.8	543.8	542.1	540.4	539.2	538.7	539.8	540.9	542.6	543.2
p_1(bar)	1.013	1.013	1.013	1.013	1.013	1.013	1.013	1.013	1.013	1.013	1.013	1.013
p_2(bar)	10.95	10.94	10.94	10.94	10.97	10.99	11	11.01	11	10.98	10.96	10.95
$\dot{m}_a$(kg/s)	491.1	490.2	490.2	490.2	492.7	495.3	496.9	497.8	496.1	494.4	491.9	491.1
$\dot{m}_f$(kg/s)	11.23	11.25	11.25	11.25	11.2	11.14	11.11	11.09	11.12	11.16	11.21	11.23
P_{net}(MW)	147.6	146.8	146.8	146.8	149	151.3	152.8	153.5	152	150.5	148.3	147.6

Table A7: GT13 Average Operating Data for 2018

Item	Jan	Feb	Mar	Apr	May	June	July	Aug	Sep	Oct	Noiv	Dec
t_{o1} (^{0}C)	NA	NA	40	43	43	42	43	43	42	42	41	40
t_{02}(^{0}C)	NA	NA	77	78	77	77	77	77	77	77	77	77
t_{w1}(^{0}C)	NA	NA	36	37	37	38	39	38	38	38	36	36
t_{w2}(^{0}C)	NA	NA	51	51	51	51	51	50	51	51	51	51
$t_{1(}$^{0}C)	NA	NA	31	28.45	27.5	26.5	25.5	25	26	26.87	28	30
t_2(^{0}C)	NA	NA	384.8	379.1	377	374.8	372.6	371.5	373.7	375.6	378.1	382.5
t_3(^{0}C)	NA	NA	1108	1107	1106	1106	1105	1105	1106	1106	1107	1108
t_4(^{0}C)	NA	NA	544.7	541.7	540.6	539.4	538.2	537.7	538.8	539.8	541.2	543.5
p_1(bar)	NA	NA	1.014	1.014	1.014	1.013	1.013	1.013	1.013	1.013	1.014	1.014
p_2(bar)	NA	NA	10.93	10.97	10.98	11	11.01	11.02	11.01	10.99	10.98	10.95
$\dot{m}_a$(kg/s)	NA	NA	487.4	491.7	493.3	495	496.6	497.5	495.8	494.3	492.4	489.1
$\dot{m}_f$(kg/s)	NA	NA	11.25	11.16	11.13	11.09	11.06	11.04	11.07	11.11	11.15	11.22
P_{net}(MW)	NA	NA	145.3	149.2	150.6	152.1	153.6	154.4	152.9	151.6	149.9	146.8

Table A8: GT13 Average Operating Data for 2019

Item	Jan	Feb	Mar	Apr	May	June	July	Aug	Sep	Oct	Noiv	Dec
t_{o1} (^{0}C)	41	42	40	43	43	42	43	44	42	42	42	41
t_{02}(^{0}C)	77	77	77	78	77	77	77	77	77	77	77	77
t_{w1}(^{0}C)	37	36	35	37	37	38	39	38	38	38	36	37
t_{w2}(^{0}C)	52	51	51	51	51	51	51	51	51	51	51	52
$t_{1(}$^{0}C)	30.7	31.5	32	29	25.23	24	24.5	25.8	28.1	28	29	30
t_2(^{0}C)	384.1	385.9	387	380.3	372	369.2	370.3	373.2	378.3	378.1	380.3	382.5
t_3(^{0}C)	1108	1108	1109	1107	1105	1105	1105	1106	1107	1107	1107	1108
t_4(^{0}C)	544.3	545.2	545.8	542.3	537.9	536.5	537.1	538.6	541.3	541.2	542.3	543.5
p_1(bar)	1.014	1.014	1.014	1.014	1.013	1.013	1.013	1.013	1.014	1.014	1.014	1.014
p_2(bar)	10.93	10.92	10.92	10.96	11.02	11.04	11.03	11.01	10.97	10.98	10.96	10.95
$\dot{m}_a$(kg/s)	487.9	486.6	485.7	490.8	497.1	499.2	498.3	496.1	492.3	492.4	490.8	489.1
$\dot{m}_f$(kg/s)	11.24	11.27	11.29	11.18	11.05	11	11.02	11.07	11.15	11.15	11.18	11.22
P_{net}(MW)	145.8	144.6	143.8	148.4	154	155.9	155.1	153.2	149.7	149.9	148.4	146.8

Table A9: GT13 Average Operating Data for 2020

t_{o1} (^{0}C)	Jan	Feb	Mar	Apr	May	June	July	Aug	Sep	Oct	Noiv	Dec
t_{02}(^{0}C)	41	41	40	43	43	43	43	43	42	42	41	41
t_{w1}(^{0}C)	77	77	77	78	77	77	77	77	77	77	77	77
t_{w2}(^{0}C)	36	36	36	37	37	38	38	39	38	38	37	36
$t_{1(}$^{0}C)	51	51	51	51	51	51	51	51	51	51	51	51
t_2(^{0}C)	28.5	29.2	30	29	27.5	27	25.5	24	26.52	26.5	28	28
t_3(^{0}C)	379.2	380.8	382.5	380.3	377.0	375.9	372.6	369.2	374.8	374.8	378.1	378.1
t_4(^{0}C)	1107.0	1107.3	1107.7	1107.2	1106.5	1106.2	1105.5	1104.7	1106.0	1106.0	1106.7	1106.7
p_1(bar)	541.7	542.6	543.5	542.3	540.6	540.0	538.2	536.5	539.4	539.4	541.2	541.2
p_2(bar)	1.014	1.014	1.014	1.014	1.014	1.013	1.013	1.013	1.013	1.013	1.014	1.014
$\dot{m}_a$(kg/s)	10.97	10.96	10.95	10.96	10.98	10.99	11.01	11.04	11.00	11.00	10.98	10.98
$\dot{m}_f$(kg/s)	491.61	490.43	489.09	490.77	493.29	494.13	496.65	499.17	494.93	494.97	492.45	492.45
P_{net}(MW)	11.16	11.19	11.22	11.18	11.13	11.11	11.06	11.00	11.09	11.09	11.15	11.15
t_{o1} (^{0}C)	149.11	148.05	146.84	148.35	150.62	151.37	153.64	155.90	152.10	152.13	149.86	149.86

The summary of monthly ambient air temperatures during period of the study are presented in Table A10

Table A10: Summary of Mean Monthly Ambient Air Temperature for Azura Edo Power Plant

S/N	Ambient Air Temperature (^{0}C)	Frequency
1	23	2
2	24	11
3	25	17
4	26	14
5	27	17
6	28	14
7	29	19
8	30	4
9	31	4
10	32	2
11	33	2

Table A11: Collected Operating Data for GT11

S/N	P_{net} (MW)	T_1 (^{0}C)	T_2 (^{0}C)	p_1 (bar)	p_2 (bar)	P_f (bar)	P_3 (bar)	P_4 (bar)	T_f (^{0}C)	T_3 (^{0}C)	T_4 (^{0}C)	$\dot{m}_a$ (kg/s)	$\dot{m}_f$ (kg/s)	$\dot{m}_g$ (kg/s)	T_{w1} (^{0}C)	T_{w2} (^{0}C)	T_{o1} (^{0}C)	T_{o2} (^{0}C)
1	159.41	21	363.6	1.0091	11.06	24	10.839	1.0191	60	1103.0	534.0	504.01	10.74	514.75	39	51	45	77
2	157.86	22	365.8	1.0093	11.04	24	10.824	1.0193	60	1103.5	535.1	502.33	10.78	513.11	39	51	44	77
3	156.16	23	368.0	1.0094	11.03	24	10.809	1.0194	60	1104.0	536.3	500.65	10.82	511.46	38	51	43	77
4	154.46	24	370.2	1.0096	11.01	24	10.794	1.0196	60	1104.5	537.5	498.97	10.85	509.82	37	51	42	77
5	152.82	25	372.5	1.0097	11.00	24	10.780	1.0197	60	1105.0	538.6	497.29	10.89	508.18	36	51	42	77
6	149.86	27	376.9	1.0100	10.97	24	10.750	1.0200	60	1106.0	541.0	493.93	10.96	504.89	36	51	42	77
7	147.14	29	381.3	1.0103	10.94	24	10.721	1.0203	60	1107.0	543.3	490.57	11.03	501.60	37	51	43	77
8	145.49	30	383.5	1.0105	10.92	24	10.706	1.0205	60	1107.5	544.5	488.89	11.07	499.95	36	51	42	77
9	144.04	31	385.8	1.0106	10.91	24	10.692	1.0206	60	1108.0	545.7	487.20	11.10	498.31	36	51	43	78
10	142.60	32	388.0	1.0108	10.89	24	10.677	1.0208	60	1108.5	546.9	485.52	11.14	496.66	36	51	42	77
11	141.27	33	390.0	1.0109	10.88	24	10.662	1.0209	60	1109.0	548.0	483.84	11.18	495.02	36	51	42	77
12	139.80	35	392.0	1.0112	10.85	24	10.633	1.0212	60	1110.0	550.0	480.48	11.25	491.73	36	51	42	77

Table A12: Collected Operating Data for GT12

S/N	P_{net} (MW)	T_1 (^{0}C)	T_2 (^{0}C)	p_1 (bar)	p_2 (bar)	P_f (bar)	P_3 (bar)	P_4 (bar)	T_f (^{0}C)	T_3 (^{0}C)	T_4 (^{0}C)	$\dot{m}_a$ (kg/s)	$\dot{m}_f$ (kg/s)	$\dot{m}_g$ (kg/s)	T_{w1} (^{0}C)	T_{w2} (^{0}C)	T_{o1} (^{0}C)	T_{o2} (^{0}C)
1	158.24	22	365.8	1.0108	11.05	24	10.83	1.0208	60	1104.0	535.0	502.83	10.98	513.8	39	51	44	78
2	156.66	23	368.0	1.0109	11.04	24	10.82	1.0209	60	1104.5	536.3	501.15	11.02	512.2	39	51	43	77
3	155.17	24	370.2	1.0111	11.02	24	10.80	1.0211	60	1105.0	537.5	499.47	11.05	510.5	39	51	43	77
4	152.04	26	374.7	1.0114	10.99	24	10.77	1.0214	60	1106.0	539.8	496.11	11.12	507.2	38	51	43	77
5	150.16	27	376.9	1.0115	10.98	24	10.76	1.0215	60	1106.5	541.0	494.43	11.16	505.6	36	51	41	77
6	147.23	29	381.3	1.0118	10.95	24	10.73	1.0218	60	1107.5	543.3	491.07	11.23	502.3	36	51	41	77
7	145.77	30	383.5	1.0120	10.93	24	10.72	1.0220	60	1108.0	544.5	489.39	11.27	500.7	36	51	41	77
8	144.33	31	385.8	1.0121	10.92	24	10.70	1.0221	60	1108.5	545.7	487.70	11.30	499.0	37	52	41	77
9	142.88	32	388.0	1.0123	10.90	24	10.69	1.0223	60	1109.0	546.9	486.02	11.34	497.4	36	51	42	78
10	141.45	33	390.2	1.0124	10.89	24	10.67	1.0224	60	1109.5	548.0	484.34	11.38	495.7	36	51	42	78
11	140.02	34	392.4	1.0126	10.87	24	10.66	1.0226	60	1110.0	549.2	482.66	11.41	494.1	36	51	42	78
12	139.67	35	394.0	1.0127	10.86	24	10.64	1.0227	60	1110.5	549.0	480.98	11.45	492.4	36	51	42	78

Table A13: Collected Operating Data for GT13

S/N	P_{net} (MW)	T_1 (^{0}C)	T_2 (^{0}C)	p_1 (bar)	p_2 (bar)	P_f (bar)	P_3 (bar)	P_4 (bar)	T_f (^{0}C)	T_3 (^{0}C)	T_4 (^{0}C)	$\dot{m}_a$ (kg/s)	$\dot{m}_f$ (kg/s)	$\dot{m}_g$ (kg/s)	T_{w1} (^{0}C)	T_{w2} (^{0}C)	T_{o1} (^{0}C)	T_{o2} (^{0}C)
1	160.70	21	362.6	1.0111	11.08	24	10.86	1.0211	60	1103.2	533.0	504.21	10.89	515.10	39	51	43	77
2	157.69	23	367.0	1.0114	11.05	24	10.83	1.0214	60	1104.2	535.3	500.85	10.97	511.81	38	50	42	76
3	155.82	24	369.2	1.0116	11.03	24	10.81	1.0216	60	1104.7	536.5	499.17	11.00	510.17	37	51	42	77
4	154.13	25	371.5	1.0117	11.02	24	10.80	1.0217	60	1105.2	537.6	497.49	11.04	508.53	36	51	41	77
5	152.65	26	373.7	1.0119	11.00	24	10.78	1.0219	60	1105.7	538.8	495.81	11.07	506.88	36	51	41	77
6	149.70	28	378.1	1.0122	10.97	24	10.76	1.0222	60	1106.7	541.2	492.45	11.15	503.59	37	52	42	78
7	148.23	29	380.3	1.0123	10.96	24	10.74	1.0223	60	1107.2	542.3	490.77	11.18	501.95	36	51	41	77
8	146.78	30	382.5	1.0125	10.94	24	10.73	1.0225	60	1107.7	543.5	489.09	11.22	500.30	35	50	41	77
9	145.28	31	384.8	1.0126	10.93	24	10.71	1.0226	60	1108.2	544.7	487.40	11.25	498.66	36	51	40	77
10	143.84	32	387.0	1.0128	10.91	24	10.70	1.0228	60	1108.7	545.9	485.72	11.29	497.01	36	51	40	77
11	142.40	33	389.2	1.0129	10.90	24	10.68	1.0229	60	1109.2	547.0	484.04	11.33	495.37	36	51	40	77
12	141.08	34	391.4	1.0131	10.88	24	10.67	1.0231	60	1109.7	548.0	482.36	11.36	493.73	36	51	40	77

APPENDIX III

AZURA EDO POWER PLANT SITE AMBIENT AIR TEMPERATURE AND RELATIVE HUMIDITY RELATION

How the relation between relative humidity and ambient air temperature was obtained. The values of relative humidity and ambient temperature for Azura Edo Power Plant site were obtained from Azura EIA (2013) as shown in Table B1. The values for relative hhumidity and ambient temperature were plotted in Microsoft Excel as shown in Figure B1. The line of best fit for the relation was obtained from the graph as shown in Figure B1.

Table B1: Ambient Air Temperature and Relative Humidity of Azura Edo Power Plant Site

S/N	Ambient Air Temperature (^{0}C)	Relative Humidity (%)
1	22.3	89.68
2	22.35	89.61
3	22.4	76.23
4	22.54	86.48
5	22.74	88.16
6	22.95	85.9
7	23.44	83.61
8	23.57	82.61
9	23.63	77.29
10	23.92	82.16
11	24.12	80.48
12	28.27	82.35
13	28.68	82.13
14	28.87	78.1
15	29.24	79.77
16	30.35	76.1
17	30.5	72.61
18	31.97	71
19	32.47	61.84
20	32.72	53.35
21	33.01	66.39
22	33.09	48.97
23	33.8	60.16
24	34.48	49.9

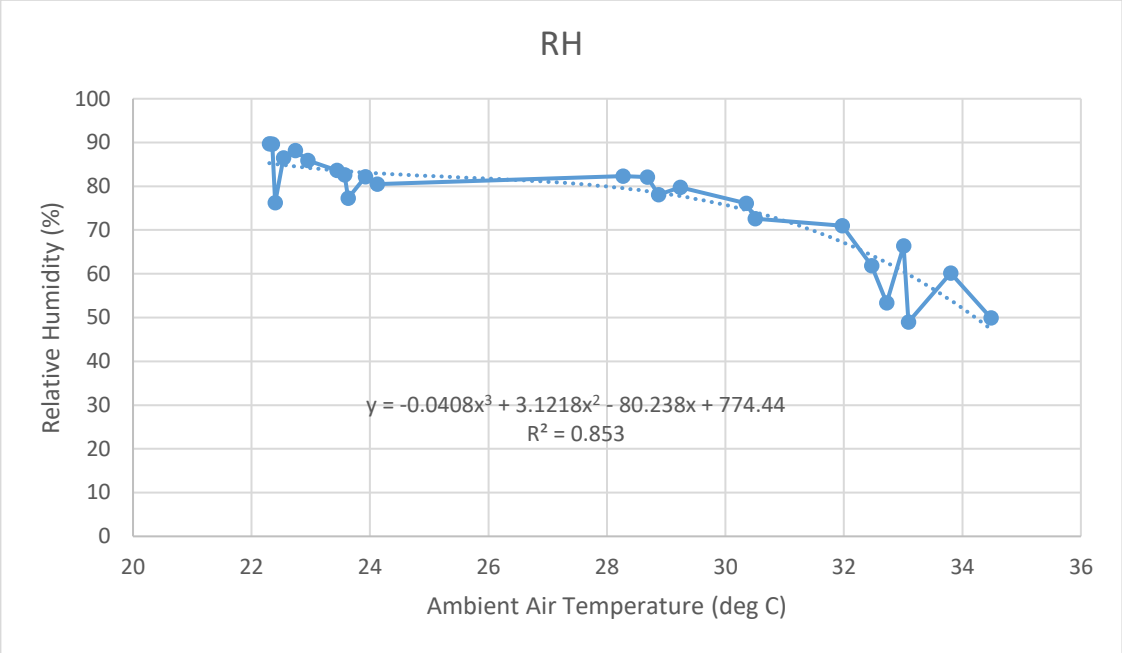

Figure B1: The Relative Humidity Against Ambient Air Temperature Curve for Azura Edo Power Plant

APPENDIX IV

PICTORIAL VIEW OF AZURA EDO POWER PLANT

APPENDIX V

SOME ENERGY ANALYSIS RESULTS

Table C1: Variation of Parameters with Ambient Air temperature Off – Design

T_1 (^{0}C)	T_2 (^{0}C)	T_3 (^{0}C)	T_4 (^{0}C)	p_2 (bar)	p_3 (bar)	$\dot{m}_a$ (kg/s)	$\dot{m}_f$ (kg/s)	$\dot{m}_g$ (kg/s)	P_{net} (MW)	η_{thnet} (%)	$\dot{m}_{CO2}$ (kg/s)	ξ_{co2} (kg/MWh)
15	363.8	1091.2	542.4	12.00	12.00	514.40	10.61	525.00	165.15	34.58	27.86	607.21
21	360.1	1093.6	551.2	11.77	11.77	503.90	10.36	514.26	157.72	33.80	27.21	620.97
22	361.3	1093.9	552.5	11.73	11.73	503.20	10.32	513.51	156.50	33.67	27.10	623.34
23	362.5	1094.1	553.8	11.69	11.69	500.50	10.27	510.77	155.28	33.54	26.99	625.73
24	363.7	1094.2	555.1	11.65	11.65	498.82	10.24	509.05	154.07	33.41	26.88	628.12
25	364.8	1094.3	556.4	11.61	11.61	497.19	10.19	507.39	152.85	33.28	26.77	630.54
26	366.2	1094.5	557.5	11.58	11.58	495.80	10.16	505.96	151.82	33.17	26.68	632.65
27	367.2	1094.4	559.0	11.54	11.54	493.83	10.11	503.94	150.44	33.03	26.55	635.40
28	368.4	1094.4	557.9	11.50	11.50	492.19	10.07	502.26	147.28	32.90	26.44	646.38
29	369.6	1094.2	561.0	11.46	11.46	490.56	10.03	500.59	148.02	32.77	26.33	640.43
30	370.8	1094.1	562.1	11.42	11.42	488.94	9.99	498.93	146.84	32.64	26.22	642.90
31	371.9	1093.9	563.9	11.38	11.38	487.36	9.94	497.30	145.64	32.51	26.11	645.44
32	373.1	1093.6	564.1	11.35	11.34	485.94	9.90	495.84	144.43	32.38	26.00	648.02
33	374.2	1093.3	565.0	11.37	11.31	484.15	9.86	494.01	143.25	32.24	25.89	650.56
34	375.3	1092.8	565.9	11.27	11.27	482.58	9.81	492.39	142.02	32.11	25.77	653.31
35	376.4	1092.3	567.0	11.23	11.23	481.009	9.77	490.78	140.82	31.98	25.66	656.00

Table C2: Performance Results for GT11

S/N	t_1 (^{0}C)	r_{pc}	HS (MW)	η_{thg} (%)	Q_{flue} (MW)	$P_{mec\ hloss}$ (MW)	$P_{gen\ loss}$ (MW)	P_{aux} (MW)	η_{mech} (%)	η_{gen} (%)	P_{net} (MW)	η_{net} (%)
1	21	10.96	483.60	33.65	303.12	1.41	1.92	0.23	99.13	98.81	159.41	32.96
2	22	10.94	485.22	33.23	302.26	1.45	1.92	0.23	99.10	98.80	157.86	32.53
3	23	10.93	486.84	32.81	301.39	1.50	2.08	0.23	99.06	98.69	156.16	32.08
4	24	10.91	488.46	32.40	300.52	1.54	2.24	0.23	99.03	98.57	154.46	31.62
5	25	10.89	490.08	31.99	299.65	1.54	2.40	0.23	99.02	98.46	152.82	31.18
6	27	10.86	493.32	31.18	297.91	1.54	2.40	0.23	99.00	98.43	149.86	30.38
7	29	10.83	496.56	30.38	296.17	1.50	2.24	0.23	99.01	98.50	147.14	29.63
8	30	10.81	498.18	29.99	295.30	1.54	2.40	0.23	98.97	98.38	145.49	29.20
9	31	10.80	499.80	29.61	294.43	1.54	2.40	0.23	98.96	98.36	144.04	28.82
10	32	10.78	501.42	29.22	293.55	1.54	2.40	0.23	98.95	98.35	142.60	28.44
11	33	10.76	503.04	28.87	292.67	1.54	2.40	0.23	98.94	98.33	141.27	28.08
12	35	10.73	506.28	28.39	290.72	1.54	2.40	0.23	98.93	98.31	139.80	27.61

Table C3: Performance Results for GT12

S/N	t_1 (^{0}C)	r_{pc}	HS (MW)	η_{thg} (%)	Q_{flue} (MW)	$P_{mec\ hloss}$ (MW)	$P_{gen\ loss}$ (MW)	P_{aux} (MW)	η_{mech} (%)	η_{gen} (%)	P_{net} (MW)	η_{net} (%)
1	22	10.94	494.22	32.76	302.59	1.50	1.92	0.23	99.08	98.80	158.24	32.02
2	23	10.92	495.84	32.33	301.80	1.50	1.92	0.23	99.07	98.79	156.66	31.60
3	24	10.90	497.46	31.92	300.93	1.50	1.92	0.23	99.06	98.78	155.17	31.19
4	26	10.87	500.70	31.13	299.20	1.50	2.08	0.23	99.04	98.65	152.04	30.37
5	27	10.85	502.32	30.73	298.33	1.58	2.40	0.23	98.97	98.43	150.16	29.89
6	29	10.82	505.56	29.95	296.59	1.58	2.40	0.23	98.95	98.40	147.23	29.12
7	30	10.81	507.18	29.57	295.71	1.58	2.40	0.23	98.94	98.39	145.77	28.74
8	31	10.79	508.80	29.19	294.84	1.58	2.40	0.23	98.93	98.37	144.33	28.37
9	32	10.77	510.42	28.82	293.97	1.58	2.40	0.23	98.92	98.35	142.88	27.99
10	33	10.76	512.05	28.45	293.09	1.58	2.40	0.23	98.91	98.34	141.45	27.62
11	34	10.74	513.67	28.08	292.22	1.58	2.40	0.23	98.90	98.32	140.02	27.26
12	35	10.72	515.29	27.92	290.57	1.58	2.40	0.23	98.90	98.32	139.67	27.11

Table C4: Performance Results for GT13

S/N	t_1 (^{0}C)	r_{pc}	HS (MW)	η_{thg} (%)	Q_{flue} (MW)	$P_{mec\ hloss}$ (MW)	$P_{gen\ loss}$ (MW)	P_{aux} (MW)	η_{mech} (%)	η_{gen} (%)	P_{net} (MW)	η_{net} (%)
1	21	10.96	490.35	33.47	302.74	1.50	1.917	0.23	99.09	98.82	160.70	32.77
2	23	10.92	493.59	32.64	301.01	1.50	1.917	0.23	99.07	98.80	157.69	31.95
3	24	10.91	495.21	32.23	300.14	1.54	2.237	0.23	99.03	98.59	155.82	31.47
4	25	10.89	496.83	31.82	299.28	1.58	2.396	0.23	99.00	98.47	154.13	31.02
5	26	10.88	498.45	31.42	298.41	1.58	2.396	0.23	98.99	98.45	152.65	30.62
6	28	10.84	501.69	30.63	296.67	1.58	2.396	0.23	98.97	98.42	149.70	29.84
7	29	10.83	503.31	30.24	295.80	1.58	2.396	0.23	98.96	98.41	148.23	29.45
8	30	10.81	504.93	29.86	294.93	1.58	2.396	0.23	98.95	98.39	146.78	29.07
9	31	10.79	506.55	29.48	294.06	1.63	2.396	0.23	98.91	98.38	145.28	28.68
10	32	10.78	508.17	29.10	293.19	1.63	2.396	0.23	98.90	98.36	143.84	28.31
11	33	10.76	509.79	28.72	292.32	1.63	2.396	0.23	98.89	98.35	142.40	27.93
12	34	10.74	511.41	28.37	291.33	1.63	2.396	0.23	98.88	98.33	141.08	27.59

Table C5: The Values of Compression and Expansion Pressure Ratios for Model and Actual Operating Data

Compressor Ratio			Expansion Ratio		
Model r_{pc}	Actual r_{pc}	difference	Model r_{pt}	Model r_{pt}	difference
11.663	10.960	0.703	11.546	10.635	0.911
11.622	10.943	0.679	11.506	10.619	0.887
11.582	10.927	0.655	11.466	10.603	0.863
11.543	10.910	0.632	11.427	10.587	0.840
11.502	10.894	0.608	11.387	10.571	0.816
11.423	10.861	0.562	11.310	10.539	0.770
11.344	10.828	0.516	11.231	10.507	0.723
11.304	10.812	0.492	11.192	10.491	0.700
11.264	10.795	0.469	11.152	10.476	0.676
11.225	10.779	0.446	11.113	10.460	0.654
11.244	10.762	0.482	11.073	10.444	0.630
11.105	10.729	0.376	10.995	10.412	0.583

PUBLISHED ARTICLE

Egware H.O, Obanor A.I, Aniekwu A.N, Omoifo O.I and Ighodaro O.O (2021): Modelling and Simulation of the SGT5-2000E Gas Turbine Model for Power Generation. *Journal of Energy Technology and Environment Vol. 3(2) pp 88 – 107.*